UNIVERSIDADE ESTADUAL PAULISTA
"JÚLIO DE MESQUITA FILHO"
INSTITUTO DE BIOCIÊNCIAS – RIO CLARO

PROGRAMA DE PÓS-GRADUAÇÃO EM CIÊNCIAS BIOLÓGICAS
(ZOOLOGIA)

# SISTEMÁTICA E DIVERSIFICAÇÃO DAS ESPÉCIES DA SUBFAMÍLIA PARATELMATOBIINAE (ANURA: LEPTODACTYLIDAE)

**MARCUS THADEU TEIXEIRA SANTOS**

Tese apresentada ao Instituto de Biociências do Câmpus de Rio Claro, Universidade Estadual Paulista, como parte dos requisitos para obtenção do título de doutor em Ciências Biológicas (Zoologia)

**Junho - 2020**

**MARCUS THADEU TEIXEIRA SANTOS**

# SISTEMÁTICA E DIVERSIFICAÇÃO DAS ESPÉCIES DA SUBFAMÍLIA PARATELMATOBIINAE (ANURA: LEPTODACTYLIDAE)

Tese apresentada ao Instituto de Biociências do Câmpus de Rio Claro, Universidade Estadual Paulista, como parte dos requisitos para obtenção do título de doutor em Ciências Biológicas (Zoologia)

**Orientador:** Prof. Dr. Célio Fernando Baptista Haddad

**Coorientador:** Prof. Dr. Paulo Christiano Anchietta Garcia

Rio Claro, SP

Junho - 2020

S237s

Santos, Marcus Thadeu Teixeira
Sistemática e diversificação das espécies da subfamília Paratelmatobiinae (Anura: Leptodactylidae) / Marcus Thadeu Teixeira Santos. -- Rio Claro, 2020
126 f. : tabs., fotos, mapas

Tese (doutorado) - Universidade Estadual Paulista (Unesp), Instituto de Biociências, Rio Claro
Orientador: Célio Fernando Baptista Haddad
Coorientador: Paulo Christiano Anchietta Garcia

1. Anuros. 2. Filogenia. 3. Taxonomia. 4. Evolução. 5. Biogeografia. I. Título.

Sistema de geração automática de fichas catalográficas da Unesp. Biblioteca do Instituto de Biociências, Rio Claro. Dados fornecidos pelo autor(a).

Essa ficha não pode ser modificada.

**UNIVERSIDADE ESTADUAL PAULISTA**

**Câmpus de Rio Claro**

## CERTIFICADO DE APROVAÇÃO

TÍTULO DA TESE: SISTEMÁTICA E DIVERSIFICAÇÃO DAS ESPÉCIES DA SUBFAMÍLIA PARATELMATOBIINAE (ANURA: LEPTODACTYLIDAE)

**AUTOR: MARCUS THADEU TEIXEIRA SANTOS**
**ORIENTADOR: CELIO FERNANDO BAPTISTA HADDAD**
**COORIENTADOR: PAULO CHRISTIANO DE ANCHIETTA GARCIA**

Aprovado como parte das exigências para obtenção do Título de Doutor em CIÊNCIAS BIOLÓGICAS (ZOOLOGIA), pela Comissão Examinadora:

Prof. Dr. CELIO FERNANDO BAPTISTA HADDAD
Departamento de Zoologia / UNESP - Instituto de Biociências de Rio Claro - SP

Prof. Dr. JOSE PEREZ POMBAL JUNIOR
Museu Nacional-UFRJ /Rio de Janeiro-RJ

Prof. Dr. FABIO RAPOSO DO AMARAL
Biologia Evolutiva e Filogeografia / Universidade Federal de São Paulo- Campus Diadema

Profa. Dra. MARIA TEREZA CHIARIONI THOMÉ
Departamento de Biologia e Ecologia Evolutiva / UFSCAR - Centro de Ciências Biológicas e da Saúde

Prof. Dr. BORIS LEONARDO BLOTTO ACUÑA
Departamento de Zoologia / Universidade de São Paulo - Instituto de Biociências

Rio Claro, 30 de junho de 2020

Dedico esta tese aos cientistas brasileiros e às universidades públicas pela luta constante e aos amantes da biodiversidade pela inspiração.

## AGRADECIMENTOS

Certamente várias pessoas e instituições contribuíram enormemente para a realização desta tese. Sou especialmente grato ao meu orientador, Prof. Célio Haddad por acreditar no projeto, pela oportunidade de fazer parte do seu grupo de pesquisa, pelos ensinamentos e pelo apoio em momentos difíceis. Obrigado também por sua eficiência, por incentivar minhas escolhas e por estar sempre disposto a ajudar. Tudo isso foi crucial para a conclusão do projeto.

A meu coorientador, Prof. Paulo Garcia, pelos ensinamentos, pela ajuda e dicas nos trabalhos de campo, que foram fundamentais. Sou muito grato também pela ideia de trabalhar com os Paratelmatobiinae, que se iniciou lá atrás (em 2012), e que desde então tem sido o principal foco de meus estudos.

À Profa. Ana Carolina Carnaval, por me receber de portas abertas em seu laboratório no *City College of New York* durante o período de doutorado sanduíche. Obrigado também pela disposição em ajudar, empolgação, e pelas ótimas dicas. O período em Nova York foi muito importante para o desenvolvimento do estudo e proporcionou um amplo crescimento acadêmico.

Agradeço imensamente ao amigo, Prof. Rafael F. Magalhães, por toda ajuda, desde as conversas iniciais, que contribuíram para a elaboração do projeto, até às ideias, ajudas com análises de dados e indicações de bibliografia. Obrigado também por toda a disponibilidade, paciência e amizade.

À Mariana Lyra, por toda ajuda no laboratório de biologia molecular, pela serenidade e ótimas conversas. Muitas vezes eu achava que, após diversas tentativas, não havia mais alternativa para conseguir amplificar um determinado fragmento e a Mari, na maior calma e otimismo, chegava com novas ideias, que quase sempre funcionavam.

Aos demais colaboradores, Thiago de Carvalho, Rodrigo Ferreira, Fabrício Santos, Luciana Lourenço, Felipe Leite, Iuri Dias, Stenio Vittorazzi, Hussam Zaher, Luís Giasson, Sílvia Oliveira, Bárbara Zaidan, Nelson da Silva e Bianca Berneck, pelas contribuições.

À Maria Tereza Thomé, pelas valiosas dicas ao longo de várias etapas do doutorado, como durante as avaliações de projeto, progresso e qualificação. Suas ideias e incentivos foram muito importantes. Também agradeço à Priscila Lemes, Délio Baêta e Cinthia Brasileiro, pelas contribuições em uma ou mais dessas etapas.

Um agradecimento especial a todos que me ajudaram em campo, Juliane Monteiro, Thaís Condez, Thiago de Carvalho, Nadya Pupin, Elicarlos Nardin, Paulo Garcia, Bárbara Zaidan, Bianca Berneck, Izabela Barata, Sofia Martins, Fabiana Dallacorte e Javier Toso. Também agradeço a todos os colegas que me enviaram amostras de tecido, Miguel Rodrigues, Sabrina Baroni, Rodrigo Ferreira, Ricardo Sawaya, Luiz Ugioni, Paulo Costa, Milena Wacklevski e Iuri Dias.

À Sofia Lamerato Costa, por toda a ajuda com a organização dos dados e com a morfometria e aos colegas João Giovanelli e Maurício Vancine pelas ajudas com mapas.

Aos amigos do Laboratório de Herpetologia da UNESP, Pedro Taucce, Paulo Pinheiro, Thiago de Carvalho, Thaís Condez, Leo Malagoli, Juliane Monteiro, Ana Paula Motta, Mariana Lyra, Nadya Pupin, Tulipa da Costa, Francisco Brusquetti, Kaleb Pretto Gatto, Tereza Thomé, Boris Blotto, Fábio de Sá, João Giovanelli, Anyelet Aguilar, Amanda Silva, Délio Baêta, Ariadne Sabbag, Carla Lopes, Priscila Lemes, Bianca Berneck, Ana Carolina Lourenço, Danilo Delgado, Lucas Nicioli, Natalia Salles, Aline Aguiar e José Ribeiro Júnior. A ótima convivência, conversas e momentos de descontração e lazer foram muito importantes para a conclusão da tese e para suportar as angústias em tempos tão difíceis.

Aos colegas do Departamento de Biologia da *City College of New York*, Mariana Vasconcellos, Kathryn Mercier, Patrick Shea, Karin Seger, Andrea Paz, Connor French, Laura Bertola. Obrigado pelas dicas, conversas e pelos *Lab Meetings* e *Happy Hours*. Foram muito importantes para a adaptação. Agradeço especialmente à Kathryn, Patrick e Connor pela ajuda com o inglês nos trabalhos que compõem a tese.

Aos colegas do Laboratório de Herpetologia da UFMG, Tiago Pezzuti, Rafael Magalhães, Caroline Oswald, Bárbara Zaidan, Igor Rodrigues, João Víctor Lacerda, Henrique Costa, Emanuel da Silva, Samuel Gomides, Fernando Leal, Brenda Silva, Daniela Fonseca, Sofia Martins, Isabel Marques, Rachel Montesinos e Hans Thomassen, pela convivência, amizade e momentos de lazer, especialmente durante os congressos de Herpeto.

Também agradeço aos demais amigos espalhados por esse mundão afora, em especial ao João, Bárbara, Fernando, Isabelle, Lucas, Ana Carolina, Guilherme, Amanda, Klever, Tereza, Flávio e Marina pela amizade de tantos anos.

Aos curadores e técnicos das coleções herpetológicas consultadas, José Pombal Jr., Manoela Woitovicz e Pedro Pinna (MNRJ), Hussam Zaher, Taran Grant e Aline Benetti (MZUSP), Helio Fernandes, Thiago Soares e Juliana Silva (MBML), Oswaldo Peixoto (EI),

Sérgio Carvalho e Silva (ZUFRJ), Victor Orrico (MZUESC), Selvino Oliveira (CHUFSC), Ariovaldo Giaretta (AAG-UFU), Júlio Moura Leite (MHNCI), Célio Haddad e Nadya Pupin (CFBH), Paulo Garcia e Camila Almeida (UFMG), Ronald Heyer e Kevin de Queiroz (USNM), José Rosado e Jonathan Woodward (MCZ). As amostras e espécimes depositados nas diversas coleções foram fundamentais para a elaboração dessa tese.

Aos docentes e discentes do Programa de Pós-Graduação em Ciências Biológicas (Zoologia) por contribuírem para minha formação. Também sou muito grato a todos os funcionários da UNESP de Rio Claro.

Às agências de fomento pelas bolsas e auxílios concedidos, sem as quais eu não conseguiria realizar o doutorado. O presente trabalho foi realizado com apoio da Coordenação de Aperfeiçoamento de Pessoal de Nível Superior - Brasil (CAPES) - Código de Financiamento 001. À Pró-Reitoria de Pós-Graduação da UNESP por recursos disponibilizados para visitas a coleções zoológicas. Também agradeço à Fundação de Amparo à Pesquisa do Estado de São Paulo (FAPESP) por auxílios proporcionados por projetos coordenados pelo Prof. Célio Haddad (2013/50741-7 e 2014/50342).

Ao Instituto Chico Mendes de Conservação da Biodiversidade (ICMBio), Instituto Estadual de Meio Ambiente e Recursos Hídricos (IEMA-ES), Instituto Estadual de Florestas (IEF-MG), Instituto Estadual do Ambiente (INEA-RJ), Comissão Técnico-Científica do Instituto Florestal (COTEC-SP), Instituto Ambiental do Paraná (IAP-PR), Fundação do Meio Ambiente (FATMA-SC), e Comissão de Ética no Uso de Animal do Instituto de Biociências, UNESP, Rio Claro (CEUA-IB) pelas licenças concedidas.

Ao Centro de Estudos de Insetos Sociais (CEIS, UNESP) por permitir o uso do Laboratório de Biologia Molecular. Ao CIPRES Science Gateway e ao Núcleo de Computação Científica (NCC/GridUNESP) da UNESP pelos recursos computacionais disponibilizados para análises de dados. Ao Sci-Hub pela disseminação gratuita de conhecimento científico, sem o qual ficaria inviável acessar boa parte da literatura consultada.

Aos meus pais, Mirtes e Flávio por todo amor, apoio, reconhecimento, cuidado e incentivo ao longo desses anos. Obrigado também pela educação e por incentivarem o pensamento crítico sobre os mais variados temas. Aos meus irmãos Melissa, João e Pedro pelo apoio e incentivo. Aos meus queridos sobrinhos Henrique e Gustavo pelos bons momentos compartilhados e pelas risadas. A meu cunhado Reinaldo e minha cunhada Rafaella pelo apoio.

A minha companheira Thaís, por todo seu amor, carinho, paciência e pelos ótimos momentos compartilhados ao longo de todos esses anos. Obrigado também por apoiar minhas escolhas, pelos valiosos conselhos e por tanto me ajudar nos momentos mais difíceis.

Por fim, agradeço aos *Crossodactylodes*, *Paratelmatobius*, *Scythrophrys* e *Rupirana*, esses pequenos anuros que tanto me intrigam. A empolgação gerada a cada encontro em campo e a cada dado analisado foi fundamental para eu conseguir chegar ao final dessa etapa.

*“It seems to me that the natural world is the greatest source of excitement; the greatest source of visual beauty; the greatest source of intellectual interest. It is the greatest source of so much in life that makes life worth living”*

(Sir David F. Attenborough)

## RESUMO GERAL

A subfamília Paratelmatobiinae é um grupo de anuros pouco estudado constituído por 14 espécies de distribuição geográfica restrita alocadas nos gêneros *Crossodactylodes*, *Paratelmatobius*, *Scythrophrys* e *Rupirana*. Até o momento, estudos filogenéticos focados na subfamília foram baseados em amostragens gênica e/ou taxonômica limitadas. No primeiro capítulo desse trabalho, propusemos uma hipótese filogenética para o gênero *Crossodactylodes*, avaliamos a evolução de alguns caracteres fenotípicos e de história natural e realizamos uma revisão taxonômica para o grupo. Recuperamos *Crossodactylodes* como monofilético e diagnosticado por sete sinapomorfias putativas em caracteres morfológicos e de história natural. Evidências suportam algumas sinapomorfias morfológicas como adaptações ao hábito bromelígena. No segundo capítulo, propusemos uma nova hipótese filogenética para Paratelmatobiinae, baseada em ampla amostragem gênica e taxonômica. Além disso, delimitamos linhagens evolutivamente independentes e estimamos os tempos dos eventos de diversificação. Recuperamos Paratelmatobiinae e cada um de seus quatro gêneros como monofiléticos e bem suportados. Cinco espécies potencialmente novas incluídas em nosso estudo foram suportadas como linhagens evolutivamente independentes nas árvores filogenéticas e nas análises de delimitação. Também recuperamos outras linhagens profundamente divergentes e geograficamente estruturadas nos quatro gêneros de Paratelmatobiinae. Nossa estimativa dos tempos de divergência indica que a diversificação na subfamília se iniciou no Eoceno e continuou durante o Oligoceno, Neógeno e Pleistoceno. Mudanças climáticas passadas, eventos neotectônicos e características relacionadas à história natural possivelmente influenciaram a diversificação de Paratelmatobiinae. Por fim, no terceiro capítulo formalizamos a descrição de uma nova espécie de *Paratelmatobius*, que ocorre na Mata Atlântica do estado do Paraná, sul do Brasil. Descrevemos adultos, girinos e vocalizações. A nova espécie é facilmente diagnosticável de outras espécies do gênero por seu canto de anúncio, que é composto por dois tipos de notas e compreende uma série de duas a quatro notas. Uma análise filogenética e caracteres morfológicos suportam que a nova espécie pertence ao grupo de espécies de *P. cardosoi*.



**Palavras-chave:** Campo rupestre; *Crossodactylodes*; Filogenia; Mata Atlântica; *Paratelmatobius*; *Rupirana*; *Scythrophrys*; Taxonomia.

## GENERAL ABSTRACT

The subfamily Paratelmatobiinae is a poorly studied group of frogs consisting of 14 species with restricted geographical distribution allocated to the genera *Crossodactylodes*, *Paratelmatobius*, *Scythrophrys* and *Rupirana*. To date, phylogenetic studies focused on this subfamily have been based on limited taxon and/or character sampling. In the first chapter of this work, we proposed a phylogenetic hypothesis for the genus *Crossodactylodes*, evaluated the evolution of some phenotypical and natural history traits and performed a taxonomic revision for the group. We recovered *Crossodactylodes* as monophyletic and diagnosed by seven putative synapomorphies in morphological and natural history characters. Evidence supports some morphological synapomorphies as adaptations to the bromeligenous habit. In the second chapter, we proposed a new phylogenetic hypothesis for Paratelmatobiinae, based on extensive taxon and character sampling. In addition, we delimitated independently evolving lineages within the group and estimated the timing of diversification events. We recovered Paratelmatobiinae and each of its four genera as monophyletic and robustly supported. Five potentially new species included in our study were supported as independently evolving lineages in the phylogenetic trees and in the delimitation analyses. We also recovered other deeply divergent and geographically structured lineages within the four genera of Paratelmatobiinae. Our estimation of divergence times indicates that diversification in the subfamily began in the Eocene and continued during the Oligocene, Neogene and Pleistocene. Past climate changes, neotectonic events, and life history traits likely influenced the diversification of Paratelmatobiinae. Finally, in the third chapter, we formalized the description of a new species of *Paratelmatobius*, which occurs in the Atlantic Forest of the state of Paraná, southern Brazil. We described adults, tadpoles, and vocalizations. The new species can be readily distinguished from its congeners by its advertisement call being composed of two note types and comprised of a series of two to four notes. Morphological traits and phylogenetic analysis place the new species within the *P. cardosoi* species group.



**Keywords:** Atlantic Forest; Campo rupestre; *Crossodactylodes*; *Paratelmatobius*; Phylogeny; *Rupirana*; *Scythrophrys*; Taxonomy.

**SUMÁRIO**

**INTRODUÇÃO GERAL** ..... 14

Referências Bibliográficas ..... 17

**CAPÍTULO I**

Systematic Revision of the Rare Bromeligenous Genus *Crossodactylodes* Cochran, 1938 (Anura: Leptodactylidae: Paratelmatobiinae) ..... 21

**CAPÍTULO II**

Multilocus phylogeny of Paratelmatobiinae (Anura: Leptodactylidae) reveals strong spatial structure and previously unknown diversity in the Atlantic Forest hotspot ..... 64

**CAPÍTULO III**

A new species of *Paratelmatobius* (Anura: Leptodactylidae: Paratelmatobiinae) from the Atlantic Forest of southern Brazil ..... 103

**CONCLUSÕES GERAIS** ..... 125

**PERSPECTIVAS** ..... 126

# INTRODUÇÃO GERAL

A família Leptodactylidae Werner, 1896 é atualmente composta por 214 espécies alocadas em três subfamílias: Leiuperinae Bonaparte, 1850, Leptodactylinae Werner, 1896 e Paratelmatobiinae Ohler & Dubois, 2012 (Frost, 2020). Tanto Leiuperinae, quanto Leptodactylinae compreendem aproximadamente 100 espécies e são amplamente distribuídas na América do Sul, sendo também registradas em pequenas porções da América Central e América do Norte (Frost, 2020). Em contrapartida, Paratelmatobiinae é composta por apenas 14 espécies e apresenta distribuição mais restrita, que se estende da região central do estado da Bahia ao centro-leste de Santa Catarina, Brasil (Frost, 2020). A subfamília é composta pelos gêneros *Crossodactylodes* Cochran, 1938, *Paratelmatobius* Lutz & Carvalho, 1958, *Rupirana* Heyer, 1999 e *Scythrophrys* Lynch, 1971 (Frost, 2020).

Os quatro gêneros estão distribuídos ao longo de um gradiente norte-sul e são associados a regiões serranas (Fouquet et al., 2013). O gênero *Rupirana* é endêmico dos campos rupestres da porção setentrional da Serra do Espinhaço, na região central do estado da Bahia (Juncá & Lugli, 2009). *Crossodactylodes* ocorre no domínio da Mata Atlântica desde o sul do estado da Bahia até o Rio de Janeiro e em uma área de campo rupestre no estado de Minas Gerais (Barata et al., 2013; Teixeira et al., 2013). *Paratelmatobius* é endêmico da Mata Atlântica e distribuído na Serra da Mantiqueira e na Serra do Mar, desde a fronteira entre os estados de Minas Gerais, Rio de Janeiro e São Paulo até o norte do estado do Paraná (Frost, 2020). Por fim, o gênero *Scythrophrys*, também endêmico da Mata Atlântica, é distribuído na porção sul da Serra do Mar e nas Serras do Leste Catarinense, nos estados do Paraná e Santa Catarina. A maioria das espécies de Paratelmatobiinae tem distribuição restrita a uma ou poucas localidades (Frost, 2020). A ocorrência em ambientes específicos em áreas remotas e os encontros recentes de novas espécies (Barata et al., 2013; Teixeira et al., 2013) sugerem que o número de espécies de Paratelmatobiinae pode estar subestimado.

As hipóteses sobre as relações dos gêneros atualmente incluídos em Paratelmatobiinae com outros grupos de anuros sofreram amplas modificações ao longo dos anos. Cochran (1955) sugeriu afinidade de *Crossodactylodes* com o gênero *Crossodactylus* Duméril & Bibron, 1841. Lynch (1971) investigou as relações entre os Leptodactylidae (*sensu lato*) e alocou *Crossodactylodes* na subfamília Telmatobiinae, tribo Grypiscini, juntamente com os gêneros *Cycloramphus* Tschudi, 1838 e *Zachaenus* Cope, 1866. Por outro lado, *Paratelmatobius* foi alocado na subfamília Leptodactylinae, juntamente com *Barycholos*

Heyer, 1969, *Edalorhina* Jiménez de la Espada, 1870, *Hydrolaetare* Gallardo, 1963, *Leptodactylus* Fitzinger, 1826, *Limnomedusa* Fitzinger, 1843, *Lithodytes*, Fitzinger, 1843, *Physalaemus*, Fitzinger, 1826, *Pleurodema* Tschudi, 1838 e *Pseudopaludicola* Miranda-Ribeiro, 1926. Já o gênero *Scythrophrys* foi classificado como *incertae sedis* dentro da subfamília Telmatobiinae.

Heyer (1975) foi o primeiro autor a relatar um relacionamento próximo entre os gêneros *Crossodactylodes*, *Paratelmatobius* e *Scythrophrys*, ao incluí-los em um agrupamento denominado "gripiscíneos", juntamente com os gêneros *Cycloramphus*, *Zachaenus*, *Craspedoglossa* (posteriormente sinonimizado à *Cycloramphus*), *Crossodactylus*, *Hylodes* Fitzinger, 1826, *Megaelosia* Miranda-Ribeiro, 1923 e *Thoropa* Cope, 1865. O gênero *Rupirana* foi descrito somente em 1999. Na descrição original, Heyer (1999) incluiu o gênero em Leptodactylidae (*sensu lato*), mas não conseguiu estabelecer com quais gêneros *Rupirana* é proximamente relacionado. Posteriormente, Dubois (2005) propôs uma classificação baseada no agrupamento de Heyer (1975), incluindo *Crossodactylodes*, *Paratelmatobius*, *Scythrophrys* e *Rupirana* na família Leptodactylidae, subfamília Cycloramphinae, juntamente com os gêneros *Cycloramphus*, *Zachaenus* e *Thoropa*.

O uso de sequências de DNA e o aumento na capacidade de processamento computacional possibilitaram o desenvolvimento de estudos com grande amostragem taxonômica (e.g., Frost et al., 2006; Pyron & Wiens, 2011). Frost et al. (2006) recuperaram os gêneros *Paratelmatobius* e *Scythrophrys* como irmãos e proximamente relacionados aos gêneros *Adenomera* Steindachner, 1867, *Lithodytes*, *Leptodactylus*, *Vanzolinius* Heyer, 1974 (posteriormente sinonimizado a *Leptodactylus*), *Edalorhina*, *Engystomops* Jiménez de la Espada, 1872, *Eupemphix* Steindachner, 1863 (posteriormente sinonimizado a *Physalaemus*), *Pleurodema*, *Physalaemus*, *Somuncuria* Lynch, 1978 (posteriormente sinonimizado a *Pleurodema*) e *Pseudopaludicola*, compondo a família Leptodactylidae, que passou a ser menos abrangente a partir desse estudo. Lourenço et al. (2008), utilizando um maior número de terminais de *Paratelmatobius* e *Scythrophrys*, também recuperaram os gêneros como irmãos.

Pyron & Wiens (2011), em análise com maior abrangência taxonômica, também recuperaram *Paratelmatobius* como táxon irmão de *Scythrophrys* e propuseram a subfamília Paratelmatobiinae para alocá-los. No entanto, os autores não apresentaram uma diagnose para o novo táxon proposto, tornando Paratelmatobiinae *nomen nudum*. Essa diagnose foi posteriormente apresentada por Ohler & Dubois (2012), que validaram assim

Paratelmatobiinae. Em seguida, Fouquet et al. (2013) incluíram pela primeira vez os gêneros *Crossodactylodes* e *Rupirana* em uma análise filogenética baseada em sequências de DNA. Os autores recuperaram os dois gêneros como proximamente relacionados a *Paratelmatobius* e *Scythrophrys*. Desconhecendo a validação de Paratelmatobiinae feita por Ohler & Dubois (2012), Fouquet et al. (2013) propuseram a subfamília Crossodactylodinae para alocar os quatro gêneros. Dessa forma, o nome proposto é um sinônimo júnior de Paratelmatobiinae (Dubois, 2013).

Apesar do avanço recente sobre o conhecimento das relações filogenéticas em Paratelmatobiinae, todos os estudos filogenéticos focados na subfamília até o momento foram baseados em amostragens gênica e/ou taxonômica limitadas (Lourenço et al., 2008; Fouquet et al., 2013; Teixeira et al., 2013), dificultando o entendimento da história evolutiva do grupo. Diante do padrão de distribuição geográfica dos gêneros e espécies de Paratelmatobiinae, uma hipótese filogenética mais completa para o grupo pode ter implicações para um melhor entendimento de eventos de diversificação que ocorreram na Mata Atlântica em diferentes escalas temporais, assim como da relação entre a biota da Mata Atlântica e a biota dos campos rupestres. Além disso, hipóteses filogenéticas abrangentes são importantes para o reconhecimento de espécies ainda não descritas e, dessa forma, constituem uma etapa importante para a descrição de novos táxons (Wiens, 2007; Caminer et al., 2017; Grabowski et al., 2017). Isso é especialmente relevante diante das taxas alarmantes de perda de hábitat na Mata Atlântica e nos campos rupestres nas últimas décadas (Ribeiro et al., 2009; Silveira et al., 2016), fazendo com que algumas espécies possam ter sido extintas antes mesmo de serem descobertas (Lees & Pimm, 2015).

Assim, o objetivo geral deste trabalho foi aprimorar o conhecimento sobre as relações evolutivas em Paratelmatobiinae e os fatores associados à sua diversificação e contribuir para o refinamento da taxonomia do grupo. Esta tese está organizada em três capítulos. O primeiro capítulo é focado no gênero *Crossodactylodes*. Nesse capítulo, propusemos uma hipótese filogenética para o gênero, avaliamos a evolução de alguns caracteres fenotípicos e de história natural e realizamos uma revisão taxonômica, abordando ainda a distribuição geográfica, a história natural e a conservação das espécies. Esse capítulo foi publicado no periódico *Herpetological Monographs*. No segundo capítulo, aumentamos a amostragem gênica e taxonômica, incluindo diversos terminais dos quatro gêneros de Paratelmatobiinae e propusemos uma nova hipótese filogenética para a subfamília. Além disso, delimitamos linhagens evolutivamente independentes e estimamos os tempos dos eventos de diversificação

dentro da subfamília. Esse capítulo foi publicado no periódico *Molecular Phylogenetics and Evolution*. Por fim, no terceiro capítulo, publicado no periódico *Zootaxa*, formalizamos a descrição de uma nova espécie de *Paratelmatobius*.

## REFERÊNCIAS BIBLIOGRÁFICAS


Barata, I.M., Santos, M.T.T., Leite, F.S.F., Garcia, P.C.A. 2013. A new species of *Crossodactylodes* (Anura: Leptodactylidae) from Minas Gerais, Brazil: first record of genus within the Espinhaço Mountain Range. *Zootaxa*, 3731, 552–560.

Bonaparte, C.L.J.L. 1850. Conspectus Systematum. Herpetologiae et Amphibiologiae. Editio altera reformata. Lugdini Batavorum: E. J. Brill.

Caminer, M.A., Milá, B., Jansen, M., Fouquet, A., Venegas, P.J., Chávez, G., Lougheed, S.C., Ron, S.R. 2017. Systematics of the *Dendropsophus leucophyllatus* species complex (Anura: Hylidae): Cryptic diversity and the description of two new species. *PLoS ONE*, 12, e0171785.

Cochran, D.M. 1938. Diagnoses of new frogs from Brazil. *Proceedings of the Biological Society of Washington*, 51, 41–42.

Cochran, D.M. 1955. Frogs of Southeastern Brazil. *United States National Museum Bulletin*, 206, 1–423.

Cope, E.D. 1865. Sketch of the primary groups of Batrachia s. Salientia. *Natural History Review. New Series*, 5, 97–120.

Cope, E.D. 1866. On the structures and distribution of the genera of the arciferous Anura. *Journal of the Academy of Natural Sciences of Philadelphia*. *Series 2*, 6, 67–112.

Dubois, A. 2005. Amphibia Mundi. 1.1. An ergotaxonomy of recent amphibians. *Alytes*, 23, 1–24.

Dubois, A. 2013. Crossodactylodinae Fouquet, Blotto, Maronna, Verdade, Juncá, de Sá & Trefaut Rodrigues, 2013 is an invalid junior synonym of Paratelmatobiinae Ohler & Dubois, 2012 (Amphibia, Anura). *Zootaxa*, 3700, 499–500.

Duméril, A.M.C., Bibron, G. 1841. Erpétologie Générale ou Histoire Naturelle Complète des Reptiles. Volume 8. Paris: Librarie Enclyclopedique de Roret.

Fitzinger, L.J.F.J. 1826. Neue Classification der Reptilien nach ihren Natürlichen Verwandtschaften nebst einer Verwandtschafts-Tafel und einem Verzeichnisse der Reptilien-Sammlung des K.K. Zoologisch Museum's zu Wien. Wien: J. G. Heubner.

Fitzinger, L.J.F.J. 1843. Systema Reptilium. Fasciculus Primus. Wien: Braumüller et Seidel.

Fouquet, A., Blotto, B.L., Maronna, M.M., Verdade, V.K., Juncá, F.A., de Sá, R., Rodrigues, M.T. 2013. Unexpected phylogenetic positions of the genera *Rupirana* and *Crossodactylodes* reveal insights into the biogeography and reproductive evolution of leptodactylid frogs. *Molecular Phylogenetics and Evolution*, 67, 445–457.

Frost, D.R. 2020. Amphibian Species of the World: an online reference. Version 6.0. Electronic Database accessible at http://research.amnh.org/herpetology/amphibia/index.html. American Museum of Natural History, New York, USA. (acessado em 04 de março de 2020).

Frost, D.R., Grant, T., Faivovich, J., Bain, R., Haas, A., Haddad, C.F.B, de Sá, R.O., Donnellan, S. C., Raxworthy, C.J., Wilkinson, M., Channing, A., Campbell, J.A., Blotto, B.L., Moler, P., Drewes, R.C., Nussbaum, R.A., Lynch, J.D., Green, D., Wheeler, W.C. 2006. The amphibian tree of life. *Bulletin of the American Museum of Natural History*, 297, 1–370.

Gallardo, J.M. 1963. *Hydrolaetare*, nuevo genero de Leptodactylidae (Amphibia) neotropical. *Neotropica. La Plata*, 9, 42–48.

Grabowski, M., Wysocka, A., Mamos, T. 2017. Molecular species delimitation methods provide an insight in taxonomy of the endemic gammarid species flock from the ancient Lake Ohrid. *Zoological Journal of the Linnean Society*, 181, 272–285.

Heyer, W.R. 1969. Studies on the genus *Leptodactylus* (Amphibia, Leptodactylidae) III. A redefinition of the genus *Leptodactylus* and a description of a new genus of leptodactylid frogs. *Contributions in Science. Natural History Museum of Los Angeles County*, 155, 1–14.

Heyer, W.R. 1974. *Vanzolinius*, a new genus proposed for *Leptodactylus discodactylus* (Amphibia, Leptodactylidae). *Proceedings of the Biological Society of Washington*, 87, 81–90.

Heyer, W.R. 1975. A preliminary analysis of the intergeneric relationships of the frog family Leptodactylidae. *Smithsonian Contributions to Zoology*, 199, 1–55.

Heyer, W.R. 1999. A new genus and species of frog from Bahia, Brazil (Amphibia: Anura: Leptodactylidae) with comments on the zoogeography of the Brazilian campos rupestres. *Proceedings of the Biological Society of Washington*, 112, 19–30.

Jiménez de la Espada, M. 1870. Fauna neotropicalis species quaedam nondum cognitae. *Jornal de Sciências, Mathemáticas, Physicas e Naturaes*. *Lisboa*, 3, 57–65.

Jiménez de la Espada, M. 1872. Nuevos batráquios Americanos. *Anales de la Sociedad Española de Historia Natural. Madrid*, 1, 84–88.

Juncá, F.A., Lugli, L. 2009. Reproductive biology, vocalizations, and tadpole morphology of *Rupirana cardosoi*, an anuran with uncertain affinities. *South American Journal of Herpetology*, 4, 173–178.

Lees, A.C., Pimm, S.L. 2015. Species, extinct before we know them? *Current Biology*, 25, R177–R180.

Lourenço, L.B., Bacci-Junior, M., Martins, V.G., Recco-Pimentel, S.M., Haddad, C.F. 2008. Molecular phylogeny and karyotype differentiation in *Paratelmatobius* and *Scythrophrys* (Anura, Leptodactylidae). *Genetica*, 132, 255–266.

Lutz, B., Carvalho, A.L. 1958. Novos anfíbios anuros das Serras Costeiras do Brasil. *Memórias do Instituto Oswaldo Cruz. Rio de Janeiro*, 56, 239–249.

Lynch, J.D. 1971. Evolutionary relationships, osteology, and zoogeography of leptodactyloid frogs. *Miscellaneous Publication. Museum of Natural History, University of Kansas*, 53, 1–238.

Lynch, J.D. 1978. A re-assessment of the telmatobiine leptodactylid frogs of Patagónia. *Occasional Papers of the Museum of Natural History, University of Kansas*, 72, 1–57.

Miranda-Ribeiro, A. 1923. *Elosia*, Tsch. e os generos correlatos. *Revista do Museu Paulista. São Paulo*, 13, 813–821.

Miranda-Ribeiro, A. 1926. Notas para servirem ao estudo dos Gymnobatrachios (Anura) Brasileiros. *Arquivos do Museu Nacional. Rio de Janeiro*, 27, 1–227.

Ohler, A., Dubois, A. 2012. Validation of two familial nomina nuda of Amphibia Anura. *Alytes*, 28, 162–167.

Pyron, R.A., Wiens, J.J. 2011. A large-scale phylogeny of Amphibia including over 2800 species, and a revised classification of advanced frogs, salamanders, and caecilians. *Molecular Phylogenetics and Evolution*, 61, 543–583.

Ribeiro, M.C., Metzger, J.P., Martensen, A.C., Ponzoni, F.J., Hirota, M.M. 2009. The Brazilian Atlantic forest: how much is left, and how is the remaining forest distributed? Implications for conservation. *Biological Conservation*, 142, 1141–1153.

Silveira, F.A.O., Negreiros, D., Barbosa, N.P.U., Buisson, E., Carmo, F.F., Carstensen, D.W., Conceição, A.A., Cornelissen, T.G., Echternacht, L., Fernandes, G.W., Garcia, Q.S., Guerra, T.J., Jacobi, C.M., Lemos-Filho, J.P., Le Stradic, S., Morellato, L.P.C., Neves, F.S., Oliveira, R.S., Schaefer, C.E., Viana, P.L., Lambers, H. 2016. Ecology and

evolution of plant diversity in the endangered campo rupestre: a neglected conservation priority. *Plant Soil*, 403, 129–152.

Steindachner, F. 1863. Über einige neue Batrachier aus den Sammlungen des Wiener Museums. *Sitzungsberichte der Kaiserlichen Akademie der Wissenschaften, Mathematisch-Naturwissenschaftliche Classe*, 48, 186–192.

Steindachner, F. 1867. Reise der österreichischen Fregatte Novara um die Erde in den Jahren 1857, 1858, 1859 unter den Bafehlen des Commodore B. von Wüllerstorf-Urbair. Zologischer Theil. 1. Amphibien. Wien: K. K. Hof- und Staatsdruckerei.

Teixeira, M. Jr., Recoder, R.S, Amaro, R.C, Damasceno, R.P, Cassimiro, J., Rodrigues, M.T. 2013. A new *Crossodactylodes* Cochran, 1938 (Anura: Leptodactylidae: Paratelmatobiinae) from the highlands of the Atlantic Forests of southern Bahia, Brazil. *Zootaxa*, 3702, 459–472.

Tschudi, J.J. von. 1838. Classification der Batrachier mit Berücksichtigung der fossilen Thiere dieser Abtheilung der Reptilien. Neuchâtel: Petitpierre.

Werner, F. 1896. Beiträge zur Kenntniss der Reptilien und Batrachier von Centralamerika und Chile, sowie einiger seltenerer Schlangenarten. *Verhandlungen des Zoologisch-Botanischen Vereins in Wien*, 46, 344–365.

Wiens, J.J. 2007. Species delimitation: new approaches for discovering diversity. *Systematic Biology*, 56: 875–878.

# CAPÍTULO I

## Systematic Revision of the Rare Bromeligenous Genus *Crossodactylodes* Cochran, 1938

## (Anura: Leptodactylidae: Paratelmatobiinae)

*Herpetological Monographs*, 34, 2020, 1–38
© 2020 by The Herpetologists' League, Inc.

# Systematic Revision of the Rare Bromeligenous Genus *Crossodactylodes* Cochran 1938 (Anura: Leptodactylidae: Paratelmatobiinae)

Marcus Thadeu T. Santos[1,2,10], Rafael F. Magalhães[2,3], Rodrigo B. Ferreira[4], Stenio E. Vittorazzi[5], Iuri R. Dias[6], Felipe S. F. Leite[7], Luciana B. Lourenço[8], Fabrício R. Santos[2], Célio F. B. Haddad[1,9], and Paulo C. A. Garcia[2]

[1] Programa de Pós-graduação em Zoologia, Instituto de Biociências, Universidade Estadual Paulista (UNESP), Caixa Postal 199, 13506-900, Rio Claro, SP, Brazil
[2] Programa de Pós-graduação em Zoologia, Instituto de Ciências Biológicas, Departamento de Zoologia, Universidade Federal de Minas Gerais, 31270-901, Belo Horizonte, MG, Brazil
[3] Departamento de Ciências Naturais, Universidade Federal de São João del-Rei, 36301-160, São João del-Rei, MG, Brazil
[4] Projeto Bromeligenous, Instituto Marcos Daniel, 29090-160, Vitória, ES, Brazil
[5] Departamento de Ciências Biológicas, Universidade do Estado de Mato Grosso, 78300-000, Tangará da Serra, MT, Brazil
[6] Departamento de Ciências Biológicas, Universidade Estadual de Santa Cruz, 45662-900, Ilhéus, BA, Brazil
[7] Sagarana Lab, Instituto de Ciências Biológicas e da Saúde, Universidade Federal de Viçosa, Campus Florestal, 35690-000, Florestal, MG, Brazil
[8] Departamento de Biologia Estrutural e Funcional, Instituto de Biologia, Universidade Estadual de Campinas, 13083-863, Campinas, SP, Brazil
[9] Universidade Estadual Paulista (UNESP), Instituto de Biociências, Departamento de Biodiversidade e Centro de Aquicultura (CAUNESP), Caixa Postal 199, 13506-900, Rio Claro, SP, Brazil

Abstract: *Crossodactylodes* is a poorly known genus of small-sized bromeligenous frogs, endemic to Brazil. They have a patchy distribution across the mountains of the Atlantic Forest and the "campo rupestre" ecosystem. To better resolve their evolutionary relationships, we performed phylogenetic analyses using a multigene DNA matrix and representative sampling within the genus. We then evaluated the evolution of phenotypical and natural history traits with the inferred phylogeny. We recovered *Crossodactylodes* as monophyletic, diagnosed by seven putative synapomorphies in morphological and natural history characters. Evidence supports some morphological synapomorphies as adaptations to the bromeligenous habit. We found high genetic distances among closely distributed lineages within *C. bokermanni* and *C. izecksohni*. Some of these lineages might represent undescribed cryptic species. We provide detailed accounts for each species including data on their geographic range, conservation, and natural history. All species of *Crossodactylodes* occur in highly threatened environments, are restricted to very small geographic ranges, and probably have limited dispersal capacity due to their small body size and dependence on bromeliads. These factors emphasize the need for habitat protection to safeguard species viability.

**Key words:** Atlantic Forest; Campo rupestre; Character evolution; Endemism; Molecular phylogenetics; Taxonomic revision

The Brazilian anuran fauna is the richest in the world, with more than 1090 species within 105 genera and 20 families (Segalla et al. 2019). This is likely still an underestimation, given that 262 new species were described between 2004 and 2016 (Tapley et al. 2018). The Atlantic Forest contributes greatly to this number, harboring 625 species, most of which are endemic to the domain (Rossa-Feres et al. 2017). This high richness and endemism within the Atlantic Forest might be due to the wide latitudinal range, variable climatic gradient, presence of distinct ecoregions, high topographical complexity, and intense sampling effort (Vasconcelos et al. 2014; Rodríguez et al. 2015; Oliveira et al. 2016). Even with high sampling efforts along the Atlantic Forest, several new species of anurans are still described every year (e.g., Bornschein et al. 2015; Forlani et al. 2017; Taucce et al. 2018; Carvalho et al. 2019). Factors such as the many remote and still-unsampled areas, limited geographical range, and low abundance of some species, cryptic habits, and the difficulty to differentiate some species from related congeners can explain the high rate of new descriptions (Pimm et al. 2014; Costello et al. 2015).

Although the description of new species is an important step to overcome knowledge gaps on biodiversity, decreasing the Linnean shortfall (see Hortal et al. 2015), this is only a small fraction of the biological complexity of the organisms and their interaction networks. Beyond the recognition of species, there are shortfalls related to the geographic distributions, evolution, and biotic interactions (i.e., Wallacean, Darwinian, and Eltonian shortfalls, respectively; Hortal et al. 2015). Overcoming these shortfalls is especially important for species that are rare, geographically constrained, and habitat-specialized because they are more prone to be threatened (Pimm et al. 2014; Toledo et al. 2014). In the Brazilian Atlantic Forest, a high proportion of the anuran species have these characteristics (Haddad et al. 2013; Villalobos et al. 2013; Toledo et al. 2014). Therefore, comprehensive studies addressing these taxa are crucial for a better understanding of their life history traits and an accurate evaluation of their conservation status.

Among the endemic and habitat-specialized anurans of Atlantic Forest, the leptodactylid genus *Crossodactylodes* Cochran 1938 clearly illustrates the aforementioned biological shortfalls. It currently comprises five bromeligenous species (i.e., life cycle in some way dependent on bromeliads; Peixoto 1995): *C. pintoi* Cochran 1938; *C. bokermanni* Peixoto 1983 "1982"; *C. izecksohni* Peixoto 1983 "1982"; *C. septentrionalis* Teixeira, Recoder, Amaro, Damasceno, Cassimiro, and Rodrigues 2013; and *C. itambe* Barata, Santos, Leite, and Garcia 2013. Four species inhabit montane regions of Atlantic Forest across the Brazilian states of Bahia, Espírito Santo, and Rio de Janeiro (Cochran 1938; Peixoto 1983; Teixeira et al. 2013). A single species inhabits a transitional zone between Atlantic Forest and Cerrado in the "campo rupestre" ecosystem (rupestrian grasslands; Silveira

[10] Correspondence: email, mthadeusantos@gmail.com



Downloaded From: https://bioone.org/journals/Herpetological-Monographs on 20 May 2020
Terms of Use: https://bioone.org/terms-of-use Access provided by Universidade Estadual Paulista Julio de Mesquita Filho (UNESP)

et al. 2016) of the Espinhaço Mountain Range in the state of Minas Gerais, Brazil (Barata et al. 2013). All species are narrow-range endemics, mostly known from only the type locality (Frost 2019). The recent species discoveries after more than 3 decades without new descriptions (i.e., *C. itambe* and *C. septentrionalis*; Barata et al. 2013 and Teixeira et al. 2013, respectively), as well as the record of the genus in an unexpected environment (i.e., campo rupestre; Barata et al. 2013), could indicate that the richness and geographic range of *Crossodactylodes* are underestimated. The small body size, the strict association to bromeliads, the occurrence in remote areas, and the lack of knowledge on vocalization (Barata et al. 2013; Teixeira et al. 2013) hamper further study of the genus and location of unknown populations.

Taxonomic studies on *Crossodactylodes* began with Cochran (1938), who proposed it to allocate *C. pintoi* based on distinct morphological traits compared to other genera of Leptodactylidae Werner 1896. Originally, Cochran (1938) briefly diagnosed the species. Decades later, Cochran (1955) complemented the description and suggested that *Crossodactylodes* is closely related to the genus *Crossodactylus* Duméril and Bibron 1841 (Hylodidae) based on the presence of spines on the inner surface of the first finger set in a round mass, similarity of the tooth development, and bilobed appearance of toe when dried.

Lynch (1971) provided a more complete diagnosis of *Crossodactylodes*, mainly based on characters of skull osteology. Lynch's diagnosis differs from that of Cochran (1955) due to Y-shaped terminal phalanges (T-shaped in Cochran 1955) and an absent tympanum (hidden in Cochran 1955). Lynch (1971) suggested that *Crossodactylodes* is closely related to *Cycloramphus* Tschudi 1838 and *Zachaenus* Cope 1866 due to similarity in the architecture of the temporal region and size of the roofing bones. Therefore, Lynch (1971) placed *Crossodactylodes* into the Grypiscini tribe of Leptodactylidae. Lynch (1971) also mentioned the oviposition of a few large eggs attached to bromeliads for *Crossodactylodes*.

Following Lynch's work, Heyer (1975) proposed an informal unit named "grypiscines" to allocate *Crossodactylodes*, *Cycloramphus*, *Zachaenus*, *Craspedoglossa* Müller 1922 (later synonymized to *Cycloramphus*), *Crossodactylus*, *Hylodes* Fitzinger 1826, *Megaelosia* Miranda-Ribeiro 1923, *Thoropa* Cope 1865, *Paratelmatobius* Lutz and Carvalho 1958, and *Scythrophrys* Lynch 1971. Dubois (2005) made minor adjustments and formalized the arrangement proposed by Heyer (1975) including *Crossodactylodes* in Leptodactylidae, subfamily Cycloramphinae, along with *Cycloramphus*, *Zachaenus*, *Rupirana* Heyer 1999, *Paratelmatobius*, *Scythrophrys*, and *Thoropa*. The genera *Crossodactylus*, *Hylodes*, and *Megaelosia* were transferred to the subfamily Hylodinae (Dubois 2005).

The first molecular phylogenetic studies with extensive taxonomic sampling on amphibians resulted in substantial modifications on the anuran classification (Frost et al. 2006; Pyron and Wiens 2011). However, these studies did not include *Crossodactylodes* in the analyses. Thus, Frost et al. (2006) classified the genus in the tribe Cycloramphini, family Cycloramphidae, based on the phylogenetic placement found for its putative relatives according to Lynch (1971), while Pyron and Wiens (2011) left *Crossodactylodes* as an incertae sedis genus within Hyloidea. Fouquet et al. (2013) were the first authors to include *Crossodactylodes* in an extensive molecular phylogenetic analysis and the genus was unambiguously grouped with *Rupirana*, *Paratelmatobius*, and *Scythrophrys* within Leptodactylidae. For this clade, Fouquet et al. (2013) proposed the new subfamily Crossodactylodinae, which is a junior synonym of Paratelmatobiinae Ohler and Dubois 2012 (Dubois 2013). Further, Teixeira et al. (2013) provided the first phylogenetic arrangement within *Crossodactylodes* and included the three formally recognized species for which tissue samples were available (*C. bokermanni*, *C. izecksohni*, and *C. septentrionalis*).

Although there are recent contributions on phylogenetic relationships of *Crossodactylodes* (Fouquet et al. 2013; Teixeira et al. 2013), the phylogenetic placement of *C. itambe* remains unknown. This information has implications for the diversification pattern of the genus, as it is the only species that occurs in the campo rupestre. Moreover, the knowledge about behavior, geographical distribution, and evolution of morphological characters is limited for the genus. The diagnosis of *Crossodactylodes* was based solely on its type species (*C. pintoi*; Cochran 1938, 1955; Lynch 1971), and the morphological variation within the genus is poorly understood because the earliest species descriptions (*C. pintoi*, *C. bokermanni*, and *C. izecksohni*) are hardly comparable to the more recent ones (*C. septentrionalis* and *C. itambe*). In addition, *C. septentrionalis* was described based solely on one female specimen (Teixeira et al. 2013) and thus some morphological characters observed in males, which are commonly used in the taxonomy of the genus, have not been evaluated for this species.

In this study, we provide phylogenetic analyses of a matrix composed of mitochondrial (mtDNA) and nuclear (nDNA) gene fragments, including for the first time specimens of *Crossodactylodes itambe* and increasing the sampling within *C. bokermanni*, *C. izecksohni*, and *C. septentrionalis*. We also evaluate the evolution of several phenotypic and natural history traits and provide a systematic revision of *Crossodactylodes*, with updated diagnoses for the genus, comparing it with the other genera of Paratelmatobiinae. We redescribe *C. pintoi*, *C. bokermanni*, and *C. izecksohni* to enhance comparisons and offer the first assessment of male morphological characters for *C. septentrionalis*. Lastly, we provide detailed accounts for each species including data on geographic range, natural history, and conservation. Our main goal is to afford an extensive taxonomic framework for *Crossodactylodes*, which can benefit future species descriptions and contribute to the overcoming of Wallacean, Darwinian, and Eltonian shortfalls regarding these poorly known bromeligenous anurans.

## Materials and Methods

### Phylogenetics and Character Evolution

**Taxon and genetic sampling.**—As an ingroup, we included specimens of four of the five species of *Crossodactylodes*. The missing species, *C. pintoi*, is known only from its type series and has not been recorded since 1909 (Peixoto and Carvalho-e-Silva 2004). We included for the first time specimens of *C. itambe* and increased the sampling within *C. septentrionalis*, *C. bokermanni*, and *C. izecksohni*. For the last two species, we included specimens from

Downloaded From: https://bioone.org/journals/Herpetological-Monographs on 20 May 2020
Terms of Use: https://bioone.org/terms-of-use Access provided by Universidade Estadual Paulista Julio de Mesquita Filho (UNESP)

localities not included in previous analyses (Fouquet et al. 2013; Teixeira et al. 2013). Outgroups were selected based on the results of Pyron and Wiens (2011), Fouquet et al. (2013), Teixeira et al. (2013), and Pyron (2014). We broadly sampled the other Paratelmatobiinae genera, with three of the seven species of *Paratelmatobius* (*P. cardosoi* Pombal and Haddad 1999, *P. gaigeae* [Cochran 1938], and *P. poecilogaster* Giaretta and Castanho 1990) and three specimens for each of the two monotypic genera *Scythrophrys* and *Rupirana*. We also sampled genera of the other two subfamilies of Leptodactylidae: *Pleurodema* Tschudi 1838 and *Physalaemus* Fitzinger 1826 for Leiuperinae and *Adenomera* Steindachner 1867 and *Leptodactylus* Fitzinger 1826 for Leptodactylinae. We used an allophrynid, *Allophryne ruthveni* Gaige 1926, to root the trees due to its close relationship with Leptodactylidae (Pyron and Wiens 2011; Pyron 2014).

Our matrix included sequences for six genes. Noncoding mtDNA gene sequences produced for this study include gene fragments of the heavy strand transcription unit 1 (H1: 12S and 16S rRNA genes, plus the intervening tRNA valine gene). Protein-coding mtDNA gene sequences included fragments of cytochrome oxidase subunit I (COI), and cytochrome b (cytb). The nDNA protein-coding gene sequences included fragments of proopiomelanocortin A (POMC), recombination-activating protein 1 (RAG-1), and tyrosinase (Tyr). Our sampling was complemented with GenBank sequences. GenBank accession numbers are listed in Appendix I.

**DNA amplification and sequencing.**—We extracted genomic DNA from ethanol-preserved tissues using standard phenol-chloroform extraction protocols (Sambrook and Russel 2001). For all the amplifications, the polymerase chain reaction program included an initial denaturing step of 60 s at 94°C followed by 35 cycles of amplification (94°C for 30 s; variable annealing temperatures and times, Appendix II; and 72°C for 60 s for extension), with a final extension step at 72°C for 7 min. Amplifications were performed in a 15-µL volume reaction containing: 20 ng of genomic DNA, 1× buffer, 2.5 mM $MgCl_2$, 1.25 µM each primer, 3 mM dNTPs, 0.72 µg bovine serum albumin, and 0.625 U Platinum Taq DNA polymerase (Thermo Fisher Scientific). Primers are listed in Appendix II. The amplification products were cleaned using polyethylene glycol 20% protocol with modifications (Sambrook and Russel 2001; Santos et al. 2015) and sequenced using fluorescent dye-labelled terminators (ABI Prism BigDye™ Terminators v1.1 cycle sequencing kit; Applied Biosystems) with an ABI 3130XL (Applied Biosystems). All sequences were made in both directions to check for potential errors and confirm heterozygous nucleotide position. Chromatograms obtained from the automated sequencer were read and assembled using the sequence editing software SeqScape (v2.6, Thermo Fisher Scientific Inc.).

**Phylogenetic analyses and genetic distance.**—We performed a multiple sequence alignment for each fragment with MAFFT v7.394 (Katoh and Standley 2013) using the MAFFT online service (Katoh et al. 2019). We used the G-INS-i algorithm and default transition/transversion cost ratio and gap opening penalty, with minor adjustments by eye for H1. For the Bayesian analysis, we selected the optimal partition scheme and nucleotide substitution models for each data block in PartitionFinder v2.1.1 (Lanfear et al. 2017) under the linked model of branch lengths and greedy search algorithm. For this, we defined 18 a priori partitions, including the 12S rRNA, the tRNA valine, the 16S rRNA genes, and the first, second, and third codon positions of COI, cytb, POMC, RAG-1, and Tyr separately. The analysis was repeated to check congruence in results and the best model was selected through Bayesian Information Criterion (BIC). We performed the Bayesian phylogenetic inference analysis using MrBayes v3.2.6. (Ronquist et al. 2012) implemented in online CIPRES Science gateway portal (Miller et al. 2010). For this analysis, we made two parallel runs, using eight chains (seven heated and one cold) with $5 \times 10^7$ generations each. The runs were summarized in a 50% majority rule consensus tree after a discarded burn-in of 25% first trees. Convergence and minimal effective sample sizes (ESS > 200) of all parameters were verified in Tracer v1.6 (Rambaut et al. 2014).

For the most-parsimonious trees reconstruction we used TNT v1.5 (Goloboff and Catalano 2016), applying equal weights to all transformations and considering gaps as a fifth state. Searches were conducted using the traditional search option consisting of 1000 random addition sequences followed by tree bisection and reconnection swapping and holding a maximum of 100 trees each step. The optimal trees obtained were submitted to an additional round of tree bisection and reconnection swapping. Parsimony jackknife absolute frequencies (Farris et al. 1996) were estimated using a traditional search, with 1000 resampling iterations.

For comparative purposes, we estimated mtDNA uncorrected *p*-distances inside and between the monophyletic and geographically structured lineages found in the phylogenetic reconstructions. For this we used concatenated mtDNA fragments and each of the fragments separately (COI, cytb, and H1). We also computed the distances for the 16S rRNA gene fragment limited by the primers 16SAR and 16SBR (Palumbi et al. 1991), which is commonly used for genetic distances calculations in anurans (Fouquet et al. 2007). The distances were estimated in MEGA v7.0 (Kumar et al. 2016). This analysis was made to highlight putative cryptic species or deep conspecific lineages within *Crossodactylodes*.

**Character evolution analysis.**—We assembled a discrete matrix composed of 30 morphological and natural history characters (Appendices III, IV) using Mesquite v3.2 (Maddison and Maddison 2017). Then, we optimized unambiguous characters in a simplified tree of the Paratelmatobiinae clade derived from our previous analyses using WinClada v1.00.08 (Nixon 2002). This simplification was made by collapsing multiple individuals from a single species or lineage into a single branch. In this case, variation in characters within each branch was treated as a multistate character. This analysis was made to show putative synapomorphies of each node emphasizing *Crossodactylodes*. Data were obtained through direct examination of specimens (see Referred specimens sections and Appendix V) or from literature in the absence of primary data. All characters were equally weighted without any ordering. We also included the morphometric character foot length, which is represented by the ratio foot length:snout–vent length (SVL; Appendices III, IV). This character was optimized as a continuous character. For this, we reconstructed ancestral states using the Trace Character History and Reconstruct

Downloaded From: https://bioone.org/journals/Herpetological-Monographs on 20 May 2020
Terms of Use: https://bioone.org/terms-of-use Access provided by Universidade Estadual Paulista Julio de Mesquita Filho (UNESP)

Ancestral States modules from Mesquite v3.2 (Maddison and Maddison 2017) under a squared-change parsimony model. We obtained the measurements for other Paratelmatobiinae from literature when individual values were available or through direct examination when only the means were provided in the literature (Appendix V).

**Phylogenetic placement of *Crossodactylodes pintoi*.**—We also used the discrete matrix, supplemented with the DNA sequences matrix, to perform a total evidence analysis in TNT v1.5 (Goloboff and Catalano 2016). This analysis was made to provide a phylogenetic placement for *C. pintoi*, for which DNA sequences were unavailable. For this, we used a single terminal per species or lineage and rooted the analysis in *Rupirana cardosoi*. The optimal trees and parsimony jackknife absolute frequencies (1000 resampling iterations) were obtained using implicit enumeration.

### Taxonomic Analyses

All collected specimens were euthanized in 5% lidocaine solution, fixed in 10% commercial grade formalin, and preserved in 70% ethanol. All geographic coordinates are in the system datum WGS84. Museum acronyms follow Sabaj (2016), except by MZUESC, which stands for Museu de Zoologia of the Universidade Estadual de Santa Cruz, Ilhéus, Bahia, Brazil. We examined types of all species of *Crossodactylodes*. For comparative purposes, we examined representatives of each genus of Paratelmatobiinae (Appendix V).

We analyzed external qualitative and morphometric characters. Terminology for external qualitative characters follows Duellman (1970), Heyer et al. (1990), and Duellman and Lehr (2009). To the nearest 0.1 mm with a digital caliper under a stereomicroscope, we measured SVL (from the tip of snout to the posterior margin of the vent), head length (from the tip of snout to the angle of the jaw), head width (between the angles of the jaws), arm length (from the anterior insertion of the arm to the elbow), arm width (greatest width), forearm length (from the elbow to the proximal edge of the inner metacarpal tubercle), forearm width (greatest width), hand length (from the proximal edge of the inner metacarpal tubercle to the tip of the third finger), thigh length (from the posterior margin of the vent to the outer edge of the knee), tibia length (from the outer edge of the knee to the outer edge of the heel), tarsal length (from the outer edge of the heel to the inner metatarsal tubercle), foot length (from the proximal edge of the inner metatarsal tubercle to the tip of the fourth toe). We used ImageTool v3.0 (Wilcox et al. 1996) to take measurements to the nearest 0.1 mm for eye diameter (between the anterior and posterior margins of the eye), interorbital distance (between the anterior margins of the eyes), eye–nostril distance (from the anterior corner of the eye to the posterior margin of the nostril), nostril–snout distance (from the posterior margin of the nostril to the tip of snout), internarial distance (between the inner margins of the nostrils), third finger disc diameter (greatest horizontal distance between the outer edges of the third finger disk), and fourth toe disc diameter (greatest horizontal distance between the outer edges of the fourth toe disk). For details of this method, see Barata et al. (2013). For one specimen of *C. pintoi* (MCZ 25707), we only measured SVL from a scaled photograph. All measurements were taken by MTTS.

Descriptions of coloration in life are based on field observations and photographs. Sex was determined by observation of gonads or secondary sexual characters (arm and forearm hypertrophy and nuptial pads on males). Variations are based on adult specimens. To verify the presence of tympanic annulus concealed by the skin and internal vocal sac, we made dissections in the skin on the lateral side of the head and on the gular region of some specimens (*Crossodactylodes bokermanni*: UFMG 13769, 14198; *C. itambe*: UFMG 14031, 14037; *C. izecksohni*: UFMG 14174, 14178, 14182, 14219). To verify the size of the zygomatic process of squamosal, and if a columella was present in *C. itambe*, we cleared and double-stained two specimens (UFMG 14033, 14034) with alizarin red and alcian blue following the protocol of Taylor and Van Dyke (1985). Due to the poor preservation of coloration in the specimens of *C. pintoi*, we did not consider characters related to color pattern in its diagnosis and comparisons with congeners. Terminology for egg morphology and ovipositional mode follow Altig and McDiarmid (2007).

For *Crossodactylodes pintoi*, *C. bokermanni*, and *C. izecksohni* we provided redescriptions of the holotypes because the original descriptions were hardly comparable to the more-recent descriptions. For *C. septentrionalis* and *C. itambe*, we provided new diagnoses, comparisons, and additional information on morphological variation.

### Conservation Accounts

We provided relevant data on geographic distribution, habitat, and potential threats for the species of *Crossodactylodes* following the suggestion of Tapley et al. (2018). For this, we calculated the extent of occurrence for the species known from more than two occurrence points (*C. bokermanni* and C. *izecksohni*). First, we generated minimum convex polygons using ArcGis (v10.0, ESRI Inc., Redlands, CA), following the International Union for Conservation of Nature (IUCN 2019) guidelines. Then, we calculated: (1) the area above 700 m elevation within the extent of occurrence, as the lower elevation limit known for these species is approximately 800 m; (2) the area of forest remnants within the extent of occurrence which is above this elevational limit, as these species occur only in forested areas; and (3) the percentage of protected areas present in the extent of occurrence. Spatial data on the protected areas were obtained from Instituto Chico Mendes de Conservação da Biodiversidade (ICMBio 2017); forest remnants data were obtained from SOS Mata Atlântica and Instituto Nacional de Pesquisas Espaciais (2018); and elevation shapefile was obtained from the Topodata project (Valeriano and Rossetti 2012). For species known only for localities in the same grid size of 2 km (i.e., a cell area of 4 $km^2$), the area of occupancy was considered equivalent to this cell, as recommended by the IUCN (2019). We then provided conservation assessments for each species of *Crossodactylodes*, applying the IUCN (2019) criteria.

## Results

### Phylogenetics and Character Evolution Analyses

Our final alignment comprised 5351 characters, with 23% of missing data, mainly in H1. The BIC in Partition Finder selected six subsets as the best partition scheme, BIC =

Downloaded From: https://bioone.org/journals/Herpetological-Monographs on 20 May 2020
Terms of Use: https://bioone.org/terms-of-use Access provided by Universidade Estadual Paulista Julio de Mesquita Filho (UNESP)

61,899.638: SYM + I + G for COI and cytb first positions; HKY + I for COI and cytb second positions; GTR + G for COI and cytb third positions; GTR + I + G for 12S rRNA, 16S rRNA, and tRNA valine genes; and two independent partitions of HKY + G for first and second positions and for third positions of nDNA fragments (POMC, RAG-1, and Tyr).

The Bayesian and parsimony phylogenetic inference analyses result in the same general topology, varying only on internal relationships among terminals within species or at intraspecific lineage level (Fig. 1). The parsimony analysis resulted in 45 trees with 5780 steps (strict consensus in Fig. S1). The analyses recovered *Crossodactylodes* as an unambiguously supported monophyletic group (100% Bayesian posterior probability and parsimony jackknife; Fig 1), diagnosed by seven putative synapomorphies in morphological and natural history characters (see genus diagnosis section; Fig. 2; Appendices III, IV). *Paratelmatobius* is strongly supported as the sister taxon of *Crossodactylodes* (99% Bayesian posterior probability; 97% parsimony jackknife; Fig. 1) and the clade containing these genera is diagnosed by one putative morphological synapomorphy (absence of tarsal fold; Fig. 2; Appendices III, IV). Within the other Paratelmatobiinae, *Scythrophrys* was unambiguously supported as the sister taxon of *Crossodactylodes* plus *Paratelmatobius* (100% Bayesian posterior probability and parsimony jackknife) and *Rupirana* was recovered as the earliest diverging genus (Fig. 1). The clade which shows *Rupirana* as the sister taxon of the other Paratelmatobiinae is unambiguously supported in the Bayesian analysis (100% posterior probability) but poorly supported in the parsimony analysis (46% jackknife frequency). Within the remaining outgroups, the two genera representing the subfamily Leptodactylinae (*Adenomera* and *Leptodactylus*) form the sister taxon of Paratelmatobiinae (Fig. 1).

Within *Crossodactylodes*, both analyses recovered *C. bokermanni* as the sister taxon of the remaining species (Fig. 1). The clade composed by *C. izecksohni*, *C. itambe*, and *C. septentrionalis* is diagnosed by three putative morphological synapomorphies (absence of vocal slit, absence of dorsolateral fold, and skin texture of males coarsely granular; Fig. 2; Appendices III, IV). In this clade, *C. izecksohni* (diagnosed by one putative morphological autapomorphy: iris coloration in life yellowish with dark brown reticulations, interrupted by a brown horizontal bar at the pupil level) is recovered as the sister taxon of *C. itambe* plus *C. septentrionalis* (Figs. 1, 2; Appendices III, IV). The clade containing these two species is diagnosed by one putative morphological synapomorphy (zygomatic process of squamosal bone long, passing the anterior margin of the optic foramen; Fig. 2; Appendices III, IV). Moreover, *C. itambe* is diagnosed by two putative morphological autapomorphies (presence of an anterior projection in medial region of the upper lip and iris coloration in life uniformly black or brownish black; Fig. 2; Appendices III, IV) while *C. septentrionalis* is supported by one putative autapomorphy (disc of Finger I acute, i.e., no apparent disc; Fig. 2; Appendices III, IV). The total evidence analysis resulted in three trees with 3052 steps (strict consensus in Fig. S2) and recovered *C. pintoi* in a clade together with *C. itambe*, *C. septentrionalis*, and *C. izecksohni* (97% jackknife frequency). However, the relationships among terminals within this clade were not fully resolved.

The uncorrected *p*-distances among recognized species of *Crossodactylodes* vary from 7.8% to 11.4% for the concatenated mtDNA fragments and from 3.2% to 7.9% for the 16S rRNA fragment (Table 1). For COI, cytb, and H1 the distances vary from 11.3% to 17.3%, 11.2% to 16.0%, and 5.2% to 9.2%, respectively (Appendices VI, VII).

Within *Crossodactylodes bokermanni*, the analyses recovered three well-supported clades, exclusives of different localities in the state of Espírito Santo: a lineage from Estação Biológica de Santa Lúcia, municipality of Santa Teresa (Lineage A); a lineage from Parque Estadual do Forno Grande, municipality of Castelo (Lineage B); and a lineage from Penha district, municipality of Santa Teresa, vicinities of the type locality (Lineage C). The Lineage C forms the sister group of Lineage A plus Lineage B (Fig. 1). The uncorrected *p*-distances among these lineages vary from 2.6% to 5.4% for the concatenated mtDNA and from 0.7% to 4.3% for the 16S rRNA fragment (Table 1). For COI, cytb, and H1, the distances vary from 5.0% to 9.3%, 4.6% to 9.0%, and 1.3% to 3.5%, respectively (Appendices VI, VII). None of the morphological and natural history characters of our matrix supported these lineages (Fig. 2; Appendices III, IV). Moreover, these lineages are not distinguishable on the basis of morphological characters analyzed for the taxonomic descriptions.

Within *Crossodactylodes izecksohni*, two well-supported and nonsympatric clades are recovered: a lineage from four different localities in the municipality of Santa Teresa, vicinities of the type locality (Lineage A), and a lineage from Estação Biológica de Santa Lúcia, also in the municipality of Santa Teresa (Lineage B). The range of uncorrected *p*-distances between the lineages is 5.3–5.4% for the concatenated mtDNA and 3.5–4.3% for the 16S rRNA fragment (Table 1). For COI, cytb, and H1, the ranges are 6.0–6.8%, 7.7–8.9%, and 3.8–3.9%, respectively (Appendices VI, VII). None of the morphological and natural history characters of our matrix supported these lineages (Fig. 2; Appendices III, IV). In addition, these lineages do not differ on the basis of morphological characters analyzed for the taxonomic descriptions.

## Taxonomic Accounts

### *Crossodactylodes* Cochran

*Crossodactylodes* Cochran 1938: Cochran 1938:41–42.

**Type species.**—*Crossodactylodes pintoi* Cochran 1938, by monotypy.

**Diagnosis.**—*Crossodactylodes* can be distinguished and diagnosed from the other genera of Paratelmatobiinae by the following combination of characters: (1) nuptial pads of males formed by few (less than 20) and well-developed keratinized spines; (2) discs of fingers II–IV expanded (i.e., more dilated than the base); (3) toes II–V lacking lateral ridges, fringes, or webs; (4) cloacal flap conspicuous (i.e., with long free distal portion); (5) reproductive mode 6 (i.e., eggs and exotrophic tadpoles in water in aerial plants; Haddad and Prado 2005); (6) deposition of single eggs, positioned isolated from other eggs; (7) tympanic middle ear (i.e., tympanic membrane, tympanic annulus, and columella; see Pereyra et al. 2016) completely lacking; (8) absence of

Downloaded From: https://bioone.org/journals/Herpetological-Monographs on 20 May 2020
Terms of Use: https://bioone.org/terms-of-use Access provided by Universidade Estadual Paulista Julio de Mesquita Filho (UNESP)

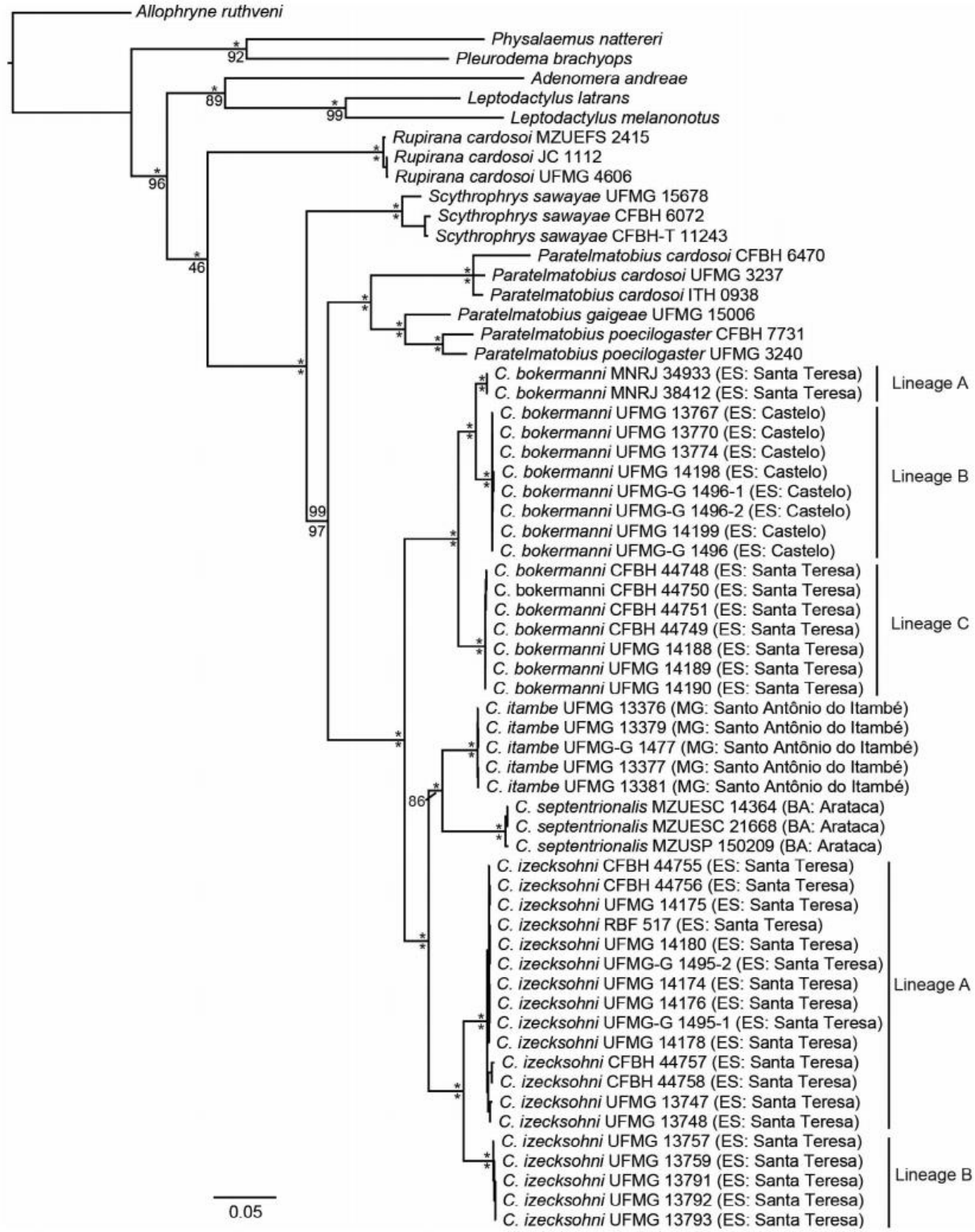


FIG. 1.—The 50% majority rule consensus tree from Bayesian phylogenetic inference of concatenated mtDNA (H1, COI, cytb) and nDNA (POMC, RAG-1, tyr) genes. Values above branches indicate posterior probabilities proportions and those under branches are jackknife proportions achieved in the parsimony analysis of the same matrix, which resulted in the same general topology (strict consensus available in Fig. S1). Asterisks indicate 100% values.

Downloaded From: https://bioone.org/journals/Herpetological-Monographs on 20 May 2020
Terms of Use: https://bioone.org/terms-of-use Access provided by Universidade Estadual Paulista Julio de Mesquita Filho (UNESP)

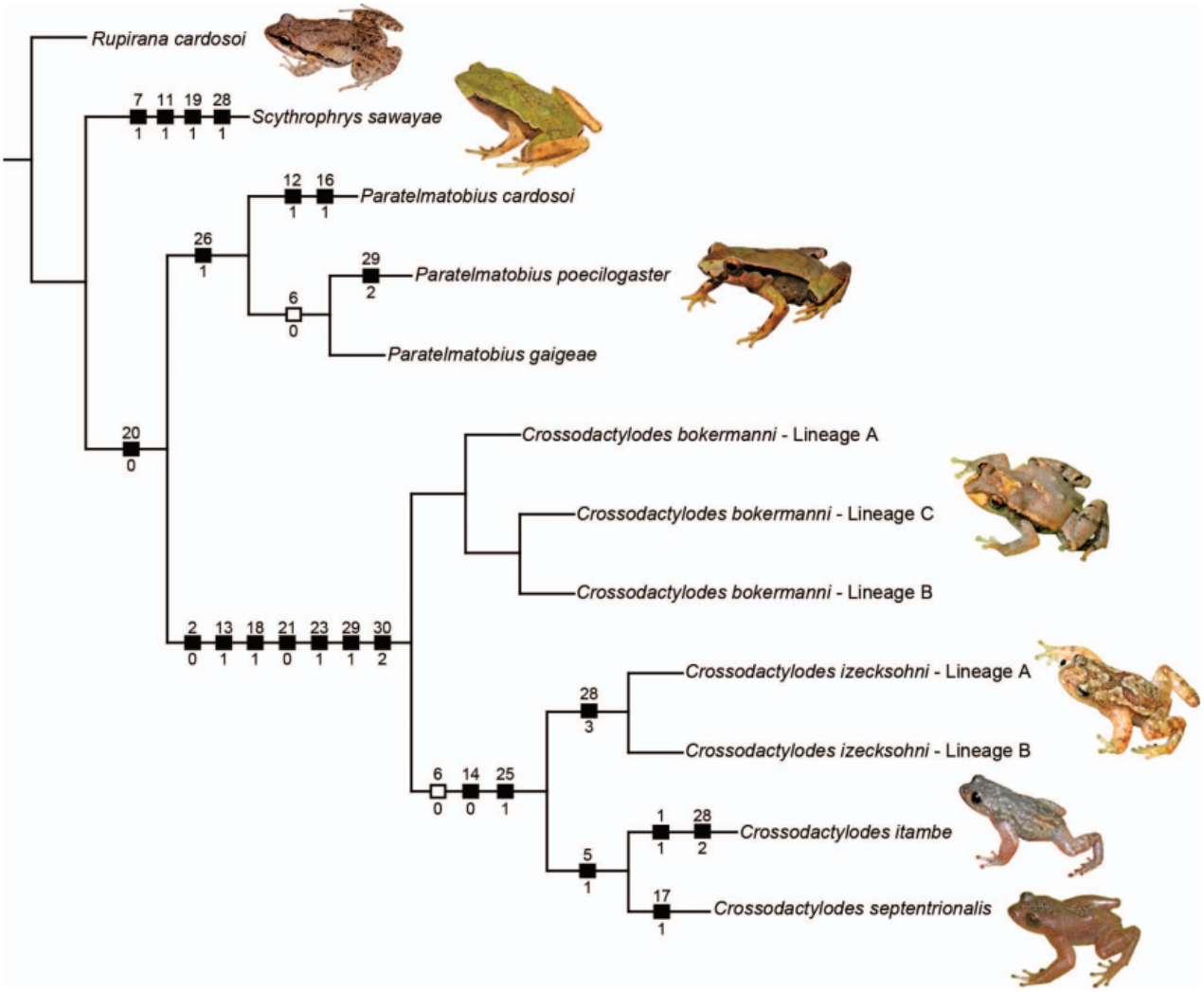


FIG. 2.—A simplified phylogenetic tree of Paratelmatobiinae showing optimization of unambiguous morphological and natural history characters (see Appendices III, IV). For each node the list of the unambiguous synapomorphies is given and each synapomorphy is represented by a black square (nonhomoplasic synapomorphy) or a white square (homoplasic synapomorphy). The upper numbers indicate the character number and the lower numbers their respective states. A color version of this figure is available online.

tarsal fold; (9) in life, ventral surfaces of arm lacking bright and contrasting coloration; (10) males lacking white tubercles on dorsum; (11) SVL 10.8–18.6 mm; (12) foot length/SVL 0.31–0.41; (13) snout rounded to truncate in dorsal view; (14) vocal sac absent, or externally indistinct; (15) tubercles on upper eyelid rounded or absent; (16) absence of a small meniscus on the upper iris; (17) absence of a tubercle on outer margin of heel; (18) in life, ventral surfaces of belly lacking bright and contrasting coloration. The characters 1–7 are putative synapomorphies of *Crossodactylodes* (Characters 2, 13, 18, 21, 23, 29, and 30 in Fig. 2 and Appendices III, IV).

**Comparison with other genera of Paratelmatobiinae.**—*Crossodactylodes* can be distinguished from all other genera of Paratelmatobiinae (characters in parentheses) by having nuptial pads of males formed by few (less than 20) and well-developed spines; Fig. 3A (nuptial pads lacking spines or spicules in *Paratelmatobius lutzii*, and formed by numerous (more than 20) small spicules in all remaining species of Paratelmatobiinae; Fig. 3B); discs of fingers II–IV expanded, i.e., more dilated than the base; Fig. 3C (narrow, i.e., same width or less dilated than the base in the other genera; Figs. 3D–F); toes II–V lacking lateral ridges, fringes, or webs; Fig. 3G (with lateral ridges in *Rupirana* and *Scythrophrys*, Figs. 3J, K; with well-developed webs in *P. lutzii*, Fig. 3I; and with well-developed flexible fringes in other species of *Paratelmatobius*, Fig. 3H); cloacal flap conspicuous, i.e., with long free distal portion; Fig. 4A (inconspicuous, i.e., with short free distal portion in the other genera; Figs. 4B, C); reproductive mode 6 sensu Haddad and Prado (2005), with eggs and exotrophic tadpoles associated to bromeliads (mode 18, eggs on rock above water, exotrophic tadpoles move to water) in *P. poecilogater* (mode 1, eggs and exotrophic tadpoles in lentic water) in other species of Paratelmatobiinae (Garcia 1996; Haddad and Prado 2005; Juncá and Lugli 2009); and deposition of

Downloaded From: https://bioone.org/journals/Herpetological-Monographs on 20 May 2020
Terms of Use: https://bioone.org/terms-of-use Access provided by Universidade Estadual Paulista Julio de Mesquita Filho (UNESP)

TABLE 1.—Uncorrected *p*-distances (percentage) among species and lineages of *Crossodactylodes*. Distances for all concatenated mtDNA fragments (ca. 3700 bp) are shown under the diagonal and distances for the 16S rRNA fragment (ca. 550 bp) are shown above the diagonal. Intraspecific or intralineage distances are shown as concatenated mitochondrial/16S rRNA (along diagonal). NC = not calculated because there was only one individual.

| | *C. bokermanni* Lineage A | *C. bokermanni* Lineage B | *C. bokermanni* Lineage C | *C. itambe* | *C. izecksohni* Lineage A | *C. izecksohni* Lineage B | *C. septentrionalis* |
|---|---|---|---|---|---|---|---|
| *C. bokermanni* Lineage A | NC / 0 ($n$ = 2) | 0.7 | 3.3–3.6 | 5.1 | 4.9–5.5 | 6.6–6.8 | 6.1 |
| *C. bokermanni* Lineage B | 2.6–2.7 | 0.0–0.2 ($n$ = 7) / 0 ($n$ = 8) | 4.0–4.3 | 5.1 | 4.9–5.5 | 6.6–6.8 | 6.1 |
| *C. bokermanni* Lineage C | 4.9–5.0 | 5.1–5.4 | 0.0–0.1 ($n$ = 3) / 0 ($n$ = 7) | 4.9–5.3 | 5.7–6.3 | 7.1–7.9 | 6.1 |
| *C. itambe* | 10.2–10.4 | 10.0–10.2 | 9.9–10.1 | 0.1–0.2 ($n$ = 5) / 0 ($n$ = 5) | 3.5–4.0 | 4.9–5.1 | 3.2 |
| *C. izecksohni* Lineage A | 10.8–10.9 | 10.5–10.9 | 11.0–11.2 | 8.0–8.4 | 0.0–0.7 ($n$ = 7) / 0.0–0.4 ($n$ = 12) | 3.5–4.3 | 4.6–4.9 |
| *C. izecksohni* Lineage B | 11.0–11.2 | 10.8–11.2 | 11.1–11.4 | 8.5–8.8 | 5.3–5.4 | 0.1 ($n$ = 3) / 0.0–0.2 ($n$ = 3) | 5.8–6.1 |
| *C. septentrionalis* | 11.4 | 11.1–11.4 | 11.2–11.3 | 7.8–7.9 | 9.4–9.7 | 9.9–10.2 | NC / NC |

single eggs, positioned isolated, i.e., not adjacent to any other egg (50–200 eggs in a single group in *Rupirana*; Juncá and Lugli 2009; 10–40 eggs positioned in haphazard groups, or in groups of 2–20 in other species of Paratelmatobiinae; Garcia 1996; Pombal and Haddad 1999). Moreover, *Crossodactylodes* differs from all other Paratelmatobiinae, except from *P. lutzii* (see Lynch 1971), by tympanic middle ear completely lacking (tympanic membrane, annulus, and columella present in *Rupirana*; tympanic membrane absent, tympanic annulus present and visible through the skin, columella present in *Scythrophrys*, *P. cardosoi*, *P. mantiqueira*, and *P. yepiranga*; and tympanic membrane absent, tympanic annulus present and concealed by skin, and columella present in *P. gaigeae* and *P. poecilogaster* (Figs. 5, 6).

Additionally, *Crossodactylodes* differs from *Rupirana* by the absence of a tarsal fold; Fig. 3G (presence; Fig. 3J), absence of white tubercles on males' dorsum; Fig. 5A (presence; Fig. 5D); by the smaller body size considering males and females, SVL = 10.8–18.6 mm (SVL = 27.8–34.4 mm; Heyer 1999), and smaller foot, foot length/SVL = 0.31–0.43 (foot length/SVL = 0.52–0.55). In addition, the optimization of the continuous character foot length showed a decrease of foot in *Crossodactylodes* compared with all other genera of Paratelmatobiinae (Fig. 7). From *Scythrophrys* it differs by having snout rounded to truncate in dorsal view (acuminate), vocal sac absent or externally indistinct (externally distinct), tubercle on upper eyelid rounded or absent (acuminate, which resembles a small dermal horn), absence of a small meniscus on the upper iris (presence), dorsolateral fold absent or weakly developed (well-developed), absence of a tubercle on outer margin of heel (presence), absence of a tarsal fold; Fig. 3G (presence; Fig. 3K), absence of bright and contrasting coloration on ventral surfaces of arm and forearm (presence). From *Paratelmatobius* it differs by the absence of bright and contrasting coloration on ventral surfaces of belly, arm, and forearm (presence).

**Distribution.**—Four of the five species of *Crossodactylodes* occur across the Atlantic Forest in the states of Bahia, Espírito Santo, and Rio de Janeiro, Brazil, at elevations between 770–1480 m (Cochran 1938; Peixoto 1983; Teixeira et al. 2013). A single species (*C. itambe*) occurs in the campo rupestre of the Espinhaço Range in the state of Minas Gerais, Brazil (Barata et al. 2013) at elevations between 1800–2000 m (Fig. 8).

**Natural history.**—In the Atlantic Forest domain, species of *Crossodactylodes* inhabit montane and submontane ombrophilous rain forests and are found in ground or epiphytic bromeliads. The only species that occupies the high-altitude campo rupestre of the Espinhaço Range is found exclusively in rupicolous bromeliads. The main locomotor mode of the species is a slow walking (Barata et al. 2018a; Ferreira et al. 2019a; this study). When disturbed, specimens dive quickly to the bottom of the water accumulated in bromeliad axils and rarely jump outside the bromeliads. When this occurs, some individuals display death-feigning on the ground. It is common to find adults together with different ontogenetic stages (e.g., eggs, tadpoles, and juveniles) in the same bromeliad or bromeliad cluster (Santos et al. 2017; Ferreira et al. 2019a; this study). Eggs are found as single large eggs

Downloaded From: https://bioone.org/journals/Herpetological-Monographs on 20 May 2020
Terms of Use: https://bioone.org/terms-of-use Access provided by Universidade Estadual Paulista Julio de Mesquita Filho (UNESP)

FIG. 3.—Some diagnostic characters for the genera of Paratelmatobiinae. Nuptial pads of males of (A) *C. itambe* UFMG 14032, showing few, and well-developed spines (this state is also observed in all other species of *Crossodactylodes*); and (B) *P. gaigeae* MZUSP 138661, showing numerous and small spicules (this state is also observed in *Scythrophrys*, *Rupirana*, and other species of *Paratelmatobius*, except in *P. lutzii*, for which nuptial pads lack spicules or spines). Scale bars = 0.2 mm. Left hand of (C) *C. itambe* UFMG 11239, showing expanded discs on fingers II–IV, i.e., more dilated than the base of finger (state also observed in other species of *Crossodactylodes*); and of (D) *P. cardosoi* CFBH 3269, (E) *R. cardosoi* UFMG 7924, and (F) *S. sawayae* UFMG 19546, showing narrow discs on fingers II–IV, i.e., same width or less dilated than the base of finger (state also observed in other species of *Paratelmatobius*). Scale bars = 0.5 mm. Right foot of (G) *C. bokermanni* UFMG 13767, showing absence of tarsal fold, and toes II–V lacking lateral ridges, fringes, or webs (states also observed in other species of *Crossodactylodes*); (H) *P. gaigeae* UFMG 15008, showing absence of tarsal fold, and toes II–V with well-developed flexible fringes (states also observed in other species of *Paratelmatobius*, except in *P. lutzii*); (I) *P. lutzii* MZUSP 94633, showing absence of tarsal fold, and toes II–V with well-developed webs; (J) *R. cardosoi* UFMG 4353, and (K) *S. sawayae* UFMG 19546, showing presence of tarsal fold, indicated by white arrowheads, and toes II–V with lateral ridges; some of them are indicated by black arrowheads. Scale bars = 1.0 mm. A color version of this figure is available online.

Downloaded From: https://bioone.org/journals/Herpetological-Monographs on 20 May 2020
Terms of Use: https://bioone.org/terms-of-use Access provided by Universidade Estadual Paulista Julio de Mesquita Filho (UNESP)

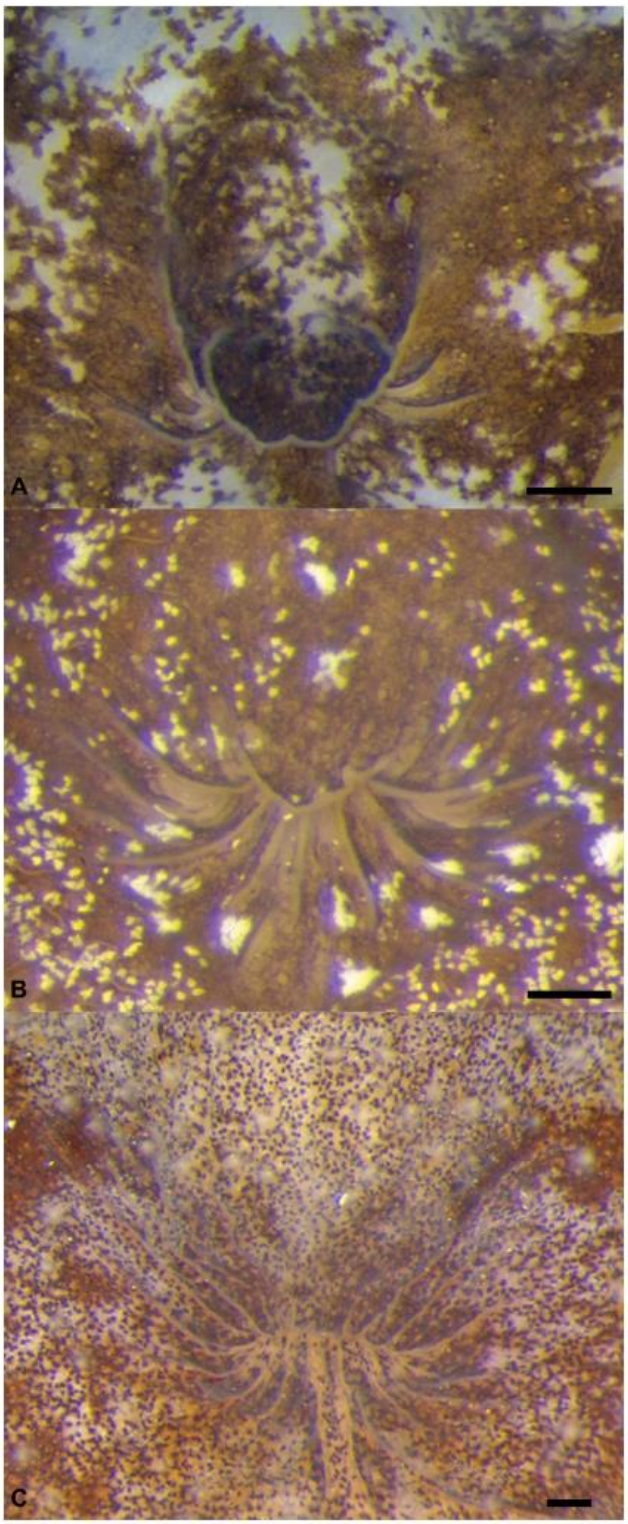


FIG. 4.—Some diagnostic characters for the genera of Paratelmatobiinae. Cloacal region of (A) *C. izecksohni* UFMG 14174, showing a conspicuous cloacal flap, i.e., with long free distal portion (state also observed in other species of *Crossodactylodes*), and of (B) *P. gaigeae* UFMG 15008, and (C) *R. cardosoi* UFMG 4353, showing an inconspicuous cloacal flap, i.e., with short free distal portion (state also observed in *Scythrophrys* and in other species of *Paratelmatobius*). Scale bars = 0.2 mm. A color version of this figure is available online.

submerged or slightly above the water surface, positioned isolated from other eggs (Santos et al. 2017; Ferreira et al. 2019a). We observed five well-formed eggs in the ovisac (i.e., posterior part of the oviduct) of one dissected female of *C. itambe* (UFMG 11237). As eggs were found singly in the field, at least females of *C. itambe* seem to partition their clutches into nearby axils or bromeliads. After hatching, tadpoles complete their development in the water accumulated in leaf axils (Peixoto 1983; Santos et al. 2017). Parental care (egg and tadpole guarding) was reported for *C. izecksohni* (Ferreira et al. 2019a) and hypothesized for *C. itambe* (Santos et al. 2017).

**Content.**—*Crossodactylodes pintoi* Cochran 1938, *C. bokermanni* Peixoto 1983 "1982", *C. izecksohni* Peixoto 1983 "1982", *C. septentrionalis* Teixeira, Recoder, Amaro, Damasceno, Cassimiro, and Rodrigues 2013, and *C. itambe* Barata, Santos, Leite, and Garcia 2013.

## Species Accounts

### *Crossodactylodes pintoi* Cochran
Figs. 9A, 10A–C

*Crossodactylodes pintoi* Cochran 1938: Cochran 1938:42. Holotype male (MZUSP 56467, formerly USNM 102606, examined in this study) from Serra de Macaé, municipality of Nova Friburgo, state of Rio de Janeiro, southeastern Brazil (Bokermann 1966), collected by E. Garbe between September and December 1909.

**Referred specimens.**—We examined four paratopotypes of *Crossodactylodes pintoi* including three males (MNRJ 4097 [formerly USNM 102610]; MZUSP 104; USNM 102608) and one female (MCZ 25707, formerly USNM 102609 [via photograph]). The specimen MNRJ 4097 was not considered in the Variation section due to its poor preservation condition.

**Diagnosis.**—*Crossodactylodes pintoi* is diagnosable from all congeners by the following combination of characters: (1) absence of vomerine odontophores; (2) snout not flattened in lateral view; (3) bilobed cloacal flap; (4) thumbs in adult males weakly widened; (5) zygomatic process of squamosal bone short, not passing the anterior margin of the optic foramen; (6) males lacking vocal slits; (7) absence of dorsolateral fold; (8) discs of fingers II–IV slightly expanded; (9) skin on males' dorsum coarsely granular; (10) disc of Finger I rounded; (11) medial region of the upper lip not anteriorly projected; (12) SVL 15.9 mm (female) and 16.2–18.0 mm (males).

**Comparisons.**—*Crossodactylodes pintoi* is distinguished from its congeners (characters in parentheses) by the absence of vomerine odontophores; Fig. 11B (presence in *C. bokermanni* and *C. septentrionalis*; Fig. 11A); snout not flattened in lateral view; Fig. 10A (flattened in *C. bokermanni* [Fig. 10D] and *C. septentrionalis* [Fig. 11C]); thumbs in adult males weakly widened; Fig. 12D (broadly widened in *C. izecksohni* [Fig. 12C] and *C. septentrionalis* [Fig. 12E]); cloacal flap bilobed; Fig. 13B (undivided, or with a small indentation in *C. izecksohni* and *C. itambe*; Fig. 13A); zygomatic process of squamosal bone short, not passing the anterior margin of the optic foramen (long, passing the anterior margin of the optic foramen in *C. septentrionalis* and *C. itambe*; see Teixeira et al. 2013). Additionally, *C. pintoi* can be distinguished from *C. bokermanni* by the

Downloaded From: https://bioone.org/journals/Herpetological-Monographs on 20 May 2020
Terms of Use: https://bioone.org/terms-of-use Access provided by Universidade Estadual Paulista Julio de Mesquita Filho (UNESP)

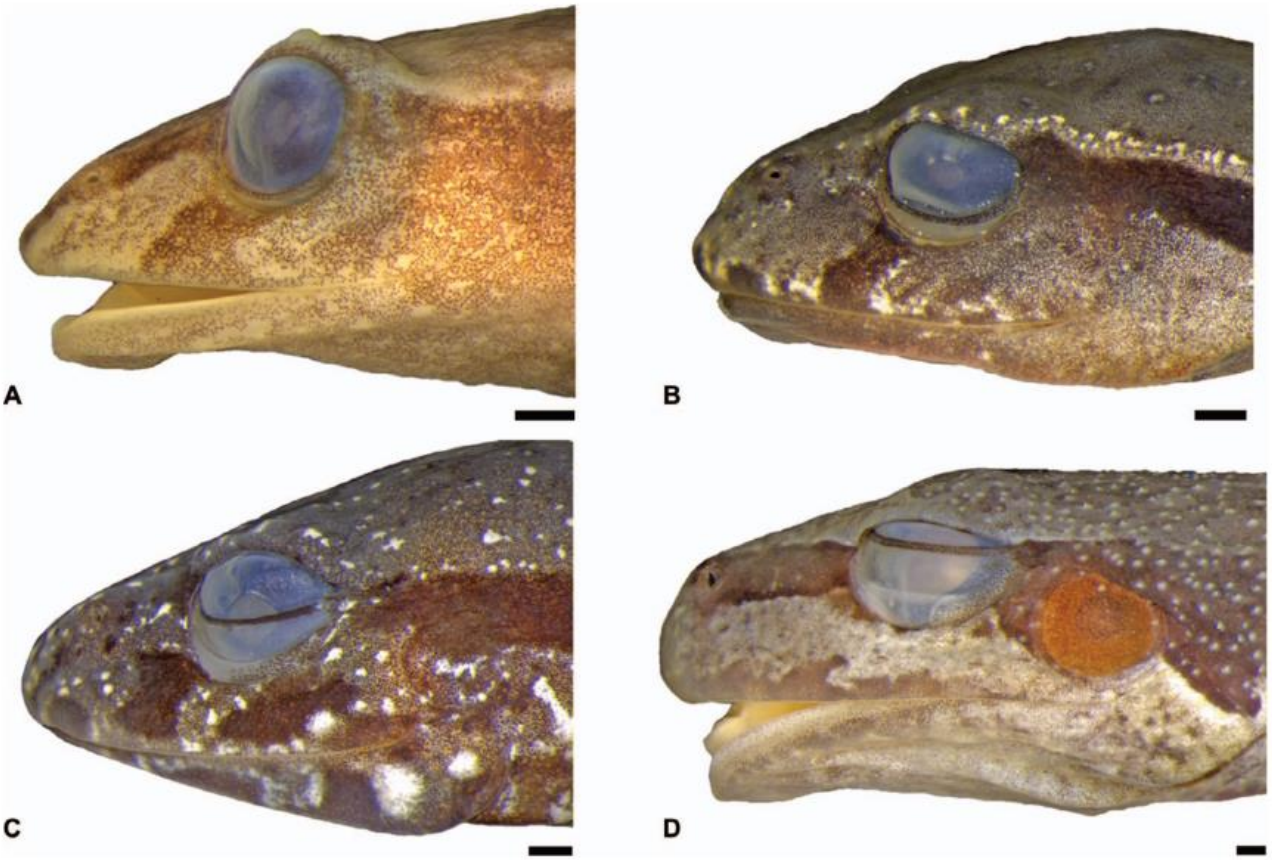


FIG. 5.—Some diagnostic characters related to tympanic middle ear elements for the genera of Paratelmatobiinae. Lateral side of the head in (A) *C. bokermanni* ZUFRJ 1933 and in (B) *P. gaigeae* UFMG 15005, showing absence of tympanic membrane and no apparent tympanic annulus externally (states also observed in other species of *Crossodactylodes*, and in *P. lutzii* and *P. poecilogaster*); in (C) *P. cardosoi* CFBH 28975, showing absence of tympanic membrane and tympanic annulus visible through the skin (states also observed in *P. mantiqueira*, *P. yepiranga*, and *S. sawayae*); in (D) *R. cardosoi* UFMG 4353, showing presence of tympanic membrane and tympanic annulus visible through the skin. Scale bars = 0.5 mm. A color version of this figure is available online.

absence of vocal slits in males (presence); absence of dorsolateral fold; Fig. 14B (presence; Fig. 14A); discs of fingers II–IV slightly expanded; Fig. 12D (broadly expanded; Fig. 12A); skin on males' dorsum coarsely granular (shagreen). Differs from *C. izecksohni* by its larger size, with SVL 15.9 mm in female and 16.2–18.0 mm in males (females SVL = 10.8–13.9 mm; males SVL = 10.8–15.0 mm; Table 2). It is distinguished from *C. septentrionalis* by having disc of Finger I rounded; Fig. 12D (acute; Fig. 12E). Differs from *C. itambe* by the absence of anterior projection in the medial region of the upper lip; Fig. 13C (presence; Figs. 11D, 13D).

**Redescription of the holotype.**—Adult male, SVL 16.2 mm; body slightly robust, dorsoventrally flattened; head slightly wider than long (head width/head length = 1.02); head width = 0.36 SVL; head length = 0.35 SVL; snout not flattened, truncated in dorsal view, rounded in lateral view; eye–nostril distance shorter than eye diameter (eye–nostril distance/eye diameter = 0.75); canthus rostralis slightly curved in dorsal view and rounded in cross-section; loreal region slightly concave; nostrils slightly protuberant, rounded, dorsolaterally directed, opening in the apices of small dermal elevations; interorbital area flat and approximately twice as long as eye diameter (interorbital distance/eye diameter = 2.00). Eyes medium-sized and protuberant (eye diameter/head length = 0.25; eye diameter/head width = 0.24), laterally oriented; upper eyelid margin smooth. Tympanic membrane and annulus absent. A poorly developed dermal fold from posterior edge of eye curving downward to arm insertion. Dorsolateral fold absent.

Choanae small, nearly rounded, spaced 1.6 mm from each other. Vomerine odontophores absent. Tongue ovoid, not notched, free behind for about one third of its length. Vocal slits absent; vocal sac externally indistinct. Single, small, toothlike process present on front of lower jaw with a socket between premaxillae.

Forelimb robust, hypertrophied, lacking fold or fringe; forearm nearly as robust as arm (forearm width/arm width = 1.02); fingers long; relative length of fingers I < II ≈ IV < III; discs of fingers II–IV slightly expanded, nearly rounded; disc of Finger I rounded, less expanded than the others; fingers II–IV slender; Finger I weakly widened, with nuptial pad formed by strongly aggregate keratinized spines covering most of its lateral margin and dorsal surface (12 spines on left and 13 on right thumbs); subarticular tubercles small, flat, oval in ventral view on Finger I and round in ventral view on fingers II–IV; supernumerary tubercles slightly distinct; inner metacarpal tubercle flat, elliptical; outer metacarpal

Downloaded From: https://bioone.org/journals/Herpetological-Monographs on 20 May 2020
Terms of Use: https://bioone.org/terms-of-use Access provided by Universidade Estadual Paulista Julio de Mesquita Filho (UNESP)

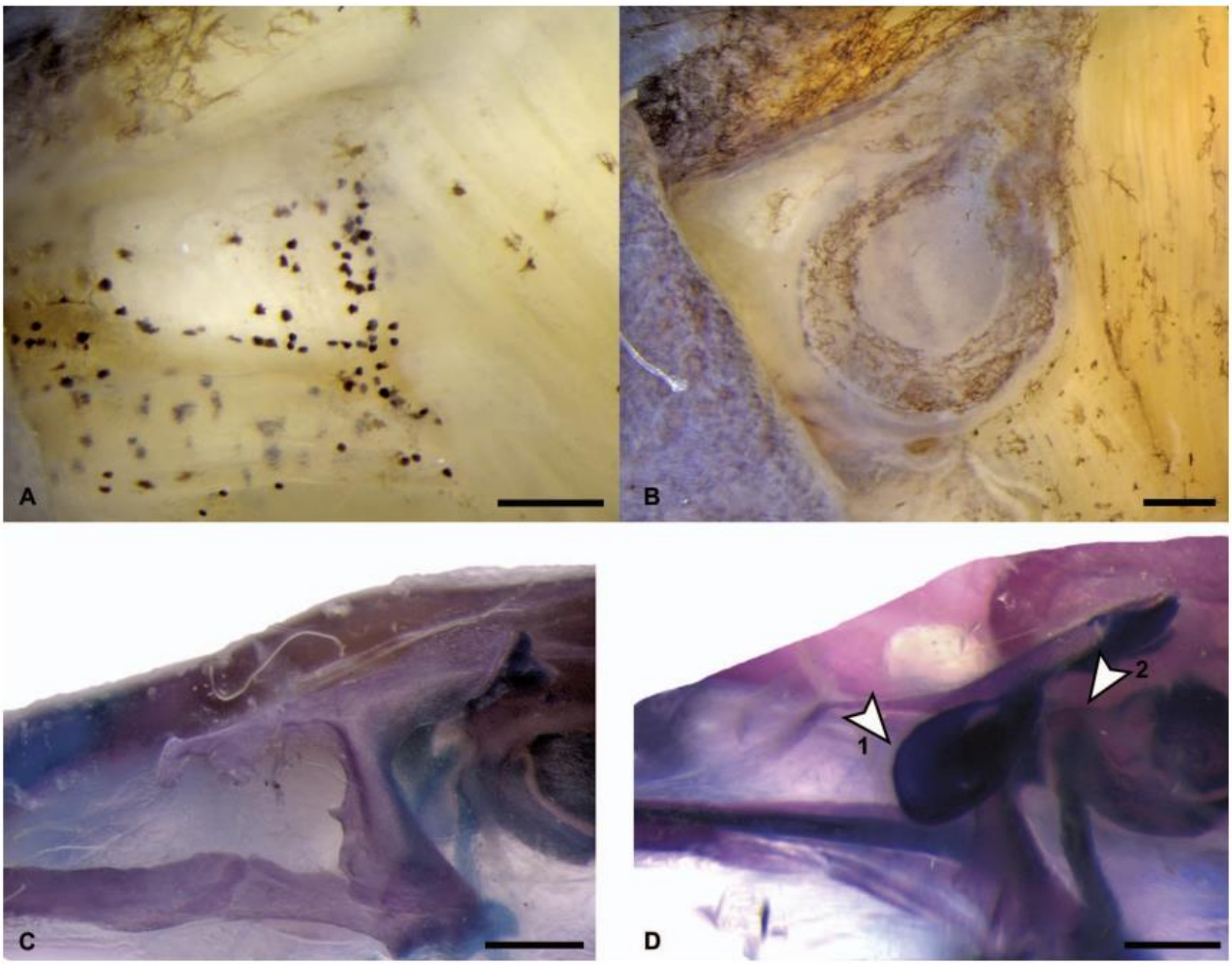


FIG. 6.—Some diagnostic characters related to tympanic middle ear elements for the genera of Paratelmatobiinae. Lateral side of the head shown after a dissection in the skin in (A) *C. bokermanni* UFMG 13769, showing absence of tympanic annulus (the same is observed in other species of *Crossodactylodes*), and in (B) *P. poecilogaster* UFMG 3240, showing presence of tympanic annulus concealed by the skin (the same state is observed in *P. gaigeae*). Scale bars = 0.25 mm. Cleared and double-stained specimens of (C) *C. itambe* UFMG 14033, showing absence of columella (state also reported for other species of *Crossodactylodes*), and of (D) *P. gaigeae* MZUSP 132608, showing presence of columella indicated by white arrowhead 2 (note also the presence of tympanic annulus, stained in blue and indicated by white arrowhead 1). Scale bars = 0.25 mm). A color version of this figure is available online.

tubercle large, flat, and nearly round in ventral view; vestigial digital webbing.

Hindlimb medium-sized and moderately robust (thigh length/SVL = 0.43; tibia length/SVL = 0.41); tarsal fold absent; toes long, slender, with expanded and nearly rounded discs, larger than finger discs (fourth toe disc diameter/third finger disc diameter = 1.29); relative length of toes I < II < III ≈ V < IV; subarticular tubercles small, flat, and rounded in ventral view; supernumerary tubercles indistinct; inner metatarsal tubercle large, flat, and elliptical in ventral view; outer metatarsal tubercle small, nearly rounded in ventral view, slightly conical in profile; digital webbing absent.

Skin on dorsal surface of body, dorsal and ventral surfaces of arm, flank, belly, and chest coarsely granular; skin on dorsal surface of head, dorsal and ventral surfaces of hindlimbs, and on throat shagreen. Cloacal opening directed posteriorly, at upper level of thighs, covered by a bilobed cloacal flap.

**Measurements of the holotype (in mm).**—SVL 16.2; head length 5.7; head width 5.8; eye diameter 1.4; eye–nostril distance 1.1; nostril–snout distance 0.8; internarial distance 1.2; interorbital distance 2.8; arm length 4.9; forearm length 2.8; hand length 4.1; third finger disk diameter 0.5; thigh length 6.8; tibia length 6.7; tarsal length 4.5; foot length 5.6; fourth toe disk diameter 0.6; arm width 1.8; forearm width 1.8.

**Coloration of the holotype in preservative.**—Translucent coloration on head and body, showing the superficial musculature. Dorsum and venter pale yellow; eyelids grayish; spines on nuptial pad black.

**Variation.**—Snout in dorsal view varies from truncate (MZUSP 56467) to rounded (MCZ 25707; MZUSP 104; USNM 102608) and in lateral view from rounded (MZUSP 56467; USNM 102608) to slightly sloping (MCZ 25707;

Downloaded From: https://bioone.org/journals/Herpetological-Monographs on 20 May 2020
Terms of Use: https://bioone.org/terms-of-use Access provided by Universidade Estadual Paulista Julio de Mesquita Filho (UNESP)

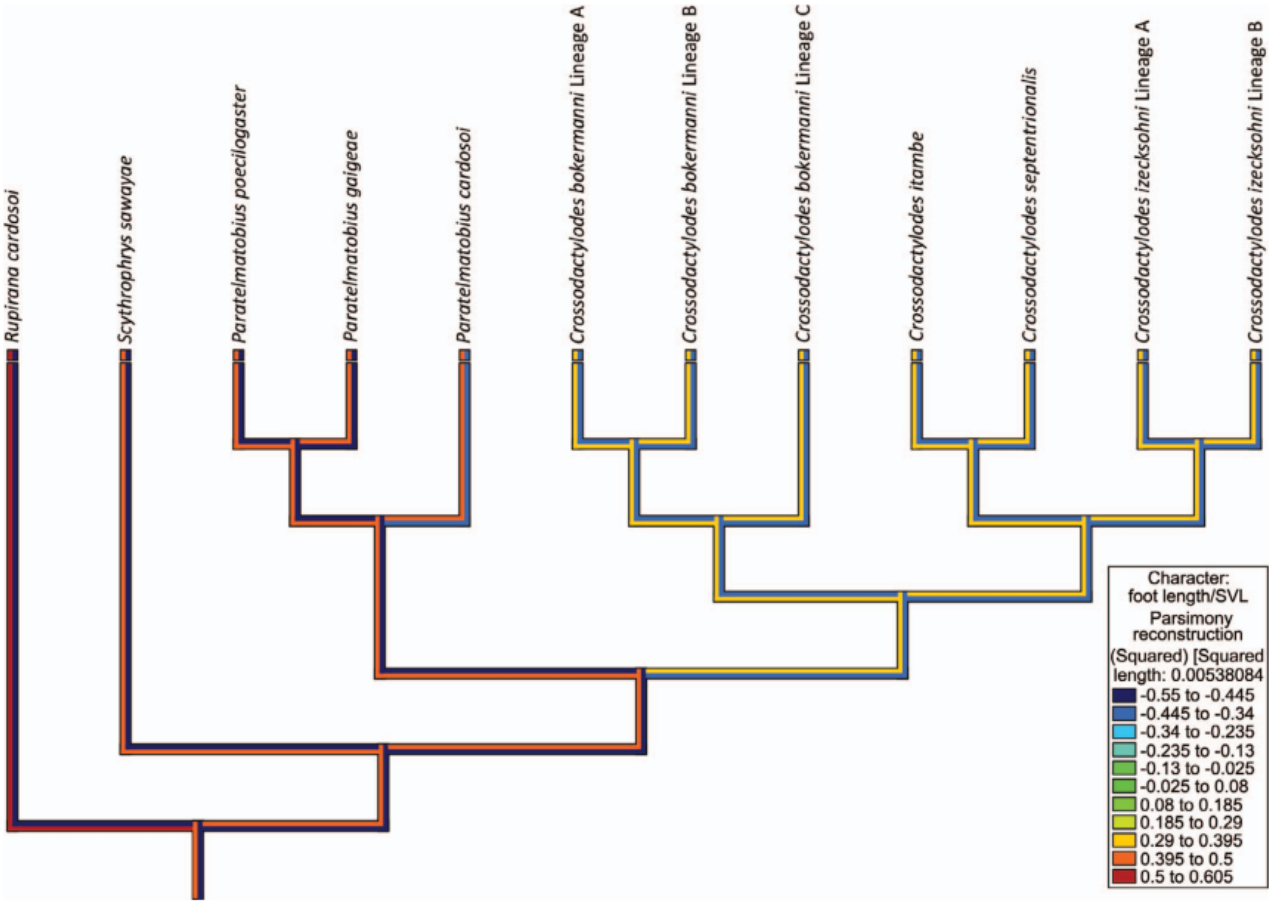


FIG. 7.—Optimization of the continuous character foot length, represented by minimum and maximum values of the ratio foot length/SVL, under Squared Change Parsimony model. Shades of the extremes blue and red represent, respectively, the highest values of minimum and maximum that indicate larger foots. Intermediate values represent smaller foots (i.e., lower values both in minimum and maximum). Note the decrease of foot length in *Crossodactylodes*. A color version of this figure is available online.

MZUSP 104). Males are distinguished from females by the presence of nuptial pads, hypertrophy of arms and forearms, and a rougher dorsal skin. The spines on nuptial pads vary in number (from one in a juvenile male to 13 in the holotype; the other males paratypes have 7–9 spines; Cochran 1955).

**Distribution.**—*Crossodactylodes pintoi* is known only from its type locality at Serra de Macaé, municipality of Nova Friburgo in the state of Rio de Janeiro, southeastern Brazil (Fig. 8).

**Conservation.**—*Crossodactylodes pintoi* is listed as Data Deficient by the IUCN Red List (Peixoto and Carvalho-e-Silva 2004) and the Brazilian Red List (Haddad et al. 2016a) due to the lack of information on its distribution and ecological requirements. On the other hand, Morais et al. (2013) suggested that the species status should be Critically Endangered based on the limited extent of occurrence and the long time no further individual is collected. It is noteworthy that Morais et al. (2013) used the publication year of *C. pintoi* description (1938) as evidence of the last collection, even though it is well documented that the species is known only from its type series collected in 1909.

The region of Serra de Macaé is also known as "Macaé de Cima" or headwaters of the Macaé River. It is located at the northern stretch of the escarpment of the Serra do Mar and covers the districts of Mury, Lumiar, and São Pedro da Serra in the municipality of Nova Friburgo. The region has extensive remnants of well-preserved ombrophilous dense forest (Instituto Estadual do Ambiente 2014). Two, short-term fieldworks were conducted in the region by MTTS (one between 18–24 January 2013 in the surroundings of the districts of Lumiar and São Pedro da Serra and one between 07–10 February 2017 in the surroundings of Macaé de Cima). Macaé de Cima was also visited by RBF between 11–15 December 2017, employing extensive bromeliad sampling at several sites with six collectors, totaling 46 sampling hours and 31.2 km tracked. We could not find new individuals of *Crossodactylodes pintoi*. The visited localities have high richness and abundance of bromeliads across different types of environments and strata. In this way, more sampling effort around the mountains of Nova Friburgo still needs to be done.

Although the type locality of *Crossodactylodes pintoi* has not been exactly recorded (see Remarks), all specimens of the type series were collected in the same locality (Cochran 1938). Thus, the estimated area of occupancy is ~4 km$^2$. Following the precautionary approach (IUCN 2019) and based on the available evidence, *C. pintoi* can be listed as

Downloaded From: https://bioone.org/journals/Herpetological-Monographs on 20 May 2020
Terms of Use: https://bioone.org/terms-of-use Access provided by Universidade Estadual Paulista Julio de Mesquita Filho (UNESP)

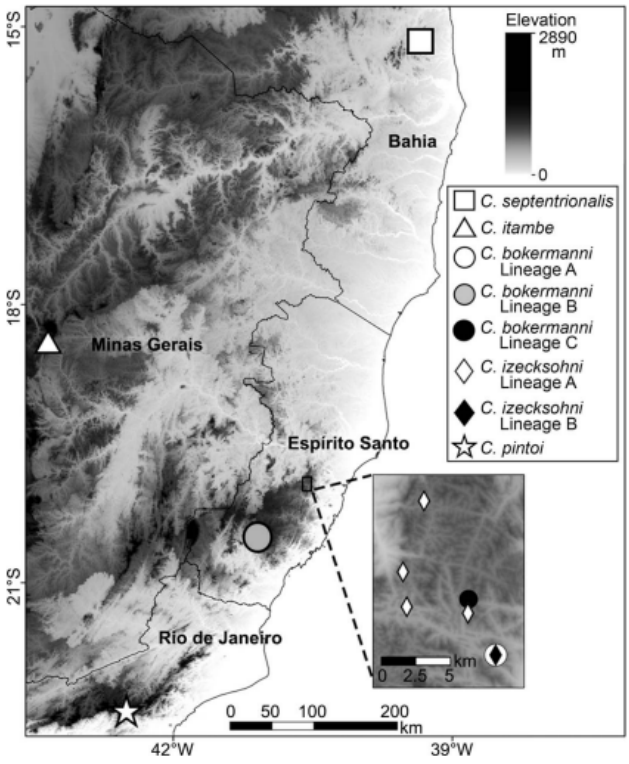


FIG. 8.—Geographic distribution of the species and lineages of *Crossodactylodes* on northeastern and southeastern Brazil. The black diamond overlapping the white circle indicates the sympatry of Lineage A of *C. bokermanni* and Lineage B of *C. izecksohni*.

Vulnerable under Criterion D2 because it is known from a single location and can become Critically Endangered or even Extinct within a short time period due to the effects of anthropic pressures or stochastic events.

**Advertisement call.**—Unknown.

**Tadpole.**—Unknown. A lot of tadpoles from municipality of Santa Teresa, described by Peixoto (1981), was wrongly assigned to *Crossodactylodes pintoi*. Later, Peixoto (1983) suggested that the same lot should belong to either one or both *C. bokermanni* or *C. izecksohni*.

**Natural history.**—Unknown.

**Remarks.**—Cochran (1938, 1955) reported that the tympanum of *Crossodactylodes pintoi* is hidden. However, Lynch (1971) and Teixeira et al. (2013) re-evaluated this character and considered the tympanum absent. We agree with Lynch (1971) and Teixeira et al. (2013) but considered all tympanic middle ear elements (i.e., tympanic membrane, tympanic annulus, and columella) absent. Cochran (1955) considered the snout of the holotype as rounded in dorsal view. However, our study and Teixeira et al. (2013) considered it truncated. This variation might be due to differences in interpretation or due to fixation artifact related to the long time the specimen was collected. Cochran (1955) and Barata et al. (2013) reported that *C. pintoi* has a median subgular vocal sac. However, after careful analysis, we conclude that the skinfold these authors interpreted as vocal sac is a fixation artifact and that a vocal sac is absent in *C. pintoi*. Peixoto (1983) erroneously reported MZUSP 56473 as the holotype of *C. pintoi*. Lynch (1971) reported natural history data for *C. pintoi*. However, the information refers to *C. bokermanni* or *C. izecksohni*, and the natural history of *C. pintoi* remains unknown.

It is well documented that Ernst Garbe (1853–1925), a traveling naturalist of the Museu de Zoologia of Universidade de São Paulo, was in the Serra de Macaé, municipality of Nova Friburgo, between September and December 1909, the year in which he collected the type series of *Crossodactylodes pintoi* (see Ihering and Ihering 1911; Pinto 1945; Paynter and Traylor 1991). According to Bokermann (1966), various species of birds collected by E. Garbe in the region are only found at elevations close to 1000 m. Because of this, Bokermann (1966) states that E. Garbe possibly collected the specimens along an old path that linked the municipality of Nova Friburgo to the headwaters of the Macaé River. However, it is not possible to precisely determine the type locality of *C. pintoi*.

*Crossodactylodes bokermanni* Peixoto
Figs. 9B, 10D–F

*Crossodactylodes bokermanni* Peixoto 1983 "1982": Peixoto 1983:619–621, 623, 626. Holotype male (EI 7173, examined in this study) from Alto Santo Antônio, municipality of Santa Teresa, state of Espírito Santo, southeastern Brazil, about 19°54′40.13″S, 40°35′29.37″W, 832 m, collected by O.L. Peixoto and colleagues on 22 December 1980 (O.L. Peixoto, personal communication).

**Referred specimens.**—We examined 33 paratopotypes of *Crossodactylodes bokermanni* including six males (EI 7174, 7180–7181; MZUSP 58077, 73759–73760 [formerly WCAB 48001–48002]), 15 females (EI 7175–7176, 7182–7183, 7189; MNRJ 4166, 14223–14226, 14237; MZUSP 58079; USNM 221885–87), and 12 juveniles (EI 7177–7179, EI 7184–7188; MNRJ 4165, 14222–14223; MZUSP 58078). To this species we refer four additional males (ZUFRJ 1377–1378, 1380, 1933) and two additional females (ZUFRJ 1382, 1934) from the type locality; one male (CFBH 44754) from Reserva Biológica Augusto Ruschi, municipality of Santa Teresa, state of Espírito Santo, southeastern Brazil, 19°53′50.31″S, 40°32′46.13″W, 811 m; one male (UFMG 14188), seven females (CFBH 44748–44753; UFMG 14189), and one juvenile (UFMG 14190) from Penha District, municipality of Santa Teresa, state of Espírito Santo, southeastern Brazil, 19°55′44.62″S, 40°32′55.33″W, 811 m; three males (MBML 3975, 3984–85), one female (MNRJ 38412), and one juvenile (MNRJ 34933) from Estação Biológica de Santa Lúcia, municipality of Santa Teresa, state of Espírito Santo, southeastern Brazil, 19°57′45.76″S, 40°31′55.66″W, 915 m; four males (UFMG 13767, 13769, 13774, 14197) and three females (UFMG 13770, 14198–14199) from Parque Estadual do Forno Grande, municipality of Castelo, state of Espírito Santo, southeastern Brazil, 20°30′40.07″S, 41°5′26.92″W, 1477 m; and one female (MBML 1774) and two juveniles (MBML 1779–80) from Sítio Fassarela, municipality of Domingos Martins, state of Espírito Santo, southeastern Brazil, 20°21′47.47″S, 41°4′47.16″W, 1018 m.

**Diagnosis.**—*Crossodactylodes bokermanni* is diagnosable from all congeners by the following combination of characters: (1) males with vocal slits; (2) presence of

Downloaded From: https://bioone.org/journals/Herpetological-Monographs on 20 May 2020
Terms of Use: https://bioone.org/terms-of-use Access provided by Universidade Estadual Paulista Julio de Mesquita Filho (UNESP)

FIG. 9.—Dorsal (left) and ventral (right) views of holotypes of (A) *C. pintoi* MZUSP 56467, male, SVL = 16.2 mm; (B) *C. bokermanni* EI 7173, male, SVL = 15.2 mm; and (C) *C. izecksohni* EI 7192, male, SVL = 13.4 mm. A color version of this figure is available online.

Downloaded From: https://bioone.org/journals/Herpetological-Monographs on 20 May 2020
Terms of Use: https://bioone.org/terms-of-use Access provided by Universidade Estadual Paulista Julio de Mesquita Filho (UNESP)

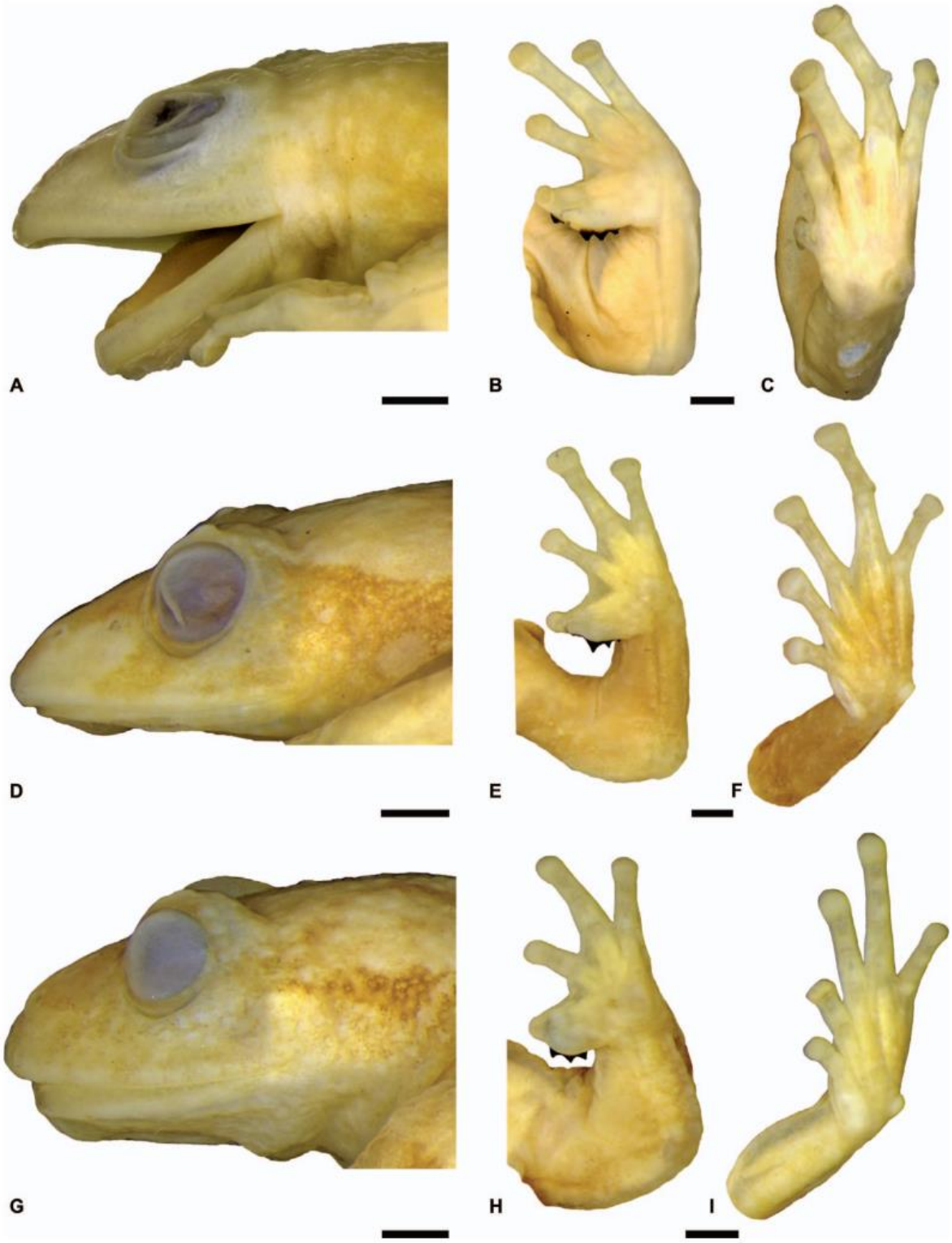


FIG. 10.—Head in lateral view, left hand, and left foot of holotypes of (A–C) *C. pintoi* MZUSP 56467, (D–F) *C. bokermanni* EI 7173, and (G–I) *C. izecksohni* EI 7192. Scale bars = 1 mm. A color version of this figure is available online.

Downloaded From: https://bioone.org/journals/Herpetological-Monographs on 20 May 2020
Terms of Use: https://bioone.org/terms-of-use Access provided by Universidade Estadual Paulista Julio de Mesquita Filho (UNESP)

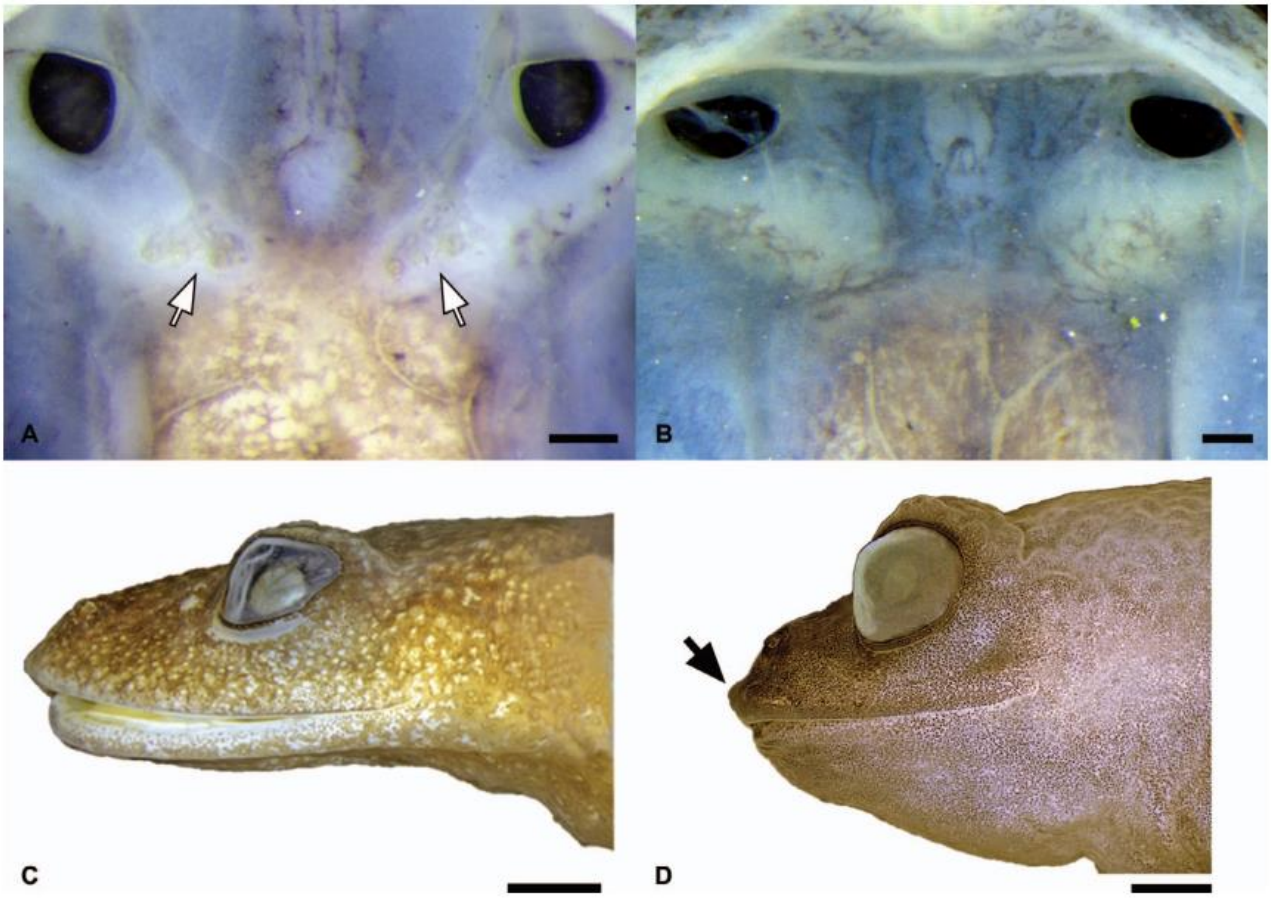


FIG. 11.—Some diagnostic characters for species of *Crossodactylodes*. Buccal roof in (A) *C. bokermanni* UFMG 14197, showing presence of vomerine odontophores indicated by white arrows (state also observed in *C. septentrionalis*), and in (B) *C. itambe* UFMG 14040, showing absence of vomerine odontophores (state also observed in *C. pintoi* and *C. izecksohni*). Scale bars = 0.2 mm. Head in lateral view in (C) *C. septentrionalis* MZUESC 14363, showing a flattened snout, and in (D) *C. itambe* UFMG 11239, showing a not-flattened snout and an anterior projection in the medial region of the upper lip indicated by a black arrow (for this character also refer to Fig. 13D). Scale bars = 1 mm. A color version of this figure is available online.

dorsolateral fold; (3) discs of fingers II–IV broadly expanded; (4) skin on males' dorsum shagreen; (5) presence of vomerine odontophores; (6) snout flattened in lateral view; (7) thumbs in adult males weakly widened; (8) in life, iris coppery or reddish with dark brown fine reticulations; (9) zygomatic process of squamosal bone short, not passing the anterior margin of the optic foramen; (10) presence of a black canthal stripe; (11) presence of a black lateral band from posterior corner of the eye to the posterior third of body; (12) hindlimbs with black transverse bars; (13) disc of Finger I rounded; (14) medial region of the upper lip not anteriorly projected; (15) in preservative, dorsal background coloration varying from pale cream to pale yellow, or brown.

**Comparisons.**—*Crossodactylodes bokermanni* is distinguished from its congeners (characters in parentheses) by the presence of vocal slits in males (absence in *C. pintoi*, *C. izecksohni*, *C. septentrionalis*, and *C. itambe*); presence of a dorsolateral fold from posterior corner of the eye to the posterior third of body; Fig. 14A (absence in *C. pintoi*, *C. izecksohni*, *C. septentrionalis*, and *C. itambe*; Fig. 14B); discs of fingers II–IV broadly expanded; Fig. 12A (slightly expanded in *C. pintoi*, *C. izecksohni*, *C. septentrionalis*, and *C. itambe*; Figs. 12B–E); skin on males' dorsum shagreen (coarsely granular in *C. pintoi*, *C. izecksohni*, *C. septentrionalis*, and *C. itambe*); presence of vomerine odontophores; Fig. 11A (absence in *C. pintoi*, *C. izecksohni*, and *C. itambe*; Fig. 11B); snout flattened in lateral view; Fig. 10D (not flattened in *C. pintoi* [Fig. 10A], *C. izecksohni* [Fig. 10G], and *C. itambe* [Fig. 11D]); thumbs in adult males weakly widened; Fig. 12A (broadly widened in *C. izecksohni* [Fig. 12C] and *C. septentrionalis* [Fig. 12E]); iris in life coppery to reddish, with dark brown fine reticulations; Fig. 15A (yellowish with dark brown fine reticulations, interrupted by a brown horizontal bar at the pupil level in *C. izecksohni* [Fig. 16A] and uniformly black or brownish black in *C. itambe* [Fig. 15B]); zygomatic process of squamosal bone short, not passing the anterior margin of the optic foramen (long, passing the anterior margin of the optic foramen in *C. septentrionalis* and *C. itambe*; see Teixeira et al. 2013); presence of a black canthal stripe; Fig. 14A (absence in *C. septentrionalis* and *C. itambe*; Fig. 14B); presence of a black lateral band from posterior corner of the eye to the posterior third of body; Fig. 14A (absence in *C. septentrionalis* and *C. itambe*; Fig. 14B); presence of black transverse bars on hindlimbs; Fig. 14A (absence in *C. septentrionalis* and *C. itambe*; Fig. 14B). Additionally, *C.*

Downloaded From: https://bioone.org/journals/Herpetological-Monographs on 20 May 2020
Terms of Use: https://bioone.org/terms-of-use Access provided by Universidade Estadual Paulista Julio de Mesquita Filho (UNESP)

Fig. 12.—Diagnostic characters for species of *Crossodactylodes*. Left hand of (A) a female (UFMG 13770) and a male (UFMG 13767) of *C. bokermanni*; (B) a female (UFMG 11246) and a male (UFMG 11239) of *C. itambe*; (C) a female (ZUFRJ 365) and a male (UFMG 14174) of *C. izecksohni*; (D) a male of *C. pintoi* (USNM 102608); and a female (MZUESC 14364) and a male (MZUESC 14363) of *C. septentrionalis*. Note the broadly expanded discs of fingers II–IV in *C. bokermanni* (A); the broadly widened thumbs in males of *C. izecksohni* (C), and *C. septentrionalis* (E); and the acute disc on Finger I in *C. septentrionalis* (E). Scale bars = 1 mm. A color version of this figure is available online.

*bokermanni* can be distinguished from *C. septentrionalis* by having disc of Finger I rounded; Fig. 12A (acute; Fig. 12E); from *C. itambe* by the absence of anterior projection in the medial region of the upper lip; Fig. 13C (presence; Figs. 11D, 13D); and dorsal background coloration in preservative pale cream, pale yellow, or brown; Fig. 17A (dark gray or brownish black; Fig. 17B).

**Redescription of the holotype.**—Adult male, SVL 15.2 mm; body slender, dorsoventrally flattened; head slightly longer than wide (head width/head length 0.97); head width 0.38 SVL; head length 0.40 SVL; snout flattened, rounded in dorsal view, slightly sloping in lateral view; eye–nostril distance slightly shorter than eye diameter (eye–nostril distance/eye diameter 0.97); canthus rostralis slightly curved in dorsal view and rounded in cross-section; loreal region slightly concave; nostrils protuberant, elliptical, dorsolaterally directed, opening in the apices of small dermal elevations; interorbital area flat and more than twice as long as eye diameter (interorbital distance/eye diameter = 2.24). Eyes medium-sized and protuberant (eye diameter/head length = 0.23; eye diameter/head width = 0.24), laterally oriented; upper eyelid margin with a prominent rounded tubercle in its medial region. Tympanic membrane and annulus absent. A poorly developed dermal fold from posterior edge of eye curving downward to arm insertion. A weakly developed dorsolateral fold extending from the posterior corner of the eye to the posterior third of body.

Choanae small, nearly rounded, spaced 1.5 mm from each other. Vomerine odontophores present, positioned posterior to the level of the choanae, broadly separated from each other. Tongue ovoid, not notched, free behind for about one third of its length. Vocal slits short, located at the level of the posterior third of tongue; vocal sac externally indistinct. Single, small tooth-like process present on front of lower jaw with a socket between premaxillae.

Forelimb slightly robust, moderately hypertrophied, lacking fold or fringe; forearm nearly as robust as arm (forearm width/arm width = 1.04); fingers long; relative length of fingers I ≈ II < IV < III; discs of fingers II–IV broadly expanded, elliptical; disc of Finger I rounded, less expanded than the others; fingers II–IV slender; Finger I weakly widened, with nuptial pad formed by regularly spaced keratinized spines covering most of its lateral margin and dorsal surface (eight spines on each thumb); subarticular tubercles small, flat, and rounded in ventral view; supernumerary tubercles slightly distinct; inner metacarpal tubercle flat, elliptical; outer metacarpal tubercle large, flat, and nearly round in ventral view; vestigial digital webbing.

Hindlimb medium-sized and slender (thigh length/SVL = 0.44; tibia length/SVL = 0.45); tarsal fold absent; toes long, slender; discs of toes II–V broadly expanded, elliptical; disc of Toe I rounded, less expanded than the others; discs with similar size to the finger discs (fourth toe disc diameter/third finger disc diameter = 1.02); relative length of toes I < II < V < III < IV; subarticular tubercles small, flat, and rounded

Downloaded From: https://bioone.org/journals/Herpetological-Monographs on 20 May 2020
Terms of Use: https://bioone.org/terms-of-use Access provided by Universidade Estadual Paulista Julio de Mesquita Filho (UNESP)

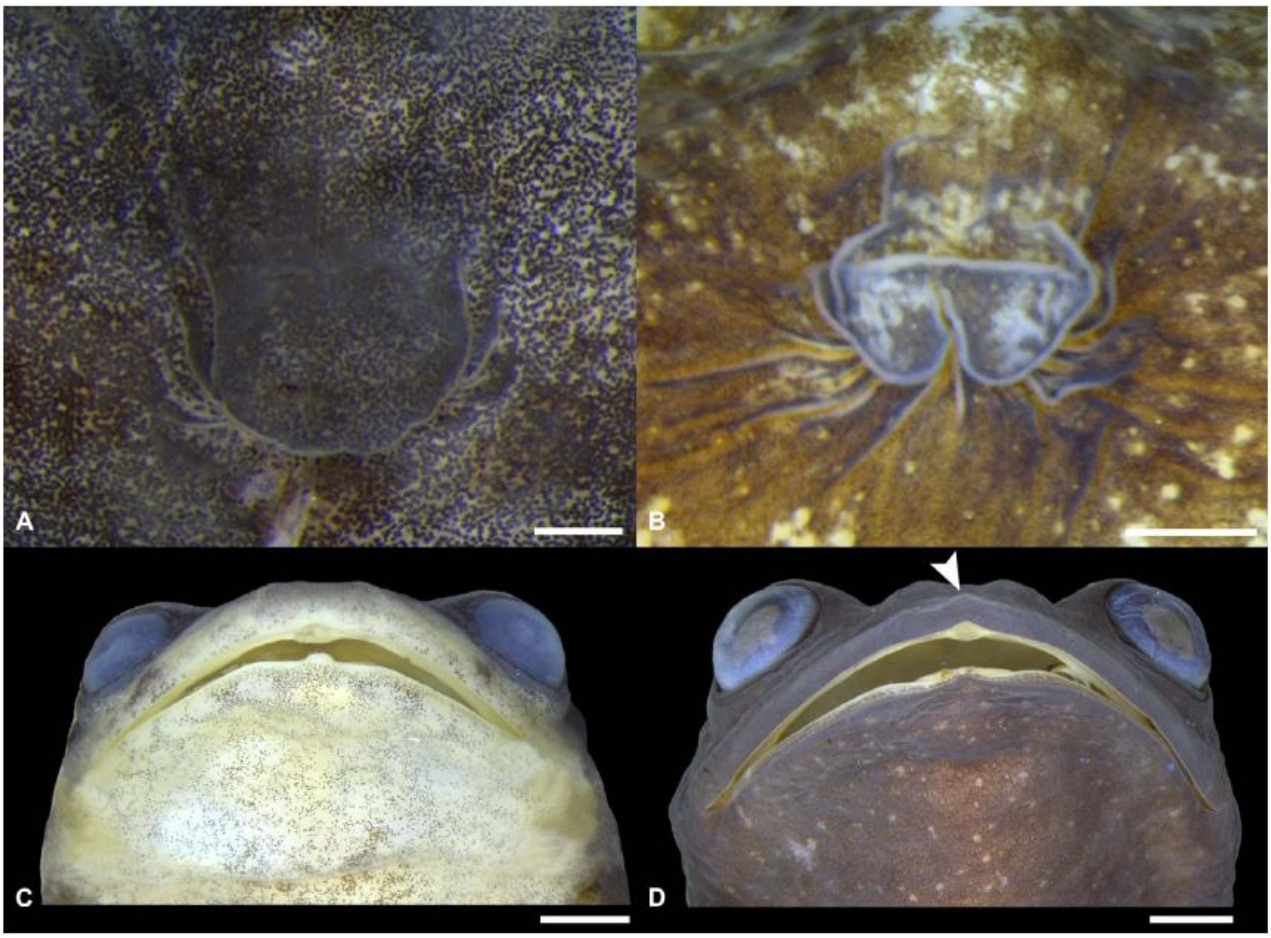


FIG. 13.—Diagnostic characters for species of *Crossodactylodes*. Cloacal region in (A) *C. itambe* UFMG 13382, showing an undivided cloacal flap (state also observed in *C. izecksohni*—in both species the flap can also show a small distal indentation); and in (B) *C. septentrionalis* MZUESC 14363, showing a bilobed cloacal flap (state also observed in *C. pintoi*). This character is polymorphic in *C. bokermanni*. Scale bars = 0.5 mm. Head in ventral view in (C) *C. bokermanni* UFMG 13767, showing medial region of the upper lip lacking an anterior projection (state also observed in *C. pintoi*, *C. izecksohni*, and *C. septentrionalis*); and in (D) *C. itambe* UFMG 13380, showing medial region of the upper lip with an anterior projection, indicated by a white arrow head. Scale bars = 1 mm. A color version of this figure is available online.

in ventral view; supernumerary tubercles indistinct; inner metatarsal tubercle large, flat, and elliptical in ventral view; outer metatarsal tubercle small, nearly rounded in ventral view, slightly conical in profile; digital webbing absent.

Skin on flank, dorsal, and ventral surfaces shagreen. Cloacal opening directed posteriorly, at upper level of thighs, covered by an undivided cloacal flap. Few small scattered tubercles near the cloacal opening.

**Measurements of the holotype (in mm).**—SVL 15.2; head length 6.0; head width 5.8; eye diameter 1.4; eye–nostril distance 1.3; nostril–snout distance 0.9; internarial distance 1.4; interorbital distance 3.1; arm length 4.2; forearm length 3.0; hand length 3.8; third finger disk diameter 0.6; thigh length 6.6; tibia length 6.9; tarsal length 3.8; foot length 5.7; fourth toe disk diameter 0.6; arm width 1.5; forearm width 1.5.

**Coloration of the holotype in life.**—Based on the description and photographs provided by Peixoto (1983), we could infer that the holotype had dorsal surfaces of head, body, and limbs reddish brown with scattered black flecks. Dorsum with two conspicuous reddish blotches lighter than the background, one with an inverted triangular shape on posterior third of head and the other somewhat rectangular extends from the scapular region to the posterior third of body. These blotches are delimited by whitish green flecks. Eyelid tubercle whitish. A black, rounded blotch in the lumbar region. Loreal region reddish, lighter than the background; a thick black canthal stripe and a black labial bar. A cream narrow dorsolateral fold extends from behind the eye to posterior third of body. Flank with a black band, dorsally delimited by the dorsolateral fold. This band is expanded after the arm insertion. A black transverse bar in the wrist; spines on nuptial pad black. Hindlimb with black transverse bars (three on thigh and tibia and one on tarsus). A thick black stripe on anterior surface of thigh. Venter dark brown with marbled blotches lighter than the background.

**Coloration of the holotype in preservative.**—The color is faded, turning into pale tones. The reddish-brown dorsal surfaces of head, body, and limbs become pale cream. The conspicuous reddish blotches on dorsum are translu-

Downloaded From: https://bioone.org/journals/Herpetological-Monographs on 20 May 2020
Terms of Use: https://bioone.org/terms-of-use Access provided by Universidade Estadual Paulista Julio de Mesquita Filho (UNESP)

FIG. 14.—Some diagnostic characters for species of *Crossodactylodes*. (A) *C. bokermanni* in life, showing the dorsolateral fold (white arrow), the black canthal stripe, the black lateral band from posterior corner of the eye to the posterior third of body, and the black transverse bars on hindlimbs (white arrowheads 1, 2, and 3, respectively). (B) *C. septentrionalis* in life, in which dorsolateral fold and the black stripe, band, and bars are absent. Dorsolateral fold is also absent in *C. pintoi*, *C. izecksohni*, and *C. itambe*. The black stripe, band, and bars are also absent in *C. itambe*, are polymorphic in *C. izecksohni* (Fig. S3), and states for these characters are unknown for *C. pintoi*. A color version of this figure is available online.

cent, as well as the dorsal and ventral surfaces of hand and foot. The black flecks, blotches, bands, and bars are pale brown and less evident. Venter continues darker than dorsum. Thoracic skin is translucent, showing pectoral musculature. Eyelid tubercle, dorsolateral fold, carpal, and tarsal tubercles are whitish.

**Variation.**—Snout in lateral view varies from slightly sloping (~71%) to acuminate (~29%). The cloacal flap is usually undivided (~61%), but may have a small distal indentation (~35%) and is rarely bilobed (~4%). Specimens from municipality of Castelo are slightly larger than specimens from municipality of Santa Teresa (Castelo, females SVL = 16.2–17.7 mm, mean = 17.2 mm, males SVL = 16.6–17.9 mm, mean = 17.1 mm; Santa Teresa, females SVL = 12.3–16.1 mm, mean = 14.1 mm, males SVL

TABLE 2.—Morphometric characters (mean ± SD, range in parentheses) in mm for males and females of species of *Crossodactylodes*.

| Character | *C. bokermanni* | | *C. izecksohni* | | *C. itambe* | | *C. septentrionalis* | | *C. pintoi* |
|---|---|---|---|---|---|---|---|---|---|
| | Males ($n$ = 20) | Females ($n$ = 19) | Males ($n$ = 39) | Females ($n$ = 43) | Males ($n$ = 17) | Females ($n$ = 18) | Males ($n$ = 1) | Females ($n$ = 2) | Males ($n$ = 3) |
| Snout–vent length | 15.0 ± 1.5 (12.7–17.9) | 14.5 ± 1.7 (12.2–17.7) | 13.5 ± 1.0 (10.8–15.0) | 12.4 ± 0.9 (10.8–13.9) | 16.5 ± 1.3 (14.0–17.9) | 16.4 ± 0.8 (15.2–18.0) | 18.6 | 16.3 ± 0.3 (16.1–16.5) | 17.0 ± 0.9 (16.2–18.0) |
| Head length | 5.7 ± 0.4 (5.2–6.6) | 5.6 ± 0.4 (4.9–6.5) | 5.1 ± 0.3 (4.5–5.4) | 4.8 ± 0.3 (4.3–5.2) | 6.2 ± 0.3 (5.6–6.6) | 6.1 ± 0.2 (5.7–6.5) | 7.2 | 6.4 ±0.0 (6.4–6.4) | 5.8 ± 0.1 (5.7–6.0) |
| Head width | 5.6 ± 0.4 (5.0–6.4) | 5.4 ± 0.5 (4.7–6.4) | 5.4 ± 0.3 (4.6–5.8) | 4.9 ± 0.3 (4.3–5.4) | 6.6 ± 0.3 (6.2–7.2) | 6.4 ± 0.2 (6.1–6.9) | 7.3 | 6.3 ± 0.1 (6.2–6.3) | 6.0 ± 0.2 (5.8–6.3) |
| Eye diameter | 1.4 ± 0.1 (1.2–1.6) | 1.4 ± 0.1 (1.1–1.6) | 1.2 ± 0.1 (1.1–1.4) | 1.2 ± 0.1 (1.1–1.3) | 1.8 ± 0.1 (1.6–2.0) | 1.8 ± 0.1 (1.4–2.0) | 1.7 | 1.6 ± 0.1 (1.6–1.7) | 1.4 ± 0.1 (1.4–1.5) |
| Interorbital distance | 3.1 ± 0.3 (2.7–3.6) | 3.0 ± 0.2 (2.6–3.5) | 2.8 ± 0.2 (2.4–3.3) | 2.7 ± 0.2 (2.3–3.0) | 3.4 ± 0.2 (3.1–3.7) | 3.3 ± 0.2 (2.9–3.6) | 3.9 | 3.4 ± 0.1 (3.3–3.5) | 3.1 ± 0.4 (2.8–3.5) |
| Eye–nostril distance | 1.3 ± 0.2 (1.0–1.6) | 1.2 ± 0.1 (1.0–1.5) | 1.2 ± 0.1 (1.0–1.4) | 1.1 ± 0.1 (0.9–1.3) | 1.4 ± 0.1 (1.3–1.6) | 1.4 ± 0.1 (1.3–1.5) | 1.7 | 1.5 ± 0.0 (1.5–1.5) | 1.2 ± 0.1 (1.1–1.3) |
| Nostril–snout distance | 1.0 ± 0.1 (0.9–1.2) | 1.0 ± 0.1 (0.9–1.2) | 0.8 ± 0.1 (0.7–1.0) | 0.8 ± 0.1 (0.7–0.9) | 1.1 ± 0.1 (0.9–1.2) | 1.0 ± 0.1 (0.9–1.1) | 1.0 | 0.9 ± 0.0 (0.9–0.9) | 0.9 ± 0.1 (0.8–0.9) |
| Internarial distance | 1.3 ± 0.1 (1.1–1.5) | 1.3 ± 0.1 (1.1–1.5) | 1.1 ± 0.1 (1.0–1.3) | 1.1 ± 0.1 (1.0–1.3) | 1.3 ± 0.1 (1.2–1.4) | 1.3 ± 0.1 (1.1–1.4) | 1.4 | 1.2 ± 0.0 (1.2–1.2) | 1.3 ± 0.2 (1.2–1.4) |
| Arm length | 4.2 ± 0.5 (3.5–5.1) | 4.0 ± 0.4 (3.3–4.8) | 3.9 ± 0.4 (3.0–4.5) | 3.4 ± 0.2 (3.0–3.8) | 4.8 ± 0.3 (4.1–5.1) | 4.6 ± 0.2 (4.2–4.9) | 6.1 | 4.5 ± 0.1 (4.4–4.5) | 4.7 ± 0.4 (4.2–5.0) |
| Arm width | 1.3 ± 0.3 (0.9–1.9) | 1.0 ± 0.1 (0.8–1.2) | 1.6 ± 0.4 (0.8–2.1) | 0.8 ± 0.1 (0.7–1.0) | 1.8 ± 0.3 (1.3–2.3) | 1.2 ± 0.1 (1.0–1.3) | 2.4 | 1.1 ± 0.0 (1.1–1.1) | 1.8 ± 0.0 (1.8–1.8) |
| Forearm length | 2.9 ± 0.2 (2.6–3.4) | 2.9 ± 0.3 (2.5–3.6) | 2.5 ± 0.2 (2.0–3.0) | 2.4 ± 0.2 (2.1–3.4) | 3.6 ± 0.2 (3.1–3.9) | 3.6 ± 0.2 (3.2–3.9) | 3.4 | 3.3 ± 0.1 (3.2–3.3) | 2.8 ± 0.2 (2.7–3.0) |
| Forearm width | 1.4 ± 0.2 (1.1–1.9) | 1.1 ± 0.1 (0.9–1.3) | 1.5 ± 0.3 (1.0–1.9) | 1.0 ± 0.1 (0.7–1.1) | 1.9 ± 0.3 (1.5–2.4) | 1.4 ± 0.1 (1.2–1.6) | 2.3 | 1.1 ± 0.1 (1.1–1.2) | 1.9 ± 0.1 (1.8–2.0) |
| Hand length | 3.8 ± 0.4 (3.2–4.4) | 3.5 ± 0.4 (2.9–4.5) | 3.2 ± 0.3 (2.6–3.8) | 2.8 ± 0.2 (2.5–3.4) | 4.7 ± 0.3 (4.0–5.2) | 4.4 ± 0.3 (3.8–4.9) | 5.4 | 4.2 ± 0.1 (4.1–4.3) | 4.2 ± 0.3 (4.0–4.5) |
| Third finger disc diameter | 0.7 ± 0.1 (0.5–0.9) | 0.6 ± 0.1 (0.5–0.9) | 0.4 ± 0.1 (0.3–0.6) | 0.4 ± 0.1 (0.3–0.5) | 0.6 ± 0.1 (0.5–0.7) | 0.6 ± 0.1 (0.5–0.7) | 0.8 | 0.6 ± 0.1 (0.6–0.7) | 0.6 ± 0.1 (0.5–0.6) |
| Thigh length | 6.6 ± 0.6 (5.6–7.7) | 6.4 ± 0.6 (5.4–7.6) | 5.4 ± 0.4 (4.4–6.1) | 4.9 ± 0.3 (4.3–5.8) | 6.6 ± 0.3 (5.9–7.1) | 6.6 ± 0.3 (6.0–7.3) | 8.8 | 7.2 ± 0.3 (7.0–7.4) | 7.1 ± 0.4 (6.8–7.6) |
| Tibia length | 6.7 ± 0.6 (5.7–7.6) | 6.4 ± 0.6 (5.6–7.4) | 5.4 ± 0.3 (4.5–6.0) | 5.0 ± 0.3 (4.5–5.7) | 6.3 ± 0.3 (5.5–6.7) | 6.3 ± 0.3 (5.7–6.7) | 8.6 | 6.8 ± 0.1 (6.7–6.9) | 6.4 ± 0.3 (6.1–6.7) |
| Tarsal length | 3.8 ± 0.3 (3.1–4.3) | 3.5 ± 0.3 (3.0–4.1) | 3.1 ± 0.2 (2.5–3.7) | 2.9±0.2 (2.5–3.3) | 3.7 ± 0.2 (3.4–4.1) | 3.8 ± 0.2 (3.5–4.3) | 5.2 | 4.1 ± 0.2 (4.0–4.2) | 4.6 ± 0.2 (4.5–4.8) |
| Foot length | 5.9 ± 0.6 (4.9–6.9) | 5.4 ± 0.7 (4.5–7.0) | 4.8 ± 0.4 (3.9–5.5) | 4.4 ± 0.3 (3.8–5.1) | 5.8 ± 0.4 (5.1–6.4) | 5.8 ± 0.3 (5.3–6.3) | 7.5 | 5.8 ± 0.3 (5.6–6.0) | 5.7 ± 0.6 (5.1–6.3) |
| Fourth toe disk diameter | 0.7 ± 0.1 (0.5–0.9) | 0.6 ± 0.1 (0.5–0.9) | 0.5 ± 0.1 (0.3–0.7) | 0.4 ± 0.1 (0.4–0.6) | 0.7 ± 0.1 (0.5–0.8) | 0.7 ± 0.1 (0.5–0.8) | 0.8 | 0.6 ± 0.0 (0.6–0.6) | 0.7 ± 0.1 (0.6–0.8) |

Downloaded From: https://bioone.org/journals/Herpetological-Monographs on 20 May 2020
Terms of Use: https://bioone.org/terms-of-use Access provided by Universidade Estadual Paulista Julio de Mesquita Filho (UNESP)

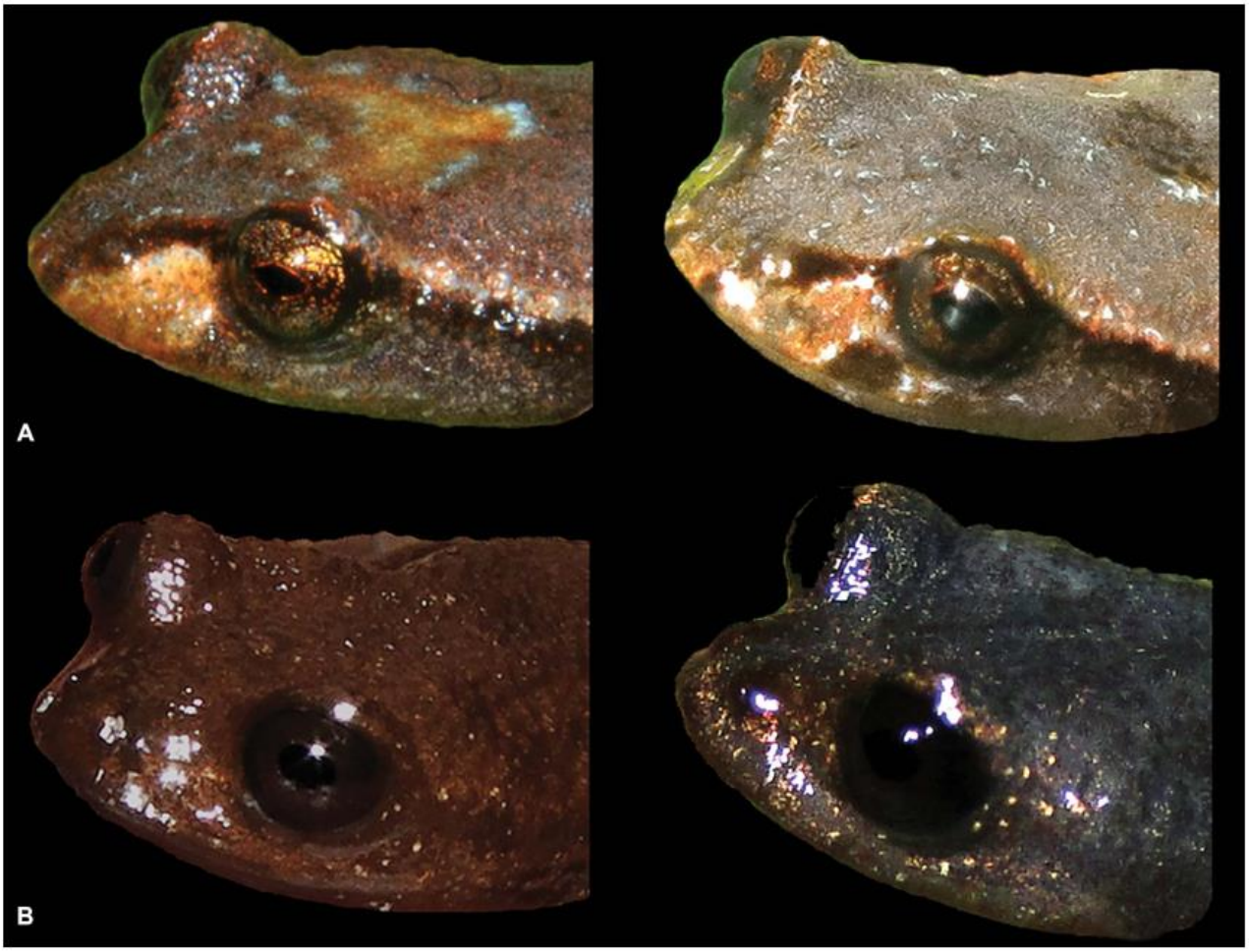


FIG. 15.—Diagnostic character states of iris coloration in life in *Crossodactylodes*. (A) Two specimens of *C. bokermanni*, showing a coppery or reddish iris with dark brown fine reticulations; (B) *C. itambe*, showing a uniformly black or brownish black iris. The state for this character is unknown for *C. pintoi*. For the states observed in *C. izecksohni* and *C. septentrionalis* refer to Fig. 16. A color version of this figure is available online.

= 12.7–16.3 mm, mean = 14.5 mm). Males are distinguished from females by the presence of nuptial pads, moderate hypertrophy of arms and forearms (females arm width/arm length = 0.20–0.27, mean = 0.24; forearm width/forearm length = 0.32–0.40, mean = 0.37; males arm width/arm length = 0.25–0.39, mean = 0.30; forearm width/forearm length = 0.40–0.61, mean = 0.46), and a slightly rougher dorsal skin. In addition, males have a single, median subgular vocal sac, visible only after dissection in the skin of gular region (e.g., UFMG 13769). The spines on nuptial pads vary in number (from one to eight), size, and degree of aggregation. The number of spines can vary between the right and left thumbs of a same specimen. Males with larger SVL and more-hypertrophied forelimbs have higher number and aggregation of spines. The dorsal background coloration in life varies from light gray, light lilac, and brown. The pattern of dorsal blotches is quite variable. The two conspicuous blotches described for the holotype vary in size and shape, can be black rather than reddish, and one or both may be absent. A black labial bar is usually present but can be absent. Some individuals have an orange coloration in different regions: loreal region; posterior surfaces of arm, thigh, tibia, and tarsus; and cloacal region (e.g., Fig. 14A). The black stripe, band, and bars vary in thickness and can be more or less marked. Venter might have orange scattered flecks on gular, abdominal, and cloacal regions.

**Distribution.**—*Crossodactylodes bokermanni* is only known from the state of Espírito Santo, southeastern Brazil. The species is known from four sites in the municipality of Santa Teresa: (1) Alto Santo Antônio (type locality), about 19°54′40.10″S, 40°35′29.37″W, 843 m (O.L. Peixoto, personal communication); (2) Reserva Biológica Augusto Ruschi, 19°53′50.31″S, 40°32′46.13″W, 811 m; (3) Penha district, 19°55′44.62″S, 40°32′55.33″W, 800 m; and (4) Estação Biológica de Santa Lúcia, about 19°57′47, 68″S, 40°31′55,85″W, 908 m. It is also recorded from another two localities: (1) Sítio Fassarela, municipality of Domingos Martins, 20°21′47.47″S, 41°4′47.16″W, 1018 m; and (2) Parque Estadual do Forno Grande, municipality of Castelo, 20°30′40.07″S, 41°5′26.92″W, 1477 m.

Peixoto (1983) used approximate geographic coordinates from the city of Santa Teresa. Other studies also used these coordinates, which misleads that *Crossodactylodes bokermanni* occurs between 650–675 m elevation (Silvano and

Downloaded From: https://bioone.org/journals/Herpetological-Monographs on 20 May 2020
Terms of Use: https://bioone.org/terms-of-use Access provided by Universidade Estadual Paulista Julio de Mesquita Filho (UNESP)

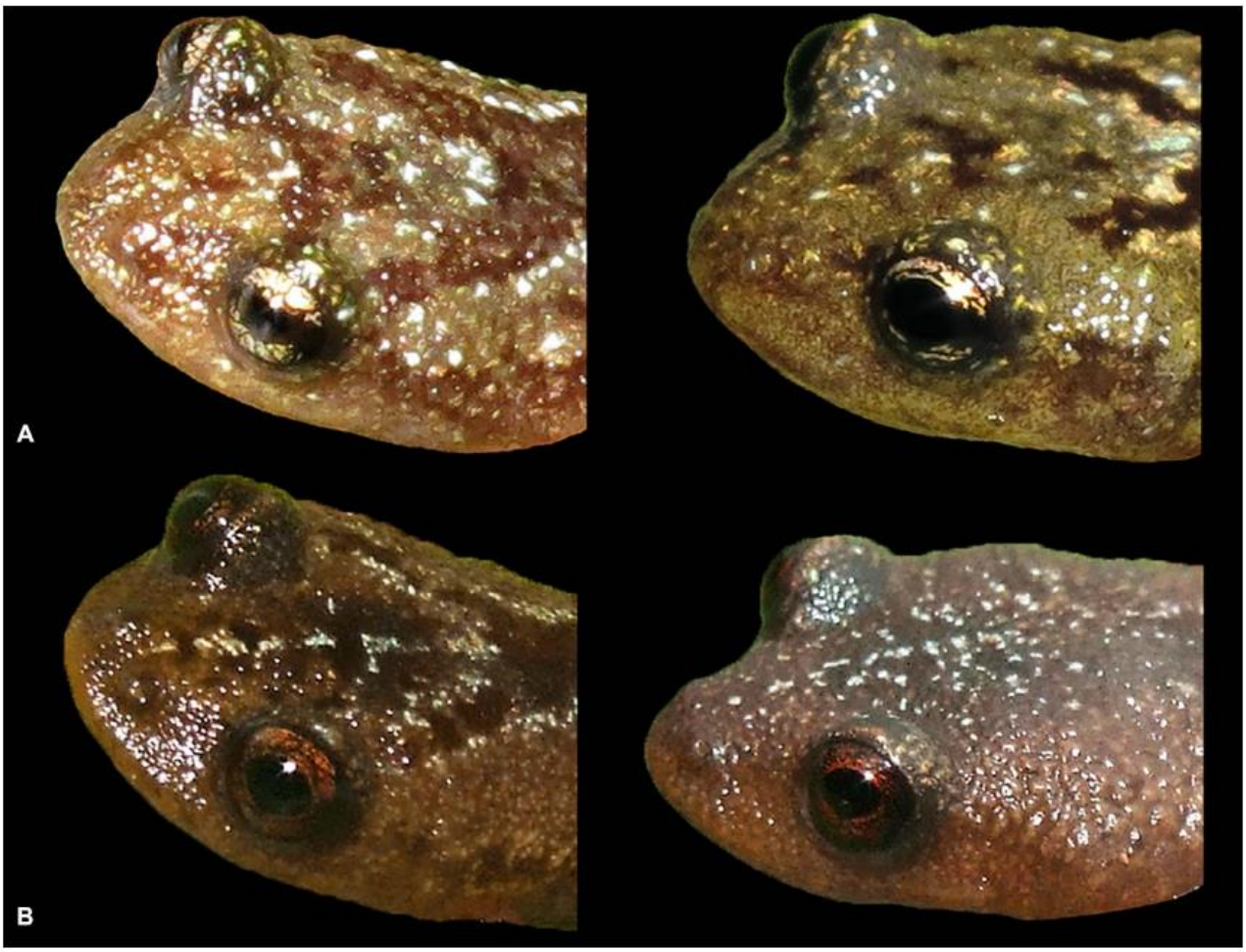


FIG. 16.—Diagnostic character states of iris coloration in life in *Crossodactylodes*. (A) Two specimens of *C. izecksohni*, showing a yellowish iris with dark brown fine reticulations, interrupted by a brown horizontal bar at the pupil level; (B) *C. septentrionalis*, showing a reddish iris with dark brown fine reticulations. The state for this character is unknown for *C. pintoi*. For the states observed in *C. bokermanni* and *C. itambe* refer to Fig. 15. A color version of this figure is available online.

Peixoto 2004a; Teixeira et al. 2013). In fact, *C. bokermanni* is known to occur between 800–1477 m elevations. Haddad et al. (2016b) stated that the species occurs in the Parque Estadual Mata das Flores, municipality of Castelo in the state of Espírito Santo, but we could not find voucher specimens from this locality in taxonomic collections.

**Conservation.**—According to the IUCN Red List, *Crossodactylodes bokermanni* has a decreasing population trend and is listed as Near Threatened (close to qualifying as Vulnerable) due to extent of occurrence <5000 $km^2$ and the probable declining on the extent and quality of habitat (Silvano and Peixoto 2004a). However, due to the extent of occurrence considered by the authors the species should almost qualify as Endangered, not Vulnerable (see IUCN 2019). In the Brazilian Red List, the species was also listed as Near Threatened, but close to qualifying as Endangered (Haddad et al. 2016b). According to these authors, there is no evidence that the species was more abundant in the past. Considering the six records currently known for *C. bokermanni*, our analysis shows an extent of occurrence of 765 $km^2$, with elevation ranging from 218–1718 m. Considering only areas above 700 m (see Materials and Methods), the extent of occurrence has 700 $km^2$, of which 174 $km^2$ are covered by Atlantic Forest remnants and 8 $km^2$ are inside protected areas.

*Crossodactylodes bokermanni* occurs at two strictly protected areas (IUCN category II; Dudley 2008): Reserva Biológica Augusto Ruschi (35.62 $km^2$) and Parque Estadual do Forno Grande (9.13 $km^2$). In addition, the species occurs at the Estação Biológica de Santa Lúcia (4.4 $km^2$). We point out that the main threat to the species is habitat loss in the private properties around the protected areas due to replacement of the forest by monocultures for wood production (*Pinus* and *Eucalyptus*), coffee plantations, and human settlements (Sabagh et al. 2017; Ferreira et al. 2019b). In addition, illegal collection of bromeliads, livestock grazing, logging, tourism (Silvano and Peixoto 2004a; Stuart et al. 2008; Haddad et al. 2016b), and burning (Scardua 2000) might be reducing the breeding habitat of *C. bokermanni*. Thus, following the IUCN (2019) guidelines, the species can be categorized as Near Threatened (close to qualifying as Endangered) due to its limited extent of occurrence (<5000 $km^2$; Criterion B1), fragmented popula-

Downloaded From: https://bioone.org/journals/Herpetological-Monographs on 20 May 2020
Terms of Use: https://bioone.org/terms-of-use Access provided by Universidade Estadual Paulista Julio de Mesquita Filho (UNESP)

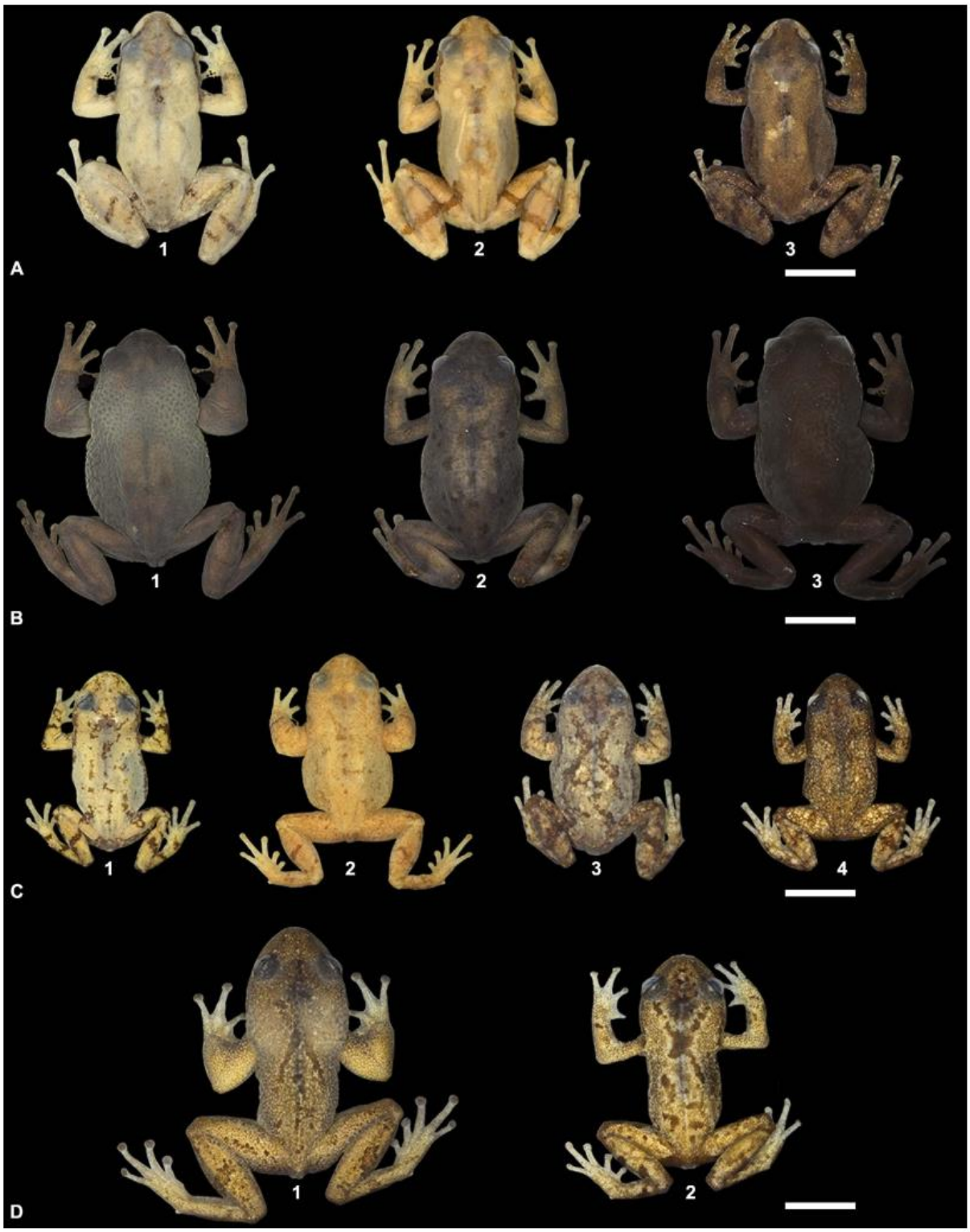


FIG. 17.—Dorsal background coloration in preservative in species of *Crossodactylodes*. (A) In *C. bokermanni*, the coloration varies from pale cream (1) UFMG 13767, pale yellow (2) ZUFRJ 1377, and brown (3) UFMG 14189. (B) In *C. itambe*, can be dark gray (1–2) UFMG 13377, and UFMG 13383, respectively, or brownish black (3) UFMG 11247. (C) In *C. izecksohni*, varies from pale cream (1) UFMG 13749, pale yellow (2) ZUFRJ 1935, and light brown (3–4) UFMG 14175, and UFMG 14216, respectively. (D) In *C. septentrionalis*, can be light brown (1) MZUESC 14363, and cream (2) MZUESC 14364. Note the difference comparing *C. itambe* with the other species. This character is not considered for *C. pintoi*, because all known specimens are faded. Scale bars = 5 mm. A color version of this figure is available online.

Downloaded From: https://bioone.org/journals/Herpetological-Monographs on 20 May 2020
Terms of Use: https://bioone.org/terms-of-use Access provided by Universidade Estadual Paulista Julio de Mesquita Filho (UNESP)

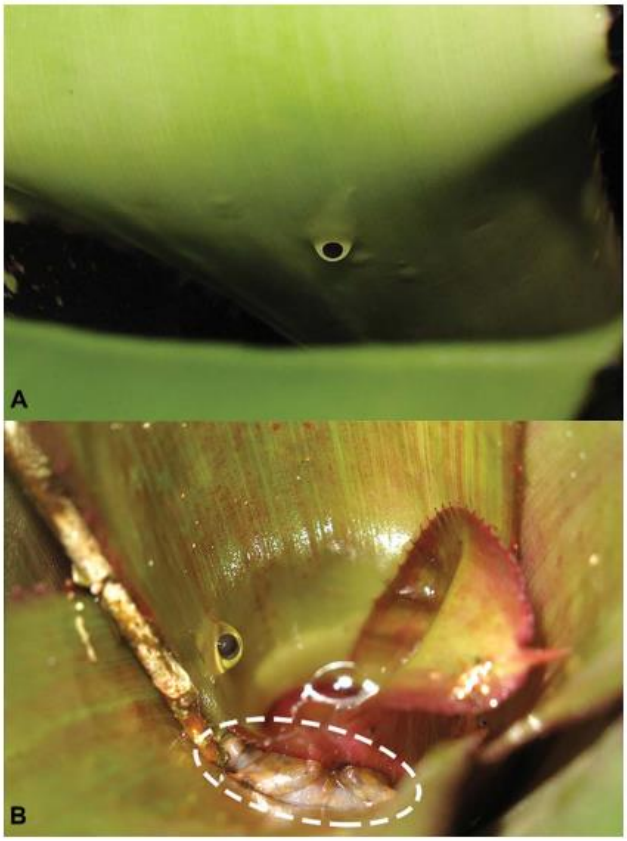


FIG. 18.—A single egg of (A) *C. bokermanni* attached to the abaxial surface of a *Billbergia* sp. from the Parque Estadual do Forno Grande, municipality of Castelo, Espírito Santo State, and of (B) *C. izecksohni* attached to the adaxial surface of a *Aechmea capixabae*, from Alto Santo Antônio, municipality of Santa Teresa, Espírito Santo State. Note the presence of a male (white ellipse), which was sitting alongside the egg, but dove quickly while being photographed. A color version of this figure is available online.

tions (Subcriterion a), and decline on the quality of habitat outside and around protected areas (approaching Subcriterion b[iii]).

**Advertisement call.**—Unknown.

**Tadpole.**—Unknown. The tadpole described by Peixoto (1981) was wrongly attributed to *Crossodactylodes pintoi* (Peixoto 1983) and might belong to either or both *C. bokermanni* or *C. izecksohni*.

**Natural history.**—*Crossodactylodes bokermanni* was found throughout the year inside bromeliads in the montane and submontane ombrophilous rain forest at the northern portion of the Mantiqueira Mountain Range (sensu Gontijo-Pascutti et al. 2012), in the Atlantic Forest domain. In the municipality of Santa Teresa, *C. bokermanni* was recorded in epiphytic (i.e., from 33 cm to 12 m from the ground) and terrestrial bromeliads of the following species: *Billbergia* sp., *Edmundoa lindenii*, *Neoregelia guttata*, *N. macrosepala*, *N. pauciflora*, and *Vriesea bituminosa*. The species was mostly found using large epiphytic bromeliads with many axils (e.g., *V. bituminosa*). In the municipality of Castelo, *C. bokermanni* was recorded in terrestrial and epiphytic bromeliads (i.e., up to 4 m from the ground) exclusively of the genus *Billbergia* (a small-sized bromeliad with few axils), despite the occurrence of several other species of bromeliads in the visited areas.

Individuals of *Crossodactylodes bokermanni* were mostly found partially submerged inside the water accumulated in bromeliads but were also found fully submerged or on the leaf out of the water. Most individuals were found alone or in pairs in the bromeliads. In one occasion, a male was found with two females in a *Billbergia* spp. cluster. The field observations indicate that individuals of *C. bokermanni* are found much more rarely and sparsely than are individuals of *C. izecksohni* and *C. itambe*. In the municipality of Santa Teresa, *C. bokermanni* occurs in sympatry with *C. izecksohni*, but they were not found in syntopy. Females lay single large eggs, positioned isolated from other eggs. Eggs are uniformly dark pigmented, submerged or above the water surface, attached to bromeliad leaves (Fig. 18A).

**Remarks.**—Peixoto (1983) stated that males of *Crossodactylodes bokermanni* have a less modified thumb, compared to males of *C. pintoi*, without specifying in which aspect. Possibly, Peixoto (1983) referred to a higher enlargement of the thumb and a higher number and degree of aggregation of spines on nuptial pads of *C. pintoi*. Our examination indicates that this is valid considering most of the individuals of both species. However, a few males of *C. bokermanni* show a similar thumb to that observed in males of *C. pintoi* and thus this character is not diagnostic between these species. Peixoto (1983) considered the iris in life of *C. bokermanni* black with intense, copper-colored dots while Teixeira et al. (2013) considered that the iris is brown. Our examination of specimens in life indicates that the iris coloration varies from coppery to reddish, with dark brown fine reticulations (Fig. 15A).

*Crossodactylodes izecksohni* Peixoto
Figs. 9C, 10G–I

*Crossodactylodes izecksohni* Peixoto 1983 "1982": Peixoto: 1983:621–622, 625–626. Holotype male (EI 7192, examined in this study) from Alto Santo Antônio, municipality of Santa Teresa, state of Espírito Santo, southeastern Brazil, about 19°54′40.13″S, 40°35′29.37″W, 832 m, collected by O.L. Peixoto and colleagues on 22 December 1980 (O.L. Peixoto, personal communication).

**Referred specimens.**—We examined 45 paratopotypes of *Crossodactylodes izecksohni* including 18 males (EI 7193, 7196, 7198, 7200, 7206–7207, 7209, 7213, 7217, 7220; MZUSP 58080, 58082, 58084, 58086; USNM 221878–221880, 221884) and 27 females (EI 7194–7195, 7197, 7199, 7201–7205, 7208, 7210–7212, 7214–7216, 7218–7219, 7221–7222; MNRJ 4167; MZUSP 58081, 58083, 58085; USNM 221881–221883). To this species we refer 10 additional topotypes including six males (UFMG 397, 13747; ZUFRJ 361, 1400, 1932, 1935) and four females (UFMG 399; ZUFRJ 365, 1392, 1401); 12 males (UFMG 14174–14175, 14177–14181, 14215, 14219–14220, 14222–14223) and 11 females (UFMG 14176, 14182–14186, 14214, 14216–14217, 14221, 14224) from another locality in Alto Santo Antônio, municipality of Santa Teresa, state of Espírito Santo, southeastern Brazil, 19°51′53.28″S, 40°34′39.68″W, 933 m; seven males (MBML 3835–3836, 3977–3979; UFMG 13753, 14030) and four females (MBML 3834; UFMG

Downloaded From: https://bioone.org/journals/Herpetological-Monographs on 20 May 2020
Terms of Use: https://bioone.org/terms-of-use Access provided by Universidade Estadual Paulista Julio de Mesquita Filho (UNESP)

13748–13749, 14029) from hill in front of Escola Superior São Francisco de Assis, municipality of Santa Teresa, state of Espírito Santo, southeastern Brazil, 19°56′01.02″S, 40°35′21.68″W, 770 m; two males (UFMG 14222–14223) and one female (UFMG 14224) from the vicinity of Reserva Biológica Augusto Ruschi, municipality of Santa Teresa, state of Espírito Santo, southeastern Brazil, 19°54′35,97″S, 40°32′9,89″W, 888 m; six males (MBML 3958–3959, 4605, 6784; UFMG 13760, 13791) and five females (MBML 3956–3957; UFMG 13757, 13759, 13793) from Estação Biológica de Santa Lúcia, municipality of Santa Teresa, state of Espírito Santo, southeastern Brazil, 19°57′45.76″S, 40°31′55.66″W, 915 m; and one female (MBML 768) from Nova Lombardia, municipality of Santa Teresa, state of Espírito Santo, southeastern Brazil (not georeferenced).

**Diagnosis.**—*Crossodactylodes izecksohni* is diagnosable from all known congeners by the following combination of characters: (1) thumbs in adult males broadly widened; (2) SVL 10.8–13.9 mm (females) and 10.8–15.0 mm (males); (3) in life, iris yellowish with dark brown fine reticulations, interrupted by a brown horizontal bar at the pupil level; (4) cloacal flap undivided or with a small distal indentation; (5) absence of vomerine odontophores; (6) snout not flattened in lateral view; (7) zygomatic process of squamosal bone short, not passing the anterior margin of the optic foramen; (8) males lacking vocal slits; (9) absence of dorsolateral fold; (10) discs of fingers II–IV slightly expanded; (11) skin on male dorsum coarsely granular; (12) disc of Finger I rounded; (13) medial region of the upper lip not anteriorly projected; (14) in preservative, dorsal background coloration varying from pale cream to pale yellow, or light brown.

**Comparisons.**—*Crossodactylodes izecksohni* is distinguished from its congeners (characters in parentheses) by having thumbs in adult males broadly widened; Fig. 12C (weakly widened in *C. pintoi* [Fig. 12D], *C. bokermanni* [Fig. 12A], and *C. itambe* [Fig. 12B]); iris in life yellowish with dark brown fine reticulations, interrupted by a brown horizontal bar at the pupil level; Fig. 16A (coppery to reddish with dark brown fine reticulations in *C. bokermanni* [Fig. 15A], reddish with dark brown fine reticulations in *C. septentrionalis* [Fig. 16B], uniformly black or brownish black in *C. itambe* [Fig. 15B]); males and females with smaller size, SVL 10.8–13.9 mm in females and 10.8–15.0 mm in males (female SVL = 15.9 mm, males SVL = 16.2–18.0 mm in *C. pintoi*; females SVL = 16.1–16.5 mm, male SVL = 18.6 mm in *C. septentrionalis*; Table 2); females with a smaller size, SVL 10.8–13.9 mm (females SVL = 15.2–18.0 mm in *C. itambe*; Table 2); cloacal flap undivided or with a small indentation; Fig. 13A (bilobed in *C. pintoi* and *C. septentrionalis*; Fig. 13B); absence of vomerine odontophores; Fig. 11B (presence in *C. bokermanni* and *C. septentrionalis*; Fig. 11A); snout not flattened in lateral view; Fig. 10G (flattened in *C. bokermanni* [Fig. 10D] and *C. septentrionalis* [Fig. 11C]); zygomatic process of squamosal bone short, not passing the anterior margin of the optic foramen (long, passing the anterior margin of the optic foramen in *C. septentrionalis* and *C. itambe*; see Teixeira et al. 2013). Additionally, *C. izecksohni* can be distinguished from *C. bokermanni* by the absence of vocal slits in males (presence); absence of dorsolateral fold; Fig. 14B (presence; Fig. 14A); discs of fingers II–IV slightly expanded; Fig. 12C (broadly expanded; Fig. 12A); skin on male dorsum coarsely granular (shagreen). From *C. septentrionalis* by having disc of Finger I rounded; Fig. 12C (acute; Fig. 12E). It differs from *C. itambe* by the absence of anterior projection in the medial region of the upper lip; Fig. 13C (presence; Figs. 11D, 13D); and dorsal background coloration in preservative pale cream, pale yellow, or light brown; Fig. 17C (dark gray or brownish black; Fig. 17B).

**Redescription of the holotype.**—Adult male, SVL 13.4 mm; body slightly robust, dorsoventrally flattened; head wider than long (head width/head length = 1.09); head width 0.43 SVL; head length = 0.40 SVL; snout not flattened, rounded in dorsal and lateral views; eye–nostril distance slightly longer than eye diameter (eye–nostril distance/eye diameter = 1.05); canthus rostralis slightly curved in dorsal view and rounded in cross-section; loreal region slightly concave; nostrils protuberant, elliptical, dorsolaterally directed, opening in the apices of small dermal elevations; interorbital area flat, more than twice as long as eye diameter (interorbital distance/eye diameter = 2.48). Eyes medium-sized and protuberant (eye diameter/head length = 0.23; eye diameter/head width = 0.21), laterally oriented; upper eyelid margin granular, with a nearly elliptic tubercle in its medial region. Tympanic membrane and annulus absent. A poorly developed dermal fold from posterior edge of eye curving downward to arm insertion. Dorsolateral fold absent.

Choanae small, nearly rounded, spaced 1.4 mm from each other. Vomerine odontophores absent. Tongue ovoid, not notched, free behind for about one third of its length. Vocal slits absent; vocal sac externally indistinct. Single, small, tooth-like process present on front of lower jaw with a socket between premaxillae.

Forelimb robust, hypertrophied, lacking fold or fringe; forearm less robust than arm (forearm width/arm width = 0.82); fingers medium-sized; relative length of fingers I < II ≈ IV < III; discs of fingers II–IV slightly expanded, rounded; disc of Finger I rounded, less expanded than the others; fingers II–IV slender; Finger I broadly widened, with nuptial pad formed by strongly aggregate keratinized spines covering most of its lateral margin and dorsal surface (nine spines on left and 10 on right thumbs); subarticular tubercles small, flat, and rounded in ventral view; supernumerary tubercles slightly distinct; inner metacarpal tubercle flat, elliptical; outer metacarpal tubercle large, flat, and nearly round in ventral view; vestigial digital webbing.

Hindlimb medium-sized and moderately robust (thigh length/SVL = 0.39; tibia length/SVL = 0.43); tarsal fold absent; toes long, slender, with slightly expanded and nearly rounded discs, slightly larger than finger discs (fourth toe disc diameter/third finger disc diameter = 1.07); relative length of toes I < II < V < III < IV; subarticular tubercles small, flat, and rounded in ventral view; supernumerary tubercles indistinct; inner metatarsal tubercle large, flat, and elliptical in ventral view; outer metatarsal tubercle small, nearly rounded in ventral view, slightly conical in profile; digital webbing absent.

Skin on dorsal surfaces of head, body and arm, flanks, belly, chest, and ventral surface of arm coarsely granular; skin on dorsal and ventral surfaces of hindlimbs and on throat shagreen. Cloacal opening directed posteriorly, at upper level of thighs, covered by a cloacal flap with a small distal indentation.

Downloaded From: https://bioone.org/journals/Herpetological-Monographs on 20 May 2020
Terms of Use: https://bioone.org/terms-of-use Access provided by Universidade Estadual Paulista Julio de Mesquita Filho (UNESP)

**Measurements of the holotype (in mm).**—SVL 13.4; head length 5.3; head width 5.8; eye diameter 1.2; eye–nostril distance 1.3; nostril–snout distance 0.8; internarial distance 1.2; interorbital distance 3.1; arm length 4.3; forearm length 2.7; hand length 3.4; third finger disk diameter 0.4; thigh length 5.3; tibia length 5.7; tarsal length 3.4; foot length 5.2; fourth toe disk diameter 0.5; arm width 2.0; forearm width 1.6.

**Coloration of the holotype in life.**—Based on description and photographs provided by Peixoto (1983), we could infer that the holotype had cream dorsal surfaces of head, body, and limbs, with scattered brown flecks and blotches. An X-shaped brown blotch extends from the scapular region to the middle third of body; an oblique band of the same color, connected to this blotch, extends into the lumbar region. Flank with a brown band extending from behind the eye to the arm insertion. A brown transverse bar in the wrist; nuptial pads black colored. Hindlimbs with brown marbled blotches and interrupted bands. Venter lighter than the dorsum and with few brown flecks and blotches.

**Coloration of the holotype in preservative.**—The color is faded, turning into pale tones. The cream dorsal surfaces of head, body, and limbs become pale yellow. The brown blotches, flecks, and bands become pale brown and less evident. Venter continues lighter than dorsum. The ventral surfaces of hand and foot are translucent, showing superficial musculature. Eyelid tubercles, carpal, and tarsal tubercles are whitish.

**Variation.**—Snout in lateral view varies from rounded (~67%) to slightly sloping (~33%). The cloacal flap has a small distal indentation (~69%) or is undivided (~31%). The tubercle on medial region of upper eyelid margin is usually present (~70%) but can be absent (~30%). The shape of this tubercle is usually elliptical (~73%) but can be elongated (~27%). Few specimens have 2–4 elliptical tubercles arranged in a line (~11%) or scattered (~4%). Males are distinguished from females by the presence of nuptial pads, hypertrophy of arms and forearms (males arm width/arm length = 0.28–0.54, mean = 0.41; females arm width/arm length = 0.21–0.28, mean = 0.25; and males forearm width/forearm length = 0.46–0.80, mean = 0.61; females forearm width/forearm length = 0.29–0.45, mean = 0.40), and a rougher dorsal skin. In addition, males have wider thumbs than do females. This is possibly related to the presence of a well-developed prepolex in males (see Gomes 1988). The spines on nuptial pads vary in number (from two to 14), size, and degree of aggregation. The number of spines can vary between the right and left thumbs of a same specimen. Males with larger SVL and pronounced hypertrophy of forelimbs have a higher number and aggregation of spines, wider thumbs, and rougher skin.

The coloration pattern in life shows high variation. The dorsal background coloration can be pale pink, pale cream, beige, pale lilac, light brown, brownish gray, pale yellow, and brownish yellow (Fig. S3). Froglets are usually dark brown with numerous small white, bluish, and/or yellowish spots. The pattern of blotches, flecks, bands, and bars is also highly variable. Most specimens have a dorsal X-shaped blotch that can be strongly or weakly marked, continuous, or interrupted, but this blotch can be absent. A few specimens have a black lateral band from posterior corner of the eye to the posterior third of body, but this band is usually incomplete or fragmented. A few specimens have transverse bars on hindlimbs that can be strongly or weakly marked (Fig. S3). In preservative, the dorsal background coloration varies from pale cream, pale yellow, until light brown, and the pattern of blotches, flecks, bands, and bars is also highly variable (Fig. 17C).

**Distribution.**—*Crossodactylodes izecksohni* is known only from the municipality of Santa Teresa in the state of Espírito Santo, from seven sites: (1) Alto Santo Antônio (type locality), about 19°54′40.10″S, 40°35′29.37″W, 843 m (O.L. Peixoto, personal communication); (2) another locality in Alto Santo Antônio 19°51′53.28″S, 40°34′39.68″W, 933 m; (3) hill in front of the Escola Superior São Francisco de Assis (ESFA), 19°56′1.02″S, 40°35′21.68″W, 770 m; (4) Penha district, 19°56′17.45″S, 40°32′56.96″W, 867 m; (5) vicinity of Reserva Biológica Augusto Ruschi, 19°54′35, 97″S, 40°32′9, 89″W, 888 m; (6) Estação Biológica de Santa Lúcia, 19°57′45.76″S, 40°31′55.66″W, 915 m; and (7) Lombardia (not georeferenced data).

Peixoto (1983) used geographic coordinates from the city of Santa Teresa. Other studies used these approximate coordinates, which misleads that *Crossodactylodes izecksohni* occurs between 650–675 m elevation. (Silvano and Peixoto 2004b; Teixeira et al. 2013). In fact, *C. izecksohni* is only known from elevations between 770–933 m.

**Conservation.**—*Crossodactylodes izecksohni* is listed as Near Threatened (close to qualifying as Vulnerable) by the IUCN Red List due to extent of occurrence <5000 $km^2$ and the probable declining on the extent and quality of habitat (Silvano and Peixoto 2004b). However, due to the extent of occurrence considered by the authors, the species should almost qualify as Endangered, not Vulnerable (see IUCN 2019). It is listed as Data Deficient by the Brazilian Red List (Haddad et al. 2016c). These authors erroneously stated that the species has not been found in the last 30 yr, sampling effort has not been enough, and that the extent of occurrence is 435.73 $km^2$. Actually, the species was recorded in 1997, 2005, 2006, 2012, and 2013 (vouchered in MBML), and the sampling effort has been extensively conducted since 2012. Our analysis indicates an extent of occurrence of 39 $km^2$, of which 23 $km^2$ are covered by Atlantic Forest remnants and 12 $km^2$ are inside protected areas with elevations ranging from 689–933 m.

*Crossodactylodes izecksohni* occurs inside and in vicinities of Reserva Biológica Augusto Ruschi (35.62 $km^2$), a strictly protected area (IUCN Category II; Dudley 2008), and in the Estação Biológica de Santa Lúcia (4.4 $km^2$). These areas possibly mitigate negative impacts on lineages A and B, respectively. We point out that the main threat to *C. izecksohni* is habitat loss in the private properties around the protected areas due to wood plantations (*Pinus* and *Eucalyptus*), coffee plantations, and human settlements. In addition, illegal collection of bromeliads for gardening might be reducing the breeding habitat of *C. izecksohni* (Silvano and Peixoto 2004b; Stuart et al. 2008; Haddad et al. 2016c; Sabagh et al. 2017; Ferreira et al. 2019b). Despite these threats, almost 31% of the extent of occurrence of *C. izecksohni* is under protected areas. Therefore, following the IUCN (2019) guidelines, the species can be categorized as Near Threatened (close to qualifying as Critically Endangered) due to its limited extent of occurrence (<100 $km^2$; Criterion B1), fragmented populations (Subcriterion a), and

Downloaded From: https://bioone.org/journals/Herpetological-Monographs on 20 May 2020
Terms of Use: https://bioone.org/terms-of-use Access provided by Universidade Estadual Paulista Julio de Mesquita Filho (UNESP)

decline on the quality of habitat outside and around protected areas (approaching Subcriterion b[iii]).

**Advertisement call.**—*Crossodactylodes izecksohni* call has not been described. Ferreira et al. (2019a) video recorded males calling but the infrared video camera did not record high standard calls.

**Tadpole.**—Unknown. The tadpole described by Peixoto (1981) was wrongly attributed to *Crossodactylodes pintoi* (Peixoto 1983) and might belong to either or both *C. izecksohni* or *C. bokermanni*.

**Natural history.**—The natural history of *Crossodactylodes izecksohni* was described in detail by Ferreira et al. (2019a). A photograph of a single egg of *C. izecksohni* is provided (Fig. 18B) for comparison with the egg of *C. bokermanni*.

**Remarks.**—Teixeira et al. (2013) stated that the iris of *Crossodactylodes izecksohni* is brown. However, our examination indicates that the iris coloration is yellowish with dark brown fine reticulations, interrupted by a brown horizontal bar at the pupil level (Fig. 16A).

*Crossodactylodes septentrionalis* Teixeira, Recoder, Amaro, Damasceno, Cassimiro, and Rodrigues

*Crossodactylodes septentrionalis* Teixeira, Recoder, Amaro, Damasceno, Cassimiro, and Rodrigues 2013: Teixeira et al. 2013:461–469. Holotype female (MZUSP 150209, examined in this study) from Peito de Moça, Parque Nacional da Serra das Lontras, municipality of Arataca, state of Bahia, northeastern Brazil, 15°9′47.68″S, 39°20′34.03″W, 931 m, collected by M. Teixeira, Jr., R.S, Recoder, R.C Amaro, R.P. Damasceno, J. Cassimiro, and M.T. Rodrigues on 6 March 2009.

**Referred specimens.**—We examined two topotypes of *Crossodactylodes septentrionalis*, one male (MZUESC 14363) and one female (MZUESC 14364).

**Diagnosis.**—*Crossodactylodes septentrionalis* is diagnosable from all congeners by the following combination of characters: (1) disc of Finger I acute (no apparent disc); (2) zygomatic process of squamosal bone long, passing the anterior margin of the optic foramen; (3) thumbs in adult males broadly widened; (4) presence of vomerine odontophores; (5) snout flattened in lateral view; (6) cloacal flap bilobed; (7) in life, iris reddish with dark brown fine reticulations; (8) males lacking vocal slits; (9) absence of dorsolateral fold; (10) discs of fingers II–IV slightly expanded; (11) absence of a black canthal stripe; (12) absence of a black lateral band from posterior corner of the eye to the posterior third of body; (13) hindlimbs lacking transverse bars; (14) skin on male dorsum coarsely granular; (15) SVL 16.1–16.5 mm (females) and 18.6 mm (male); (16) medial region of the upper lip not anteriorly projected; (17) in preservative, dorsal background coloration varying from light brown to cream.

**Comparisons.**—*Crossodactylodes septentrionalis* is distinguished from its congeners (characters in parentheses) by having disc of Finger I acute; Fig. 12E (rounded in *C. pintoi*, *C. bokermanni*, *C. izecksohni*, and *C. itambe*; Figs. 12A–D); zygomatic process of squamosal bone long, passing the anterior margin of the optic foramen (short, not passing the anterior margin of the optic foramen in *C. pintoi*, *C. bokermanni*, and *C. izecksohni*; see Teixeira et al. 2013); thumbs in adult males broadly widened; Fig. 12E (weakly widened in *C. pintoi*, Fig. 12D; *C. bokermanni*, Fig. 12A; and *C. itambe*, Fig. 12B); presence of vomerine odontophores; Fig. 11A (absence in *C. pintoi*, *C. izecksohni*, and *C. itambe*; Fig. 11B); snout flattened in lateral view; Fig. 11C (not flattened in *C. pintoi*, Fig. 10A; *C. izecksohni*, Fig. 10G; and *C. itambe*, Fig. 11D); cloacal flap bilobed; Fig. 13B (undivided or with a small indentation in *C. izecksohni* and *C. itambe*; Fig. 13A); iris in life reddish with dark brown fine reticulations; Fig. 16B (yellowish with dark brown fine reticulations, interrupted by a brown horizontal bar at the pupil level in *C. izecksohni*, Fig. 16A; uniformly black or brownish black in *C. itambe*, Fig. 15B). Additionally, *C. septentrionalis* can be distinguished from *C. bokermanni* by the absence of vocal slits in males (presence); discs of fingers II–IV slightly expanded; Fig. 12E (broadly expanded; Fig. 12A); absence of dorsolateral fold; Fig. 14B (presence; Fig. 14A); absence of a black canthal stripe; Fig. 14B (presence; Fig. 14A); absence of a black lateral band from posterior corner of the eye to the posterior third of body; Fig. 14B (presence; Fig. 14A); absence of black transverse bars on hindlimbs; Fig. 14B (presence; Fig. 14A); and skin on male dorsum coarsely granular (shagreen). From *C. izecksohni* by its larger size, with SVL 16.1–16.5 mm in females and 18.6 mm in male (females SVL = 10.8–13.9 mm; males SVL = 10.8–15.0 mm; Table 2). It differs from *C. itambe* by the absence of anterior projection in the medial region of the upper lip; Fig. 13C (presence; Figs. 11D, 13D); and dorsal background coloration in preservative light brown or cream; Fig. 17D (dark gray or brownish black; Fig. 17B).

**Description of the holotype.**—See Teixeira et al. (2013).

**Variation.**—The separation between the two lobes of cloacal flap can be strongly (MZUESC 14363; MZUSP 150209) or moderately developed (MZUESC 14364). A tubercle on medial region of upper eyelid margin can be present (MZUESC 14363–14364) or absent (MZUSP 150209). The shape of this tubercle can be elliptical (MZUESC 14364) or elongated (MZUESC 14363). The only known male (MZUESC 14363) is distinguished from females by the presence of nuptial pads formed by regularly spaced keratinized spines covering most of the lateral margin and dorsal surface of thumbs (nine spines on each thumb) and by hypertrophy of arms and forearms (male arm width/arm length = 0.39; females arm width/arm length = 0.23–0.24; and male forearm width/forearm length = 0.66; females forearm width/forearm length = 0.34–0.35). In addition, the male has rougher dorsal skin and wider thumbs than a female.

**Distribution.**—*Crossodactylodes septentrionalis* is known only from the type locality at Peito de Moça in the Parque Nacional da Serra das Lontras, 15°09′47.68″S, 39°20′34.03″W, 931 m, municipality of Arataca, in the state of Bahia, northeastern Brazil (Fig. 8).

**Conservation.**—*Crossodactylodes septentrionalis* has not been assessed by the IUCN and Brazilian red lists. So far, only three adult specimens have been recorded from Peito de Moça summit in the Parque Nacional da Serra das Lontras, a strictly protected area of 113.36 km$^2$ (IUCN category II; Dudley 2008). Another eight mountainous sites (above 700 m) in the Atlantic Forest of the state of Bahia were surveyed by IRD, sampling at least 50 h/person in each

Downloaded From: https://bioone.org/journals/Herpetological-Monographs on 20 May 2020
Terms of Use: https://bioone.org/terms-of-use Access provided by Universidade Estadual Paulista Julio de Mesquita Filho (UNESP)

area (Fig. S4). In one of these sites (Reserva Particular do Patrimônio Natural Serra Bonita), a sampling effort of ~16 mo was performed (see Dias et al. 2014). Bromeliads were inspected in all sites, but no other specimen of *C. septentrionalis* was found. Thus, the known area of occupancy of the species is ~4 $km^2$.

The type locality of *Crossodactylodes septentrionalis* is quite distinct from the other visited sites and also from the surrounding forest areas in the Parque Nacional da Serra das Lontras. At the type locality, the vegetation develops over a rocky formation composed predominantly of low-height trees with a high abundance of epiphytes (lichens, mosses, and bromeliads). Although the species occurs in a strictly protected area, the available data on geographic distribution, ecological requirements, and possible threats are insufficient to classify the taxon into a category. Thus, *C. septentrionalis* can be categorized as Data Deficient.

**Advertisement call.**—Unknown.

**Tadpole.**—Unknown.

**Natural history.**—All known specimens of *Crossodactylodes septentrionalis* were found in the bromeliad *Vriesea dictyographa*, a species recorded from few highland areas, being endemic to the Atlantic Forest of Bahia State (Martinelli et al. 2008). A female (MZUESC 14364), a male (MZUESC 14363), and a tadpole of *C. septentrionalis* were found together in an ~1-m diameter bromeliad partially exposed to the sun at ~1 m above the ground. Four froglets were found together in a bromeliad at 1.5 m above the ground and 15–20 m apart from the bromeliad where the adults were found. In a neighboring bromeliad, two tadpoles were found at ~2.5 m above the ground. All the tadpoles were lost in the field. Apparently, *C. septentrionalis* has low abundance or prefers high canopy bromeliads.

**Remarks.**—*Crossodactylodes septentrionalis* has an iris in vivid red with dark brown fine reticulations (instead of only vivid red as in Teixeira et al. 2013). Some characters used by Teixeira et al. (2013) to distinguish *C. septentrionalis* from other species show polymorphisms. The SVL of *C. septentrionalis* is only larger than *C. izecksohni* (instead of *C. bokermanni* and *C. izecksohni*). The absence of well-defined bars pattern on hindlimb distinguish *C. septentrionalis* only from *C. bokermanni* (instead of *C. bokermanni* and *C. izecksohni*) because this character is polymorphic in *C. izecksohni*.

*Crossodactylodes itambe* Barata, Santos, Leite, and Garcia

*Crossodactylodes itambe* Barata, Santos, Leite, and Garcia 2013: Barata et al. 2013:553–559. Holotype male (UFMG 11239, examined in this study) from Parque Estadual do Pico do Itambé, municipality of Santo Antônio do Itambé, state of Minas Gerais, southeastern Brazil, 18°23′53.1″S, 43°20′39.6″W, 1921 m, collected by I.M. Barata, C.M. Correia, and R. Ancântara on 13 January 2010.

**Referred specimens.**—We examined 24 paratopotypes of *Crossodactylodes itambe* including 10 males (UFMG 11241–11242, 11244, 11247, 11249, 13375, 13377, 13379, 13382, 13384) and 14 females (UFMG 11236–11238, 11240, 11243, 11245–11246, 13376, 13378, 13380–13381, 13383, 13385, 13387). To this species we refer 10 additional topotypes including six males (UFMG 14031–14036) and four females (UFMG 14037–14040).

**Diagnosis.**—*Crossodactylodes itambe* is diagnosable from all known congeners by the following combination of characters: (1) medial region of the upper lip anteriorly projected; (2) in preservative, dorsal background coloration varying from dark gray to brownish black; (3) zygomatic process of squamosal bone long, passing the anterior margin of the optic foramen; (4) in life, iris uniformly black or brownish black; (5) cloacal flap undivided or with a small distal indentation; (6) absence of vomerine odontophores; (7) snout not flattened in lateral view; (8) thumbs in adult males weakly widened; (9) males lacking vocal slits; (10) absence of dorsolateral fold; (11) discs of fingers II–IV slightly expanded; (12) absence of a black canthal stripe; (13) absence of a black lateral band from posterior corner of the eye to the posterior third of body; (14) hindlimbs lacking transverse bars; (15) skin on male dorsum coarsely granular; (16) SVL 15.2–18.0 mm (females) and 14.0–17.9 mm (males); (17) disc of Finger I rounded.

**Comparisons.**—*Crossodactylodes itambe* is distinguished from its congeners (characters in parentheses) by having medial region of the upper lip anteriorly projected; Figs. 11D, 13D (not anteriorly projected in *C. pintoi*, *C. bokermanni*, *C. izecksohni*, and *C. septentrionalis*; Fig. 13C); dorsal background coloration in preservative dark gray or brownish black; Fig. 17B (pale cream, pale yellow, or brown in *C. bokermanni*, Fig. 17A; pale cream, pale yellow, or light brown in *C. izecksohni*, Fig. 17C; light brown or cream in *C. septentrionalis*, Fig. 17D); iris in life uniformly black or brownish black; Fig. 15B (coppery to reddish with dark brown fine reticulations in *C. bokermanni*, Fig. 15A; yellowish with dark brown fine reticulations, interrupted by a brown horizontal bar at the pupil level in *C. izecksohni*, Fig. 16A; reddish with dark brown fine reticulations in *C. septentrionalis*, Fig. 16B); zygomatic process of squamosal bone long, passing the anterior margin of the optic foramen (short, not passing the anterior margin of the optic foramen in *C. pintoi*, *C. bokermanni*, and *C. izecksohni*; see Teixeira et al. 2013); cloacal flap undivided or with a small distal indentation, Fig. 13A (bilobed in *C. pintoi* and *C. septentrionalis*; Fig. 13B); thumbs in adult males weakly widened, Fig. 12B (broadly widened in *C. izecksohni*, Fig. 12C; and *C. septentrionalis*, Fig. 12E); absence of vomerine odontophores, Fig. 11B (presence in *C. bokermanni* and *C. septentrionalis*, Fig. 11A); snout not flattened in lateral view; Fig. 11D (flattened in *C. bokermanni*, Fig. 10D; and *C. septentrionalis*, Fig. 11C). Additionally, *C. itambe* can be distinguished from *C. bokermanni* by the absence of vocal slits in males (presence); discs of fingers II–IV slightly expanded; Fig. 12B (broadly expanded; Fig. 12A); absence of a dorsolateral fold; Fig. 14B (presence; Fig. 14A); absence of a black canthal stripe; Fig. 14B (presence; Fig. 14A); absence of a black lateral band from posterior corner of the eye to the posterior third of body; Fig. 14B (presence; Fig. 14A); absence of black transverse bars on hindlimbs; Fig. 14B (presence; Fig. 14A); skin on male dorsum coarsely granular (shagreen). From *C. izecksohni* by females with larger size, SVL 15.2–18.0 mm (females SVL = 10.8–13.9 mm; Table 2). It differs from *C. septentrionalis* by having disc of Finger I rounded; Fig. 12B (acute; Fig. 12E).

**Description of the holotype.**—See Barata et al. (2013).

Downloaded From: https://bioone.org/journals/Herpetological-Monographs on 20 May 2020
Terms of Use: https://bioone.org/terms-of-use Access provided by Universidade Estadual Paulista Julio de Mesquita Filho (UNESP)

**Variation.**—The cloacal flap is usually undivided (~71%) but can have a small distal indentation (~29%). A tubercle on medial region of upper eyelid margin can be absent (~60%) or present (~40%). When present, this tubercle can be elongated (~57%) or elliptical (~43%). Few specimens have 2–3 elliptical tubercles arranged in a line (~6%). For differences between males and females, and other variations, see Barata et al. (2013).

**Distribution.**—*Crossodactylodes itambe* is known only from its type locality at Itambé summit in the Parque Estadual do Pico do Itambé, 18°23′53.1″S, 43°20′39.6″W, 1921 m, municipality of Santo Antônio do Itambé, in the state of Minas Gerais, southeastern Brazil (Fig. 8).

**Conservation.**—*Crossodactylodes itambe* has not been assessed by the IUCN and is listed as Data Deficient in the Brazilian Red List (Haddad et al. 2016d). The Itambé summit (type locality) is a singular environment within the Espinhaço Range due to its high elevation, humid microclimate, and high abundance of bromeliads (Barata et al. 2013). The most similar nearby area is the Pico Dois Irmãos (18°12′27.84″S; 43°18′36.60″W, ~1800 m) in the Parque Estadual do Rio Preto, at the boundaries of the municipalities of São Gonçalo do Rio Preto and Felício dos Santos in the state of Minas Gerais. This site is ~20 km distant from the type locality and harbors the same species of bromeliad (*Vriesea medusa*) which *C. itambe* inhabits. This bromeliad is only known from these two localities (Versieux et al. 2010). Fieldwork was conducted by MTTS on March 2015 at the Pico Dois Irmãos, surveying bromeliads, and he did not find any individual of *C. itambe*. The same locality was visited by another researcher in 2015 and 2017, who also did not find any individual (I. Barata, personal communication).

Occasional fires could lead to continuous decline in the area, extent and/or quality of habitat of *Crossodactylodes itambe*, even the species occurring in a strictly protected area (Barata et al. 2013, 2018b). Indeed, in November 2015, a fire destroyed natural vegetation at the Itambé summit (S.J. Duarte, personal communication) and burned part of the reproductive habitat of *C. itambe* (i.e., clumps of bromeliads). The species is known only from a single location, thus having a very small extent of occurrence and area of occupancy (i.e., 4 $km^2$) in an environment which was and still could be threatened by fires. Therefore, following the IUCN (2019) guidelines, *C. itambe* can be listed as Critically Endangered under criteria B1ab(iii) and B2ab(iii), as previously suggested by Barata et al. (2018b).

**Advertisement call.**—Barata et al. (2018a) have reported that *Crossodactylodes itambe* exhibits calling activity but have not recorded the call.

**Tadpole.**—Tadpole was described by Santos et al. (2017).

**Natural history.**—See Barata et al. (2013), Santos et al. (2017), Barata et al. (2018a,b).

**Remarks.**—Some morphological characters used by Barata et al. (2013) to distinguish *Crossodactylodes itambe* from other species are misinterpreted or polymorphic. The absence of marks on the dorsum and limbs cannot be used to distinguish *C. itambe* from *C. izecksohni* because a few specimens of *C. izecksohni* have no marks. The absence of vocal sac cannot distinguish *C. itambe* from *C. pinto*i (see Remarks of *C. pintoi*).

## KEY TO SPECIES OF *CROSSODACTYLODES*

1a. Males with vocal slits; fingers II–IV broadly expanded (Fig. 12A); presence of dorsolateral fold (Fig. 14A)..... *C. bokermanni*

1b. Males lacking vocal slits; fingers II–IV slightly expanded (Figs. 12B–E); absence of dorsolateral fold (Fig. 14B)..... 2

2a. Presence of vomerine odontophores (Fig. 11A); disc of Finger I acute (no apparent disc; Fig. 12E)..... *C. septentrionalis*

2b. Absence of vomerine odontophores (Fig. 11B); disc of Finger I rounded (Figs. 12A–D)..... 3

3a. Medial region of the upper lip anteriorly projected (Figs. 11D, 13D)..... *C. itambe*

3b. Medial region of the upper lip not anteriorly projected (Fig. 13C)..... 4

4a. Thumbs in adult males broadly widened (Fig. 12C); cloacal flap undivided or with a small distal indentation (Fig. 13A)..... *C. izecksohni*

4b. Thumbs in adult males weakly widened (Fig. 12D); cloacal flap bilobed (Fig. 13B)..... *C. pintoi*

## DISCUSSION

We recovered *Crossodactylodes* as a monophyletic and unambiguously supported clade, in accordance with the two previous phylogenetic hypotheses (Fouquet et al. 2013; Teixeira et al. 2013). We also recovered a monophyletic Paratelmatobiinae, and the relationships among the four genera were consistent with the two analyses that included all of them (Fouquet et al. 2013; Faivovich et al. 2014). We found a well-supported position of *Rupirana* as the sister taxon of the remaining Paratelmatobiinae in the Bayesian analysis, with 100% posterior probability. Nevertheless, this relationship was poorly supported in the parsimony analysis, with a jackknife frequency <50% (Fig. 1; Fig. S1). These methods tend to differ considerably, with an underestimation of support values by jackknife and an overestimation by the Bayesian method (Simmons et al. 2004). Moreover, these support indices are not directly comparable (Simmons et al. 2004), especially in our analyses in which each index was based on a distinct method of phylogenetic reconstruction. The same phylogenetic placement for *Rupirana* was recovered with high support under other parsimony and Bayesian analyses (Fouquet et al. 2013; Faivovich et al. 2014). This may be a result of differences in taxon and character sampling, as these authors used few terminals of Paratelmatobiinae but a considerably larger outgroup sampling and a larger number of nDNA fragments.

Similar to other phylogenetic hypotheses, we recovered the subfamily Leptodactylinae as the sister taxon of Paratelmatobiinae (Fouquet et al. 2013, complete matrix approach; Faivovich et al. 2014). However, other analyses recovered Paratelmatobiinae as the sister taxon of Leiuperinae (Pyron and Wiens 2011) or as the sister taxon of Leiuperinae plus Leptodactylinae (Fouquet et al. 2013, super matrix approach; Pyron 2014), but with low support values. These studies employed a more comprehensive coverage of outgroups and a larger number of DNA fragments but used fewer sequences of Paratelmatobiinae and have more missing data per species on average. Moreover, Pyron and Wiens (2011) and Pyron (2014)

Downloaded From: https://bioone.org/journals/Herpetological-Monographs on 20 May 2020
Terms of Use: https://bioone.org/terms-of-use Access provided by Universidade Estadual Paulista Julio de Mesquita Filho (UNESP)

employed the maximum likelihood method of phylogenetic reconstruction. All these methodological differences might explain the contrasting results.

Within *Crossodactylodes*, we recovered *C. bokermanni* as the sister taxon of the remaining species (Fig. 1), in accordance with Teixeira et al. (2013). This phylogenetic placement is consistent with the distinct morphology of *C. bokermanni* in comparison with congeners. Some of the morphological diagnostic characters of *C. bokermanni* seem to be plesiomorphic among Paratelmatobiinae (e.g., presence of dorsolateral fold, skin on male dorsum shagreen, and presence of vocal slits). Also, *C. bokermanni* seems to be ecologically distinct by having sparse distribution and low population abundance and by selecting epiphyte bromeliads in higher vertical strata. The higher expansion on finger II–IV discs found in the species (Fig. 12A) is likely an adaptation to arboreality.

*Crossodactylodes pintoi* was strongly supported as part of a clade which also includes *C. itambe*, *C. septentrionalis*, and *C. izecksohni* (Fig. S2) and shares three putative morphological synapomorphies with these species: absence of vocal slit, absence of dorsolateral fold, and coarsely granular skin texture of males (Appendices III, IV). However, the phylogenetic relationships within this clade were not fully resolved and should be further investigated, either by means of DNA sequences of *C. pintoi* from historical museum specimens (see Rowe et al. 2011) or by incorporating a more robust phenotypic dataset in phylogenetic reconstruction.

The subfamily Paratelmatobiinae is a morphologically diverse group of frogs, with remarkable characters distinguishing the genera (e.g., presence of numerous white tubercles on males' dorsum in *Rupirana*; presence of a meniscus on the upper iris in *Scythrophrys*; presence of well-developed and flexible fringes or webs on foot in *Paratelmatobius*; and nuptial pads of males formed by few and well-developed keratinized spines in *Crossodactylodes*; Figs. 2–6; Appendices III, IV). Stochastic events associated with the long divergence times between the genera (Fouquet et al. 2013), and the divergent selection associated with different habitats or environments in which the genera occur (i.e., shallow temporary ponds and backwaters in campo rupestre in *Rupirana*; temporary ponds and backwaters in forest areas in *Scythrophrys* and *Paratelmatobius*; and bromeliads in forest areas or campo rupestre in *Crossodactylodes*), might explain these differences. *Crossodactylodes* exhibits a life cycle strictly associated with bromeliads, which is a synapomorphic character within Leptodactylidae (Fouquet et al. 2013; this study). Some of the putative morphological synapomorphies that we found for the genus (Figs. 2–6; Appendices III, IV) seem to be related to this bromeligenous habit. The expanded discs on fingers and the lack of lateral ridges, fringes, or webs on toes seem to be adaptations to a distinct locomotor mode (i.e., slow walking on bromeliad leaves). On the other hand, other Paratelmatobiinae have narrow discs on fingers and the presence of lateral ridges, fringes, or webs on toes, which seem to be adaptions to semiaquatic habits (to varying degrees). The decrease in foot length in *Crossodactylodes*, compared with other Paratelmatobiinae (Fig. 7), might also be related to the distinct locomotor mode. A smaller foot might perform better while walking whereas a larger foot might favor higher propulsive forces during swimming and jumping (Emerson 1978; Pough 2007).

The absence of columella was already reported for *Crossodactylodes pintoi*, *C. bokermanni*, *C. izecksohni*, and *C. septentrionalis* (Lynch 1971; Gomes 1988; Teixeira et al. 2013) and we report it for *C. itambe* (Fig. 6C). Based on examination of external morphology, dissection of the skin on the lateral head of some specimens, and following the assumption of Pereyra et al. (2016), i.e., absence of columella implies absence of tympanic annulus and tympanic membrane, we consider the tympanic middle ear as completely lacking in all species of *Crossodactylodes*. This is another putative synapomorphy for the genus (Figs. 2, 5, 6; Appendices III, IV). However, among other Paratelmatobiinae, the absence of columella was reported for *Paratelmatobius lutzii* (Lynch 1971), and the knowledge of the phylogenetic placement of this species is important for a more accurate optimization of this character (Pereyra et al. 2016). Extratympanic hearing pathways were already reported for many species of different anuran families (Pereyra et al. 2016). In *Crossodactylodes* it might be related to the evolution of a different type of communication associated with breeding in bromeliads, as at least *C. izecksohni* and *C. itambe* are known to exhibit calling activity (Barata et al. 2018a; Ferreira et al. 2019a).

The nuptial pad formed by a few, well-developed spines (Figs. 2, 3A; Appendices III, IV) is another putative synapomorphy of *Crossodactylodes* (Fouquet et al. 2013; this study). Agonistic encounters between males were reported for *C. izecksohni* (Ferreira et al. 2019a). Therefore, this character seems to be associated with territoriality. Bromeliads, tree holes, and pools in torrential streams are limited resources which select males with the ability to defend them (e.g., Mendelson et al. 2008; Magalhães et al. 2018; Ferreira et al. 2019a). Territorial males usually have secondary sexual characters such as tusks, spines, odontids, keratinized nuptial pads, and hypertrophied forearms (Kupfer 2007); these last two are present in *Crossodactylodes*. However, the spines can also be used to attack potential predators of eggs and tadpoles, as *C. izecksohni* and *C. itambe* are known to exhibit egg and/or tadpole guarding behavior (Santos et al. 2017; Ferreira et al. 2019a). Therefore, both territoriality and parental care might be related to the evolution of the different type of nuptial pad in *Crossodactylodes* males. In addition, *C. izecksohni* females have also been observed displaying egg and tadpole guarding as well as in female–female combat (Ferreira et al. 2019a). The deposition of single eggs positioned isolated from other eggs, another putative synapomorphy of *Crossodactylodes* (Figs. 2, 18; Appendices III, IV), is another indication of high maternal investment and parental care (Santos et al. 2017; Ferreira et al. 2019a).

The sexual dimorphism related to hypertrophy of arms and forearms is more accentuated in *Crossodactylodes izecksohni* and *C. itambe* than it is in *C. bokermanni* (Table 2). This dimorphism seems also to be accentuated in *C. pintoi* and *C. septentrionalis*, but a higher number of specimens need to be analyzed for confirmation. In addition, *C. izecksohni* and *C. itambe* were found in higher abundance, with aggregations of individuals occupying the same bromeliad or bromeliad patch (Santos et al. 2017; Ferreira et al. 2019a). This favors agonistic encounters which

Downloaded From: https://bioone.org/journals/Herpetological-Monographs on 20 May 2020
Terms of Use: https://bioone.org/terms-of-use Access provided by Universidade Estadual Paulista Julio de Mesquita Filho (UNESP)

probably increase the selective pressure on characters related to territoriality. Therefore, we hypothesize that territoriality might be an important issue in the evolution and diversification of the clade comprising *C. izecksohni*, *C. itambe*, *C. septentrionalis*, and *C. pintoi*.

We found high genetic distances and striking relationships among lineages within both *Crossodactylodes bokermanni* and *C. izecksohni* (Fig. 1; Table 1; Appendices VI, VII). In *C. bokermanni*, Lineage A is more closely related to Lineage B (which occurs ~85 km apart) than to Lineage C (which occurs ~5 km apart; Figs. 1, 8). In *C. izecksohni*, we found two distinct lineages which occur ~5 km apart (Figs. 1, 8). Fouquet et al. (2007) suggested a mean genetic distance of 3% for 16S rDNA to identify lineages that could correspond to candidate species in Neotropical frogs. The distances between Lineages A and C and Lineages B and C of *C. bokermanni*, and between Lineages A and B of *C. izecksohni*, are above this threshold (Table 1). In addition, these same distances are similar to some interspecific distances (e.g., between *C. itambe* and Lineage A of *C. izecksohni* and between *C. itambe* and *C. septentrio*nalis) and much higher than all other intraspecific or intralineage distances (Table 1). The same pattern occurs in the other mtDNA fragments (Appendices VI, VII). Although thresholds for species recognition based in genetic distances are arbitrary because different phenomena drive the evolutionary processes in different species (Padial et al. 2009), the mtDNA distances among these lineages are unexpectedly high considering the small geographic distances separating them. The small body size and the occurrence in topographically complex forests have been associated with high genetic divergences in other taxa of tropical anurans (Pabijan et al. 2012; Rodríguez et al. 2015). In *Crossodactylodes*, the high genetic distances might be related to ecological barriers to gene flow associated with a high concentration of bromeliads in mountaintops and unfavorable conditions in depressions, forming islands with low connectivity. This type of isolation in highland environments was already reported for other Atlantic Forest anurans (Pie et al. 2018; Ramos et al. 2019). Alternatively, this might be related to multiple bottlenecks or founder events, isolating lineages which previously had a continuous distribution, as observed for some African montane frogs (Lawson et al. 2015). These scenarios (i.e., gradual isolation or bottlenecks/founder events) could be tested with a more extensive sampling using demographic simulations (Knowles 2009).

Despite the high genetic divergences among the lineages within *Crossodactylodes bokermanni* and *C. izecksohni*, we did not detect morphological characters distinguishing them. For this reason, we considered that these lineages are deep conspecific lineages (sensu Padial et al. 2010). However, we suggest further investigation using alternative character systems and methods such as a multispecies coalescent in an integrative taxonomic approach (Fujita et al. 2012). Acoustic and larval characters, which are poorly known for *Crossodactylodes*, may provide the alternative source of characters for a more accurate identification of these lineages. These characters constitute important sources of evidence to delimit cryptic species in anurans (Randrianiaina et al. 2009; Grosjean et al. 2015; Köhler et al. 2017). Furthermore, samples from more localities will be required to discern between true allopatry or extremes of clinal variation.

Moreover, and in addition to the possible morphologically cryptic species, the high discontinuity among the geographic range of the different species of *Crossodactylodes*, associated with the recent findings of new species and populations (Teixeira et al. 2013; Barata et al. 2013; this study), indicate that the real diversity within the genus might be underestimated. The geographic distribution of the genus resembles that of other taxa of small-sized anurans with a high proportion of narrow endemic species associated with highland forest islands (e.g., *Brachycephalus* Fitzinger 1826; *Ischnocnema venancioi* species series; and *Paratelmatobius* [Pie et al. 2013; Taucce et al. 2018; Santos et al. 2019, respectively]). In *Brachycephalus*, 22 of its 36 constituent species were described in the last 10 yr (Frost 2019).

The phylogenetic placement of *Crossodactylodes itambe* (Figs. 1, 2), the only nonforest species of the genus, suggests that the common ancestor of *Crossodactylodes* inhabited forests and the colonization of campo rupestre was secondary. *Crossodactylodes itambe* was recovered as the sister taxon of *C. septentrionalis* (Fig. 1), indicating a close relationship between campo rupestre and southern Bahia Atlantic Forest. This relation was also reported by Ramos et al. (2019) based on the close relationships between the treefrog *Pithecopus megacephalus* (Miranda-Ribeiro 1926), endemic from campo rupestre, and one lineage of *P. rohdei* (Mertens 1926) that occurs on southern Bahia. On the other hand, Sabbag et al. (2018) found that the rock frog *Thoropa megatympanum* Caramaschi and Sazima 1984, another endemic species from campo rupestre, diverged after *T. saxatilis* Cocroft and Heyer 1988 from southern Atlantic Forest and before a clade comprising lineages from southeastern and northeastern Atlantic Forest, including one inhabiting southern Bahia. Our results support the idea that at least part of the endemic anuran fauna from campo rupestre originates from Atlantic Forest ancestors, even though the relationships between these two regions are complex.

The genus *Crossodactylodes* is distributed in highland forest islands in the Atlantic Forest domain and in one location in the campo rupestre of the Espinhaço Range (Fig. 8). According to current knowledge, all species are restricted to very small geographic ranges (i.e., *C. pintoi*, *C. itambe*, and *C. septentrionalis* are known only from their type locality; and the predicted extent of occurrence is 174 $km^2$ for *C. bokermanni*, and 23 $km^2$ for *C. izecksohni*). Both the Atlantic Forest domain and the campo rupestre of the Espinhaço Range are considered very endangered environments (Myers et al. 2000; Silveira et al. 2016). Among the threats to global amphibian conservation, habitat loss and fragmentation are considered the most prominent (Cushman 2006; Stuart et al. 2008), as they lead to isolation of populations and loss of genetic diversity (Weeks et al. 2016). Furthermore, the extinction associated with fragmentation is inversely proportional to species dispersal capacity (Cushman 2006), an important factor for species of *Crossodactylodes* due to their small body size and dependency on bromeliads, which probably limits their dispersal. In addition, species with restricted ranges are more vulnerable to natural stochastic events and the negative anthropogenic

Downloaded From: https://bioone.org/journals/Herpetological-Monographs on 20 May 2020
Terms of Use: https://bioone.org/terms-of-use Access provided by Universidade Estadual Paulista Julio de Mesquita Filho (UNESP)

activities, and hence are more prone to extinction (Sodhi et al. 2008; Pimm et al. 2014; Toledo et al. 2014; Weeks et al. 2016). All these factors emphasize the need for effective conservation measures to safeguard *Crossodactylodes* species.

**Acknowledgments.**—We thank H.Q. Boudet (MBML), J.P. Pombal, Jr. (MNRJ), H. Zaher, T. Grant (MZUSP), O.L. Peixoto (EI), S.P. Carvalho-e-Silva (ZUFRJ), W.R. Heyer and K. de Queiroz (USNM), and V.G.D. Orrico (MZUESC) for loan of specimens or providing access to the collections. J. Rosado and J. Woodward (MCZ) provided photographs of a specimen under their care. P.P.G. Taucce took pictures of some specimens at USNM. We are grateful to the Centro de Estudos de Insetos Sociais (CEIS), UNESP, Rio Claro, Brazil, for allowing the utilization of the facilities for some molecular analyses. P. Shea and C. French helped with English. P.D.P. Pinheiro helped with dissections and phylogenetic analyses. D. Baêta and B.F. Zaidan helped with cleared and double-stained specimens. We are grateful to G.H.F. Azevedo, I.L.F. Magalhães, B. Faleiro, J.V.A. Lacerda, F. Leal, I.R. Fernandes, A.P. Motta, M.B. Harvey, and two anonymous reviewers for comments and suggestions that improved the manuscript. M. Vancine helped with the map. We thank L. Kollman, A. Amorin, M. Sena, and T. Mota for identification of bromeliads. J.E. Santos, Jr. and M.L. Lyra provide laboratory assistance. We thank P.H. Martins, P. Rocha, B.H. Fehlberg, C.Z. Zocca, A.T. Monico, F.C. Lirio, and R.S. Cipriano for fieldwork assistance, and the Bromeligenous project for logistical support. This work was financed by Fundação de Amparo à Pesquisa do Estado de São Paulo (FAPESP), Grant 2013/50741-7; Fundação de Amparo à Pesquisa do Estado de Minas Gerais (FAPEMIG), Grant APQ-01120-16; Mohamed bin Zayed; Utah State University; and Rufford Foundation. This study was financed in part by the Coordenação de Aperfeiçoamento de Pessoal de Nível Superior – Brasil (CAPES) – Finance Code 001. Support was provided to MTTS by FAPEMIG and CAPES (Grants 88881.189822/2018-01 and 88882.434124/2019-01); to RFM by CAPES (Programa Nacional de Pós-Doutorado); and IRD thanks Conselho Nacional de Desenvolvimento Científico e Tecnológico (CNPq), Grant 155198/2018-1 and FSFL thanks FAPEMIG and Vale, Grants APQ-01796-15 and RDP-00004-17. In addition, CFBH, FRS, and PCAG were supported by research fellowships from CNPq. Sampling permits were issued by ICMBio (28607, 35198-2, and 50402); Instituto Estadual de Florestas, Minas Gerais 108/12; Instituto Estadual de Meio Ambiente e Recursos Hídricos, Espírito Santo 021-2012 and 005-2016; Institutional Animal Care and Use Committee, Utah State University 2002; and Comissão de Ética no Uso de Animais, Universidade Vila Velha 355-2015.

## Supplemental Material

Supplemental material associated with this article can be found online at https://doi.org/10.1655/HERPMONOGRAPHS-D-19-00008.S1; https://doi.org/10.1655/HERPMONOGRAPHS-D-19-00008.S2; https://doi.org/10.1655/HERPMONOGRAPHS-D-19-00008.S3; https://doi.org/10.1655/HERPMONOGRAPHS-D-19-00008.S4.

## Literature Cited

Altig, R., and R.W. McDiarmid. 2007. Morphological diversity and evolution of egg and clutch structure in amphibians. Herpetological Monographs 21:1–32.

Barata, I.M., M.T.T. Santos, F.S.F. Leite, and P.C.A. Garcia. 2013. A new species of *Crossodactylodes* (Anura: Leptodactylidae) from Minas Gerais, Brazil: First record of genus within the Espinhaço Mountain Range. Zootaxa 3731:552–560.

Barata, I.M., R.A. Griffiths, and G.B. Ferreira. 2018a. Activity pattern and behavior of an endemic bromeliad frog observed through camera trapping. Herpetological Review 49:432–438.

Barata, I.M., E.P. Silva, and R.A. Griffiths. 2018b. Predictors of abundance of a rare bromeliad-dwelling frog (*Crossodactylodes itambe*) in the Espinhaço Mountain Range of Brazil. Journal of Herpetology 52:321–326.

Bornschein, M.R., C.R. Firkowski, D. Baldo, L.F. Ribeiro, R. Belmonte-Lopes, L. Corrêa, S.A.A. Morato, and M.R. Pie. 2015. Three new species of phytotelm-breeding *Melanophryniscus* from the Atlantic Rainforest of southern Brazil (Anura: Bufonidae). PLoS ONE 10:e0142791. DOI: https://dx.doi.org/10.1371/journal.pone.0142791

Bossuyt, F., and M.C. Milinkovitch. 2000. Convergent adaptive radiations in Madagascan and Asian ranid frogs reveal covariation between larval and adult traits. Proceedings of the National Academy of Science of the United States of America 97:6585–6590.

Bokermann, W.C.A. 1966. Lista Anotada das Localidades Tipo de Anffbios Brasileiros. Serviço de Documentação da Reitoria da Universidade de São Paulo, Brasil.

Caramaschi, U., and I. Sazima. 1984. Uma nova espécie de *Thoropa* da Serra do Cipó, Minas Gerais, Brasil (Amphibia, Leptodactylidae). Revista Brasileira de Zoologia 2:139–146.

Carvalho, T.R., C.S. Cassini, P.P.G. Taucce, and C.F.B. Haddad. 2019. A new, morphologically cryptic species of *Adenomera* closely related to *Adenomera araucaria* from the Atlantic Forest of southern Brazil (Anura, Leptodactylidae). Journal of Herpetology 53:131–143.

Cochran, D.M. 1938. Diagnoses of new frogs from Brazil. Proceedings of the Biological Society of Washington 51:41–42.

Cochran, D.M. 1955. Frogs of southeastern Brazil. United States National Museum Bulletin 206:1–423.

Cocroft, R.B., and W.R. Heyer. 1988. Notes on the frog genus *Thoropa* (Amphibia: Leptodactylidae) with a description of a new species (*Thoropa saxatilis*). Proceedings of the Biological Society of Washington 101:209–220.

Cope, E.D. 1865. Sketch of the primary groups of Batrachia s. Salientia. Natural History Review, New Series 5:97–120.

Cope, E.D. 1866. On the structures and distribution of the genera of the arciferous Anura. Journal of the Academy of Natural Sciences of Philadelphia, Series 2 6:67–112.

Costello, M.J., B. Vanhoorne, and W. Appeltans. 2015. Conservation of biodiversity through taxonomy, data publication, and collaborative infrastructures. Conservation Biology 29:1094–1099.

Cushman, S.A. 2006. Effects of habitat loss and fragmentation on amphibians: A review and prospectus. Biological Conservation 128:231–240.

Dias, I.R., T.T. Medeiros, M.V. Nova, and M. Solé. 2014. Amphibians of Serra Bonita, southern Bahia: A new hotpoint within Brazil's Atlantic Forest hotspot. Zookeys 449:105–130.

Dubois, A. 2005. Amphibia Mundi 1.1. An ergotaxonomy of recent amphibians. Alytes 23:1–24.

Dubois, A. 2013. Crossodactylodinae Fouquet, Blotto, Maronna, Verdade, Juncá, de Sá and Trefaut Rodrigues, 2013 is an invalid junior synonym of Paratelmatobiinae Ohler and Dubois, 2012 (Amphibia, Anura). Zootaxa 3700:499–500.

Dudley, N. 2008. Guidelines for Applying Protected Areas Management Categories. International Union for Conservation of Nature, Switzerland.

Duellman, W.E. 1970. The hylid frogs of Middle America. Monograph of the Museum of Natural History, The University of Kansas 1:1–754.

Duellman, W.E., and E. Lehr. 2009. Terrestrial Breeding Frogs (Strabomantidae) in Peru. Natur und Tier-Verlag, Germany.

Duméril, A.M.C., and G. Bibron. 1841. Erpétologie Générale ou Histoire Naturelle Complète des Reptiles, Volume 8. Librairie Encyclopédique de Roret, France.

Emerson, S.B. 1978. Allometry and jumping in frogs: Helping the twain to meet. Evolution 32:551–564.

Faivovich, J., C.F.B. Haddad, P.C.A. Garcia, D.R. Frost, J.A. Campbell, and W.C. Wheeler. 2005. Systematic review of the frog family Hylidae, with special reference to Hylinae: Phylogenetic analysis and taxonomic revision. Bulletin of the American Museum of Natural History 294:1–240.

Faivovich, J., L. Nicoli, B.L. Blotto, M.O. Pereyra, D. Baldo, J.S. Barrionuevo, M. Fabrezi, E.R. Wild, and C.F.B. Haddad. 2014. Big, bad, and beautiful: Phylogenetic relationships of the horned frogs (Anura: Ceratophryidae). South American Journal of Herpetology 9:207–227.

Farris, J.S., V.A. Albert, M. Kallersjo, D. Lipscomb, and A.G. Kluge. 1996. Parsimony jackknifing outperforms neighbor-joining. Cladistics 12:99–124.

Feller, A.E., and S.B. Hedges. 1998. Molecular evidence for the early history of living amphibians. Molecular Phylogenetics and Evolution 9:509–516.

Ferreira, R.B., A.T. Mônico, C.Z. Zocca,... C. Duca. 2019a. Uncovering the natural history of the bromeligenous frog *Crossodactylodes izecksohni* (Leptodactylidae, Paratelmatobiinae). South American Journal of Herpetology 14:136–145.

Ferreira, R.B., A.T. Mônico, E.T. Silva, F.C.F. Lírio, C.Z. Zocca, M.M. Mageski, J.F.R. Tonini, K.H. Beard, C. Duca, and T. Silva-Soares. 2019b. Amphibians of Santa Teresa, Brazil: The hotspot further evaluated. ZooKeys 857:139–162.

Fitzinger, L.J.F.J. 1826. Neue Classification der Reptilien nach ihren

Downloaded From: https://bioone.org/journals/Herpetological-Monographs on 20 May 2020
Terms of Use: https://bioone.org/terms-of-use Access provided by Universidade Estadual Paulista Julio de Mesquita Filho (UNESP)

Natürlichen Verwandtschaften nebst einer Verwandtschafts-Tafel und einem Verzeichnisse der Reptilien-Sammlung des K.K. Zoologisch Museum's zu Wien. J.G. Heubner, Austria.

Forlani, M.C., J.F.R. Tonini, C.A.G. Cruz, H. Zaher, and R.O. de Sá. 2017. Molecular and morphological data reveal three new cryptic species of *Chiasmocleis* (Mehely 1904) (Anura, Microhylidae) endemic to the Atlantic Forest, Brazil. PeerJ 5:e3005. DOI: http://dx.doi.org/10.7717/peerj.3005

Fouquet, A., A. Gilles, M. Vences, C. Marty, M. Blanc, and N.J. Gemmell. 2007. Underestimation of species richness in Neotropical frogs revealed by mtDNA analyses. PLoS ONE 2:e1109. DOI: http://dx.doi.org/10.1371/journal.pone.0001109

Fouquet, A., B.L. Blotto, M.M. Maronna, V.K. Verdade, F.A. Juncá, R. de Sá, and M.T. Rodrigues. 2013. Unexpected phylogenetic positions of the genera *Rupirana* and *Crossodactylodes* reveal insights into the biogeography and reproductive evolution of leptodactylid frogs. Molecular Phylogenetics and Evolution 67:445–457.

Frost, D.R. 2019. Amphibian Species of the World: An Online Reference, Version 6.0. Available at http://research.amnh.org/herpetology/amphibia/index.html. American Museum of Natural History, USA. Archived by WebCite at http://www.webcitation.org/6qp8hUYGQ on 29 May 2017.

Frost, D.R., T. Grant, J. Faivovich,... W.C. Wheeler. 2006. The amphibian tree of life. Bulletin of the American Museum of Natural History 297:1–370.

Fujita, M.K., A.D. Leaché, F.T. Burbrink, J.A. McGuire, and C. Moritz. 2012. Coalescent-based species delimitation in an integrative taxonomy. Trends in Ecology and Evolution 27:480–488.

Gaige, H.T. 1926. A new frog from British Guiana. Occasional Papers of the Museum of Zoology, University of Michigan 176:1–3.

Garcia, P.C.A. 1996. Recaracterização de *Scythrophrys sawayae* (Cochran, 1953) Baseada em Morfologia, Osteologia e Aspectos da Miologia e História Natural (Amphibia, Anura, Leptodactylidae). M.S. thesis, Universidade Católica do Rio Grande do Sul, Brasil.

Giaretta, A.A., and L.M. Castanho. 1990. Nova espécie de *Paratelmatobius* (Amphibia, Anura, Leptodactylidae) da Serra do Mar, Brasil. Papéis Avulsos de Zoologia, São Paulo 37:133–139.

Goebel, A.M., J.M. Donnely, and M.E. Atz. 1999. PCR primers and amplification methods for 12S ribosomal DNA, the control region, cytochrome oxidase I, and cytochrome b in bufonids and other frogs, and an overview of PCR primers which have amplified DNA in amphibians successfully. Molecular Phylogenetics and Evolution 11:163–199.

Goloboff, P., and S. Catalano. 2016. TNT version 1.5, including a full implementation of phylogenetic morphometrics. Cladistics 32:221–238.

Gomes, N. 1988. Osteologia comparada de duas espécies do gênero *Crossodactylodes* Cochran, 1938 (Amphibia, Anura, Leptodactylidae). Memórias do Instituto Butantan 50:51–61.

Gontijo-Pascutti, A.H.F., Y. Hasui, M. Santos, A.V. Soares, Jr., and I.A. Souza. 2012. As serras do Mar e da Mantiqueira. Pp. 549–571 in Geologia do Brasil (Y. Hasui, C.D.R. Carneiro, F.F.M. Almeida, and A. Bartorelli, eds.). Beca, Brazil.

Graybeal, A. 1997. Phylogenetic relationships of bufonid frogs and tests of alternate macroevolutionary hypotheses characterizing their radiation. Zoological Journal of the Linnean Society 119:297–338.

Grosjean, S., S. Bordoloi, Y. Chuaynkern, P. Chakravarty, and A. Ohler. 2015. When young are more conspicuous than adults: A new ranid species (Anura: Ranidae) revealed by its tadpole. Zootaxa 4058:471–498.

Haddad, C.F.B., and C.P.A. Prado. 2005. Reproductive modes in frogs and their unexpected diversity in the Atlantic Forest of Brazil. BioScience 55:207–217.

Haddad, C.F.B., L.F. Toledo, C.P.A. Prado, D. Loebmann, J.L. Gasparini, and I. Sazima. 2013. Guide to the Amphibians of the Atlantic Forest: Diversity and Biology. Anolis Books, Brazil.

Haddad, C.F.B., I.F. Machado, J.G.R. Giovanelli,... R.P. Bastos. 2016a. Avaliação do Risco de Extinção de *Crossodactylodes pintoi* Cochran, 1938. Available at http://www.icmbio.gov.br/portal/biodiversidade/fauna-brasileira/estado-de-conservacao/7647-anfibios-crossodactylodes-pintoi.html. Processo de Avaliação do Risco de Extinção da Fauna Brasileira, ICMBio, Brazil. Archived by WebCite at http://www.webcitation.org/6uaCmZKjy on 29 October 2017.

Haddad, C.F.B., M.V. Segalla, Y.S.L. Bataus,... U. Caramaschi. 2016b Avaliação do Risco de Extinção de *Crossodactylodes bokermanni* Peixoto 1983 "1982". Available at http://www.icmbio.gov.br/portal/faunabrasileira/carga-estado-de-conservacao/8116-anfibios-crossodactylodes-bokermanni. Processo de Avaliação do Risco de Extinção da Fauna Brasileira, ICMBio, Brazil. Archived by WebCite at http://www.webcitation.org/6uaDE2Sbl on 29 October 2017.

Haddad, C.F.B., M.V. Segalla, Y.S.L. Bataus,... U. Caramaschi. 2016c. Avaliação do Risco de Extinção de *Crossodactylodes izecksohni* Peixoto 1983 "1982". Available at http://www.icmbio.gov.br/portal/biodiversidade/fauna-brasileira/estado-de-conservacao/7701-anfibios-crossodactylodes-izecksohni.html. Processo de Avaliação do Risco de Extinção da Fauna Brasileira, ICMBio, Brazil. Archived by WebCite at http://www.webcitation.org/6uaDUh4w4 on 29 October 2017.

Haddad, C.F.B., Y.S.L. Bataus, V.M. Uhlig,... R. Lingnau. 2016d. Avaliação do Risco de Extinção de *Crossodactylodes itambe* Barata, Santos, Leite, and Garcia 2013. Available at http://www.icmbio.gov.br/portal/biodiversidade/fauna-brasileira/estado-de-conservacao/7700-anfibios-crossodactylodes-itambe.html. Processo de Avaliação do Risco de Extinção da Fauna Brasileira, ICMBio, Brazil. Archived by WebCite at http://www.webcitation.org/6ua8FrJ61on 29 October 2017.

Hedges, S.B. 1994. Molecular evidence for the origin of birds. Proceedings of the National Academy of Sciences of the United States of America 91:2621–2624.

Heyer, W.R. 1975. A preliminary analysis of the intergeneric relationships of the frog family Leptodactylidae. Smithsonian Contributions to Zoology 199:1–55.

Heyer, W.R. 1999. A new genus and species of frog from Bahia, Brazil (Amphibia: Anura: Leptodactylidae) with comments on the zoogeography of the Brazilian campos rupestres. Proceedings of The Biological Society of Washington 112:19–30.

Heyer, W.R., A.S. Rand, C.A.G. Cruz, O.L. Peixoto, and C. Nelson. 1990. Frogs of Boracéia. Arquivos de Zoologia do Estado de São Paulo 31:231–410.

Hortal, J., F. de Bello, J.A.F. Diniz-Filho, T.M. Lewinsohn, J.M. Lobo, and R.J. Ladle. 2015. Seven shortfalls that beset large-scale knowledge of biodiversity. Annual Review of Ecology, Evolution, and Systematics 46:523–549.

Ihering, H., and R. Ihering. 1911. O Museu Paulista nos annos de 1906 a 1909. Revista do Museu Paulista 8:1–22.

Instituto Chico Mendes de Conservação da Biodiversidade (ICMBio). 2017. Unidades de Conservação. Available at http://icmbio.gov.br/portal/unidadesdeconservacao/biomas-brasileiros. Accessed on 13 November 2019. Ministério do Meio Ambiente, Brasil.

Instituto Estadual do Ambiente. 2014. APA Estadual de Macaé de Cima: Plano de Manejo: Informações Sintetizadas da UC. Executive Report. Instituto Estadual do Ambiente, Brazil.

International Union for Conservation of Nature (IUCN) Standards and Petitions Committee. 2019. Guidelines for Using the IUCN Red List Categories and Criteria, Version 14. International Union for Conservation of Nature, Switzerland.

Juncá, F.A., and L. Lugli. 2009. Reproductive biology, vocalizations, and tadpole morphology of *Rupirana cardosoi*, an anuran with uncertain affinities. South American Journal of Herpetology 4:173–178.

Katoh, K., and D.M. Standley. 2013. MAFFT multiple sequence alignment software Version 7: Improvements in performance and usability. Molecular Biology and Evolution 30:772–780.

Katoh, K., J. Rozewicki, and K.D. Yamada. 2019. MAFFT online service: Multiple sequence alignment, interactive sequence choice and visualization. Briefings in Bioinformatics 20:1160–1166.

Köhler, J., M. Jansen, A. Rodríguez, P.J.R. Kok, L.F. Toledo, M. Emmrich, F. Glaw, C.F.B. Haddad, M. Rödel, and M. Vences. 2017. The use of bioacoustics in anuran taxonomy: Theory, terminology, methods and recommendations for best practice. Zootaxa 4251:1–124.

Knowles, L.L. 2009. Statistical phylogeography. Annual Review of Ecology, Evolution, and Systematics 40:593–612.

Kumar, S., G. Stecher, and K. Tamura. 2016. MEGA7: Molecular evolutionary genetics analysis version 7.0 for bigger datasets. Molecular Biology and Evolution 33:1870–1874.

Kupfer, A. 2007. Sexual size dimorphism in amphibians: An overview. Pp. 50–59 in Sex, Size and Gender Roles: Evolutionary Studies of Sexual Size Dimorphism (D.J. Fairbairn, W.U. Blanckenhorn and T. Szekely, eds.). Oxford University Press, UK.

Lanfear, R., P.B. Frandsen, A.M. Wright, T. Senfeld, and B. Calcott. 2017. PartitionFinder 2: New methods for selecting partitioned models of evolution for molecular and morphological phylogenetic analyses. Molecular Biology and Evolution 34:772–773.

Lawson, L.P., J.M. Bates, M. Menegon, and S.P. Loader. 2015. Divergence at the edges: Peripatric isolation in the montane spiny throated reed frog

Downloaded From: https://bioone.org/journals/Herpetological-Monographs on 20 May 2020
Terms of Use: https://bioone.org/terms-of-use Access provided by Universidade Estadual Paulista Julio de Mesquita Filho (UNESP)

complex. BMC Evolutionary Biology 15:1–15. DOI: http://dx.doi.org/10.1186/s12862-015-0384-3

Lutz, B., and A.L. de Carvalho. 1958. Novos anfíbios anuros das serras costeiras do Brasil. Memórias do Instituto Oswaldo Cruz 56:239–249.

Lynch, J.D. 1971. Evolutionary relationships, osteology, and zoogeography of leptodactyloid frogs. Miscellaneous Publications of the Museum of Natural History, University of Kansas 53:1–238.

Lyra, M.L., C.F.B. Haddad, and A.M.L. de Azeredo-Espin. 2017. Meeting the challenge of DNA barcoding Neotropical amphibians: Polymerase chain reaction optimization and new COI primers. Molecular Ecology Resources 17:966–980.

Maddison, W.P., and D.R. Maddison. 2017. Mesquite: A modular system for evolutionary analysis, Version 3.2. Available at http://mesquiteproject.org. Mesquite Project, USA. Archived by WebCite at http://www.webcitation.org/6r3FdSuUV on 07 June 2017.

Magalhães, R.F., J.V.A. Lacerda, L.P. Reis, P.C.A. Garcia, and P.D.P. Pinheiro. 2018. Sexual dimorphism in *Bokermannohyla martinsi* (Bokermann, 1964) (Anura, Hylidae) with a report of male–male combat. South American Journal of Herpetology 13:202–209.

Martinelli, G., C.M. Vieira, M. González, P. Leitman, A. Piratininga, A.F. da Costa, and R.C. Forzza. 2008. Bromeliaceae da Mata Atlântica brasileira: Lista de espécies, distribuição e conservação. Rodriguésia 59:209–258.

Mendelson, J.R., J.M. Savage, E. Griffith, H. Ross, B. Kubicki, and R. Gagliardo. 2008. Spectacular new gliding species of *Ecnomiohyla* (Anura: Hylidae) from central Panama. Journal of Herpetology 42:750–759.

Mertens, R. 1926. Herpetologischen Mitteilungen VIII–XV. Senckenbergiana Biologica 8:137–155.

Miller, M.A., W. Pfeiffer, and T. Schwartz. 2010. Creating the CIPRES Science Gateway for inference of large phylogenetic trees. Proceedings of the Gateway Computing Environments Workshop 2010:1–8. DOI: https://dx.doi.org/10.1109/GCE.2010.5676129

Miranda-Ribeiro, A. 1923. *Elosia* Tsch. e os generos correlatos. Revista do Museu Paulista 13:813–821.

Miranda-Ribeiro, A. 1926. Notas para servirem ao estudo dos gymnobatrachios (Anura) brasileiros. Arquivos do Museu Nacional, Rio de Janeiro 27:1–227.

Morais, A.R., M.N. Siqueira, P. Lemes, N.M. Maciel, P. De Marco, Jr., and D. Brito. 2013. Unraveling the conservation status of Data Deficient species. Biological Conservation 166:98–102.

Moritz, C., C.J. Schneider, and D.B. Wake. 1992. Evolutionary relationships within the *Ensatina eschscholtzii* complex confirm the ring species interpretation. Systematic Biology 41:273–291.

Müller, L. 1922. Über eine Sammlung Froschlurche von Sta. Catharina nebst Beschriebung zweier neuer Arten. Blätter für Aquarien- und Terrarienkunde 33:167–171.

Myers, N., R.A. Mittermeier, C.G. Mittermeier, G.A.B. da Fonseca, and J. Kent. 2000. Biodiversity hotspots for conservation priorities. Nature 403:853–858.

Nixon, K. 2002. WinClada, Version 1.00.08. Published by the author, USA.

Ohler, A., and A. Dubois. 2012. Validation of two familial nomina nuda of Amphibia Anura. Alytes 28:162–167.

Oliveira, U., A.P. Paglia, A.D. Brescovit,... A.J. Santos. 2016. The strong influence of collection bias on biodiversity knowledge shortfalls of Brazilian terrestrial biodiversity. Diversity and Distributions 22:1232–1244.

Pabijan, M., K.C. Wollenberg, and M. Vences. 2012. Small body size increases the regional differentiation of populations of tropical mantellid frogs (Anura: Mantellidae). Journal of Evolutionary Biology 25:2310–2324.

Padial, J.M., S. Castroviejo-Fisher, J. Köhler, C. Vilà, J.C. Chaparro, and I. De la Riva. 2009. Deciphering the products of evolution at the species level: The need for an integrative taxonomy. Zoologica Scripta 38:431–447.

Padial, J.M., A. Miralles, I. De la Riva, and M. Vences. 2010. The integrative future of taxonomy. Frontiers in Zoology 7:16. DOI: http://dx.doi.org/10.1186/1742-9994-7-16

Palumbi, S.R., A.P. Martin, B.D. Kessing, and W.O. McMillan. 1991. Detecting population structure using mitochondrial DNA. Pp. 271–278 in Genetic Ecology of Whales and Dolphins (A.R. Hoelzel, ed.). International Whaling Commission, UK.

Paynter, R.A.J., and M.A. Traylor. 1991. Ornithological Gazetteer of Brazil, vol. 2. Cambridge Harvard College Press, USA.

Peixoto, O.L. 1981. Notas sobre o girino de *Crossodactylodes pintoi* Cochran (Amphibia, Anura, Leptodactylidae). Revista Brasileira de Biologia 41:339–341.

Peixoto, O.L. 1983 "1982". Duas novas espécies de *Crossodactylodes* de Santa Tereza, estado do Espírito Santo, Brasil. (Amphibia, Anura, Leptodactylidae). Revista Brasileira de Biologia 42:619–626.

Peixoto, O.L. 1995. Associação de anuros a bromeliáceas na Mata Atlântica. Revista da Universidade Federal Rural do Rio de Janeiro, Série Ciências da Vida 17:75–83.

Peixoto, O.L., and S.P. Carvalho-e-Silva. 2004. *Crossodactylodes pintoi*. The IUCN Red List of Threatened Species 2004:e.T56346A11465671. DOI: http://dx.doi.org/10.2305/IUCN.UK.2004.RLTS.T56346A11465671.en

Pereyra, M.O., M.C. Womack, Barrionuevo,J.S. ... J. Faivovich. 2016. The complex evolutionary history of the tympanic middle ear in frogs and toads (Anura). Scientific Reports 6:34130. DOI: http://dx.doi.org/10.1038/srep34130

Pie, M.R., A.L.S. Meyer, C.R. Firkowski, L.F. Ribeiro, and M.R. Bornschein. 2013. Understanding the mechanisms underlying the distribution of microendemic montane frogs (*Brachycephalus* spp., Terrarana: Brachycephalidae) in the Brazilian Atlantic Rainforest. Ecological Modelling 250:165–176.

Pie, M.R., B.C. Faircloth, L.F. Ribeiro, M.R. Bornschein, and J.E. McComarck. 2018. Phylogenomics of montane frogs of the Brazilian Atlantic Forest is consistent with isolation in sky islands followed by climatic stability. Biological Journal of the Linnean Society 125:72–82.

Pimm, S.L., C.N. Jenkins, R. Abell, T.M. Brooks, J.L. Gittleman, L.N. Joppa, P.H. Raven, C.M. Roberts, and J.O. Sexton. 2014. The biodiversity of species and their rates of extinction, distribution, and protection. Science 344:1246752. DOI: http://dx.doi.org/10.1126/science.1246752

Pinto, O.M.O. 1945. Cinqüenta anos de investigação ornitológica. Arquivos de Zoologia do Estado de São Paulo 4:261–340.

Pombal, J.P., Jr., and C.F.B. Haddad. 1999. Frogs of the genus *Paratelmatobius* (Anura: Leptodactylidae) with descriptions of two new species. Copeia 1999:1014–1026.

Pough, F.H. 2007. Amphibian biology and husbandry. ILAR Journal 48:203–213.

Pyron, R.A. 2014. Biogeographic analysis reveals ancient continental vicariance and recent oceanic dispersal in amphibians. Systematic Biology 63:779–797.

Pyron, R.A., and J.J. Wiens. 2011. A large-scale phylogeny of Amphibia with over 2800 species, and a revised classification of extant frogs, salamanders, and caecilians. Molecular Phylogenetics and Evolution 61:543–583.

Rambaut, A., M.A. Suchard, D. Xie, and A.J. Drummond. 2014. Tracer, version 1.6. Available at http://tree.bio.ed.ac.uk/software/tracer. Archived by WebCite at http://www.webcitation.org/6qpoA3u3h on 29 May 2017.

Ramos, E.K.S., R.F. Magalhães, N.C.S. Marques, D. Baêta, P.C.A. Garcia, and F.R. Santos. 2019. Cryptic diversity in Brazilian endemic monkey frogs (Hylidae, Phyllomedusinae, *Pithecopus*) revealed by multispecies coalescent and integrative approaches. Molecular Phylogenetics and Evolution 132:105–116.

Randrianiaina, R.D., R.N. Antúnez, J. Canitz,... M. Vences. 2009. Vogue or adaptive character? A tadpole's goatee helps to distinguish two cryptic treefrog species of the genus *Boophis*. Herpetology Notes 2:165–173.

Rodríguez, A., M. Börner, M. Pabijan, M. Gehara, C.F.B. Haddad, and M. Vences. 2015. Genetic divergence in tropical anurans: Deeper phylogeographic structure in forest specialists and in topographically complex regions. Evolutionary Ecology 29:765–785.

Ronquist, F., M. Teslenko, P. van der Mark, D.L. Ayres, A. Darling, S. Höhna, B. Larget, L. Liu, M.A. Suchard, and J.P. Huelsenbeck. 2012. MrBayes 3.2: Efficient Bayesian phylogenetic inference and model choice across a large model space. Systematic Biology 61:539–542.

Rossa-Feres, D.C., M.V. Garey, U. Caramaschi,... C.F.B. Haddad. 2017. Anfíbios da Mata Atlântica: Lista de espécies, histórico dos estudos, biologia e conservação. Pp. 237–314 in Revisões em Zoologia: Mata Atlântica (E.L.A Monteiro-Filho and C.E. Conte, eds.). Editora UFPR, Brazil.

Rowe, K.C., S. Singhal, M.D. Macmanes, J.F. Ayroles, T.L. Morelli, E.M. Rubidge, K. Bi, and C.C. Moritz. 2011. Museum genomics: Low-cost and high-accuracy genetic data from historical specimens. Molecular Ecology Resources 11:1082–1092.

Sabagh, L.T., R.B. Ferreira, and C.F.D. Rocha. 2017. Host bromeliads and their associated frog species: Further considerations on the importance of species interactions for conservation. Symbiosis 73:201–211.

Sabbag, A.F., M.L. Lyra, K.R. Zamudio, C.F.B. Haddad, R.N. Feio, F.S.F. Leite, J.L. Gasparini, and C.A. Brasileiro. 2018. Molecular phylogeny of Neotropical rock frogs reveals a long history of vicariant diversification in the Atlantic Forest. Molecular Phylogenetics and Evolution 122:142–156.

Downloaded From: https://bioone.org/journals/Herpetological-Monographs on 20 May 2020
Terms of Use: https://bioone.org/terms-of-use Access provided by Universidade Estadual Paulista Julio de Mesquita Filho (UNESP)

Sabaj, M.H. 2016. Standard Symbolic Codes for Institutional Resource Collections in Herpetology and Ichthyology: An Online Reference, Version 6.5. Available at http://www.asih.org/. American Society of Ichthyologists and Herpetologists, USA. Archived by WebCite at http://www.webcitation.org/6qpZPWPt3 on 29 May 2017.

Sambrook, J., and D.W. Russel. 2001. Molecular Cloning: A Laboratory Manual. Cold Spring Harbor Laboratory Press, USA.

Santos, J.E., Jr., F.R. Santos, and F.A. Silveira. 2015. Hitting an unintended target: Phylogeography of *Bombus brasiliensis* Lepeletier, 1836 and the first new Brazilian bumblebee species in a century (Hymenoptera: Apidae). PLoS ONE 10:e0125847. DOI: https://dx.doi.org/10.1371/journal.pone.0125847

Santos, M.T.T., T.L. Pezzuti, I.M. Barata, F.S.F. Leite, and P.C.A. Garcia. 2017. The tadpole of the microendemic, bromeligenous *Crossodactylodes itambe* (Anura, Leptodactylidae) from the endangered 'campo rupestre' of southeastern Brazil, with additional comments on natural history. South American Journal of Herpetology 12:14–23.

Santos, M.T.T., S.H. Oliveira, T.R. Carvalho, B.F. Zaidan, N.R. Silva, B.V. Berneck, and P.C.A. Garcia. 2019. A new species of *Paratelmatobius* (Anura: Leptodactylidae: Paratelmatobiinae) from the Atlantic Forest of southern Brazil. Zootaxa 4648:473–493.

Scardua, F.P. 2000. Plano de Manejo do Parque Estadual do Forno Grande. Technical Report. Instituto Estadual de Meio Ambiente e Recursos Hídricos, Brasil.

Segalla, M.V., U. Caramaschi, C.A.G. Cruz, P.C.A. Garcia, T. Grant, C.F.B. Haddad, D.J. Santana, L.F. Toledo, and J.A. Langone. 2019. Brazilian amphibians: List of species. Herpetologia Brasileira 8:65–96.

Silvano, D., and O.L. Peixoto. 2004a. *Crossodactylodes bokermanni*. The IUCN Red List of Threatened Species 2004:e.T56344A11465382. DOI: http://dx.doi.org/10.2305/IUCN.UK.2004.RLTS.T56344A11465382.en

Silvano, D., and O.L. Peixoto. 2004b. *Crossodactylodes izecksohni*. The IUCN Red List of Threatened Species 2004:e.T56345A11465530. DOI: http://dx.doi.org/10.2305/IUCN.UK.2004.RLTS.T56345A11465530.en

Silveira, F.A.O., D. Negreiros, N.P.U. Barbosa,... H. Lambers. 2016. Ecology and evolution of plant diversity in the endangered campo rupestre: A neglected conservation priority. Plant and Soil 403:129–152.

Simmons, M.P., K.M. Pickett, and M. Miya. 2004. How meaningful are Bayesian support values? Molecular Biology and Evolution 21:188–199.

Sodhi, N.S., D. Bickford, A.C. Diesmos, T.M. Lee, L.P. Koh, B.W. Brook, C.H. Sekercioglu, and C.J.A. Bradshaw. 2008. Measuring the meltdown: Drivers of global amphibian extinction and decline. PLoS ONE 3:e1636. DOI: https://dx.doi.org/10.1371/journal.pone.0001636

SOS Mata Atlântica and Instituto Nacional de Pesquisas Espaciais. 2018. Atlas dos Remanescentes Florestais da Mata Atlântica, Período 2016–2017. Available at http://mapas.sosma.org.br. Accessed on 13 November 2019.

Steindachner, F. 1867. Reise der österreichischen Fregatte Novara um die Erde in den Jahren 1857, 1858, 1859 unter den Bafehlen des Commodore B. von Wüllerstorf-Urbair. Zologischer Theil. 1. Amphibien. K.K. Hof- und Staatsdruckerei, Austria.

Stuart, S., M. Hoffmann, J. Chanson, N. Cox, R. Berridge, P. Ramani, and B. Young. 2008. Threatened Amphibians of the World. Lynx Edicions, IUCN, and Conservation International, Spain, Switzerland, and USA.

Tapley, B., C.J. Michaels, R. Gumbs, M. Böhm, J. Luedtke, P. Pearce-Kelly, and J.J.L. Rowley. 2018. The disparity between species description and conservation assessment: A case study in taxa with high rates of species discovery. Biological Conservation 220:209–214.

Taylor, W.R., and G.C. Van Dyke. 1985. Revised procedures for staining and clearing small fishes and other vertebrates for bone and cartilage study. Cybium 9:107–119.

Taucce, P.P.G., C. Canedo, J.S. Parreiras, L.O. Drummond, P. Nogueira-Costa, and C.F.B. Haddad. 2018. Molecular phylogeny of *Ischnocnema* (Anura: Brachycephalidae) with the redefinition of its series and the description of two new species. Molecular Phylogenetics and Evolution 128:123–146.

Teixeira, M., Jr., R.S. Recoder, R.C. Amaro, R.P. Damasceno, J. Cassimiro, and M.T. Rodrigues. 2013. A new *Crossodactylodes* Cochran, 1938 (Anura: Leptodactylidae: Paratelmatobiinae) from the highlands of the Atlantic Forests of southern Bahia, Brazil. Zootaxa 3702:459–472.

Titus, T.A., and A. Larson. 1996. Molecular phylogenetics of desmognathine salamanders (Caudata: Plethodontidae): A reevaluation of evolution in ecology, life history, and morphology. Systematic Biology 45:451–472.

Toledo, L.F., C.G. Becker, C.F.B. Haddad, and K.R. Zamudio. 2014. Rarity as an indicator of endangerment in Neotropical frogs. Biological Conservation 179:54–62.

Tschudi, J.J. 1838. Classification der Batrachier, Mit Berücksichtigung der Fossilen Thiere Dieser Abtheilung der Reptilien. In der Buchdruckerei von Petitpierre, Switzerland.

Valeriano, M.M., and D.F. Rossetti. 2012. Topodata: Brazilian full coverage refinement of SRTM data. Applied Geography 32:300–309.

Vasconcelos, T.S., V.H.M. Prado, F.R. da Silva, and C.F.B. Haddad. 2014. Biogeographic distribution patterns and their correlates in the diverse frog fauna of the Atlantic Forest hotspot. PLoS ONE 9:e104130. DOI: https://dx.doi.org/10.1371/journal.pone.0104130

Versieux, L.M., R.B. Louzada, P.L. Viana, N. Mota, and M.G.L. Wanderley. 2010. An illustrated checklist of Bromeliaceae from Parque Estadual do Rio Preto, Minas Gerais, Brazil, with notes on phytogeography and one new species of *Cryptanthus*. Phytotaxa 10:1–16.

Villalobos, F., R. Dobrovolski, D.B. Provete, and S.F. Gouveia. 2013. Is rich and rare the common share? Describing biodiversity patterns to inform conservation practices for South American anurans. PLoS ONE 8:e56073. DOI: https://dx.doi.org/10.1371/journal.pone.0056073

Weeks, A.R., J. Stoklosa, and A.A. Hoffmann. 2016. Conservation of genetic uniqueness of populations may increase extinction likelihood of endangered species: The case of Australian mammals. Frontiers in Zoology 13:31. DOI: https://dx.doi.org/10.1186/s12983-016-0163-z

Werner, F. 1896. Beiträge zur Kenntniss der Reptilien und Batrachier von Centralamerika und Chile, sowie einiger seltenerer Schlangenarten. Verhandlungen des Zoologisch-Botanischen Vereins in Wien 46:344–365.

Wilcox, D.C., B.S Dove, D.W. McDaid, and D.B. Greer. 1996. Imagetool. Available at http://compdent.uthscsa.edu/imagetool.asp. The University of Texas Health Science Center at San Antonio, USA. Archived by WebCite at http://www.webcitation.org/6qpeHshHN on 29 May 2017.

Wiens, J.J., J.W. Fetzner, C.L. Parkinson, and T.W. Reeder. 2005. Hylid frog phylogeny and sampling strategies for speciose clades. Systematic Biology 54:778–807.

**Accepted on** 22 November 2019
**Published on** 20 May 2020

Downloaded From: https://bioone.org/journals/Herpetological-Monographs on 20 May 2020
Terms of Use: https://bioone.org/terms-of-use Access provided by Universidade Estadual Paulista Julio de Mesquita Filho (UNESP)

APPENDIX I.—GenBank accession numbers for sequences employed in this study. Museum voucher numbers are reported only for sequences generated for this article. For other voucher information, refer to the GenBank accession numbers. A dash (—) indicates missing data.

| | | GenBank accession numbers | | | | | |
|---|---|---|---|---|---|---|---|
| Species | Museum number | H1 | COI | cytb | POMC | RAG-1 | Tyr |
| *Adenomera andreae* | | KC520683 | KC520689 | JQ321766 | KC604061 | KC604037/ KF674220 | KC520698 |
| *Allophryne ruthveni* | | AY843564 | KU494331 | AY843786 | AY819077 | AY844361 | KC604076 |
| *Crossodactylodes bokermanni* | | KC593358 | — | — | — | — | — |
| *C. bokermanni* | MNRJ 38412 | KC593359 | MN610690 | MN610722 | MN610759 | MN609871 | MN610796 |
| *C. bokermanni* | UFMG 14188 | MN610833 | MN610691 | MN610723 | MN610760 | MN609872 | MN610797 |
| *C. bokermanni* | UFMG 14189 | MN610834 | MN610692 | MN610724 | MN610761 | MN609873 | MN610798 |
| *C. bokermanni* | UFMG 14190 | MN610835 | MN610693 | MN610725 | MN610762 | MN609874 | MN610799 |
| *C. bokermanni* | UFMG 13767 | MN610836 | MN610694 | MN610726 | MN610763 | MN609875 | MN610800 |
| *C. bokermanni* | UFMG 13770 | MN610837 | MN610695 | MN610727 | MN610764 | MN609876 | MN610801 |
| *C. bokermanni* | UFMG 13774 | MN610838 | MN610696 | MN610728 | MN610765 | MN609877 | MN610802 |
| *C. bokermanni* | UFMG 14198 | MN610839 | MN610697 | MN610729 | MN610766 | — | MN610803 |
| *C. bokermanni* | UFMG 14199 | MN610840 | MN610698 | MN610730 | MN610767 | MN609878 | MN610804 |
| *C. bokermanni* | UFMG-G 1496-1 | MN610841 | MN610699 | MN610731 | MN610768 | MN609879 | MN610805 |
| *C. bokermanni* | UFMG-G 1496-2 | MN610842 | MN610700 | MN610732 | MN610769 | MN609880 | MN610806 |
| *C. bokermanni* | UFMG-G 1496-3 | MN610843 | — | — | — | — | — |
| *C. bokermanni* | | KF534637/ KF534647 | KF534656 | KF534665 | — | — | — |
| *C. bokermanni* | | KF534638/ KF534648 | KF534657 | KF534666 | — | — | KF534683 |
| *C. bokermanni* | | KF534639/ KF534649 | KF534658 | KF534667 | — | — | KF534684 |
| *C. bokermanni* | | KF534640/ KF534650 | KF534659 | KF534668 | — | — | KF534685 |
| *Crossodactylodes itambe* | UFMG-G 1477 | MN610844 | KY362547 | MN610733 | MN610770 | MN609881 | MN610807 |
| *C. itambe* | UFMG 13376 | MN610845 | KY362548 | MN610734 | MN610771 | MN609882 | MN610808 |
| *C. itambe* | UFMG 13377 | MN610846 | KY362549 | MN610735 | MN610772 | MN609883 | MN610809 |
| *C. itambe* | UFMG 13379 | MN610847 | KY362550 | MN610736 | MN610773 | MN609884 | MN610810 |
| *C. itambe* | UFMG 13381 | MN610848 | KY362551 | MN610737 | MN610774 | MN609885 | MN610811 |
| *Crossodactylodes izecksohni* | UFMG 13757 | MN610849 | MN610701 | MN610738 | MN610775 | MN609886 | MN610812 |
| *C. izecksohni* | UFMG 13759 | MN610850 | MN610702 | MN610739 | MN610776 | MN609887 | MN610813 |
| *C. izecksohni* | UFMG 13791 | MN610851 | MN610703 | MN610740 | MN610777 | MN609888 | MN610814 |
| *C. izecksohni* | UFMG 13792 | — | MN610704 | MN610741 | MN610778 | MN609889 | MN610815 |
| *C. izecksohni* | UFMG 13793 | — | MN610705 | MN610742 | MN610779 | MN609890 | MN610816 |
| *C. izecksohni* | UFMG 13747 | MN610852 | MN610706 | MN610743 | MN610780 | MN609891 | MN610817 |
| *C. izecksohni* | UFMG 13748 | MN610853 | MN610707 | MN610744 | MN610781 | MN609892 | MN610818 |
| *C. izecksohni* | UFMG 14174 | MN610854 | MN610708 | MN610745 | MN610782 | MN609893 | MN610819 |
| *C. izecksohni* | UFMG 14175 | MN610855 | MN610709 | MN610746 | MN610783 | MN609894 | MN610820 |
| *C. izecksohni* | UFMG 14176 | MN610856 | MN610710 | MN610747 | MN610784 | MN609895 | MN610821 |
| *C. izecksohni* | UFMG 14178 | MN610857 | MN610711 | MN610748 | MN610785 | MN609896 | MN610822 |
| *C. izecksohni* | UFMG 14180 | MN610858 | MN610712 | MN610749 | MN610786 | MN609897 | MN610823 |
| *C. izecksohni* | UFMG-G 1495-1 | MN610859 | MN610713 | MN610750 | MN610787 | MN609898 | MN610824 |
| *C. izecksohni* | UFMG-G 1495-2 | MN610860 | MN610714 | MN610751 | MN610788 | MN609899 | MN610825 |
| *C. izecksohni* | | KF534632/ KF534641 | KF534651 | KF534660 | — | — | KF534678 |
| *C. izecksohni* | | KF534633/ KF534642 | KF534652 | KF534661 | — | — | KF534679 |
| *C. izecksohni* | | KF534634/ KF534644 | KF534653 | KF534662 | — | — | KF534680 |
| *C. izecksohni* | | KF534635/ KF534645 | KF534654 | KF534663 | — | — | KF534681 |
| *C. izecksohni* | | KF534636/ KF534646 | KF534655 | KF534664 | — | — | KF534682 |
| *Crossodactylodes septentrionalis* | | KC603957/ KC603958 | KC603985 | KC603963 | KC604048 | KC604033 | KC604077 |
| *C. septentrionalis* | MZUESC 14363 | — | MN610715 | MN610752 | MN610789 | MN609900 | MN610826 |
| *C. septentrionalis* | MZUESC 21668 | — | MN610716 | MN610753 | MN610790 | MN609901 | MN610827 |
| *Leptodactylus latrans* | | AY843688 | KC603989 | AY843934 | KP295578 | AY844470 | KC604082 |
| *Leptodactylus melanonotus* | | JX564873 | JX564873 | JX564873 | — | — | — |
| *Paratelmatobius cardosoi* | | EU224413 | KU494618 | — | — | — | — |
| *P. cardosoi* | | — | JX298372 | JX298413 | JX298143 | JX298195 | JX298242 |
| *P. cardosoi* | UFMG 3237 | — | MN610717 | MN610754 | MN610791 | MN609902 | MN610828 |
| *Paratelmatobius gaigeae* | UFMG 15006 | — | MN610718 | MN610755 | MN610792 | MN609903 | MN610829 |
| *Paratelmatobius poecilogaster* | | EU224398 | KU494620 | — | — | — | — |
| *P. poecilogaster* | UFMG 3240 | — | MN610719 | MN610756 | MN610793 | MN609904 | MN610830 |
| *Physalaemus nattereri* | | — | KC603984 | KC603965 | KC604053 | — | KC604079 |
| *Pleurodema brachyops* | | AY843733 | KP295702 | AY843979 | KP295582 | AY844503 | — |
| *Rupirana cardosoi* | | KC593361 | — | KC593351 | — | — | KC593368 |
| *R. cardosoi* | | KC603955/ KC603956 | KC603987 | KC603964 | KC604049 | KC604034 | KC604078 |
| *R. cardosoi* | UFMG 4606 | — | MN610720 | MN610757 | MN610794 | MN609905 | MN610831 |
| *Scythrophrys sawayae* | | DQ283099 | — | — | — | — | DQ282926 |
| *S. sawayae* | | KU495580 | KU494787 | — | — | — | — |
| *S. sawayae* | UFMG 15678 | — | MN610721 | MN610758 | MN610795 | MN609906 | MN610832 |

Downloaded From: https://bioone.org/journals/Herpetological-Monographs on 20 May 2020
Terms of Use: https://bioone.org/terms-of-use Access provided by Universidade Estadual Paulista Julio de Mesquita Filho (UNESP)

APPENDIX II.—Sequence of primers, temperature, and time melting used for each fragment and the correlated sources.

| Locus | Primer name and sequence (5′→3′) | Temperature (°C) | Time (s) | Source |
|---|---|---|---|---|
| 12S | MVZ59: ATAGCACTGAAAAYGCTDAGATG<br>MVZ50: TYTCGGTGTAAGYGARAKGCTT | 54 | 60 | Graybeal (1997) |
| 16S | 12SL13: TTAGAAGAGGCAAGTCGTAACATGGTA<br>16STitus1: GGTGGCTGCTTTTAGGCC | 51 | 60 | Feller and Hedges (1998)<br>Titus and Larson (1996) |
| 16S | 16SL2A: CCAAACGAGCCTAGTGATAGCTGGTT<br>16SH10: TGATTACGCTACCTTTGCACGGT | 51 | 60 | Hedges (1994) |
| 16S | 16Sar: CGCCTGTTTATCAAAAACAT<br>16Sbr: CCGGTCTGAACTCAGATCACGT | 51 | 60 | Palumbi et al. (1991) |
| COI | ANF1: ACHAAYCAYAAAGAYATYGG<br>ANR1: CCRAARAATCARAADARRTGTTG | 51 | 40 | Lyra et al. (2017) |
| cytb | CytbAR-H: TAWAAGGGTCTTCTACTGGTTG<br>MVZ15: GAACTAATGGCCCACACWWTACGNAA | 53 | 30 | Goebel et al. (1999)<br>Moritz et al. (1992) |
| cytb | CytbF: TTTCTAGCAATACAYTACACAGCYGAT<br>CytbC-R: CTACTGGTTGTCCTCCGATTCATGT | 50 | 50 | M.L. Lyra (personal communication) |
| POMC | POMC-1:<br>AATGTATYAAAGMMTGCAAGATGGWCCT<br>POMC-2: TAYTGRCCCTTYTTGTGGGCRTT | 60 | 40 | Wiens et al. (2005) |
| RAG-1 | R1-GFF: GAGAAGTCTACAAAAAVGGCAAAG<br>R1-GFR: GAAGCGCCTGAACAGTTTATTAC | 61 | 40 | Faivovich et al. (2005) |
| Tyr | Tyr1C: GGCAGAGGAWCRTGCCAAGATGT<br>Tyr1G: TGCTGGGCRTCTCTCCARTCCCA | 61 | 40 | Bossuyt and Milinkovitch (2000) |

## APPENDIX III

List of morphological/natural history and morphometric characters and characters states coded for terminals of Paratelmatobiinae. To see the character states coded for each terminal, refer to Appendix IV.

### Morphological and Natural History Characters

(1) Anterior projection in medial region of the upper lip: (0) absent (Fig. 13C); (1) present (Figs. 11D, 13D).
(2) Tympanic middle ear (Figs. 5, 6): (0) absent; (1) present. The tympanic middle ear, when complete, is composed by tympanic membrane, tympanic annulus, and columella. However, one or more elements can be absent (see Pereyra et al. 2016). We coded this character as absent only when all the three elements are lacking. The absence of columella in species of *Crossodactylodes* was coded following literature data for *C. pintoi*, *C. bokermanni*, *C. izecksohni*, and *C. septentrionalis* (Lynch 1971; Gomes 1988; Teixeira et al. 2013) or by direct examination (for *C. itambe*).
(3) Tympanic membrane: (0) absent (Figs. 5A–C); (1) present (Fig. 5D).
(4) Tympanic annulus visibility (Figs. 5, 6A, B): (0) not visible through the skin; (1) visible through the skin. We made dissections to determine the presence of tympanic annulus concealed by the skin.
(5) Size of zygomatic process of squamosal bone: (0) short, not passing the anterior margin of the optic foramen; (1) long, passing the anterior margin of the optic foramen. This character was previously proposed by Teixeira et al. (2013).
(6) Vocal slit: (0) absent; (1) present.
(7) Vocal sac condition: (0) externally indistinct; (1) externally distinct. Although Heyer (1999) considered the vocal sac of *Rupirana cardosoi* as externally indicated by lateral skin folds, after examination of specimens we coded this character as externally indistinct for this species.
(8) Vomerine odontophores: (0) absent (Fig. 11B); (1) present (Fig. 11A).
(9) Tubercle on upper eyelid: (0) absent; (1) present.
(10) Shape of tubercle on upper eyelid: (0) rounded; (1) acuminate, resembling a small dermal horn.
(11) Meniscus in the upper iris: (0) absent; (1) present.
(12) Mandibular tubercle: (0) absent; (1) present.
(13) Nuptial pads: (0) numerous (more than 20) small spicules (Fig. 3B); (1) few (less than 20) well developed spines (Fig. 3A).
(14) Dorsolateral fold: (0) absent (Fig. 14B); (1) present (Fig. 14A). This fold can be poorly or well-developed (see character 15).
(15) Dorsolateral fold development: (0) weakly developed; (1) well developed. Pombal and Haddad (1999) used this character to distinguish between species of *Paratelmatobius*. To avoid subjectivity in the states assignments, we considered only the quite distinct fold of *Scythrophrys sawayae* as well developed.
(16) Relative lengths of fingers I and II: (0) Finger I as long as or shorter than Finger II; (1) Finger I longer than Finger II.
(17) Disc of Finger I: (0) acute, i.e., with no apparent disc (Fig. 12E); (1) rounded (Figs. 12A–D).
(18) Discs of fingers II–IV: (0) narrow, i.e., same width or less dilated than the base of finger (Figs. 3D–F); (1) expanded, i.e., more dilated than the base of finger (Fig. 3C).
(19) Tubercle on outer margin of heel: (0) absent; (1) present.
(20) Tarsal fold: (0) absent (Figs. 3G–I); (1) present (Figs. 3J, K).
(21) Toes II–V webbing: (0) absent (Fig. 3G); (1) present (Figs. 3H–K).
(22) Type of toes II–V webbing: (0) weak lateral ridges (Figs. 3J, K); (1) well developed, flexible fringes (Fig. 3H).
(23) Cloacal flap: (0) inconspicuous (short free distal portion; Figs. 4B, C); (1) conspicuous (long free distal portion; Fig. 4A).
(24) Numerous white tubercles on males' dorsum: (0) absent (Figs. 5A–C); (1) present (Fig. 5D).
(25) Skin texture of males' dorsum: (0) shagreen; (1) coarsely granular.
(26) Bright and contrasting coloration (in life) on ventral surfaces of belly: (0) absent; (1) present.
(27) Bright and contrasting coloration (in life) on ventral surface of arm: (0) absent; (1) present.
(28) Iris coloration in life: (0) coppery or reddish with dark brown reticulations; (1) upper half gray and lower half dark brown; (2) uniformly black or brownish black; (3) yellowish with dark brown reticulations, interrupted by a brown horizontal bar at the pupil level.
(29) Reproductive mode (sensu Haddad and Prado 2005): (0) mode 1; (1) mode 6; (2) mode 18.
(30) Number and arrangement of eggs: (0) 50–200 eggs in a single group; (1) 10–40 eggs positioned in haphazard groups, or in groups of 2–20; (2) single eggs, positioned isolated from other eggs. Data available in: Garcia (1996); Pombal and Haddad (1999); Juncá and Lugli (2009); Santos et al. (2017); and Ferreira et al. (2019a).
(31) Foot length (in mm). This continuous character was optimized as minimum and maximum values of the ratio foot length/SVL under the Squared Change Parsimony model (Fig. 7).

Downloaded From: https://bioone.org/journals/Herpetological-Monographs on 20 May 2020
Terms of Use: https://bioone.org/terms-of-use Access provided by Universidade Estadual Paulista Julio de Mesquita Filho (UNESP)

APPENDIX IV.—Character matrix for 13 taxa of Paratelmatobiinae (see Appendix III for a description of characters and character states). Polymorphic characters are coded as such. Nonapplicable characters are indicated with (–), and unknown character states are indicated with (?).

| | Characters and character states | | | | | | | | | | | | | | | | | | | | | | | | | | | | |
|---|---|---|---|---|---|---|---|---|---|---|---|---|---|---|---|---|---|---|---|---|---|---|---|---|---|---|---|---|---|
| Taxon | 1 | 2 | 3 | 4 | 5 | 6 | 7 | 8 | 9 | 10 | 11 | 12 | 13 | 14 | 15 | 16 | 17 | 18 | 19 | 20 | 21 | 22 | 23 | 24 | 25 | 26 | 27 | 28 | 29 | 30 | 31 |
| *Rupirana cardosoi* | 0 | 1 | 1 | 1 | ? | 1 | 0 | 1 | 0 | – | 0 | 0 | 0 | 1 | – | 0 | 0 | 0 | 0 | 1 | 1 | 0 | 0 | 1 | 0 | 0 | 0 | 0 | 0 | 0 | (0.5–0.55) |
| *Scythrophrys sawayae* | 0 | 1 | 0 | 0 | ? | 1 | 1 | 1 | 1 | 1 | 1 | 0 | 0 | 1 | 1 | 0 | 0 | 0 | 1 | 1 | 1 | 0 | 0 | 0 | 0 | 0 | 1 | 1 | 0 | 1 | (0.4–0.48) |
| *Paratelmatobius poecilogaster* | 0 | 1 | 0 | 0 | ? | 0 | 0 | 1 | 1 | 0 | 0 | 0 | 0 | 1 | 0 | 0 | 0 | 0 | 0 | 0 | 1 | 1 | 0 | 0 | 0 | 1 | 1 | 0 | 2 | 1 | (0.4–0.49) |
| *Paratelmatobius gaigeae* | 0 | 1 | 0 | 0 | ? | 0 | 0 | 1 | 0 | – | 0 | 0 | 0 | 1 | 0 | 0 | 0 | 0 | 0 | 0 | 1 | 1 | 0 | 0 | 0 | 1 | 1 | 0 | 0 | 1 | (0.44–0.48) |
| *Paratelmatobius cardosoi* | 0 | 1 | 0 | 1 | ? | 1 | 0 | 1 | 0 | – | 0 | 1 | 0 | 1 | 0 | 1 | 0 | 0 | 0 | 0 | 1 | 1 | 0 | 0 | 0 | 1 | 1 | 0 | 0 | 1 | (0.41–0.44) |
| *Crossodactylodes bokermanni* Lin. A | 0 | 0 | – | – | 0 | 1 | 0 | 1 | 1 | 0 | 0 | 0 | 1 | 1 | 0 | 0 | 0 | 1 | 0 | 0 | 0 | – | 1 | 0 | 0 | 0 | 0 | 0 | 1 | 2 | (0.38–0.4) |
| *Crossodactylodes bokermanni* Lin. B | 0 | 0 | – | – | 0 | 1 | 0 | 1 | 1 | 0 | 0 | 0 | 1 | 1 | 0 | 0 | 0 | 1 | 0 | 0 | 0 | – | 1 | 0 | 0 | 0 | 0 | 0 | 1 | 2 | (0.37–0.41) |
| *Crossodactylodes bokermanni* Lin. C | 0 | 0 | – | – | 0 | 1 | 0 | 1 | 1 | 0 | 0 | 0 | 1 | 1 | 0 | 0 | 0 | 1 | 0 | 0 | 0 | – | 1 | 0 | 0 | 0 | 0 | 0 | 1 | 2 | (0.34–0.41) |
| *Crossodactylodes itambe* | 1 | 0 | – | – | 1 | 0 | – | 0 | 0/1 | – | 0 | 0 | 1 | 0 | – | 0 | 0 | 1 | 0 | 0 | 0 | – | 1 | 0 | 1 | 0 | 0 | 2 | 1 | 2 | (0.31–0.4) |
| *Crossodactylodes septentrionalis* | 0 | 0 | – | – | 1 | 0 | – | 1 | 0/1 | 0 | 0 | 0 | 1 | 0 | – | 0 | 1 | 1 | 0 | 0 | 0 | – | 1 | 0 | 1 | 0 | 0 | 0 | 1 | ? | (0.36–0.4) |
| *Crossodactylodes izecksohni* Lin. A | 0 | 0 | – | – | 0 | 0 | – | 0 | 0/1 | 0 | 0 | 0 | 1 | 0 | – | 0 | 0 | 1 | 0 | 0 | 0 | – | 1 | 0 | 1 | 0 | 0 | 3 | 1 | 2 | (0.32–0.4) |
| *Crossodactylodes izecksohni* Lin. B | 0 | 0 | – | – | 0 | 0 | – | 0 | 0/1 | 0 | 0 | 0 | 1 | 0 | – | 0 | 0 | 1 | 0 | 0 | 0 | – | 1 | 0 | 1 | 0 | 0 | 3 | 1 | 2 | (0.35–0.4) |
| *Crossodactylodes pintoi* | 0 | 0 | – | – | 0 | 0 | – | 0 | 0 | 0 | 0 | 0 | 1 | 0 | – | 0 | 0 | 1 | 0 | 0 | 0 | – | 1 | 0 | 1 | 0 | 0 | ? | ? | ? | (0.31–0.35) |

## APPENDIX V

Additional Specimens examined. *Specimens for which we measured SVL and foot length.

*Paratelmatobius cardosoi*.—BRAZIL: SÃO PAULO: municipality of Bertioga, Parque das Neblinas (CFBH 38980, 38982, 38989–90, UFMG 3237); municipality of Santo André, Parque Estadual Municipal Nascentes de Paranapiacaba (topotypes: CFBH 3263–66*, 3269*, 28957–58*, 28969*, 29001*, 29004*).

*Paratelmatobius gaigeae*.—BRAZIL: SÃO PAULO: municipality of Bananal, Estação Ecológica do Bananal (CFBH 7156; MZUSP 138657*, 138659*, 138661); municipality of São José do Barreiro, Parque Nacional da Serra da Bocaina (topotypes: CFBH 36069–70*, 36079*, UFMG 15004–08*).

*Paratelmatobius lutzii*.—BRAZIL: MINAS GERAIS: Itamonte, Parque Nacional de Itatiaia (topotypes: CFBH 295, MZUSP 94629–94633).

*Paratelmatobius mantiqueira*.—BRAZIL: SÃO PAULO: Campos do Jordão, Cidade Azul (paratypes: MZUSP 15128–15132).

*Paratelmatobius poecilogaster*.—BRAZIL: SÃO PAULO: municipality of Bertioga, Parque das Neblinas (UFMG 3238–40); municipality of Santo André, Parque Estadual Municipal Nascentes de Paranapiacaba (topotypes: CFBH 866, 3253–54, CFBH 12004–05, 28959–60, 29983).

*Rupirana cardosoi*.—BRAZIL: BAHIA: municipality of Ibicoara, Parque Nacional da Chapada Diamantina (UFMG 7954–55); municipality of Lençóis, Parque Nacional da Chapada Diamantina and surroundings (CFBH 6666–67*, 6669*); municipality of Mucugê, Parque Nacional da Chapada Diamantina and surroundings (topotypes: UFMG 4252–54*, 4272*, 7915–21, 7922–23*); municipality of Palmeiras, Parque Nacional da Chapada Diamantina (CFBH 6665*).

*Scythrophrys sawayae*.—BRAZIL: PARANÁ: municipality of Piraquara, Mananciais da Serra (topotypes: CFBH 3397–98, 3400–01). SANTA CATARINA: municipality of Blumenau, Parque Nacional da Serra do Itajaí (UFMG 3241–42, 7504–07); municipality of Joinville, Castelo dos Bugres (UFMG 13896, 14470); municipality of São Bento do Sul, Rio Vermelho (CFBH 2981, 3186, 3190–91).

APPENDIX VI.—Uncorrected *p*-distances (percentage) among species and lineages of *Crossodactylodes*. Distances for COI fragment (ca. 650 bp) are shown under the diagonal, and distances for cytb fragment (ca. 770 bp) are shown above the diagonal. Intraspecific or intralineage distances are shown as COI/cytb (along diagonal). NC = not calculated because there was only one individual.

| | *C. bokermanni* Lineage A ($n$ = 1) | *C. bokermanni* Lineage B ($n$ = 7) | *C. bokermanni* Lineage C ($n$ = 7) | *C. itambe* ($n$ = 5) | *C. izecksohni* Lineage A ($n$ = 14) | *C. izecksohni* Lineage B ($n$ = 5) | *C. septentrionalis* ($n$ = 3) |
|---|---|---|---|---|---|---|---|
| *C. bokermanni* Lineage A | NC / NC | 4.6–4.7 | 6.2–6.8 | 13.1–13.4 | 13.1–14.2 | 12.5–12.6 | 13.8–14.1 |
| *C. bokermanni* Lineage B | 5.0–5.3 | 0.0–0.3 / 0.0–0.6 | 8.1–9.0 | 12.6–13.7 | 11.5–14.1 | 12.5–12.9 | 13.1–14.0 |
| *C. bokermanni* Lineage C | 7.9–8.2 | 8.5–9.3 | 0.0–0.3 / 0.0–0.2 | 14.0–14.7 | 14.2–16.0 | 13.3–13.9 | 14.7–15.2 |
| *C. itambe* | 15.2–15.5 | 15.2–15.7 | 14.1–14.6 | 0.0–0.5 / 0.0–0.3 | 11.3–13.4 | 11.2–11.6 | 11.5–12.2 |
| *C. izecksohni* Lineage A | 16.3–17.0 | 15.3–16.0 | 15.7–16.3 | 11.3–11.9 | 0.0–1.4 / 0.0–1.2 | 7.7–8.9 | 12.9–14.6 |
| *C. izecksohni* Lineage B | 16.7–17.1 | 15.7–16.1 | 16.4–16.7 | 13.3–13.8 | 6.0–6.8 | 0.0–0.2 / 0.0–0.1 | 13.6–14.0 |
| *C. septentrionalis* | 16.7–16.9 | 16.7–17.3 | 16.6–17.0 | 12.4–12.9 | 14.1–15.2 | 16.1–16.4 | 0.0–0.5 / 0.1–0.8 |

APPENDIX VII.—Uncorrected *p*-distances (percentage) of the entire H1 fragment (ca. 2300 bp) within (along diagonal) and among species and lineages of *Crossodactylodes*. NC = not calculated because there was only one individual.

| | *C. bokermanni* Lineage A ($n$ = 2) | *C. bokermanni* Lineage B ($n$ = 8) | *C. bokermanni* Lineage C ($n$ = 3) | *C. itambe* ($n$ = 5) | *C. izecksohni* Lineage A ($n$ = 7) | *C. izecksohni* Lineage B ($n$ = 3) | *C. septentrionalis* ($n$ = 1) |
|---|---|---|---|---|---|---|---|
| *C. bokermanni* Lineage A | 0.0 | | | | | | |
| *C. bokermanni* Lineage B | 1.3 | 0.0 | | | | | |
| *C. bokermanni* Lineage C | 3.4–3.5 | 3.1–3.3 | 0.0 | | | | |
| *C. itambe* | 7.7–7.9 | 7.6–7.9 | 7.3–7.5 | 0.0–0.2 | | | |
| *C. izecksohni* Lineage A | 8.2–8.3 | 8.2–8.5 | 8.1–8.3 | 5.5–5.8 | 0.0–0.4 | | |
| *C. izecksohni* Lineage B | 8.8–9.0 | 8.9–9.2 | 8.8–9.1 | 6.0–6.4 | 3.8–3.9 | 0.1 | |
| *C. septentrionalis* | 8.9 | 8.8–9.1 | 8.4 | 5.2–5.3 | 6.8–7.0 | 6.9–7.2 | NC |

Downloaded From: https://bioone.org/journals/Herpetological-Monographs on 20 May 2020
Terms of Use: https://bioone.org/terms-of-use Access provided by Universidade Estadual Paulista Julio de Mesquita Filho (UNESP)

# SUPPLEMENTAL MATERIALS

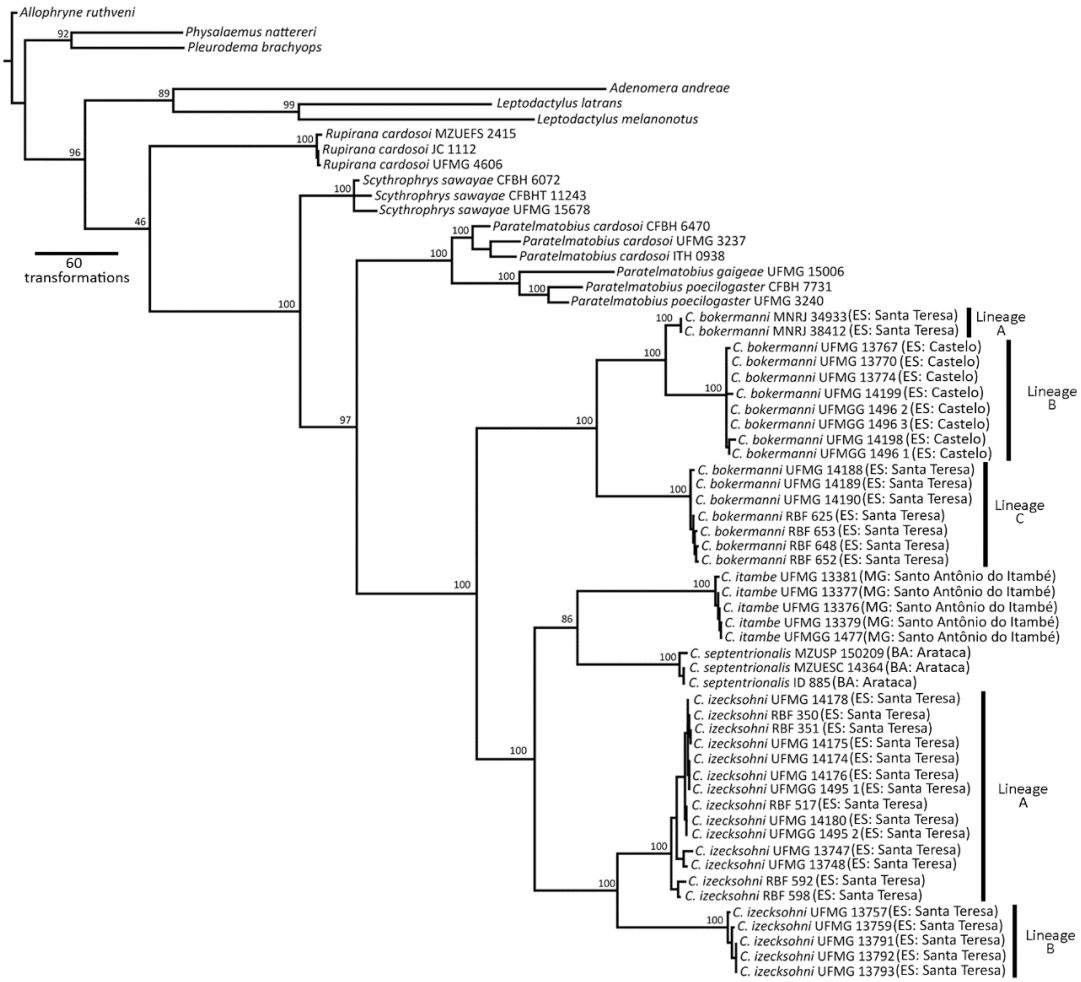


FIG. S1.—Strict consensus of the 45 equally parsimonious trees with 5780 steps each obtained from Maximum Parsimony analysis of concatenated mtDNA (H1, COI, cytb) and nDNA (POMC, RAG-1, tyr) genes. Values above branches indicate jackknife proportions.

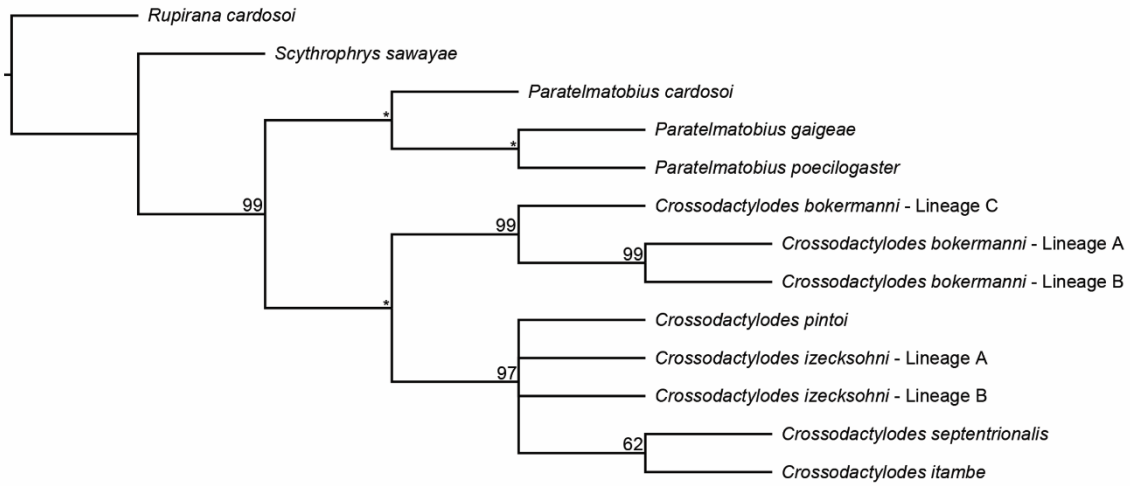


FIG. S2.—Strict consensus of the three equally parsimonious trees with 3052 steps each achieved in the total evidence analysis using TNT. Values above branches indicate jackknife proportions. Asterisks indicate 100% values.

FIG. S3.—Variation in coloration pattern in life in *Crossodactylodes izecksohni*. The dorsal background coloration may be pink (A), pale cream (B), beige (C, M, N), pale lilac (D, E), light brown (F, I), brownish gray (G, H), pale yellow (J), and brownish yellow (K, L). Froglets are usually dark brown with numerous small white, bluish and/or yellowish (O). A dorsal X-shaped blotch is usually present, and can be strongly (J, K, L, M, O), or weakly (A, D, E, G, H, I, N) marked, continuous (E, M, O), or interrupted (A, D, G, H, I, J, K, L, N), but this blotch can be absent (B, C, F). A black lateral stripe is present in few individuals, and can be from posterior margin of eye to the final third of body (B, J, L, N), or from middle to posterior third of the body (M). This stripe can be strongly (B, J, L, M), or weakly (N) marked. Transverse bars on hindlimbs is present in few individuals, and can be strongly (J, L), or weakly (H) marked.

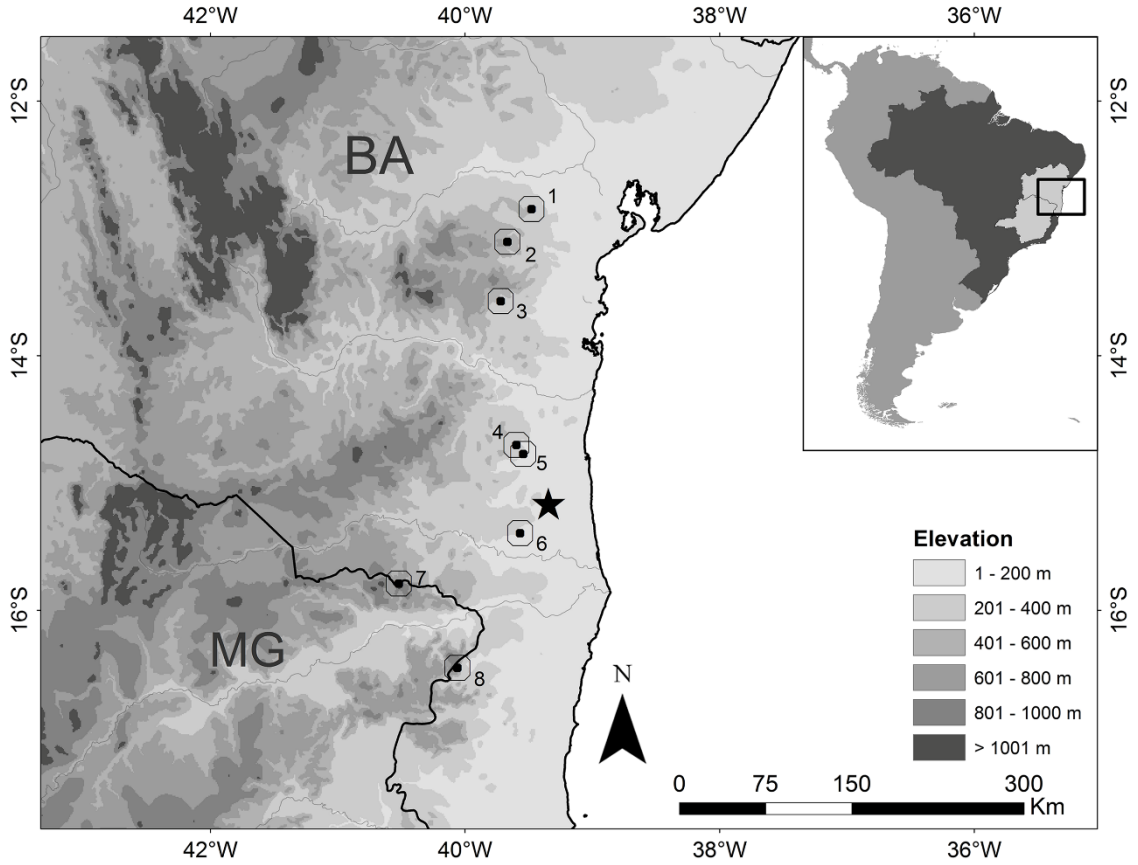


FIG. S4.—The sampled areas surrounding the type locality of *Crossodactylodes septentrionalis*, in the Parque Nacional da Serra das Lontras, municipality of Arataca in the state of Bahia (star). These areas, with approximate distances from type locality are: 1) Serra da Jiboia, municipality of Santa Teresinha, ~ 255 km north; 2) Serra do Timbó, municipality of Amargosa, ~ 230 km north; 3) Estação Ecológica de Wenceslau Guimarães, municipality of Wenceslau Guimarães, ~ 178 km north; 4) Serra do Corcovado, municipality of Almadina, ~ 55 km northwest; 5) Pedra Lascada, municipality of Barro Preto, ~ 46 km northwest; 6) Reserva Particular do Patrimônio Natural (RPPN) Serra Bonita, municipality of Camacan, ~ 35 km southwest; 7) RPPN Mata do Passarinho, municipality of Macarani, ~ 145 km southwest and 8) Parque Nacional Alto do Cariri, municipality of Guaratinga, ~ 160 km southwest. BA = Bahia; MG = Minas Gerais.

## CAPÍTULO II

# Multilocus phylogeny of Paratelmatobiinae (Anura: Leptodactylidae) reveals strong spatial structure and previously unknown diversity in the Atlantic Forest hotspot

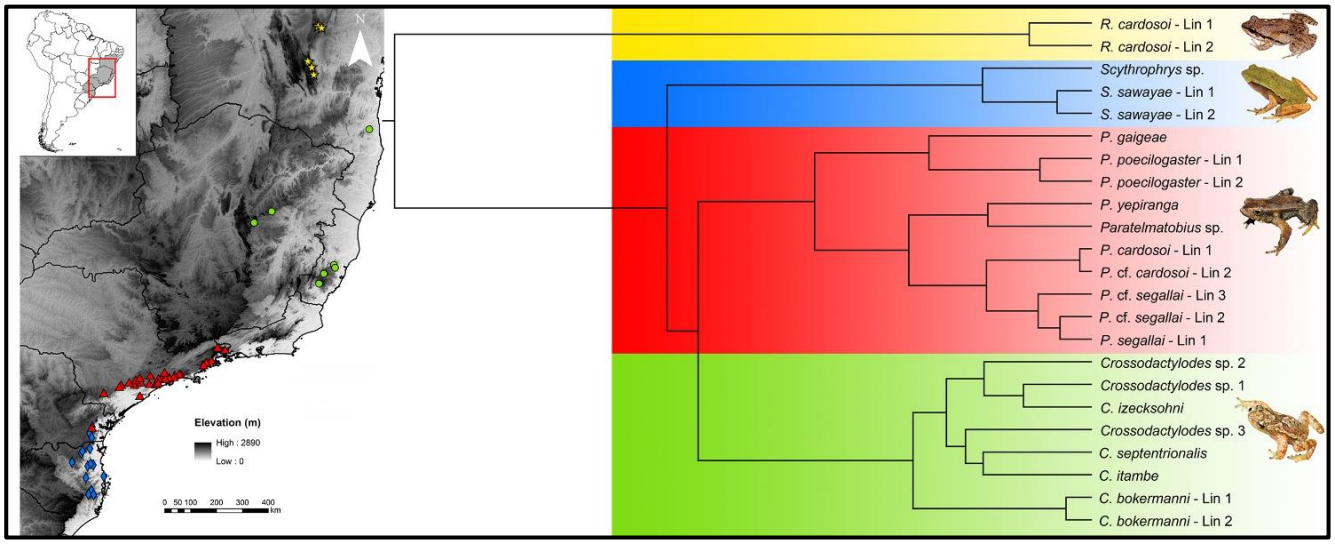


## HIGHLIGHTS

- We propose a new phylogenetic hypothesis for Paratelmatobiinae.
- We found deeply divergent and geographically structured lineages.
- Five putatively new species were supported as independently evolving lineages.
- Diversification began in the Eocene and continued until the Pleistocene.

  Past climate changes, neotectonic events, and life history traits likely influenced diversification.

Molecular Phylogenetics and Evolution 148 (2020) 106819

Contents lists available at ScienceDirect

Molecular Phylogenetics and Evolution

journal homepage: www.elsevier.com/locate/ympev

# Multilocus phylogeny of Paratelmatobiinae (Anura: Leptodactylidae) reveals strong spatial structure and previously unknown diversity in the Atlantic Forest hotspot

Marcus Thadeu T. Santos[a,b,*], Rafael F. de Magalhães[c,d], Mariana L. Lyra[b], Fabrício R. Santos[c], Hussam Zaher[e], Luís O.M. Giasson[f], Paulo C.A. Garcia[c], Ana Carolina Carnaval[g,h], Célio F.B. Haddad[a,b]

[a] Programa de Pós-Graduação em Zoologia, Instituto de Biociências, Universidade Estadual Paulista (UNESP), Avenida 24 A, 1515, Rio Claro, SP 13506-900, Brazil
[b] Departamento de Biodiversidade e Centro de Aquicultura (CAUNESP), Instituto de Biociências, Universidade Estadual Paulista (UNESP), Avenida 24 A, 1515, Rio Claro, SP 13506-900, Brazil
[c] Programa de Pós-Graduação em Zoologia, Instituto de Ciências Biológicas, Universidade Federal de Minas Gerais, Avenida Antônio Carlos, 6627, Belo Horizonte, MG 31270-010, Brazil
[d] Departamento de Ciências Naturais (DCNAT), Campus Dom Bosco, Universidade Federal de São João del-Rei (UFSJ), Praça Dom Helvécio, 74, São João del-Rei, MG 36301-160, Brazil
[e] Museu de Zoologia, Universidade de São Paulo, Avenida Nazaré, 481, São Paulo, SP 04263-000, Brazil
[f] Departamento de Ciências Naturais, Centro de Ciências Exatas e Naturais, Fundação Universidade Regional de Blumenau, Blumenau, SC 89012-900, Brazil
[g] Department of Biology, City College of New York, 160 Convent Avenue, New York, NY 10031, USA
[h] Biology Program, Graduate Center, City University of New York, 365 Fifth Avenue, New York, NY 10016, USA

ARTICLE INFO

*Keywords:*
Amphibia
*Campo rupestre*
Endemism
Genetic diversity
Molecular systematics
Species tree

ABSTRACT

The Brazilian Atlantic Forest harbors high levels of anuran diversity and endemism, including several taxa restricted to small geographic ranges. Here, we provide a multilocus phylogeny for Paratelmatobiinae, a leptodactylid subfamily composed of small-ranged species distributed in the Brazilian Atlantic Forest and in the *campo rupestre* ecosystem. We performed Bayesian inference and maximum likelihood analyses using three mitochondrial and five nuclear markers, and a matrix comprising a broad taxonomic sampling. We then delimitated independently evolving lineages within the group. We recovered Paratelmatobiinae and each of its four genera as monophyletic and robustly supported. Five putatively new species included in our analyses were unambiguously supported in the phylogenetic trees and delimitation analyses. We also recovered other deeply divergent and geographically structured lineages within the four genera of Paratelmatobiinae. Our estimation of divergence times indicates that diversification in the subfamily began in the Eocene and continued until the Pleistocene. We discuss possible scenarios of diversification for the four genera of Paratelmatobiinae, and outline the implications of our findings for taxonomy and conservation.

## 1. Introduction

The Brazilian Atlantic Forest (AF) harbors one of the highest levels of endemism and biodiversity in the world (Morellato and Haddad, 2000; Silva and Casteleti, 2003; Fonseca et al., 2004). The wide latitudinal and longitudinal ranges, broad altitudinal gradients, and the environmental complexity of this forest domain are among the main factors proposed to explain its great biological diversity (Morellato and Haddad, 2000; Oliveira-Filho and Fontes, 2000; Câmara, 2003). This biodiversity hotspot also harbors exceptionally high anuran diversity. With more than 620 species, it contains nearly one-ninth of the global anuran richness and more than 50% of the megadiverse Brazilian anuran fauna (Rossa-Feres et al., 2017; Frost, 2020). More than 75% of these species are endemic to the AF and most of them are known from

* Corresponding author at: Programa de Pós-Graduação em Zoologia, Instituto de Biociências, Universidade Estadual Paulista (UNESP), Avenida 24 A, 1515, Rio Claro, SP 13506-900, Brazil.
*E-mail addresses:* marcus.santos@unesp.br (M.T.T. Santos), rafaelmagalhaes@ufsj.edu.br (R.F.d. Magalhães), mariana.lyra@pq.cnpq.br (M.L. Lyra), fabricio-santos@ufmg.br (F.R. Santos), hzaher@usp.br (H. Zaher), lgiasson@furb.br (L.O.M. Giasson), pcagarcia@ufmg.br (P.C.A. Garcia), acarnaval@ccny.cuny.edu (A.C. Carnaval), celio.haddad@unesp.br (C.F.B. Haddad).

https://doi.org/10.1016/j.ympev.2020.106819
Received 29 September 2019; Received in revised form 15 February 2020; Accepted 1 April 2020
Available online 11 April 2020
1055-7903/ © 2020 Elsevier Inc. All rights reserved.

one or a few localities in montane environments (Haddad et al., 2013; Villalobos et al., 2013; Rossa-Feres et al., 2017).

These endemic taxa are susceptible to strong anthropogenic pressure. Over the last decades, the AF has suffered from alarming rates of vegetation loss (Ribeiro et al., 2009; Tabarelli et al., 2010), which represents the main threat to its species (Myers et al., 2000). In fact, 90% of the endangered Brazilian anurans occur only in the AF and are restricted to small geographic ranges (ICMBio, 2018). For instance, the first Brazilian anuran to be considered extinct, *Phrynomedusa fimbriata* (Hylidae: Phyllomedusinae), had a very small geographic distribution restricted to the AF (Baêta et al., 2016; Cruz and Pimenta, 2004; ICMBio, 2018). These factors highlight the need for comprehensive studies of small-ranged anurans endemic to the AF, as restricted geographic distributions represent a risk factor for extinctions due to stochastic events (Lande, 1999; Sodhi et al., 2008; Pimm et al., 2014). This knowledge will allow for a better understanding of evolutionary processes that have resulted in patterns of anuran endemism, which is important to improve conservation strategies.

Several non-mutually exclusive hypotheses have been proposed to explain the diversification of species in the AF. The most commonly invoked is the Pleistocene refugia hypothesis (Haffer, 1969; Hewitt, 2000; Moritz et al., 2000; Carnaval et al., 2009; Martins, 2011; Cazé et al., 2016), which rests on the idea that climatic fluctuations caused successive contractions and expansions of forests and open environments, with the persistence of forests in climatically stable areas. The hypothesis posits that isolation of forest fragments has prevented gene flow between populations of forest-adapted species, favoring diversification. A second class of hypotheses involves geographic barriers to gene flow, such as rivers systems and mountain chains (Pellegrino et al., 2005; Cabanne et al., 2007; Brunes et al., 2010; Thomé et al., 2014; Cazé et al., 2016). Additional factors that may have contributed to diversification, especially at small geographic scales, are topographic complexity of tropical mountains and climatic variation along altitudinal gradients, causing isolation among populations and subsequent speciation (Guarnizo and Cannatella, 2013; Graham et al., 2014; Rodríguez et al., 2015). Coupled with environmental complexity, life history traits play a key role in diversification by defining the vagility and the physiological tolerance of species (Wollenberg et al., 2011; Fusinatto et al., 2013; Polato et al., 2018).

Here, we focus on the diversification of one poorly known group of endemic anurans of AF, the leptodactylid subfamily Paratelmatobiinae Ohler and Dubois, 2012. This subfamily currently comprises 14 species in four genera: *Crossodactylodes* Cochran, 1938, *Paratelmatobius* Lutz and Carvalho, 1958, *Rupirana* Heyer, 1999, and *Scythrophrys* Lynch, 1971 (Frost, 2020). The four genera are distributed along a North-South gradient (Fig. 1; Fouquet et al., 2013), and all species are associated with montane environments. The monotypic genus *Rupirana* is endemic to the *campo rupestre* ecosystem (i.e., rupestrian grasslands; Silveira et al., 2016) in the northern Espinhaço Mountain Range, state of Bahia (Heyer, 1999; Juncá and Lugli, 2009). The genus *Crossodactylodes* includes five species distributed in the AF from southern Bahia to the state of Rio de Janeiro, and in one open environment of the *campo rupestre* in the state of Minas Gerais (Santos et al., 2020). The genus *Paratelmatobius* comprises seven species arranged in two groups (*P. cardosoi* group and *P. lutzii* group) distributed along the Serra da Mantiqueira and Serra do Mar mountain ranges, from southern Minas Gerais and Rio de Janeiro, through São Paulo, to the state of Paraná (Pombal and Haddad, 1999; Lourenço et al., 2008, Santos et al., 2019). *Scythrophrys* is also a monotypic genus distributed in the southern part of Serra do Mar and Serras do Leste Catarinense mountain ranges, in the states of Paraná and Santa Catarina (Lourenço et al., 2008).

Species of Paratelmatobiinae occupy a wide range of microhabitats, including shallow temporary ponds and small streams in open (*Rupirana*) or forested (*Paratelmatobius* and *Scythrophrys*) environments, and bromeliads (*Crossodactylodes*) (Heyer, 1999; Juncá and Lugli, 2009; Lourenço et al., 2008; Pombal and Haddad, 1999; Santos et al., 2020). Most species are rare and known from one or few localities (Frost, 2020); some of them have not been recorded for several years, such as *C. pintoi* (last record dating to 1909; Peixoto and Carvalho-e-Silva, 2004) and *P. lutzii* (last record dating to 1978; Pombal and Haddad, 1999). Although the subfamily occurs in a well-sampled and studied area (Oliveira et al., 2016; Moura et al., 2018), their rarity and occurrence in specific microhabitats, as well as the recent findings of new species (Barata et al., 2013; Santos et al., 2019; Teixeira et al., 2013), suggest that the number of species of Paratelmatobiinae may be underestimated.

Some life history traits of Paratelmatobiinae species such as small body size, restricted geographic range, and habitat specialization have already been linked to low population connectivity and, consequently, to elevated speciation rates (Losos, 2010; Wollenberg et al., 2011; Fusinatto et al., 2013; Condez et al., 2020). Therefore, the subfamily is a suitable model taxon to investigate diversification events across the AF mountains, at different temporal scales, as well as between the AF and the *campo rupestre*. However, phylogenetic studies focused on this subfamily have been based on limited taxonomic and/or character sampling (Fouquet et al., 2013; Lourenço et al., 2008; Santos et al., 2019, 2020; Teixeira et al., 2013), hampering inferences about the evolutionary history.

By combining fieldwork with samples from herpetological collections, we prepared a dataset with broad taxon sampling of Paratelmatobiinae, including species with unknown phylogenetic placement and lineages that may represent undescribed species. By sequencing eight markers from 11 named species and five putatively new species, we reconstructed the phylogeny of the Paratelmatobiinae to (1) test the monophyly of the subfamily and each of its genera; (2) delimit independently evolving lineages within *Crossodactylodes*, *Paratelmatobius*, *Scythrophrys*, and *Rupirana*; (3) estimate the timing of diversification events within the subfamily; and (4) identify evolutionary processes that might have driven diversification at different temporal scales. Given the strict association with montane environments, the restricted geographic ranges, and the life history traits of the species of Paratelmatobiinae, we expect to find deeply divergent and geographically structured species and lineages, consistent with ancient diversification events.

## 2. Material and methods

### 2.1. Sampling, laboratory procedures, and sequence editing

We gathered tissue samples from field efforts and seven institutional collections, complementing it with GenBank sequences (Tables S1 and S2). Our ingroup includes 60 samples of *Crossodactylodes*, 120 of *Paratelmatobius*, 45 of *Scythrophrys*, and nine of *Rupirana*. This includes 11 of the 14 nominal species within Paratelmatobiinae, covering almost the entirety of its known geographic range. Our sampling also includes five putatively new species: a lineage of *Paratelmatobius* (here referred as *Paratelmatobius* sp.), three lineages of *Crossodactylodes* (here referred as *Crossodactylodes* sp. 1, *Crossodactylodes* sp. 2, and *Crossodactylodes* sp. 3), for which morphological differences were observed in comparison with congeners, and a lineage of *Scythrophrys* previously proposed as a distinct taxonomic unit based on genetic and karyotypic differences (see Lourenço et al., 2003), here referred as *Scythrophrys* sp. Whenever the identification of a lineage was not absolutely certain, we added the qualifier *confer* (cf.) to the species names. Tissue samples were not available for (1) *C. pintoi*, known only from its type series collected in 1909 (Peixoto and Carvalho-e-Silva, 2004); (2) *P. lutzii*, last recorded in 1978 (Pombal and Haddad, 1999); and (3) *P. mantiqueira*, known only from its type series collected in 1953 (Pombal and Haddad, 1999) and a single specimen found 52 years later (Vrcibradic et al., 2010).

We obtained genomic DNA from ethanol-preserved tissues using a standard ammonium acetate extraction protocol (Maniatis et al., 1982). Then, we used Polymerase Chain Reaction (PCR) to amplify DNA

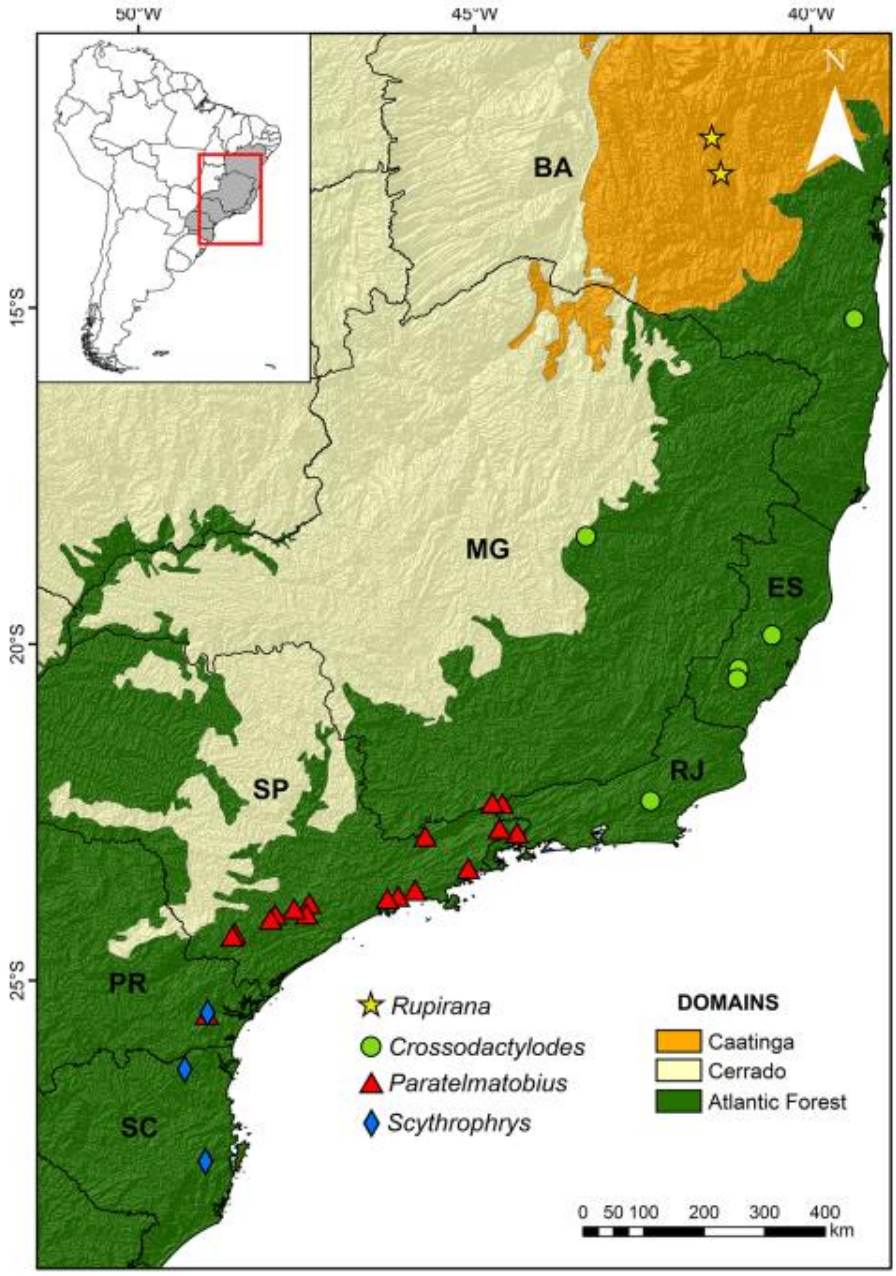


**Fig. 1.** Geographic distribution of the four genera of Paratelmatobiinae. Occurrence records were obtained from Juncá and Lugli (2009), Lourenço et al. (2008), and Santos et al. (2019, 2020). Brazilian states: BA (Bahia); ES (Espírito Santo); MG (Minas Gerais); PR (Paraná); RJ (Rio de Janeiro); SC (Santa Catarina); SP (São Paulo). For interpretation of the references to colour in this figure legend, the reader is referred to the web version of this article.

sequences for three mitochondrial (mtDNA) and five nuclear (nDNA) gene fragments. The mtDNA dataset includes the non-coding heavy strand transcription unit 1 (H1: 12S and 16S rRNA genes, plus the intervening $tRNA^{valine}$ gene), a fragment of the cytochrome *c* oxidase subunit I (COI), and cytochrome *b* (cyt-*b*). The nDNA markers include fragments of the exonic genes proopiomelanocortin A (POMC), recombination-activating protein 1 (RAG-1), rhodopsin (Rhod), tensin 3 (TNS3), and tyrosinase (Tyr). PCR primers used for amplification and sequencing and reaction conditions are shown in Table S3. We purified PCR products using a mix of thermosensitive alkaline phosphatase (FastAP) and Exonuclease I, following the manufacturer's protocol (Thermo Fisher Scientific Inc.), with modifications provided by Lyra et al. (2017). The products were sequenced in both directions by Macrogen Inc. (Seoul, South Korea), with a Big Dye v.3.0 Sequencing Kit (Applied Biosystems). We checked for quality, excluded primers sequences, and assembled the chromatograms using Geneious v.7 (Biomatters Ltd.). GenBank accession numbers and voucher information are given in Table S1 (ingroup) and Table S2 (outgroup).

We performed sequence alignments with MAFFT v.7.427 (Katoh and Standley 2013) using the MAFFT online service (Katoh et al., 2017). For coding gene fragments (COI, cyt-*b*, POMC, RAG-1, Rhod, TNS3, and Tyr) we used the G-INS-i algorithm, whereas the E-INS-i algorithm was used for H1.

### 2.2. Phylogenetic inferences

To test the monophyly of Paratelmatobiinae we used all ingroup samples, representatives of most families of Hyloidea as outgroups, and a calyptocephalellid (*Calyptocephalella gayi*) to root the trees due to its close relationship with Hyloidea (Pyron, 2014). We performed Bayesian inference (BI) and maximum likelihood (ML) analyses concatenating mtDNA and nDNA fragments. We defined 22 *a priori* partitions, including the H1 and the three codon positions for each coding fragment, separately, to estimate the best partition scheme and substitution models in PartitionFinder v.2.1.1 (Lanfear et al., 2017) under the linked model of branch lengths, greedy search algorithm, and Corrected Akaike Information Criterion (Hurvich and Tsai, 1989). For the ML analysis, we used the resulting partition scheme, but applied the GTR + G model for all partitions due to the impossibility of applying different models in RAxML. The best partition schemes and substitution models are given in Table S4 for all analyses. The BI analysis was computed with MrBayes v.3.2.6. (Ronquist et al., 2012) using two parallel runs of $4.0 \times 10^7$ generations each, and four chains (one cold), sampling every 1000 generations. We set up the runs with unlinked character state frequencies, substitution rates of GTR model, gamma shape parameter, and proportion of invariable sites between partitions. The first 25% of generations and trees were discarded as burn-in, and the remaining trees were summarized in a majority-rule consensus tree and used to calculate Bayesian posterior probabilities (PP). We verified the minimal effective sample sizes (ESS > 200) and the convergence between the runs with Tracer v.1.7 (Rambaut et al., 2018). The ML analysis was computed with RAxML v.8.2.10 (Stamatakis, 2014), with 100 independent searches for the best tree and 1000 non-parametric bootstrap replicates.

To evaluate mito-nuclear discordance, we also performed BI analyses for mtDNA and nDNA data separately. For that, we removed most of the outgroups from the previous dataset, maintaining only *Leptodactylus latrans* to root the trees due to its close relationship with Paratelmatobiinae (Faivovich et al., 2014; Santos et al., 2020; this study). We reestimated the best partition scheme and substitution models in PartitionFinder v.2.1.1 (Lanfear et al., 2017) for each dataset (Table S4). The parameters of BI analyses were the same as in the previous analyses, except for the number of generations ($3.0 \times 10^7$). We performed all phylogenetic analyses using the CIPRES Science gateway portal (Miller et al., 2010).

### 2.3. Delimitation of independently evolving lineages

To objectively define independently evolving lineages (IELs) for subsequent species tree analysis, we followed an approach of congruence, considering the reciprocal monophyly of lineages in the phylogenetic trees, the results of the lineage delimitation analyses (Generalized Mixed Yule Coalescent model - GMYC, Pons et al., 2006; and nDNA fragments network), and the 16S rRNA genetic divergences between strongly supported clades.

For delimitation of the mtDNA IELs using the GMYC model, we first constructed an ultrametric mtDNA gene tree using the same dataset of the previous mtDNA BI analysis, yet assuming each fragment as a distinct partition, and estimating substitution models in PartitionFinder v.2.1.1 (Lanfear et al., 2017); Table S4. This ultrametric gene tree was estimated in BEAST v.2.5.2 (Bouckaert et al., 2019), using the Yule model as the tree prior. A clock was estimated independently for each fragment, assuming the log-normal uncorrelated relaxed clock, without account for absolute times in the tree. The analysis was done with two independent replicates of $5.0 \times 10^7$ MCMC generations each, sampling every $5.0 \times 10^3$ generations. The convergence between the two runs, the mixing of parameters, and the minimum effective sample size (ESS > 200) were checked in Tracer v.1.7 (Rambaut et al., 2018). We combined the trees from the two runs using the LogCombiner post-processing tool (Bouckaert et al., 2019), discarding 5% burn-in. A maximum clade credibility (MCC) gene tree was then obtained through the TreeAnnotator post-processing tool (Bouckaert et al., 2019), and used in GMYC to estimate the number of IELs (Pons et al., 2006).

To run the GMYC model, we used the package *ape* v.5.3 (Paradis and Schliep, 2019) in R (R Core Team, 2017) to remove the outgroup from the MCC mtDNA tree and to keep only one random individual per locality per clade, thus avoiding the accumulation of short branches in the tree. Excessive short branches are known to result in an overestimation of candidate species in GMYC (Reid and Carstens, 2012). Specimens included in this analysis are listed in Table S1. Then we applied a maximum likelihood implementation of the GMYC using the package *splits* v.1.0.19 (Fujisawa and Barraclough, 2013) in R, assuming a single threshold among the diversification between lineages and the genealogical branching within them. Additionally, we randomly sampled $2.5 \times 10^3$ trees, using *ape* to remove the same sequences that were taken off from the MCC tree. Subsequently, we used these trees to estimate the PP of each lineage using the *bGMYC* v.1.0.2 package (Reid and Carstens, 2012) in R.

We estimated the uncorrected *p*-distances between and within the lineages delimited by the GMYC model using the 16S rRNA gene fragment limited by the primers 16Sar-L and 16Sbr-H (Palumbi et al., 1991). We calculated the distances for each genus, as well as for each species group within *Paratelmatobius*, using Mega X (Kumar et al., 2018) and treating gaps and missing data as pairwise deletions.

Since the GMYC model tends to overestimate the number of independent units, often delimiting population structure (Talavera et al., 2013), we performed an independent lineage clustering by constructing a distance network with the nDNA fragments. For this, we first used the PHASE v.2.1.1 software (Stephens et al., 2001), with SeqPHASE input/output interconversion tool (Flot, 2010) to solve the haplotype gametic phases of each fragment, considering a threshold of 0.7 PP. From the phased sequences, we constructed a matrix of multigene distances using the algorithm *genpofad*, implemented in Pofad v.1.07 (Joly et al., 2015). We corrected multiple hits in distances using the Jukes and Cantor (1969) algorithm and inferred missing nucleotides and distances using the additive method implemented in Pofad. The analysis was performed for entire Paratelmatobiinae and for each genus separately, except for *Paratelmatobius*. In the latter, we calculated distances independently for the *P. cardosoi* and *P. lutzii* species groups, due to the high levels of genetic divergence detected between them. We visualized the resulting multigene distance matrices as phylogenetic networks in SplitsTree v.4.14.8 using the neighbor-net algorithm (Huson and Bryant, 2006).

Whenever multiple mtDNA lineages belonged to a single nDNA cluster, we treated these lineages as single terminals in the subsequent species tree analysis. This was implemented because lack of gene flow is a premise of the multispecies coalescent (Liu et al., 2015). The only exception was the mtDNA lineage D of *Paratelmatobius* cf. *segallai*. Although we recovered three lineages (B, C, and D) in the same nDNA cluster, the clade formed by these lineages was paraphyletic with respect to the lineage A in the phylogenetic analyses. In addition, deep genetic divergences distinguish lineage D from all other lineages (see Results). Because of that, we decided to keep lineage D as an independent lineage for the species tree. Although alternative methods are available for lineage validation (Rannala, 2015), we opted for the protocol described above given the relatively small number of independent gene fragments (six) available for validation procedures (Knowles and Carstens, 2007; Camargo and Sites, 2013).

### 2.4. Species-tree estimation and divergence times

After the definition of IELs, we built a matrix composed only by individuals with at least six gene fragments successfully sequenced, to construct a dated species-tree. This subsampling aimed to reduce the mixing problems observed in exploratory analyses of the complete dataset. Additionally, we included samples of *Odontophrynus* and *Proceratophrys* (Odontophrynidae), *Engystomops*, *Leptodactylus*,

*Lithodytes*, and *Pleurodema* (Leptodactylidae) as outgroups. We used phased nuclear sequences in this analysis and estimated the best substitution model for each fragment through PartitionFinder, assuming that each gene fragment had independent substitution models (Table S4). The three mtDNA genes were concatenated and considered as a single fragment.

The species tree was estimated with the StarBeast2 algorithm (Ogilvie et al., 2017) implemented in BEAST v.2.5.2 (Bouckaert et al., 2019). We used the analytical population size integration and a Yule model as prior for the species tree estimation. We assumed relaxed-clock models with uncorrelated lognormal distributions for all fragments. Due to the absence of fossil records for Paratelmatobiinae, we calibrated the analysis using two secondary calibration points from Feng et al. (2017). These authors used 20 fossil-based calibrations, testing each of them by jackknife, and a comprehensive phylogenomic dataset to estimate their divergence times. We used normally distributed priors for the divergence between *Odontophrynus* and *Proceratophrys* [mean = 32.0 million years ago (Mya), sigma = 4.1], defining a 95% range of 24.8–40.0 Mya; and for the crown age of Leptodactylidae (mean = 52.8 Mya, sigma = 2.7), defining a 95% range of 48.2–58.0 Mya. The range of divergence times of *Odontophrynus/Proceratophrys* is consistent with the fossil record of the odontophrynid *Chachaiphrynus lynchi* from the Middle Oligocene (27–29 Mya) (Nicoli, 2017). To run the calibrated analysis, we initially conducted a preliminary run with $2.5 \times 10^9$ MCMC generations, sampling every $5.0 \times 10^4$ generations. Then, we adjusted the scale-factors and size of scale operators following the report of the preliminary analysis. We ran a second analysis with the adjusted parameters, performing four independent replicates of $5.0 \times 10^9$ MCMC generations each, and sampling every $1.0 \times 10^5$ generations. We assessed stationarity, convergence, and effective sample sizes with Tracer, from what we discarded 10% of the samples for each run as burn-in. The species trees of the four runs were merged, and the MCC species tree was annotated as done for the ultrametric mtDNA gene tree.

## 3. Results

### 3.1. Phylogenetic inferences

Based on a final alignment of 6739 base pairs, we obtained similar BI and ML phylogenies which mainly differed in the relationships among some of the outgroups (particularly those distantly related to Paratelmatobiinae) and support values (Figs. 2 and S1). The monophyly of Paratelmatobiinae was robustly supported (PP = 100; ML bootstrap = 98), as well as that of each of the four genera (Figs. 2–4). In both analyses, *Rupirana* was recovered as the sister taxon of the three other genera, while *Scythrophrys* was recovered as sister to *Crossodactylodes* + *Paratelmatobius* (all relationships with PP = 100 and ML bootstrap > 95; Figs. 2 and 3). The subfamily Leptodactylinae was recovered as the sister taxon of Paratelmatobiinae in both analyses, although with moderate support in the ML inference (PP = 100; ML bootstrap = 61; Figs. 2 and S1).

Within *Scythrophrys*, the monophyly of *Scythrophrys* sp. was unambiguously supported in both analyses and this taxon was recovered as sister to the nominal species *S. sawayae* (Fig. 3). In *Crossodactylodes*, the monophyly of each of the three potentially new species (*Crossodactylodes* sp. 1, *Crossodactylodes* sp. 2, and *Crossodactylodes* sp. 3) and of *C. bokermanni*, *C. septentrionalis*, and *C. itambe* was unambiguously supported in both analyses. The monophyly of *C. izecksohni* was unambiguously supported in the BI analysis and moderately supported in the ML analysis (ML bootstrap = 84). *Crossodactylodes bokermanni* was recovered as the sister taxon of a clade comprising the remaining species. Within this clade, both analyses recovered *Crossodactylodes* sp. 3, *C. septentrionalis*, and *C. itambe* in a strongly supported clade (PP = 100; ML bootstrap = 94), separated from a clade comprising *Crossodactylodes* sp. 2, *Crossodactylodes* sp. 1, and *C. izecksohni* (PP = 100; ML bootstrap = 84; Fig. 3).

Within *Paratelmatobius*, the sampled species of the *P. lutzii* group (*P. gaigeae* and *P. poecilogaster*) were recovered as monophyletic and unambiguously supported in both analyses (Fig. 4). In the *P. cardosoi* group, *P. yepiranga* was recovered as the sister taxon of *Paratelmatobius* sp., while *P. cardosoi* + *P.* cf. *cardosoi* were recovered as sisters to *P. segallai* + *P.* cf. *segallai* (all relationships and the individual monophyly of each taxon were unambiguously supported in both analyses). Considering the ingroup, the differences between BI and ML topologies were restricted to relationships within *P. cardosoi* + *P.* cf. *cardosoi*. The lineage from the municipalities of São Paulo and Itanhaém was recovered as sister to the others in the BI analysis, whereas the lineage from the municipalities of Biritiba Mirim, Mogi das Cruzes (Biritiba Ussu), and Salesópolis was recovered as sister to the others in the ML analysis (Fig. 4).

Deeply divergent and geographically structured clades were recovered within *R. cardosoi*, *S. sawayae*, *C. bokermanni*, *C. izecksohni*, *P. poecilogaster*, *P. cardosoi* + *P.* cf. *cardosoi*, and *P. segallai* + *P.* cf. *segallai* (Figs. 3 and 4).

The topology of the BI mtDNA tree was the same as that of the multigene BI tree, varying only in clade support values (Fig. S2). On the other hand, the topology of the BI nDNA tree was distinct from that of the multigene BI tree regarding relationships within *Crossodactylodes*. While *Crossodactylodes* sp. 3 was recovered as the sister taxon of *Crossodactylodes* sp. 2 + *Crossodactylodes* sp. 1 + *C. izecksohni* in the nDNA tree (PP = 87; Fig. S3), it was retrieved as sister to *C. itambe* + *C. septentrionalis* in the multigene tree (PP = 100; Fig. 3).

### 3.2. Delimitation of independently evolving lineages

Thirty-one mtDNA IELs were recovered by the GMYC model (confidence interval 8–46; Fig. 5). Within *Rupirana cardosoi*, two lineages from the state of Bahia were recovered (Fig. 5), and the uncorrected *p*-distance between them varied from 2.3% to 2.5% (Appendix A). Within *Scythrophrys*, four lineages were recovered: *Scythrophrys* sp. from the Serra do Tabuleiro and vicinities, in the state of Santa Catarina; and three lineages within *S. sawayae* from localities in the states of Paraná and Santa Catarina (Fig. 5). The uncorrected *p*-distance between *Scythrophrys* sp. and the lineages of *S. sawayae* varied from 2.9% to 4.6%, while the distances among the three lineages of *S. sawayae* varied from 1.1% to 2.5% (Appendix B).

Ten lineages were recovered within *Crossodactylodes*: *C. septentrionalis* from the south of the state of Bahia; *C. itambe* and *Crossodactylodes* sp. 3 from the Espinhaço Range in the state of Minas Gerais; and *Crossodactylodes* sp. 1, *Crossodactylodes* sp. 2, two lineages within *C. izecksohni*, and three lineages within *C. bokermanni* from the state of Espírito Santo (Fig. 5). The interspecific uncorrected *p*-distance among these lineages varied from 2.3% to 7.8% (Appendix C). The distances between the two lineages of *C. izecksohni* varied from 3.4% to 4.2%, while the distances among the three lineages of *C. bokermanni* varied from 0.9% to 4.2% (Appendix C).

For *Paratelmatobius*, the GMYC model recovered 15 lineages. Within *P. lutzii* group, five lineages were recovered: *P. gaigeae* from the Serra da Bocaina, in the state of São Paulo; and four lineages within *P. poecilogaster* from localities in the states of São Paulo and Rio de Janeiro (Fig. 5). The uncorrected *p*-distance between *P. gaigeae* and the lineages of *P. poecilogaster* varied from 4.1% to 5.5%, while the distances among the four lineages of *P. poecilogaster* varied from 0.2% to 3.2% (Appendix D). Within the *P. cardosoi* group, ten lineages distributed in the states of São Paulo and Paraná were recovered: *P. yepiranga*, *Paratelmatobius* sp., four lineages within *P. cardosoi* + *P.* cf. *cardosoi*, and four lineages within *P. segallai* + *P.* cf. *segallai* (Fig. 5). The interspecific uncorrected *p*-distance among these lineages varied from 4.4% to 8.8% (Appendix E). The distances among the four lineages within *P. cardosoi* + *P.* cf. *cardosoi* varied from 1.6% to 2.4%, whereas the distances among the four lineages within *P. segallai* + *P.* cf. *segallai* varied from 1.2% to

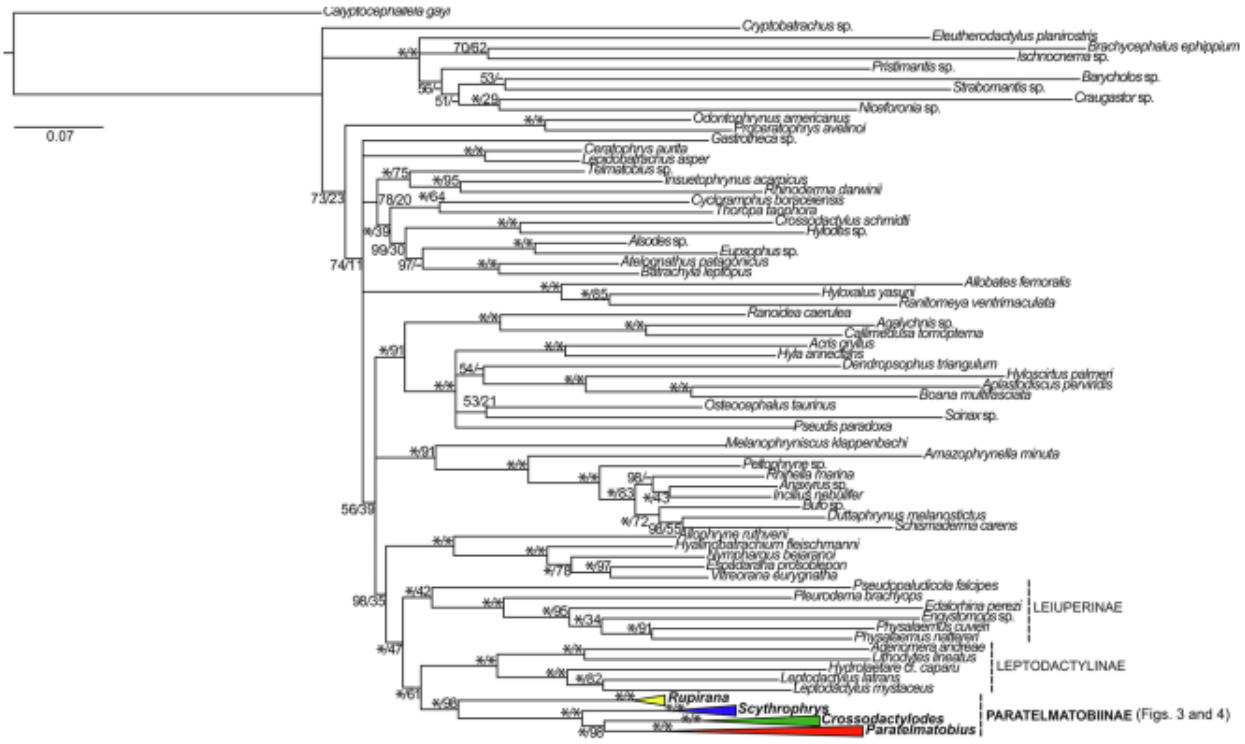


**Fig. 2.** The 50% majority rule consensus tree from Bayesian phylogenetic inference of concatenated mtDNA (H1, COI, cyt-*b*) and nDNA (POMC, RAG-1, Rhod, TNS3, Tyr) genes, showing the relationships of the four genera of Paratelmatobiinae with outgroups. For relationships within Paratelmatobiinae, please refer to Figs. 3 and 4. Posterior probabilities and maximum likelihood bootstraps are shown next to nodes (to the left and to the right of the bar, respectively). Asterisks (*) indicate unambiguously supported nodes and dashes (–) represent nodes not recovered in the maximum likelihood analysis. For the maximum likelihood topology, please refer to Fig. S1.

5.6% (Appendix E).

Although the structure of the nuclear neighbor-net generally agreed with the mtDNA lineages delimited by the GMYC model, several of the mtDNA lineages were placed in the same nDNA cluster (Fig. 6). This happened in *S. sawayae* (mtDNA lineages B + C), *C. bokermanni* (mtDNA lineages A + B), *C. izecksohni* (mtDNA lineages A + B), *P. poecilogaster* (mtDNA lineages A + B), *P. poecilogaster* (mtDNA lineages C + D), *P. cardosoi* (mtDNA lineages A + B + C), and *P.* cf. *segallai* (mtDNA lineages B + C + D); Fig. 6. These lineages were treated as single terminals in the subsequent species tree analysis, with the exception of the mtDNA lineage D of *P.* cf. *segallai*. This lineage, although belonging to the same nDNA cluster of lineages B + C, was recovered as sister to lineages A + B + C in the phylogenetic inferences (PP and ML bootstrap = 100; Fig. 4). In addition, high uncorrected *p*-distances distinguish lineage D from each of the other lineages (ranging 4.6–5.6%; Appendix E).

Each of the putatively new species (*Crossodactylodes* sp. 1, *Crossodactylodes* sp. 1, *Crossodactylodes* sp. 3, *Paratelmatobius* sp., and *Scythrophrys* sp.) was recovered as single nDNA clusters.

### 3.3. Species-tree estimation and divergence times

A total of 23 lineages of Paratelmatobiinae were included in the species tree analysis. The StarBEAST2 recovered all genera as monophyletic and unambiguously supported (Fig. 7). The relationships among the genera, as well as the relationships within each genus, were generally congruent with those of the BI and ML trees (Figs. 3 and 4). However, the relationships among *Crossodactylodes* sp. 3, *C. itambe*, and *C. septentrionalis*, as well as the relationships among the lineages within *P. segallai* + *P.* cf. *segallai*, were not robustly supported in the species tree analysis (PP < 95). The subfamily Leiuperinae was recovered as the sister taxon of Paratelmatobiinae, but with low support (PP = 53; Fig. 7).

Our estimation of divergence times (Fig. 7) suggests that the first split within Paratelmatobiinae, separating *Rupirana* from the other genera, dated back to the Middle Eocene [41.65 Mya; 35.71–48.09, 95% highest posterior density interval (HPD)]. The split between *Scythrophrys* and their sister taxa (*Crossodactylodes* and *Paratelmatobius*) was estimated to have occurred in the Upper Oligocene at 25.38 Mya (HPD 21.81–29.28), followed closely by the divergence between the latter two genera at 23.52 Mya (HPD 20.11–27.1). The split between the *P. lutzii* and *P. cardosoi* species groups dated back to the Middle Miocene at 16.57 Mya (HPD 13.85–19.27), while most of the other speciation events within the subfamily were inferred to have taken place in the Upper Miocene and the Lower Pliocene. On the other hand, divergences among what we considered intraspecific lineages appear to have taken place in the Upper Pliocene and the Lower and Middle Pleistocene (Fig. 7).

## 4. Discussion

This is the most comprehensive phylogenetic study of species in the subfamily Paratelmatobiinae conducted to date. The monophyly of Paratelmatobiinae and each of its genera was robustly supported, and the intrageneric relationships were generally well-resolved. Besides the 11 named species and the five potentially new species included in our dataset, we delimited seven other independently evolving lineages. We found strong support for our initial predictions of ancient diversification events and deeply divergent, geographically structured species and lineages. Our results reveal a complex scenario of diversification for Paratelmatobiinae, beginning with intergeneric divergences in the Eocene and Oligocene and continuing with most intrageneric

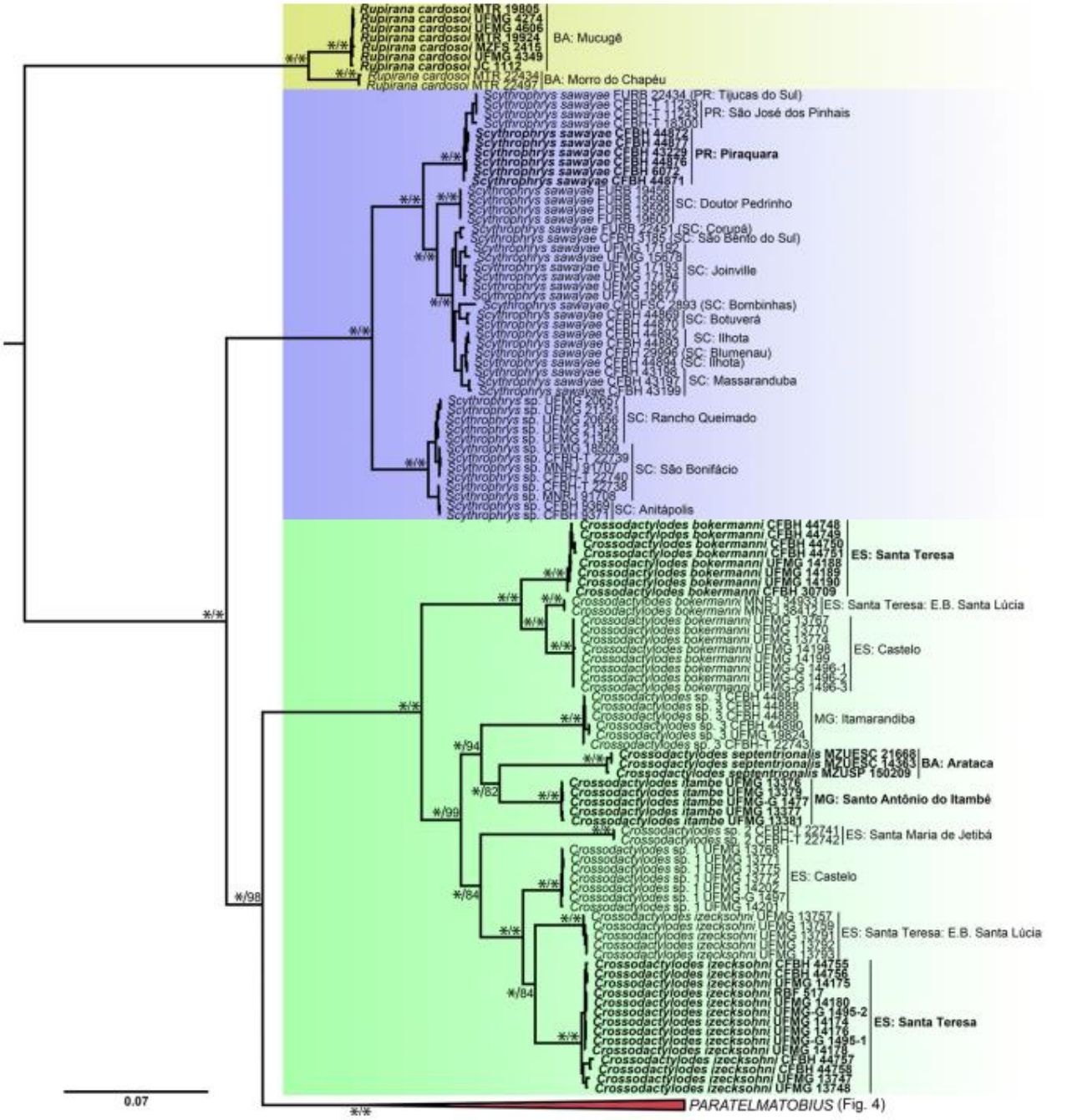


**Fig. 3.** The 50% majority rule consensus tree from Bayesian phylogenetic inference of concatenated mtDNA (H1, COI, and cyt-*b*) and nDNA (POMC, RAG-1, Rhod, TNS3, and Tyr) genes, showing the relationships within *Rupirana*, *Scythrophrys*, and *Crossodactylodes*. For relationships within *Paratelmatobius*, please refer to Fig. 4. Posterior probabilities and maximum likelihood bootstraps are shown next to nodes (to the left and to the right of the bar, respectively). Asterisks (*) indicate unambiguously supported nodes. Terminals in bold represent specimens from type localities.

diversification in the Miocene. Some diversification events cooccurred with past glaciations and tectonic activity in the Brazilian mountain ranges, but the heterogeneity of microhabitats in montane environments and the life history traits of the species of Paratelmatobiinae are likely important synergistic factors in diversification. Our results highlight the need of further taxonomic investigation, focusing on the unnamed lineages recovered by our analyses, as well as a reassessment of the conservation status of species, given their rarity and remarkably small geographic ranges.

### 4.1. Phylogenetic relationships and topological incongruences

The monophyly of Paratelmatobiinae, as well as the monophyly and relationships among the four genera, were consistent with previous studies based on smaller taxon and/or character sampling (Faivovich et al., 2014; Fouquet et al., 2013; Lourenço et al., 2008; Santos et al., 2019, 2020; Teixeira et al., 2013). We recovered the subfamily Leptodactylinae as the sister taxon of Paratelmatobiinae in both concatenated analyses, although the ML analysis shows moderate support values.

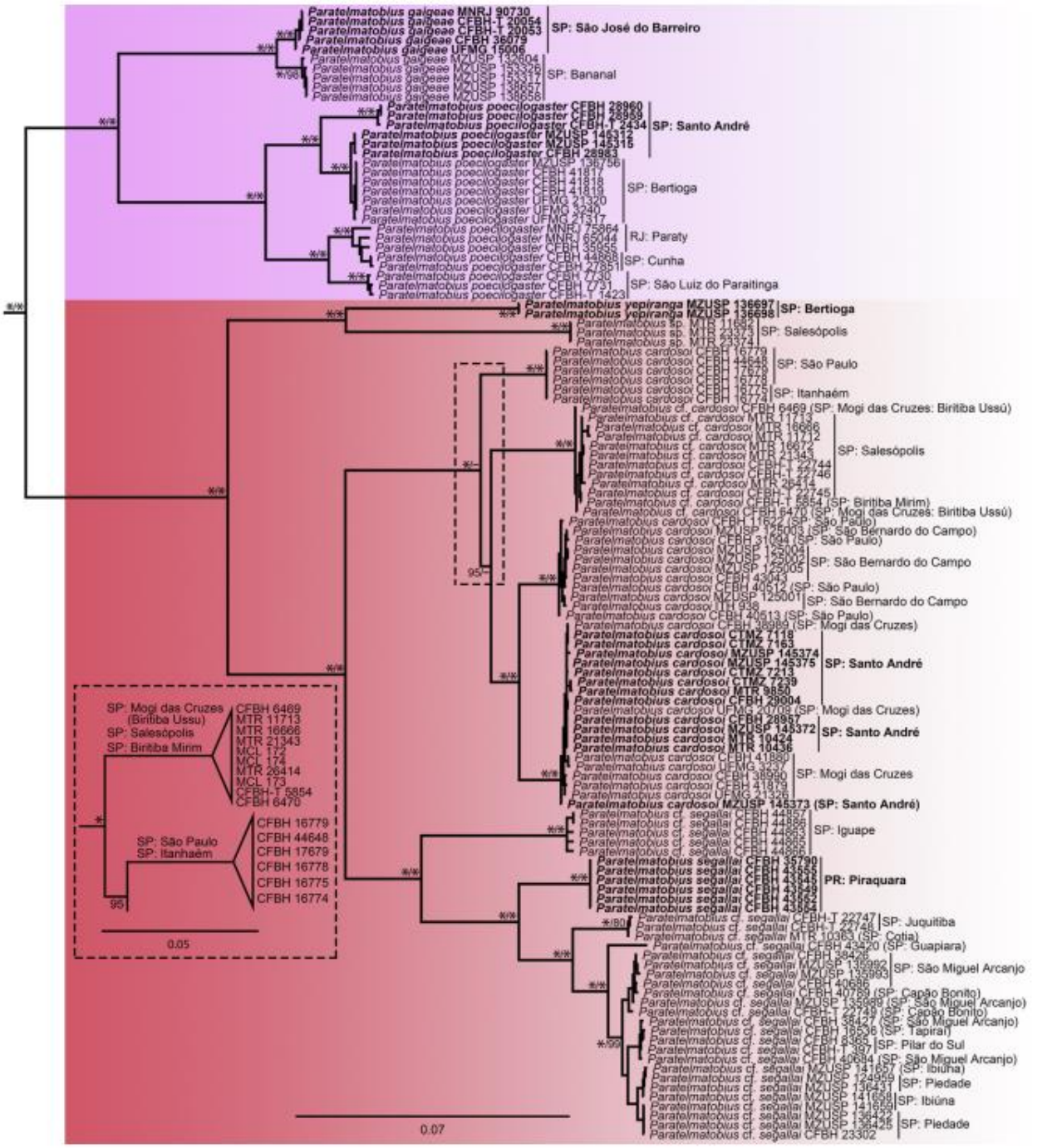


**Fig. 4.** The 50% majority rule consensus tree from Bayesian phylogenetic inference of concatenated mtDNA (H1, COI, and cyt-*b*) and nDNA (POMC, RAG-1, Rhod, TNS3, and Tyr) genes, showing the relationships within *Paratelmatobius*. Posterior probabilities and maximum likelihood bootstraps are shown next to nodes (to the left and to the right of the bar, respectively). Asterisks (*) indicate unambiguously supported nodes. Terminals in bold represent specimens from type localities. The dashed rectangle in the tree indicated the two nodes not recovered in the maximum likelihood analysis. For these nodes, the topology and support values achieved in the maximum likelihood analysis are shown in the dashed square.

This relationship is concordant with other phylogenetic hypotheses (Fouquet et al., 2013, complete matrix approach; Faivovich et al., 2014; Santos et al., 2020). Alternatively, the subfamily Leiuperinae was recovered as sister to Paratelmatobiinae in the species tree analysis, but with low support, in accordance with Pyron and Wiens (2011). On the other hand, Paratelmatobiinae was recovered as sister to Leiuperinae + Leptodactylinae in other studies (Fouquet et al., 2013, super matrix approach; Fouquet et al., 2014; Pyron, 2014), also with low support. Phylogenomic approaches have shown promise in resolving these deep nodes in the anuran phylogeny (Feng et al., 2017; Streicher et al., 2018). Sampling more loci and taxa may provide a better understanding of the relationships among the subfamilies of Leptodactylidae.

The relationships within *Scythrophrys*, *Crossodactylodes*, and the

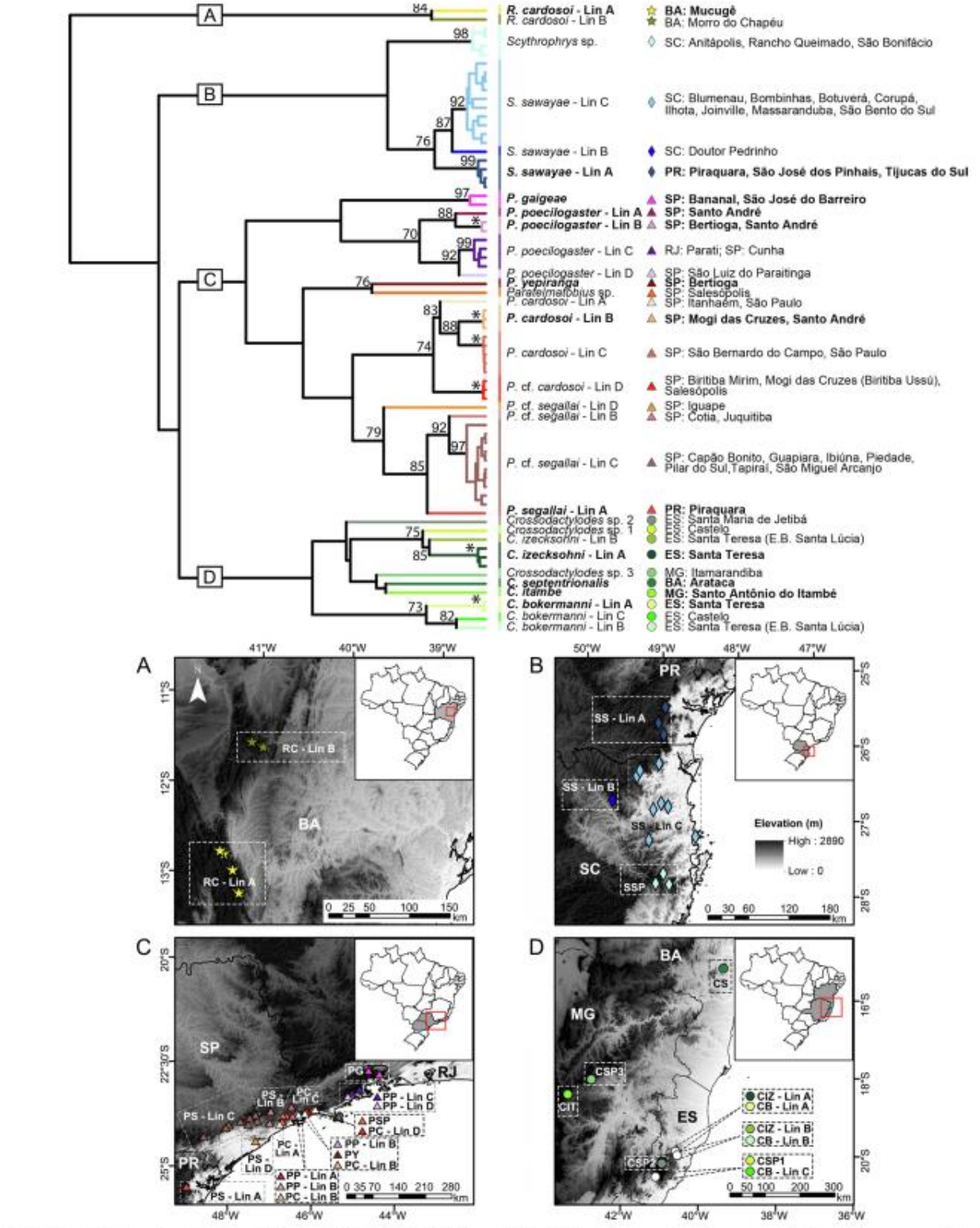


**Fig. 5.** The mtDNA gene tree showing the lineages delimited by the GMYC model. Symbols are the same for each genus, and distinct colors represent the delimited lineages. Terminals in bold represent lineages from type localities. Values next to the nodes represent the means of pairwise probabilities of co-specificity. Asterisks (*) indicate 100% values. The sampled localities for species and lineages are shown in the maps under the tree, for *Rupirana* (A), *Scythrophrys* (B), *Paratelmatobius* (C), and *Crossodactylodes* (D). White symbols in (C) and (D) indicate localities where two or more species/lineages occur in sympatry. Brazilian states: BA (Bahia); ES (Espírito Santo); MG (Minas Gerais); PR (Paraná); RJ (Rio de Janeiro); SC (Santa Catarina); SP (São Paulo). Other abbreviations: CB (*C. bokermanni*); CIT (*C. itambe*); CIZ (*C. izecksohni*); CS (*C. septentrionalis*); CSP1 (*Crossodactylodes* sp.1); CSP2 (*Crossodactylodes* sp.2); CSP3 (*Crossodactylodes* sp.3); Lin (Lineage); PC (*P. cardosoi*); PG (*P. gaigeae*); PP (*P. poecilogaster*); PS (*P. segallai*); PSP (*Paratelmatobius* sp.); PY (*P. yepiranga*); RC (*R. cardosoi*); SS (*S. sawayae*); SSP (*Scythrophrys* sp.). For interpretation of the references to colour in this figure legend, the reader is referred to the web version of this article.

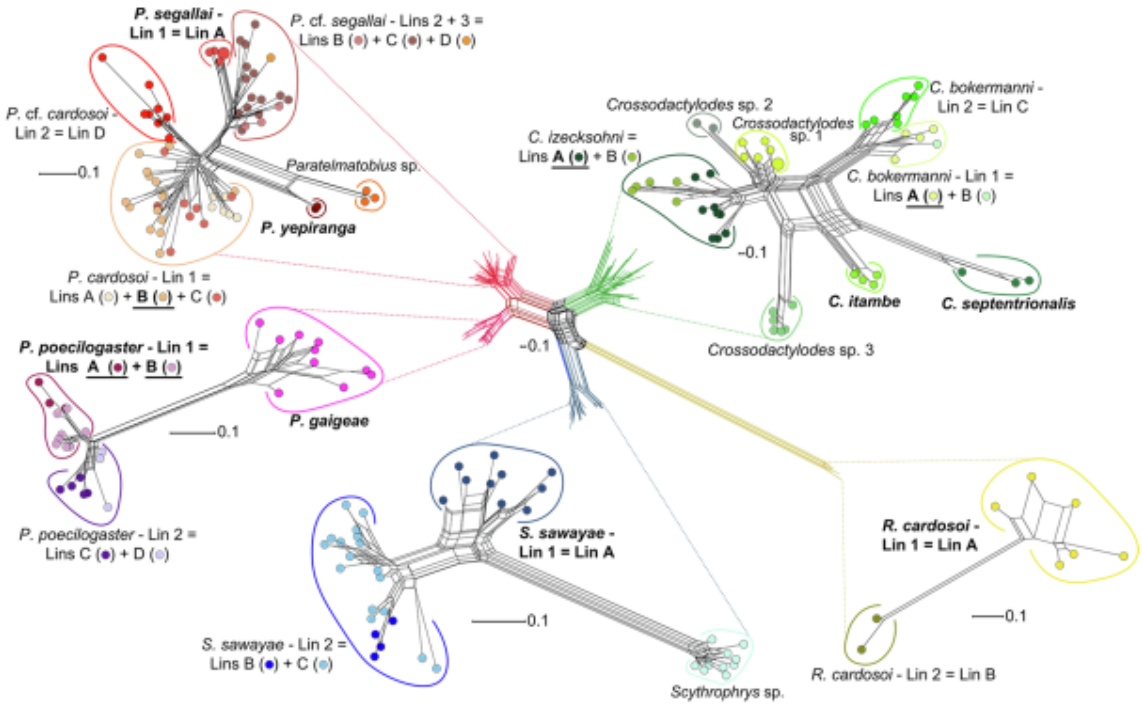


**Fig. 6.** Multilocus nDNA neighbor-net for the entire Paratelmatobiinae (small net in the center), for each genus, or species group (in the case of *Paratelmatobius*). Recovered clusters are delimited by ellipses. Note that some clusters are composed by more than one mtDNA lineage. Scale bars represent standardized genetic distances for each net (distances are not comparable among different nets). For interpretation of the references to colour in this figure legend, the reader is referred to the web version of this article.

*Paratelmatobius* species groups (*P. cardosoi* and *P. lutzii*) are in accordance with previous hypotheses (Lourenço et al., 2008; Santos et al., 2019, 2020). However, our study is the first to provide phylogenetic placements for *Crossodactylodes* sp. 1, *Crossodactylodes* sp. 2, *Crossodactylodes* sp. 3, *Paratelmatobius* sp., and *P. yepiranga*. The phylogenetic placements of *C. pintoi*, *P. lutzii*, and *P. mantiqueira*, which were not included in our study, remain uncertain. *Crossodactylodes pintoi* was recovered as closely related to *C. itambe*, *C. septentrionalis*, and *C. izecksohni* in a total evidence analysis, but the relationships within this clade were not fully resolved (Santos et al., 2020). On the other hand, no phylogenetic hypothesis exists for *P. lutzii* and *P. mantiqueira*. Morphological data suggest that *P. mantiqueira* is possibly related to *P. cardosoi*, *P. segallai*, and *P. yepiranga*, whereas *P. lutzii* is possibly related to *P. gaigeae* and *P. poecilogaster* (Pombal and Haddad, 1999; Garcia et al., 2009; Santos et al., 2019). However, *P. lutzii* has remarkable diagnostic characters in comparison with its congeners, such as the absence of columella, foot with well-developed webs, and nuptial pads lacking spicules (Lynch, 1971; Pombal and Haddad, 1999). Therefore, the species phylogenetic placement deserves further investigation.

We found topological incongruences for some intrageneric relationships when comparing our phylogenetic inferences, mainly in the relationships with short branch lengths. The relationships within *P. cardosoi* + *P.* cf. *cardosoi* differ when comparing the multigene BI and ML analyses (Fig. 4). This may be due to differences in the evolutionary models assumed in the analyses (Suchard et al., 2003), as well as an effect of short branch lengths present in these relationships, which might be difficult to solve with strong support even using multilocus datasets (Wiens et al., 2008). We also found a variable position for *Crossodactylodes* sp. 3, when comparing the BI and ML trees (Fig. 3) with the BI nDNA tree (Fig. S3). Moreover, the relationships within *P. segallai* + *P.* cf. *segallai* are incongruent when comparing the multigene concatenated and mtDNA trees (Figs. 4 and S2) with the nDNA neighbor net (Fig. 6). In both cases, the species tree topology agrees with that of the multigene BI and ML trees, but the moderate node support values indicate the same pattern of discordant gene tree topologies (Fig. 7). Therefore, our results indicate a degree of uncertainty in the relationships of these taxa, as well as a conflicting pattern between mitochondrial and nuclear fragments. This mito-nuclear discordance may be related to specific characteristics of each genome, as the faster lineage sorting of mtDNA comparing with the nDNA (Toews and Brelsford, 2012).

### 4.2. Molecular dating and scenarios of diversification

The divergence times inferred with our species tree suggest an Eocene origin for the subfamily Paratelmatobiinae (~41.7 Mya) and subsequent intergeneric diversification in the Oligocene (~23.5–25.4 Mya) (Fig. 7). These estimated divergences are more recent than those found in a previous study, which estimated the split between *Rupirana* and the other Paratelmatobiinae at ~58 Mya, and that between *Crossodactylodes* and *Paratelmatobius* at ~34 Mya (Fouquet et al., 2013). These contrasting results may be due to differences in taxon and character sampling, calibration priors, and the method used for phylogenetic reconstruction (Linder et al., 2005; Pulquério and Nichols 2007; Hipsley and Müller, 2014). Fouquet et al. (2013) included a few species of Paratelmatobiinae, but a larger outgroup sampling, and calibrated the analysis using divergences between other taxa based on different secondary calibrations and one geological event. In addition, those authors used a concatenation-based method, which tends to overestimate the divergence times when compared to the coalescent method that we applied (McCormack et al., 2011). Nevertheless, both our results and those of Fouquet et al. (2013) agree on the deep intergeneric divergence times for Paratelmatobiinae.

The divergence between *Rupirana*, distributed in the *campo rupestre*, and the three remaining Paratelmatobiinae genera in the AF (35.7–48.1 Mya) is temporally coincident with the divergence time between the AF endemic frog genus *Dendrophryniscus* and its sister taxon *Amazophrynella*, endemic to Amazonia (Fouquet et al., 2012a). This

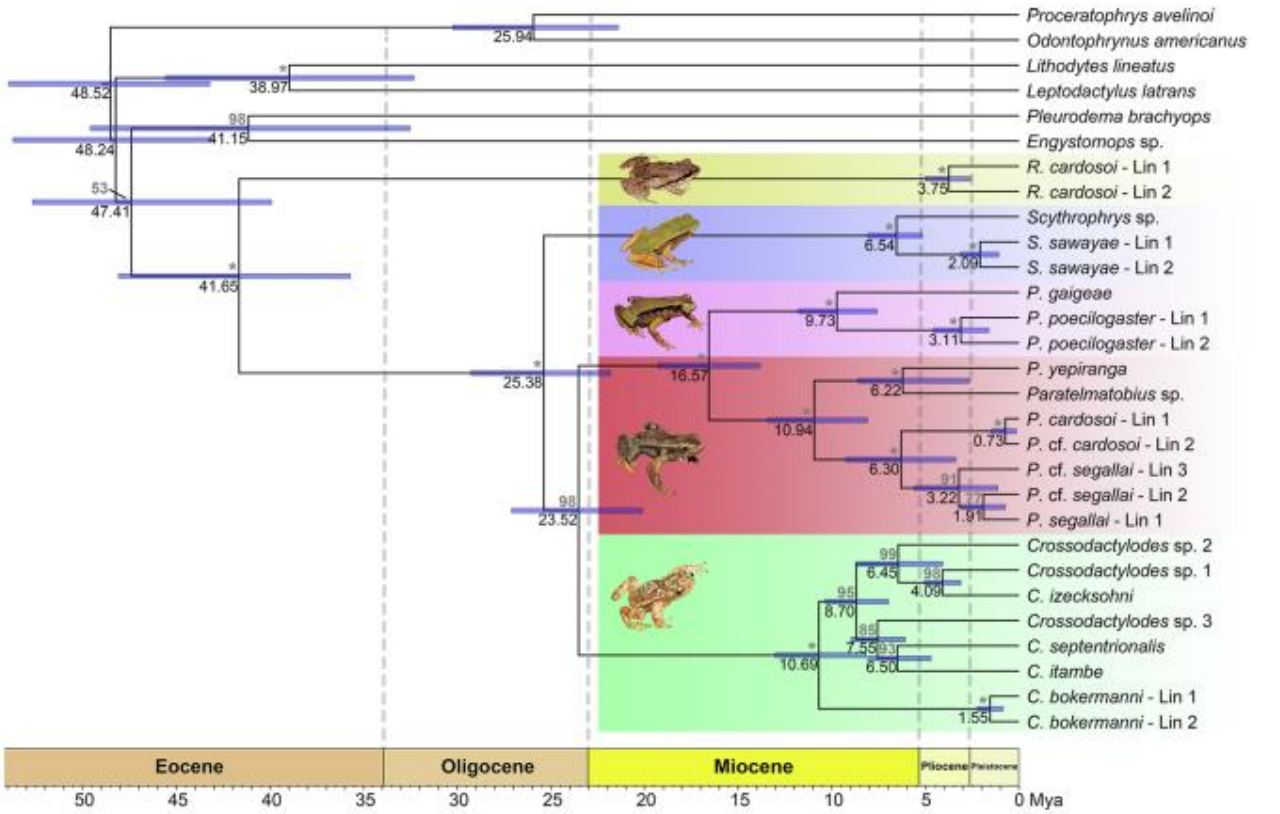


**Fig. 7.** Time-calibrated species tree annotated from StarBeast2 analysis. Values above branches (in gray) indicate posterior probabilities (asterisks mean 100% values). Values under branches (in black) indicate mean node ages, and the blue bars indicate standard deviation. For interpretation of the references to colour in this figure legend, the reader is referred to the web version of this article.

timing also coincides with divergences between major clades of Brachycephaloidea and in the subfamily Phyzelaphryninae (Eleutherodactylidae), which are mainly distributed in forested habitats of either the AF or Amazonia (Fouquet et al., 2012b; Heinicke et al., 2009). The main mechanism invoked to explain these diversifications has been ancient, pre-Pleistocenic climatically-driven forest fragmentation. The Middle-Upper Eocene was characterized by the Andean uplift and remarkable climatic changes that included a shift from wet to dry conditions, as well as marine regressions (Romero, 1986; Ortiz-Jaureguizar and Cladera, 2006; Hoorn et al., 2010). Aridification is thought to have led to a partial replacement of previously widespread rainforest by open vegetation, resulting in the formation of the South American Dry Diagonal separating the AF and Amazonia (Romero, 1986; Roig-Juñent et al., 2006). Moist forest fragments embedded in the xeric Caatinga and Cerrado savannas are relicts that attest for the dynamics between the rainforest and the open vegetation in these regions (Carnaval and Bates, 2007; Thomé et al., 2016). We hypothesize that the formation of a dry corridor at that time may have isolated the *campo rupestre* endemic genus *Rupirana* from the most common ancestor of the AF Paratelmatobiinae, explaining their long-term divergence. The *campo rupestre* has been considered a climatically stable ecosystem, with several micro-refugia, favoring persistence of old lineages (Alves and Kolbek, 1994; Silveira et al., 2016). This appears to be the case of *Rupirana*, which represents a relict taxon adapted to more seasonal environments, persisting in the *campo rupestre* as its only endemic anuran genus.

Other ancient endemic elements of the *campo rupestre* are small-sized catfishes whose nearest sister taxa occur exclusively in the AF (Ochoa et al., 2017). The genera *Copionodon* and *Glaphyropoma*, endemic to the *campo rupestre*, diverged from the AF endemic subfamily Trichogeninae in the Lower Eocene (~55.9 Mya) (Ochoa et al., 2017). On the other hand, several plant genera endemic to the *campo rupestre* are inferred to have originated later, in the Miocene (Rapini et al., 2007; Antonelli et al., 2010; Silveira et al., 2016). Neither the Eocene origin nor the close affinities with the AF biota are conditions shared among all the *campo rupestre* endemic genera. Possibly, a complex scenario of multiple sources of origin drove their diversification, as proposed for species-level endemism (Bitencourt and Rapini, 2013; Silveira et al., 2016).

Following the divergence of *Rupirana*, our results support a rapid initial diversification for the three AF genera in the Oligocene and subsequent diversification within each genus, mainly in the Miocene (Fig. 7). This is consistent with divergence times recovered for several genera belonging to various anuran families (Jetz and Pyron, 2018), including other AF anurans with similar geographic range such as *Dendrophryniscus* (Fouquet et al., 2012a), *Thoropa* (Sabbag et al., 2018), and *Brachycephalus* (Condez et al., 2020). The deep divergence between *Scythrophrys* (the southernmost genus) and its sister taxa matches the pattern and timing reported for rock frogs in the genus *Thoropa* (Sabbag et al., 2018). These results suggest that at least some AF habitats in the southern portion of the AF remained relatively stable since the Oligocene, as suggested based on the Plio–Pleistocene population persistence of *Rhinella henseli* (Thomé et al., 2010). Although previous analyses suggested that contemporary climatic heterogeneity better explains lineage endemism in the southern AF relative to historical climates (Carnaval et al., 2014), our data reinforces the notion that local endemic lineages, such as *Scythrophrys*, *R. henseli* and *Thoropa saxatilis*, have been in place for a long time.

Past climatic changes that caused forest fragmentation and isolation may have played an important role in other diversification events. A

glaciation in the Oligocene/Miocene boundary, at ~23 Mya (Zachos et al., 2001) is coincident with divergences among the three AF genera. In turn, climatic fluctuations of the Miocene (Haffer, 1997; Zachos et al., 2001; Olsen and Whiteside, 2009; Herbert et al., 2016) match the timing of most of the intrageneric divergences, while those of the Plio-Pleistocene (Haffer, 1969; Carnaval et al., 2009) coincide with the intraspecific divergences (Fig. 7). However, these geological epochs also correspond to periods of significant tectonic activity and regressive differential erosion in the Brazilian mountain ranges (Saadi, 1993, 1995; Potter, 1997; Almeida and Carneiro, 1998; Riccomini et al., 2004; Cogné et al., 2013). These might have influenced diversification by creating barriers to dispersal (see details below). The presence of several geographically restricted lineages (Figs. 3–5) suggests that processes at smaller geographic scales related to habitat heterogeneity and life history traits might have acted as synergistic factors to shape diversification in Paratelmatobiinae (Fusinatto et al., 2013; Rodríguez et al., 2015). Species of the subfamily have a small body size and are strongly associated with humid microhabitats, characteristics that are indicative of low dispersal capacity and narrow physiological tolerances (Hillman et al., 2009; Pabijan et al., 2012). These traits, along with the differential distribution of microhabitats, may have led to reduced gene flow among populations and strong spatial structure, as proposed for other small-sized and microhabitat specialist anurans (Wollenberg et al., 2011; Fusinatto et al., 2013; Rodríguez et al., 2015).

Although similar drivers likely influenced the diversification of the Paratelmatobiinae, group-specific processes are probably important for each AF genus. Diversification within *Crossodactylodes*, for instance, may have been influenced by the fact that all species and lineages are strictly associated with bromeliads on humid mountaintops. Although these bromeliad microhabitats enable species to tolerate more seasonal conditions, even those species and lineages distributed in more inland areas (i.e., the *campo rupestre* endemics *C. itambe* and *Crossodactylodes* sp. 3; Fig. 5D) inhabit wet environments with mild temperatures due to orographic rainfall and orographic fog (Barata et al., 2013; this study). Given the patchy distribution of species and lineages of the genus on isolated mountaintops (Fig. 5D), we hypothesize that climate oscillations and changes in humidity over space and time may have influenced their evolutionary history. In this context, ancestors of *Crossodactylodes* may have had a wider distribution during the Miocene colder periods, becoming isolated on mountaintops during warmer times, as previously suggested for other montane taxa with disjunctly distributed species (Firkowski et al., 2016; Prates et al., 2020). The low vagility and habitat specificity of species may have facilitated this isolation. However, the diversity of this genus may still be underestimated, as suggested by recent discoveries of new species and populations (Barata et al., 2013; Teixeira et al., 2013; Santos et al., 2020; this study). Thus, this scenario of diversification must be interpreted with caution and remains to be tested.

Considering its geographic distribution, the genus *Paratelmatobius* comprises a relatively high number of species and lineages (Figs. 1 and 5). The spatial range of the genus strongly overlaps with the Continental Rift of Southeastern Brazil (CRSB; Riccomini et al., 2004), a large fault system originating from tectonic reactivation of Precambrian shear zones between the end of the Paleocene and the end of the Oligocene (Riccomini et al., 2004; Zalán and Oliveira, 2005; Gontijo-Pascutti et al., 2012). The CRSB has been identified as the region with the most pronounced neotectonic (Neogene–Quaternary) activity in Brazil, being associated with the evolution of river systems and the increase of topographical differences between valleys and mountain ranges (Riccomini et al., 2004; Saadi, et al., 2005; Zalán and Oliveira, 2005; Gontijo-Pascutti et al., 2012). The Neogene–Quaternary divergence times among sampled species and lineages of *Paratelmatobius* (Fig. 7), and the geographical coincidence of some genetic breaks with tectonic faults and lineaments of the CRSB, indicate that these events possibly influenced the evolutionary history of the genus.

For instance, the limit between the geographical ranges of *P. cardosoi* + *P.* cf. *cardosoi* and *P. segallai* + *P.* cf. *segallai* (Fig. 5C) is somewhat coincident with a NW-SE fault of the CRSB, which had tectonic reactivation in the Miocene (Zalán and Oliveira, 2005; Riccomini et al., 2010). This is roughly congruent in time with divergences between species of *Phyllomedusa* (Hylidae; Brunes et al., 2010) and lineages of *Proceratophrys boiei* (Odontophrynidae; Amaro et al., 2012), but the break in *Paratelmatobius* is located slightly to the north in comparison with these other taxa. The divergences among the three lineages within *P. segallai* + *P.* cf. *segallai* might also be correlated with tectonic faults and lineaments, as the Cubatão-Itariri Shear System, the Serrinha Shear Zone, and the Guapiara lineament (Riccomini and Assumpção, 1999; Saadi et al., 2002; Passarelli et al., 2007) are somewhat coincident with the limits of geographic ranges of these lineages. A striking geographical and temporal discordance occur in the diversification of some lineages in the *P. cardosoi* group. The divergence between *P. yepiranga* and *Paratelmatobius* sp. is geographically congruent with the divergence between the lineages 1 (mtDNA lineages A + B + C) and 2 (mtDNA lineage D) of *P. cardosoi* + *P.* cf. *cardosoi* (Fig. 5C), but the divergence time is much older for the former taxon pair (Fig. 7). This may be indicative of a similar barrier or process limiting connectivity between lineages across multiple time periods.

Lastly, in the genus *Scythrophrys*, *S. sawayae* (lineages 1 and 2) occurs exclusively in the south of the Serra do Mar, while *Scythrophrys* sp. occurs only in the Serra do Tabuleiro and surrounding areas, an isolated mountain range in the state of Santa Catarina (Fig. 5B). This locality harbors another endemic anuran, *Boana poaju* (Hylidae; Garcia et al., 2008) and some endemic plants (Hassemer et al., 2015; Da Silva and Külkamp, 2018), but is still poorly sampled for many taxonomic groups. The deep divergence time between *Scythrophrys* sp. and *S. sawayae* (~6.5 Mya) suggests that the Serra do Tabuleiro and Serra do Mar biota experienced independent evolution since the Upper Miocene.

### 4.3. Taxonomic and conservation implications

The five putative new species included in our analyses were robustly supported in the phylogenetic trees (Figs. 3 and 4) and lineage delimitation analyses (Figs. 5 and 6). In addition, we found at least seven deeply divergent and geographically structured lineages within named species in the four genera of Paratelmatobiinae (Figs. 6 and 7). These lineages are also well-supported in all analyses, suggesting that species diversity within the subfamily is highly underestimated. Karyotypic differences were previously reported for some of these independently evolving lineages. In *Paratelmatobius*, differences were reported when comparing mtDNA lineages B and D of *P. cardosoi* + *P.* cf. *cardosoi* (karyotypes not known for lineages A and C) and mtDNA lineages A and C of *P. segallai* + *P.* cf. *segallai* (karyotypes not known for lineages B and D) (Lourenço et al., 2008). For *Scythrophrys*, it was previously suggested that *Scythrophrys* sp. belongs to a distinct species based on karyotypic and mtDNA differences (Lourenço et al., 2003; Lourenço et al., 2008).

Given the identification of several potentially new species, future taxonomic investigation and the resolution of species boundaries are crucial for an accurate assessment of extinction risks in Paratelmatobiinae (Scherz et al., 2019). Factors such as rarity and reduced geographic ranges have been suggested as important indicators of extinction risk (Pimm et al., 2014; Toledo et al., 2014) and are relevant for members of the subfamily. Several species are only known from one or a few localities (i.e., *C. itambe*, *C. izecksohni*, *C. pintoi*, *C. septentrionalis*, *P. gaigeae*, *P. lutzii*, and *P. yepiranga*) and this is also true for the five putatively new species included in our analyses (*Crossodactylodes* sp. 1, *Crossodactylodes* sp. 2, *Crossodactylodes* sp. 3, *Paratelmatobius* sp., and *Scythrophrys* sp.). Moreover, none of the species are widely distributed (Fig. 5). The long periods of time that some species remain unrecorded illustrate the rarity in Paratelmatobiinae. *Crossodactylodes pintoi*, for instance, was last seen in 1909, despite several field expeditions to the type locality (Santos et al., 2020). *Paratelmatobius lutzii* was last recorded in 1978, even after multiple visits to

the type locality (Pombal and Haddad, 1999). In addition, *P. gaigeae* was only found again 73 years after its discovery (Zaher et al., 2005) and *P. mantiqueira* after 52 years (Vrcibradic et al., 2010). Beyond their tiny geographic ranges, their low abundance and use of specific microhabitats such as bromeliads, temporary ponds, or small streams in forest areas seem to be contributing to their rarity.

Red lists of threatened species are important tools to highlight conservation priorities (Miller et al., 2006; Rodrigues et al., 2006); we argue that they can be particularly relevant for Paratelmatobiinae. Within the subfamily, one species (*P. lutzii*) is classified as Critically Endangered (CR) in the Brazilian Red List (ICMBio, 2018) and another (*C. bokermanni*) as Near Threatened. In addition, it has been suggested that *C. pintoi* and *C. itambe* should be classified as CR (Barata et al., 2018; Morais et al., 2013, respectively), although they are considered as Data Deficient (DD) in the Brazilian Red List (ICMBio, 2018). Of the remaining ten species, three are listed as DD, four as Least Concern, and two were not assessed (ICMBio, 2018). Given that DD species should also be included in conservation planning (Mace et al., 2008; Trindade-Filho et al., 2012), and considering the small geographic ranges and rarity, the Paratelmatobiinae is a highly important taxon from a conservation perspective. In the light of the new information provided by this study, it will be important to reassess the conservation status of its species to safeguard their viability and survival.

## CRediT authorship contribution statement

**Marcus Thadeu T. Santos:** Conceptualization, Formal analysis, Data curation, Writing - original draft. **Rafael F. de Magalhães:** Formal analysis, Writing - review & editing. **Mariana L. Lyra:** Data curation, Writing - review & editing. **Fabrício R. Santos:** Resources, Writing - review & editing, Funding acquisition. **Hussam Zaher:** Resources, Writing - review & editing. **Luís O.M. Giasson:** Resources, Writing - review & editing. **Paulo C.A. Garcia:** Conceptualization, Resources, Writing - review & editing. **Ana Carolina Carnaval:** Writing - review & editing, Supervision. **Célio F.B. Haddad:** Conceptualization, Resources, Writing - review & editing, Supervision, Funding acquisition.

## Acknowledgements

We thank J. P. Pombal Jr. and M. W. Cardoso (MNRJ), S. N. Oliveira (CHUFSC), and V. G. D. Orrico (MZUESC) for making available material under their care. M. T. Rodrigues, R. B. Ferreira, J. P. C. Monteiro, T. H. Condez, R. J. Sawaya, B. Berneck, L. F. Ugioni, P. N. Costa, M. Wachlevski, and I. Dias provided tissue samples. We thank J. P. C. Monteiro, T. Carvalho, T. H. Condez, I. M. Barata, S. V. Martins, B. Berneck, B. F. Zaidan, F. Dallacorte, J. Toso, P. H. Martins, E. C. Nardin, N. C. Pupin for help with field trips. J. G. R. Giovanelli for help with maps. K. Mercier helped with English. We are grateful to M. T. C. Thomé, S. T. Hiruma, T. R. Carvalho, F. R. Amaral, and two anonymous reviewers for comments and suggestions that improved the manuscript. This research benefited from resources of the Center for Scientific Computing (NCC/GridUNESP) of the Universidade Estadual Paulista (UNESP) and the Centro de Estudos de Insetos Sociais (CEIS, UNESP, Rio Claro, SP, Brazil). Field collections license provided by Instituto Chico Mendes de Conservação da Biodiversidade (ICMBio-SISBIO # 59179-1 and 59366-2); Instituto Estadual de Meio Ambiente e Recursos Hídricos (IEMA-ES # 032-2017), Instituto Estadual de Florestas (IEF-MG # 098/2017), Instituto Estadual do Ambiente (INEA-RJ # 045/2017), Comissão Técnico-Científica do Instituto Florestal (COTEC-SP # 260108 - 007.622/2017), Instituto Ambiental do Paraná (IAP-PR # 38.17), Fundação do Meio Ambiente (FATMA-SC # 5741/2017), and Ethics Committee on Animal Use of Universidade Estadual Paulista, campus Rio Claro (CEUA-IB # 24/2017).

## Funding

This work was supported by São Paulo Research Foundation, FAPESP [grant numbers 2011/50206-9, 2013/50741-7, and 2014/50342-8]; Minas Gerais Research Foundation, FAPEMIG [grant number APQ-01120-16]. MTTS was supported by Coordenação de Aperfeiçoamento de Pessoal - Brasil (CAPES 88881.189822/2018-01 and 88882.434124/2019-01). MLL thanks FAPESP for fellowship (2017/26162-8). RFM was supported by a PNPD-CAPES fellowship. CFBH, FRS, HZ, and PCAG were supported by research fellowships from Conselho Nacional de Desenvolvimento Científico e Tecnológico, CNPq (306623/2018-8, 308613/2016-3, and 306777/2014-2, respectively). AC acknowledges support by and FAPESP (BIOTA, 2013/50297-0), NSF (DEB 1343578), and NASA, through the Dimensions of Biodiversity Program.

## Declaration of Competing Interest

We declare no conflict of interest.

## Appendix A

Uncorrected *p*-distances (percentage) of mitochondrial 16S rRNA fragment (ca. 570 bp) within (highlighted in bold) and between the lineages of *Rupirana* delimited by the GMYC model. Data are shown as range (mean) when appropriate. Lin = Lineage.

| Lineage | *R. cardosoi* Lin A | *R. cardosoi* Lin B |
|---|---|---|
| *R. cardosoi* Lin A | **0.0–0.2 (0.1, n = 7)** | |
| *R. cardosoi* Lin B | 2.3–2.5 (2.3) | **.0 (n = 2)** |

## Appendix B

Uncorrected *p*-distances (percentage) of mitochondrial 16S rRNA fragment (ca. 570 bp) within (highlighted in bold) and among the lineages of *Scythrophrys* delimited by the GMYC model. Data are shown as range (mean) when appropriate. Lin = Lineage.

| Lineage | *Scythrophrys* sp. | *S. sawayae* Lin A | *S. sawayae* Lin B | *S. sawayae* Lin C |
|---|---|---|---|---|
| *Scythrophrys* sp. | **0.0–0.9 (0.4, n = 13)** | | | |
| *S. sawayae* Lin A | 3.6–4.5 (3.9) | **0.0–0.4 (0.2, n = 10)** | | |
| *S. sawayae* Lin B | 2.9–3.6 (3.2) | 1.8–2.0 (1.9) | **0.0 (n = 4)** | |
| *S. sawayae* Lin C | 3.4–4.6 (3.9) | 1.6–2.5 (2.0) | 1.1–1.6 (1.2) | **0.0–1.2 (0.5, n = 18)** |

## Appendix C

Uncorrected *p*-distances (percentage) of mitochondrial 16S rRNA fragment (ca. 570 bp) within (highlighted in bold) and among the lineages of *Crossodactylodes* delimited by the GMYC model. Data are shown as range (mean) when appropriate. Lin = Lineage.

| Lineage | *C. bokermanni* Lin A | *C. bokermanni* Lin B | *C. bokermanni* Lin C | *C. itambe* | *C. izecksohni* Lin A | *C. izecksohni* Lin B | *C. septentrionalis* | *Crossodactylodes* sp.1 | *Crossodactylodes* sp.2 | *Crossodactylodes* sp.3 |
|---|---|---|---|---|---|---|---|---|---|---|
| *C. bokermanni* Lin A | **0.0 (n = 2)** | | | | | | | | | |
| *C. bokermanni* Lin B | 3.3–3.6 (3.5) | **0.0 (n = 8)** | | | | | | | | |
| *C. bokermanni* Lin C | 0.9 | 3.9–4.2 (4.1) | **0.0 (n = 8)** | | | | | | | |
| *C. itambe* | 5.5–5.6 (5.5) | 5.1–5.7 (5.4) | 5.3–5.5 (5.3) | **0.0–0.2 (0.1, n = 5)** | | | | | | |
| *C. izecksohni* Lin A | 4.9–5.5 (5.2) | 5.8–6.5 (6.2) | 5.1–5.7 (5.4) | 3.7–4.4 (3.9) | **0.0–0.4 (0.1, n = 12)** | | | | | |
| *C. izecksohni* Lin B | 6.4–6.5 (6.4) | 7.1–7.8 (7.4) | 6.4–6.5 (6.4) | 4.6–4.9 (4.7) | 3.4–4.2 (3.7) | **0.0–0.2 (0.1, n = 5)** | | | | |
| *C. septentrionalis* | 5.8–6.0 (5.9) | 5.7–6.1 (5.9) | 5.8–6.0 (5.9) | 2.8–3.2 (2.9) | 4.2–4.7 (4.5) | 4.8–5.1 (4.9) | **0.0–0.2 (0.1, n = 3)** | | | |
| *Crossodactylodes* sp.1 | 5.3–5.5 (5.3) | 6.0–6.5 (6.2) | 5.1–5.3 (5.1) | 3.5–3.9 (3.6) | 2.3–2.7 (2.4) | 4.1–4.4 (4.1) | 4.6–4.8 (4.6) | **0.0–0.2 (0.1, n = 7)** | | |
| *Crossodactylodes* sp.2 | 5.8 | 6.7–7.2 (7.0) | 5.4 | 5.4 | 5.6–6.2 (5.8) | 6.8–7.0 (6.8) | 5.4–5.6 (5.5) | 5.6–5.8 (5.6) | **0.0 (n = 2)** | |
| *Crossodactylodes* sp.3 | 4.4–4.8 (4.6) | 4.8–5.6 (5.1) | 4.6–5.0 (4.7) | 3.2–3.4 (3.2) | 3.6–4.4 (3.9) | 4.3–4.5 (4.3) | 3.7–3.9 (3.8) | 3.8–4.5 (4.0) | 5.1–5.2 (5.1) | **0.0–0.4 (0.2, n = 6)** |

## Appendix D

Uncorrected *p*-distances (percentage) of mitochondrial 16S rRNA fragment (ca. 570 bp) within (highlighted in bold) and among the lineages of *Paratelmatobius lutzii* species group delimited by the GMYC model. Data are shown as range (mean). Lin = Lineage.

| Lineage | *P. gaigeae* | *P. poecilogaster* Lin A | *P. poecilogaster* Lin B | *P. poecilogaster* Lin C | *P. poecilogaster* Lin D |
|---|---|---|---|---|---|
| *P. gaigeae* | **0.0–1.1 (0.6, n = 9)** | | | | |
| *P. poecilogaster* Lin A | 5.2–5.5 (5.4) | **0.0–0.2 (0.1, n = 3)** | | | |
| *P. poecilogaster* Lin B | 4.3–4.8 (4.6) | 0.9–1.4 (1.2) | **0.0–0.2 (0.1, n = 10)** | | |
| *P. poecilogaster* Lin C | 4.1–4.5 (4.4) | 2.3–3.2 (2.7) | 1.6–2.4 (1.9) | **0.0–1.1 (0.7, n = 5)** | |
| *P. poecilogaster* Lin D | 4.1–4.7 (4.5) | 2.3–3.0 (2.7) | 1.6–2.2 (2.0) | 0.2–1.4 (0.7) | **0.2–0.6 (0.4, n = 3)** |

## Appendix E

Uncorrected *p*-distances (percentage) of mitochondrial 16S rRNA fragment (ca. 570 bp) within (highlighted in bold) and among the lineages of *Paratelmatobius cardosoi* species group delimited by the GMYC model. Data are shown as range (mean) when appropriate. Lin = Lineage.

| Lineage | *P. cardosoi* Lin A | *P. cardosoi* Lin B | *P. cardosoi* Lin C | *P. cardosoi* Lin D | *P. segallai* Lin A | *P. segallai* Lin B | *P. segallai* Lin C | *P. segallai* Lin D | *Paratelmatobius* sp. | *P. yepiranga* |
|---|---|---|---|---|---|---|---|---|---|---|
| *P. cardosoi* Lin A | **0.0 (n = 6)** | | | | | | | | | |
| *P. cardosoi* Lin B | 2.0–2.2 (2.1) | **0.0–0.2 (0.1, n = 20)** | | | | | | | | |
| *P. cardosoi* Lin C | 1.6–1.9 (1.8) | 2.1–2.4 (2.2) | **0.0 (n = 10)** | | | | | | | |
| *P. cardosoi* Lin D | 1.6 | 1.8–2.0 (1.9) | 1.8–2.1 (2.0) | **0.0 (n = 12)** | | | | | | |
| *P. segallai* Lin A | 4.8–5.0 (4.8) | 5.9–6.2 (6.1) | 5.4–5.6 (5.5) | 5.7–5.9 (5.9) | **0.0 (n = 6)** | | | | | |
| *P. segallai* Lin B | 5.4 | 6.4–6.8 (6.7) | 5.9–6.2 (6.0) | 6.3–6.4 (6.4) | 1.6 | **0.0 (n = 3)** | | | | |
| *P. segallai* Lin C | 4.4–5.5 (5.0) | 5.1–6.4 (5.9) | 5.0–6.2 (5.7) | 5.0–6.0 (5.7) | 1.4–2.0 (1.7) | 1.2–1.8 (1.5) | **0.0–1.2 (0.3, n = 21)** | | | |
| *P. segallai* Lin D | 5.2–5.3 (5.0) | 6.6–7.0 (6.9) | 5.5–5.8 (5.6) | 5.9–6.1 (6.0) | 4.6–4.7 (4.6) | 4.6–4.8 (4.8) | 5.0–5.6 (5.2) | **0.0 (n = 5)** | | |
| *Paratelmatobius* sp. | 7.3–7.5 (7.3) | 8.2–8.6 (8.5) | 8.4–8.8 (8.5) | 7.7–7.8 (7.8) | 7.5 | 7.7 | 7.4–8.0 (7.7) | 6.8–7.0 (6.8) | **0.0 (n = 3)** | |
| *P. yepiranga* | 7.3 | 8.5–8.8 (8.7) | 7.6–8.2 (7.9) | 7.9 | 7.0 | 7.2 | 7.2–7.9 (7.5) | 5.6–5.7 (5.7) | 5.5 | **0.0 (n = 2)** |

## Appendix F. Supplementary material

Supplementary data to this article can be found online at https://doi.org/10.1016/j.ympev.2020.106819.

## References

Almeida, F.F.M., Carneiro, C.D.R., 1998. Origem e evolução da Serra do Mar. Rev. Bras. Geoc. 28, 135–150.

Alves, R.J.V., Kolbek, J., 1994. Plant species endemism in savanna vegetation on table mountains (Campo Rupestre) in Brazil. Vegetatio 113, 125–139. https://doi.org/10.1007/BF00044230.

Amaro, R.C., Rodrigues, M.T., Yonenaga-Yassuda, Y., Carnaval, A.C., 2012. Demographic processes in the montane Atlantic rainforest: molecular and cytogenetic evidence from the endemic frog *Proceratophrys boiei*. Mol. Phylogenet. Evol. 62, 880–888. https://doi.org/10.1016/j.ympev.2011.11.004.

Antonelli, A., Verola, C.F., Parisod, C., Gustafsson, A.L.S., 2010. Climate cooling promoted the expansion and radiation of a threatened group of South American orchids (Epidendroideae: Laeliinae). Biol. J. Linn. Soc. 100, 597–607. https://doi.org/10.1111/j.1095-8312.2010.01438.x.

Baêta, D., Giasson, L.O.M., Pombal Jr., J.P., Haddad, C.F.B., 2016. Review of the rare genus *Phrynomedusa* Miranda-Ribeiro, 1923 (Anura: Phyllomedusidae) with description of a new species. Herpetol. Monogr. 30, 49–78. https://doi.org/10.1655/HERPMONOGRAPHS-D-15-00009.1.

Barata, I.M., Santos, M.T.T., Leite, F.S.F., Garcia, P.C.A., 2013. A new species of *Crossodactylodes* (Anura: Leptodactylidae) from Minas Gerais, Brazil: first record of genus within the Espinhaço Mountain Range. Zootaxa 3731, 552–560. https://doi.org/10.11646/zootaxa.3731.4.7.

Barata, I.M., Silva, E.P., Griffiths, R.A., 2018. Predictors of abundance of a rare bromeliad-dwelling frog (*Crossodactylodes itambe*) in the Espinhaço Mountain Range of Brazil. J. Herpetol. 52, 321–326. https://doi.org/10.1670/17-183.

Bitencourt, C., Rapini, A., 2013. Centres of endemism in the Espinhaço Range: identifying cradles and museums of Asclepiadoideae (Apocynaceae). Syst. Biodivers. 11, 525–536. https://doi.org/10.1080/14772000.2013.865681.

Bouckaert, R., Vaughan, T.G., Barido-Sottani, J., Duchêne, S., Fourment, M., Gavryushkina, A., Heled, J., Jones, G., Kühnert, D., De Maio, N., Matschiner, M., Mendes, F.K., Müller, N.F., Ogilvie, H.A., du Plessis, L., Popinga, A., Rambaut, A., Rasmussen, D., Siveroni, I., Suchard, M.A., Wu, C.H., Xie, D., Zhang, C., Stadler, T., Drummond, A.J., 2019. BEAST 2.5: an advanced software platform for Bayesian evolutionary analysis. PLOS Comput. Biol. 15, e1006650. https://doi.org/10.1371/journal.pcbi.1006650.

Brunes, T.O., Sequeira, F., Haddad, C.F., Alexandrino, J., 2010. Gene and species trees of a Neotropical group of treefrogs: genetic diversification in the Brazilian Atlantic Forest and the origin of a polyploid species. Mol. Phylogenet. Evol. 57, 1120–1133. https://doi.org/10.1016/j.ympev.2010.08.026.

Cabanne, G.S., Santos, F.R., Miyaki, C.Y., 2007. Phylogeography of *Xiphorhynchus fuscus* (Passeriformes, Dendrocolaptidae): vicariance and recent demographic expansion in southern Atlantic Forest. Biol. J. Linn. Soc. 91, 73–84. https://doi.org/10.1111/j.1095-8312.2007.00775.x.

Câmara, I.G., 2003. Brief history of conservation in the Atlantic Forest. In: Galindo-Leal,

C., Câmara, I.G. (Eds.), The Atlantic Forest of South America: biodiversity status, threats, and outlook. CABS and Island Press, Washington, pp. 31–42.
Camargo, A., Sites, J.J., 2013. Species delimitation: a decade after the renaissance. In: Pavlinov, I. (Ed.), The species problem: ongoing issues. InTech, New York, pp. 225–247. https://doi.org/10.5772/52664.
Carnaval, A.C., Bates, J.M., 2007. Amphibian DNA shows marked genetic structure and tracks Pleistocene climate change in northeastern Brazil. Evolution 61, 2942–2957. https://doi.org/10.1111/j.1558-5646.2007.00241.x.
Carnaval, A.C., Hickerson, M.J., Haddad, C.F.B., Rodrigues, M.T., Moritz, C., 2009. Stability predicts genetic diversity in the Brazilian Atlantic forest hotspot. Science 323, 785–789. https://doi.org/10.1126/science.1166955.
Carnaval, A.C., Waltari, E., Rodrigues, M.T., Rosauer, D., VanDerWal, J., Damasceno, R., Prates, I., Strangas, M., Spanos, Z., Rivera, D., Pie, M.R., Firkowski, C.R., Bornschein, M.R., Ribeiro, L.F., Moritz, C., 2014. Prediction of phylogeographic endemism in an environmentally complex biome. Proc. R. Soc. B. 281, 20141461. https://doi.org/10.1098/rspb.2014.1461.
Cazé, A.L.R., Mäder, G., Nunes, T.S., Queiroz, L.P., Oliveira, G., Diniz-Filho, J.A.F., Bonatto, S.B., Freitas, L.B., 2016. Could refuge theory and rivers acting as barriers explain the genetic variability distribution in the Atlantic Forest? Mol. Phylogenet. Evol. 101, 242–251. https://doi.org/10.1016/j.ympev.2016.05.013.
Cochran, D.M., 1938. Diagnoses of new frogs from Brazil. Proc. Biol. Soc. Wash. 51, 41–42.
Cogné, N., Cobbold, P.R., Riccomini, C., Gallagher, K., 2013. Tectonic setting of the Taubaté Basin (Southeastern Brazil): insights from regional seismic profiles and outcrop data. J. South Am. Earth Sci. 42, 194–204. https://doi.org/10.1016/j.jsames.2012.09.011.
Condez, T.H., Haddad, C.F.B., Zamudio, K.R., 2020. Historical biogeography and multitrait evolution in miniature toadlets of the genus *Brachycephalus* (Anura: Brachycephalidae). Biol. J. Linn. Soc. Blz 200, 1–23. https://doi.org/10.1093/biolinnean/blz200/5707641.
Cruz, C.A.G., Pimenta, B., 2004. *Phrynomedusa fimbriata*. The IUCN red list of threatened species 2004: e.T17078A6797217. https://www.iucnredlist.org/species/17078/6797217/ (accessed 08 July 2019).
Da Silva, C.R., Külkamp, J., 2018. *Valeriana iguanciana* (Valerianaceae), a new species from the highland grasslands of Serra do Tabuleiro, Santa Catarina, Brazil. Phytotaxa 364, 275–282. https://doi.org/10.11646/phytotaxa.364.3.7.
Faivovich, J., Nicoli, L., Blotto, B.L., Pereyra, M.O., Baldo, D., Barrionuevo, J.S., Fabrezi, M., Wild, E.R., Haddad, C.F.B., 2014. Big, bad, and beautiful: phylogenetic relationships of the horned frogs (Anura: Ceratophryidae). South Am. J. Herpetol. 9, 207–227. https://doi.org/10.2994/SAJH-D-14-00032.1.
Feng, Y.-J., Blackburn, D.C., Liang, D., Hillis, D.M., Wake, D.B., Cannatella, D.C., Zhang, P., 2017. Phylogenomics reveals rapid, simultaneous diversification of three major clades of Gondwanan frogs at the Cretaceous-Paleogene boundary. Proc. Natl. Acad. Sci. USA 114, E5864–E5870. https://doi.org/10.1073/pnas.1704632114.
Firkowski, C.R., Bornschein, M.R., Ribeiro, L.F., Pie, M.R., 2016. Species delimitation, phylogeny and evolutionary demography of co-distributed, montane frogs in the southern Brazilian Atlantic Forest. Mol. Phylogenet. Evol. 100, 345–360. https://doi.org/10.1016/j.ympev.2016.04.023.
Flot, J.F., 2010. Seqphase: a web tool for interconverting phase input/output files and fasta sequence alignments. Mol. Ecol. Resour. 10, 162–166. https://doi.org/10.1111/j.1755-0998.2009.02732.x.
Fonseca, G.A.B., Rylands, A.B., Paglia, A., Mittermeier, R.A., 2004. Atlantic Forest. In: Mittermeier, R.A., Gil, P.R., Hoffman, M., Pilgrim, J., Brooks, T., Mittermeier, C.G., Lamoreux, J., Fonseca, G.A.B. (Eds.), Hotspots revisited: earth's biologically richest and most endangered terrestrial ecoregions. Cemex and Agrupación Sierra Madre, Mexico City, pp. 84–88.
Fouquet, A., Blotto, B.L., Maronna, M.M., Verdade, V.K., Juncá, F.A., de Sá, R.O., Rodrigues, M.T., 2013. Unexpected phylogenetic positions of the genera *Rupirana* and *Crossodactylodes* reveal insights into the biogeography and reproductive evolution of leptodactylid frogs. Mol. Phylogenet. Evol. 67, 445–457. https://doi.org/10.1016/j.ympev.2013.02.009.
Fouquet, A., Cassini, C.S., Haddad, C.F.B., Pech, N., Rodrigues, M.T., 2014. Species delimitation, patterns of diversification and historical biogeography of the Neotropical frog genus *Adenomera* (Anura, Leptodactylidae). J. Biogeogr. 41, 855–870. https://doi.org/10.1111/jbi.12250.
Frost, D.R., 2020. Amphibian Species of the World: an online reference. Version 6.0. Am. Mus. Nat. Hist. http://research.amnh.org/herpetology/amphibia/ (accessed 07 February 2020).
Fouquet, A., Loebmann, D., Castroviejo-Fisher, S., Padial, J.M., Orrico, V.G., Lyra, M.L., Roberto, I.J., Kok, P.J.R., Haddad, C.F.B., Rodrigues, M.T., 2012b. From Amazonia to the Atlantic forest: molecular phylogeny of Phyzelaphryninae frogs reveals unexpected diversity and a striking biogeographic pattern emphasizing conservation challenges. Mol. Phylogenet. Evol. 65, 547–561. https://doi.org/10.1016/j.ympev.2012.07.012.
Fouquet, A., Recoder, R., Teixeira Jr., M., Cassimiro, J., Amaro, R.C., Camacho, A., Damasceno, R., Carnaval, A.C., Moritz, C., Rodrigues, M.T., 2012a. Molecular phylogeny and morphometric analyses reveal deep divergence between Amazonia and Atlantic Forest species of *Dendrophryniscus*. Mol. Phylogenet. Evol. 62, 826–838. https://doi.org/10.1016/j.ympev.2011.11.023.
Fujisawa, T., Barraclough, T.G., 2013. Delimiting species using single-locus data and the generalized mixed yule coalescent approach: a revised method and evaluation on simulated data sets. Syst. Biol. 62, 707–724. https://doi.org/10.1093/sysbio/syt033.
Fusinatto, L.A., Alexandrino, J., Haddad, C.F.B., Brunes, T.O., Rocha, C.F.D., Sequeira, F., 2013. Cryptic genetic diversity is paramount in small-bodied amphibians of the genus *Euparkerella* (Anura: Craugastoridae) endemic to the Brazilian Atlantic forest. PLoS ONE 8, e79504. https://doi.org/10.1371/journal.pone.0079504.
Garcia, P.C.A., Peixoto, O.L., Haddad, C.F.B., 2008. A new species of *Hypsiboas* (Anura: Hylidae) from the Atlantic Forest of Santa Catarina, southern Brazil, with comments on its conservation status. South Am. J. Herpetol. 3, 27–35. https://doi.org/10.2994/1808-9798(2008)3[27:ANSOHA]2.0.CO;2.
Garcia, P.C.A., Berneck, B.V.M., Costa, C.O.R., 2009. A new species of *Paratelmatobius* (Amphibia, Anura, Leptodactylidae) from Atlantic Rain Forest of Southeastern Brazil. South Am. J. Herpetol. 4, 217–224. https://doi.org/10.2994/057.004.0303.
Gontijo-Pascutti, A.H.F., Hasui, Y., Santos, M., Soares Jr., A.V., Souza, I.A., 2012. As Serras do Mar e da Mantiqueira. In: Hasui, Y., Carneiro, C.D.R., Almeida, F.F.M., Bartorelli, A. (Eds.), Geologia do Brasil. Beca, São Paulo, pp. 549–571.
Graham, C.H., Carnaval, A.C., Cadena, C.D., Zamudio, K.R., Roberts, T.E., Parra, J.L., McCain, C.M., Bowie, R.C.K., Moritz, C., Baines, S.B., Schneider, C.J., VanDerWal, J., Rahbek, C., Kozak, K.H., Sanders, N.J., 2014. The origin and maintenance of montane diversity: integrating evolutionary and ecological processes. Ecography 37, 1–9. https://doi.org/10.1111/ecog.00578.
Guarnizo, C.E., Cannatella, D.C., 2013. Genetic divergence within frog species is greater in topographically more complex regions. J. Zoolog. Syst. Evol. Res. 51, 333–340. https://doi.org/10.1111/jzs.12027.
Haddad, C.F.B., Toledo, L.F., Prado, C.P.A., Loebmann, D., Gasparini, J.L., Sazima, I., 2013. Guide to the amphibians of the Atlantic Forest: diversity and biology. Anolisbooks, São Paulo.
Haffer, J., 1969. Speciation in Amazonian forest birds. Science 165, 131–137. https://doi.org/10.1126/science.165.3889.131.
Haffer, J., 1997. Alternative models of vertebrate speciation in Amazonia: an overview. Biodivers. Conserv. 6, 451–476. https://doi.org/10.1023/A:1018320925954.
Hassemer, G., Ferreira, P.M.A., Trevisan, R., 2015. A review of vascular plant endemisms in Santa Catarina, southern Brazil, highlights critical knowledge gaps and urgent need of conservation efforts. J. Torrey. Bot. Soc. 142, 78–95. https://doi.org/10.3159/torrey-d-14-00033.1.
Heinicke, M.P., Duellman, W.E., Trueb, L., Means, D.B., MacCulloch, R.D., Hedges, S.B., 2009. A new frog family (Anura: Terrarana) from South America and an expanded direct-developing clade revealed by molecular phylogeny. Zootaxa 2211, 1–35. https://doi.org/10.11646/zootaxa.2211.1.1.
Herbert, T.D., Lawrence, K.T., Tzanova, A., Peterson, L.C., Caballero-Gill, R., Kelly, C.S., 2016. Late Miocene global cooling and the rise of modern ecosystems. Nat. Geosci. 9, 843–847. https://doi.org/10.1038/NGEO2813.
Hewitt, G.M., 2000. The genetic legacy of the Quaternary ice ages. Nature 405, 907–913. https://doi.org/10.1038/35016000.
Heyer, W.R., 1999. A new genus and species of frog from Bahia, Brazil (Amphibia: Anura: Leptodactylidae) with comments on the zoogeography of the Brazilian campos rupestres. Proc. Biol. Soc. Wash. 112, 19–30.
Hillman, S.S., Withers, P.C., Drewes, R.C., Hillyard, S.D., 2009. Ecological and environmental physiology of amphibians. Oxford University Press, New York. https://doi.org/10.1093/acprof:oso/9780198570325.001.0001.
Hipsley, C.A., Müller, J., 2014. Beyond fossil calibrations: realities of molecular clock practices in evolutionary biology. Front. Genet. 5, 138. https://doi.org/10.3389/fgene.2014.00138.
Hoorn, C., Wesselingh, F.P., ter Steege, H., Bermudez, M.A., Mora, A., Sevink, J., Sanmartín, I., Sanchez-Meseguer, A., Anderson, C.L., Figueiredo, J.P., Jaramillo, C., Riff, D., Negri, F.R., Hooghiemstra, H., Lundberg, J., Stadler, T., Särkinen, T., Antonelli, A., 2010. Amazonia through time: andean uplift, climate change, landscape evolution and biodiversity. Science 330, 927–931. https://doi.org/10.1126/science.1194585.
Hurvich, C., Tsai, C., 1989. Regression and time series model selection in small samples. Biometrika 76, 297–307. https://doi.org/10.1093/biomet/76.2.297.
Huson, D.H., Bryant, D., 2006. Application of phylogenetic networks in evolutionary studies. Mol. Biol. Evol. 23, 254–267. https://doi.org/10.1093/molbev/msj030.
Jetz, W., Pyron, R.A., 2018. The interplay of past diversification and evolutionary isolation with present imperilment across the amphibian tree of life. Nat. Ecol. Evol. 2, 850–858. https://doi.org/10.1038/s41559-018-0515-5.
Joly, S., Bryant, D., Lockhart, P.J., 2015. Flexible methods for estimating genetic distances from single nucleotide polymorphism. Methods Ecol. Evol. 6, 938–948. https://doi.org/10.1111/2041-210X.12343.
Jukes, T.H., Cantor, C.R., 1969. Evolution of protein molecules. In: Munro, H.N. (Ed.), Mammalian protein metabolism. Academic Press, New York, pp. 21–132. https://doi.org/10.1016/B978-1-4832-3211-9.50009-7.
Juncá, F.A., Lugli, L., 2009. Reproductive biology, vocalizations, and tadpole morphology of *Rupirana cardosoi*, an anuran with uncertain affinities. South Am. J. Herpetol. 4, 173–178. https://doi.org/10.2994/057.004.0208.
Katoh, K., Standley, D.M., 2013. MAFFT multiple sequence alignment software Version 7: improvements in performance and usability. Mol. Biol. Evol. 30, 772–780. https://doi.org/10.1093/molbev/mst010.
Katoh, K., Rozewicki, J., Yamada, K.D., 2017. MAFFT online service: multiple sequence alignment, interactive sequence choice and visualization. Brief. Bioinform. 20, 1160–1166. https://doi.org/10.1093/bib/bbx108.
Knowles, L.L., Carstens, B.C., 2007. Delimiting species without monophyletic gene trees. Syst. Biol. 56, 887–895. https://doi.org/10.1080/10635150701701091.
Kumar, S., Stecher, G., Li, M., Knyaz, C., Tamura, K., 2018. MEGA X: molecular evolutionary genetics analysis across computing platforms. Mol. Biol. Evol. 35, 1547–1549. https://doi.org/10.1093/molbev/msy096.
Lande, R., 1999. Extinction risk from anthropogenic, ecological and genetic factors. In: Landweber, L.F., Dobson, A.P. (Eds.), Genetics and the extinction of species. Princeton University Press, Princeton, pp. 1–22.
Lanfear, R., Frandsen, P.B., Wright, A.M., Senfeld, T., Calcott, B., 2017. PartitionFinder 2: new methods for selecting partitioned models of evolution for molecular and morphological phylogenetic analyses. Mol. Biol. Evol. 34, 772–773. https://doi.org/10.

1093/molbev/msw260.
Linder, H.P., Hardy, C.R., Rutschmann, F., 2005. Taxon sampling effects in molecular clock dating: an example from the African Restionaceae. Mol. Phylogenet. Evol. 35, 569–582. https://doi.org/10.1016/j.ympev.2004.12.006.
Liu, L., Xi, Z., Wu, S., Davis, C.C., Edwards, S.V., 2015. Estimating phylogenetic trees from genome-scale data. Ann. N. Y. Acad. Sci. 1360, 36–53. https://doi.org/10.1111/nyas.12747.
Losos, J.B., 2010. Adaptive radiation, ecological opportunity, and evolutionary determinism. Am. Nat. 175, 623–639. https://doi.org/10.1086/652433.
Lourenço, L.B., Garcia, P.C.A., Recco-Pimentel, S.M., 2003. Intrageneric karyotypic divergence in *Scythrophrys* and new insights into the relationship with *Paratelmatobius* (Anura, Leptodactylidae). Ital. J. Zool. 70, 183–190. https://doi.org/10.1080/11250000309356514.
Lourenço, L.B., Bacci-Júnior, M., Martins, V.G., Recco-Pimentel, S.M., Haddad, C.F.B., 2008. Molecular phylogeny and karyotype differentiation in *Paratelmatobius* and *Scythrophrys* (Anura, Leptodactylidae). Genetica 132, 255–266. https://doi.org/10.1007/s10709-007-9169-y.
Lutz, B., Carvalho, A.L., 1958. Novos anfíbios anuros das serras costeiras do Brasil. Mem. Inst. Oswaldo Cruz 56, 239–249.
Lynch, J.D., 1971. Evolutionary relationships, osteology, and zoogeography of Leptodactyloid frogs. Misc. Publ. Museum Nat. Hist. Univ. Kansas 53, 1–238.
Lyra, M.L., Haddad, C.F.B., de Azeredo-Espin, A.M.L., 2017. Meeting the challenge of DNA barcoding Neotropical amphibians: polymerase chain reaction optimization and new COI primers. Mol. Ecol. Resour. 17, 966–980. https://doi.org/10.1111/1755-0998.12648.
Mace, G.M., Collar, N.J., Gaston, K.J., Hilton-Taylor, C., Akçakaya, H.R., Leader-Williams, N., Milner-Gulland, E.J., Stuart, S.N., 2008. Quantification of extinction risk: IUCN'S system for classifying threatened species. Conserv. Biol. 22, 1424–1442. https://doi.org/10.1111/j.1523-1739.2008.01044.x.
Maniatis, T., Fritsch, E.F., Sambrook, J., 1982. Molecular cloning: a laboratory manual. Cold Spring Harbour Laboratory, New York.
Martins, F.M., 2011. Historical biogeography of the Brazilian Atlantic forest and the Carnaval-Moritz model of Pleistocene refugia: what do phylogeographical studies tell us? Biol. J. Linn. Soc. 104, 499–509. https://doi.org/10.1111/j.1095-8312.2011.01745.x.
McCormack, J.E., Heled, J., Delaney, K.S., Peterson, A.T., Knowles, L.L., 2011. Calibrating divergence times on species trees versus gene trees: implications for speciation history of *Aphelocoma* jays. Evolut. Int. J. Org. Evolut. 65, 184–202. https://doi.org/10.1111/j.1558-5646.2010.01097.x.
Miller, R.M., Rodríguez, J.P., Aniskowicz-Fowler, T., Bambaradeniya, C., Boles, R., Eaton, M.A., Gardenfors, U., Keller, V., Molur, S., Walker, S., Pollock, C., 2006. Extinction risk and conservation priorities. Science 313, 441. https://doi.org/10.1126/science.313.5786.441a.
Miller, M.A., Pfeiffer, W., Schwartz, T., 2010. Creating the CIPRES Science Gateway for inference of large phylogenetic trees. Proc. Gatew. Comput. Environ. Workshop 2010, 1–8. https://doi.org/10.1109/GCE.2010.5676129.
Instituto Chico Mendes de Conservação da Biodiversidade (ICMBio), 2018. Livro Vermelho da Fauna Brasileira Ameaçada de Extinção: Volume V – Anfíbios. In: Instituto Chico Mendes de Conservação da Biodiversidade (Ed.), Livro Vermelho da Fauna Brasileira Ameaçada de Extinção. ICMBio/MMA, Brasília, pp. 1–128.
Morais, A.R., Siqueira, M.N., Lemes, P., Maciel, N.M., De Marco Jr., P., Brito, D., 2013. Unraveling the conservation status of Data Deficient species. Biol. Conserv. 166, 98–102. https://doi.org/10.1016/j.biocon.2013.06.010.
Morellato, L.P.C., Haddad, C.F.B., 2000. Introduction: the Brazilian Atlantic forest. Biotropica 32, 786–792. https://doi.org/10.1111/j.1744-7429.2000.tb00618.x.
Moritz, C., Patton, J.L., Schneider, C.J., Smith, T.B., 2000. Diversification of rainforest faunas: an integrated molecular approach. Annu. Rev. Ecol. Syst. 31, 533–563. https://doi.org/10.1146/annurev.ecolsys.31.1.533.
Moura, M.R., Costa, H.C., Peixoto, M.A., Carvalho, A.L., Santana, D.J., Vasconcelos, H.L., 2018. Geographical and socioeconomic determinants of species discovery trends in a biodiversity hotspot. Biol. Conserv. 220, 237–244. https://doi.org/10.1016/j.biocon.2018.01.024.
Myers, N., Mittermeier, R.A., Mittermeier, C.G., Fonseca, G.A.B., Kent, J., 2000. Biodiversity hotspots for conservation priorities. Nature 403, 853–858. https://doi.org/10.1038/35002501.
Nicoli, L., 2017. New clues on anuran evolution: the oldest record of an extant hyloid clade in the Oligocene of Patagonia. Hist. Biol. 29, 1031–1044. https://doi.org/10.1080/08912963.2017.1282475.
Ochoa, L.E., Roxo, F.F., DoNascimiento, C., Sabaj, M.H., Datovo, A., Alfaro, M., Oliveira, C., 2017. Multilocus analysis of the catfish family Trichomycteridae (Teleostei: Ostariophysi: Siluriformes) supporting a monophyletic Trichomycterinae. Mol. Phylogenet. Evol. 115, 71–81. https://doi.org/10.1016/j.ympev.2017.07.007.
Ogilvie, H.A., Bouckaert, R., Drummond, A.J., 2017. StarBEAST2 brings faster species tree inference and accurate estimates of substitution rates. Mol. Biol. Evol. 34, 2101–2114. https://doi.org/10.1093/molbev/msx126.
Ohler, A., Dubois, A., 2012. Validation of two familial nomina nuda of Amphibia Anura. Alytes 28, 162–167.
Oliveira, U., Paglia, A.P., Brescovit, A.D., Carvalho, C.J.B., Silva, D.P., Rezende, D.T., Leite, F.S.F., Batista, J.A.N., Barbosa, J.P.P.P., Stehmann, J.R., Ascher, J.S., Vasconcelos, M.F., De Marco Jr., P., Löwenberg-Neto, P., Dias, P.G., Ferro, V.G., Santos, A.J., 2016. The strong influence of collection bias on biodiversity knowledge shortfalls of Brazilian terrestrial biodiversity. Divers. Distrib. 22, 1232–1244. https://doi.org/10.1111/ddi.12489.
Oliveira-Filho, A.T., Fontes, M.A.L., 2000. Patterns of floristic differentiation among Atlantic Forests in Southeastern Brazil and the influence of climate. Biotropica 32, 793–810. https://doi.org/10.1111/j.1744-7429.2000.tb00619.x.
Olsen, P.E., Whiteside, J.H., 2009. Pre-Quaternary Milankovitch cycles and climate variability. In: Gornitz, V. (Ed.), Encyclopedia of paleoclimatology and ancient environments, Encyclopedia of Earth Science Series. Springer, Dordrecht, pp. 826–835. https://doi.org/10.1007/978-1-4020-4411-3_195.
Ortiz-Jaureguizar, E., Cladera, G.A., 2006. Paleoenvironmental evolution of southern South America during the Cenozoic. J. Arid Environ. 66, 498–532. https://doi.org/10.1016/j.jaridenv.2006.01.007.
Pabijan, M., Wollenberg, K.C., Vences, M., 2012. Small body size increases the regional differentiation of populations of tropical mantellid frogs (Anura: Mantellidae). J. Evol. Biol. 25, 2310–2324. https://doi.org/10.1111/j.1420-9101.2012.02613.x.
Palumbi, S.R., Martin, A.P., Kessing, B.D., McMillan, W.O., 1991. Detecting population structure using mitochondrial DNA. In: Hoelzel, A.R. (Ed.), Genetic ecology of whales and dolphins. International Whaling Comission, UK, pp. 271–278.
Paradis, E., Schliep, K., 2019. Ape 5.0: an environment for modern phylogenetics and evolutionary analyses in R. Bioinformatics 35, 526–528. https://doi.org/10.1093/bioinformatics/bty633.
Passarelli, C.R., Basei, M.A.S., Prazeres-Filho, H.J., Siga-Jr, O., Szabó, G.A.J., Marco-Neto, J., 2007. Structural and geochronological constraints on the evolution of the Juréia Massif, Registro Domain, State of São Paulo. Brazil. An. Acad. Brasil. Ciênc. 79, 441–455. https://doi.org/10.1590/S0001-37652007000300008.
Peixoto, O.L., Carvalho-e-Silva, S.P., 2004. *Crossodactylodes pintoi*. The IUCN Red List of Threatened Species 2004: e.T56346A11465671. https://www.iucnredlist.org/species/56346/11465671/ (accessed 08 July 2019).
Pellegrino, K.C.M., Rodrigues, M.T., Waite, A.N., Morando, M., Yassuda, Y.Y., Sites Jr., J.W., 2005. Phylogeography and species limits in the *Gymnodactylus darwinii* complex (Gekkonidae, Squamata): genetic structure coincides with river systems in the Brazilian Atlantic Forest. Biol. J. Linn. Soc. 84, 13–26. https://doi.org/10.1111/j.1095-8312.2005.00472.x.
Pimm, S.L., Jenkins, C.N., Abell, R., Brooks, T.M., Gittleman, J.L., Joppa, L.N., Raven, P.H., Roberts, C.M., Sexton, J.O., 2014. The biodiversity of species and their rates of extinction, distribution, and protection. Science 344, 1246752. https://doi.org/10.1126/science.1246752.
Polato, N.R., Gill, B.A., Shah, A.A., Gray, M.M., Casner, K.L., Barthelet, A., Messer, P.W., Simmons, M.P., Guayasamin, J.M., Encalada, A.C., Kondratieff, B.C., Flecker, A.S., Thomas, S.A., Ghalambor, C.K., Poff, N.L., Funk, W.C., Zamudio, K.R., 2018. Narrow thermal tolerance and low dispersal drive higher speciation in tropical mountains. Proc. Natl. Acad. Sci. USA 115, 12471–12476. https://doi.org/10.1073/pnas.1809326115.
Pombal Jr., J.P., Haddad, C.F.B., 1999. Frogs of the genus *Paratelmatobius* (Anura: Leptodactylidae) with descriptions of two new species. Copeia 1999, 1014–1026. https://doi.org/10.2307/1447976.
Pons, J., Barraclough, T.G., Gomez-Zurita, J., Cardoso, A., Duran, D.P., Hazell, S., Kamoun, S., Sumlin, W.D., Vogler, A.P., 2006. Sequence-based species delimitation for the DNA taxonomy of undescribed insects. Syst. Biol. 55, 595–609. https://doi.org/10.1080/10635150600852011.
Potter, P.E., 1997. The Mesozoic and Cenozoic paleodrainage of South America: a natural history. J. South Am. Earth Sci. 10, 331–344. https://doi.org/10.1016/S0895-9811(97)00031-X.
Prates, I., Melo-Sampaio, P.R., de Queiroz, K., Carnaval, A.C., Rodrigues, M.T., Drummond, L.O., 2020. Discovery of a new species of *Anolis* lizards from Brazil and its implications for the historical biogeography of montane Atlantic Forest endemics. Amphibia-Reptilia 41, 87–103. https://doi.org/10.1163/15685381-20191179.
Pulquério, M.J., Nichols, R.A., 2007. Dates from the molecular clock: how wrong can we be? Trends Ecol Evol. 22, 180–184. https://doi.org/10.1016/j.tree.2006.11.013.
Pyron, R.A., 2014. Biogeographic analysis reveals ancient continental vicariance and recent oceanic dispersal in amphibians. Syst. Biol. 63, 779–797. https://doi.org/10.1093/sysbio/syu042.
Pyron, R.A., Wiens, J.J., 2011. A large-scale phylogeny of Amphibia with over 2800 species, and a revised classification of extant frogs, salamanders, and caecilians. Mol. Phylogenet. Evol. 61, 543–583. https://doi.org/10.1016/j.ympev.2011.06.012.
Rambaut, A., Drummond, A.J., Xie, D., Baele, G., Suchard, M.A., 2018. Posterior summarization in Bayesian phylogenetics using Tracer 1.7. Syst. Biol. 67, 901–904. https://doi.org/10.1093/sysbio/syy032.
Rannala, B., 2015. The art and science of species delimitation. Curr. Zool. 61, 846–853. https://doi.org/10.1093/czoolo/61.5.846.
Rapini, A., van den Berg, C., Liede-Schumann, S., 2007. Diversification of Asclepiadoideae (Apocynaceae) in the New World. Ann. Missouri Bot. Gard. 94, 407–422. https://doi.org/10.3417/0026-6493(2007)94[407:DOAAIT]2.0.CO;2.
Reid, N.M., Carstens, B.C., 2012. Phylogenetic estimation error can decrease the accuracy of species delimitation: a Bayesian implementation of the general mixed Yule coalescent model. BMC Evol. Biol. 12, 196. https://doi.org/10.1186/1471-2148-12-196.
Ribeiro, M.C., Metzger, J.P., Martensen, A.C., Ponzoni, F.J., Hirota, M.M., 2009. The Brazilian Atlantic forest: how much is left, and how is the remaining forest distributed? Implications for conservation. Biol. Conserv. 142, 1141–1153. https://doi.org/10.1016/j.biocon.2009.02.021.
Riccomini, C., Assumpção, M., 1999. Quaternary tectonics in Brazil. Episodes 22, 221–225. https://doi.org/10.18814/epiiugs/1999/v22i3/010.
R Core Team, 2017. R: a language and environment for statistical computing. R Foundation for Statistical Computing, Vienna, Austria. URL https://www.R-project.org/.
Riccomini, C., Sant'Anna, L.G., Ferrari, A.L., 2004. Evolução geológica do Rift Continental do Sudeste do Brasil. In: Mantesso-Neto, V., Bartorelli, A., Carneiro, C.D.R, Brito-Neves, B.B. (Eds.), Geologia do continente Sul-Americano: evolução da obra de Fernando Flávio Marques de Almeida. Beca, São Paulo, pp. 383–405.
Riccomini, C., Grohmann, C.H., Sant'Anna, L.G., Hiruma, S.T., 2010. A captura das cabeceiras do Rio Tietê pelo Rio Paraíba do Sul. In: Modenesi-Gauttieri, M.C., Bartorelli,

A., Mantesso-Neto, V., Carneiro, C.D.R., Lisboa, M.B.A.L. (Eds.), A Obra de Aziz Nacib Ab'Sáber. Becca, São Paulo, pp. 157–169.
Rodrigues, A.S.L., Pilgrim, J.D., Lamoreux, J.F., Hoffmann, M., Brooks, T.M., 2006. The value of the IUCN Red List for conservation. Trends Ecol. Evol. 21, 71–76. https://doi.org/10.1016/j.tree.2005.10.010.
Rodríguez, A., Börner, M., Pabijan, M., Gehara, M., Haddad, C.F.B., Vences, M., 2015. Genetic divergence in tropical anurans: deeper phylogeographic structure in forest specialists and in topographically complex regions. Evol. Ecol. 29, 765–785. https://doi.org/10.1007/s10682-015-9774-7.
Roig-Juñent, S., Domínguez, M.C., Flores, G.E., Mattoni, C., 2006. Biogeographic history of South American arid lands: a view from its arthropods using TASS analysis. J. Arid Environ. 66, 404–420. https://doi.org/10.1016/j.jaridenv.2006.01.005.
Romero, E.J., 1986. Paleogene phytogeography and climatology of South America. Ann. Missouri Bot. Gard. 73, 449–461. https://doi.org/10.2307/2399123.
Ronquist, F., Teslenko, M., Van Der Mark, P., Ayres, D.L., Darling, A., Höhna, S., Larget, B., Liu, L., Suchard, M.A., Huelsenbeck, J.P., 2012. Mrbayes 3.2: efficient Bayesian phylogenetic inference and model choice across a large model space. Syst. Biol. 61, 539–542. https://doi.org/10.1093/sysbio/sys029.
Rossa-Feres, D.C., Garey, M.V., Caramaschi, U., Napoli, M.F., Nomura, F., Bispo, A.A., Brasileiro, C.A., Thomé, M.T.C., Sawaya, R.J., Conte, C.E., Cruz, C.A.G., Nascimento, L.B., Gasparini, J.L., Almeida, A.P., Haddad, C.F.B., 2017. Anfíbios da Mata Atlântica: lista de espécies, histórico dos estudos, biologia e conservação. In: Monteiro-Filho, E.L.A., Conte, C.E. (Eds.), Revisões em zoologia: Mata Atlântica. Editora UFPR, Curitiba, pp. 237–314.
Saadi, A., 1993. Neotectônica da plataforma brasileira: esboço e interpretação preliminares. Geonomos 1, 1–15. https://doi.org/10.18285/geonomos.v1i1e2.233.
Saadi, A., 1995. A geomorfologia da Serra do Espinhaço em Minas Gerais e de suas margens. Geonomos 3, 41–63. https://doi.org/10.18285/geonomos.v3i1.215.
Saadi, A., Machette, M.N., Haller, K.M., Dart, R.L., Bradley, L., Souza, A.M.P.D., 2002. Map and database of Quaternary faults and lineaments in Brazil. U.S. Geol. Surv. Open-File Rept. 02-230, Version 1.0. Available from http://pubs.usgs.gov/of/2002/ofr-02-230/.
Saadi, A., Bezerra, F.H.R., Costa, R.D., Igreja, H.L.S., Franzinelli, E., 2005. Neotectônica da Plataforma Brasileira. In: Souza, C.R.G., Suguio, K., Oliveira, A.M.S., Oliveira, P.E. (Eds.), Quaternário do Brasil. Holos, Ribeirão Preto, pp. 211–234.
Sabbag, A.F., Lyra, M.L., Zamudio, K.R., Haddad, C.F.B., Feio, R.N., Leite, F.S., Gasparini, J.L., Brasileiro, C.A., 2018. Molecular phylogeny of Neotropical rock frogs reveals a long history of vicariant diversification in the Atlantic forest. Mol. Phylogenet. Evol. 122, 142–156. https://doi.org/10.1016/j.ympev.2018.01.017.
Santos, M.T.T., Magalhães, R.F., Ferreira, R.B., Vittorazzi, S.E., Dias, I.R., Leite, F.S.F., Lourenço, L.B., Santos, F.R., Haddad, C.F.B., Garcia, P.C.A., 2020. Systematic revision of the rare bromeligenous genus *Crossodactylodes* Cochran, 1938 (Anura: Leptodactylidae: Paratelmatobiinae). Herpetol. Monogr. https://doi.org/10.1655/HERPMONOGRAPHS-D-19-00008. In press.
Santos, M.T.T., Oliveira, S.H., Carvalho, T.R., Zaidan, B.F., Silva, N.R., Berneck, B.V., Garcia, P.C.A., 2019. A new species of *Paratelmatobius* (Anura: Leptodactylidae: Paratelmatobiinae) from the Atlantic Forest of southern Brazil. Zootaxa 4648, 473–493. https://doi.org/10.11646/zootaxa.4648.3.4.
Scherz, M.D., Glaw, F., Hutter, C.R., Bletz, M.C., Rakotoarison, A., Köhler, J., Vences, M., 2019. Species complexes and the importance of Data Deficient classification in Red List assessments: the case of *Hylobatrachus* frogs. PLoS ONE 14, e0219437. https://doi.org/10.1371/journal.pone.0219437.
Silva, J.M.C., Casteleti, C.H.M., 2003. Status of the biodiversity of the Atlantic Forest of Brazil. In: Galindo-Leal, C., Câmara, I.G. (Eds.), The Atlantic Forest of South America: biodiversity status, trends, and outlook. CABS and Island Press, Washington, pp. 43–59.
Silveira, F.A.O., Negreiros, D., Barbosa, N.P.U., Buisson, E., Carmo, F.F., Carstensen, D.W., Conceição, A.A., Cornelissen, T.G., Echternacht, L., Fernandes, G.W., Garcia, Q.S., Guerra, T.J., Jacobi, C.M., Lemos-Filho, J.P., Le Stradic, S., Morellato, L.P.C., Neves, F.S., Oliveira, R.S., Schaefer, C.E., Viana, P.L., Lambers, H., 2016. Ecology and evolution of plant diversity in the endangered campo rupestre: a neglected conservation priority. Plant Soil 403, 129–152. https://doi.org/10.1007/s11104-015-2637-8.
Sodhi, N.S., Bickford, D., Diesmos, A.C., Lee, T.M., Koh, L.P., Brook, B.W., Sekercioglu, C.H., Bradshaw, C.J.A., 2008. Measuring the meltdown: drivers of global amphibian extinction and decline. PLoS ONE 3, e1636. https://doi.org/10.1371/journal.pone.0001636.
Stamatakis, A., 2014. RAxML version 8: a tool for phylogenetic analysis and post-analysis of large phylogenies. Bioinformatics 30, 1312–1313. https://doi.org/10.1093/bioinformatics/btu033.
Stephens, M., Smith, N.J., Donnelly, P., 2001. A new statistical method for haplotype reconstruction from population data. Am. J. Hum. Genet. 68, 978–989. https://doi.org/10.1086/319501.
Streicher, J.W., Miller, E.C., Guerrero, P.C., Correa, C., Ortiz, J.C., Crawford, A.J., Pie, M.R., Wiens, J.J., 2018. Evaluating methods for phylogenomic analyses, and a new phylogeny for a major frog clade (Hyloidea) based on 2214 loci. Mol. Phylogenet. Evol. 119, 128–143. https://doi.org/10.1016/j.ympev.2017.10.013.
Suchard, M.A., Kitchen, C.M., Sinsheimer, J.S., Weiss, R.E., 2003. Hierarchical phylogenetic models for analyzing multipartite sequence data. Syst. Biol. 52, 649–664. https://doi.org/10.1080/10635150390238879.
Tabarelli, M., Aguiar, A.V., Ribeiro, M.C., Metzger, J.P., Peres, C.A., 2010. Prospects for biodiversity conservation in the Atlantic Forest: lessons from aging human-modified landscapes. Biol. Conserv. 143, 2328–2340. https://doi.org/10.1016/j.biocon.2010.02.005.
Talavera, G., Dinca, V., Vila, R., 2013. Factors affecting species delimitations with the GMYC model: insights from a butterfly survey. Methods Ecol. Evol. 4, 1101–1110. https://doi.org/10.1111/2041-210X.12107.
Teixeira Jr., M., Recoder, R.S., Amaro, R.C., Damasceno, R.P., Cassimiro, J., Rodrigues, M.T., 2013. A new *Crossodactylodes* Cochran, 1938 (Anura: Leptodactylidae: Paratelmatobiinae) from the highlands of the Atlantic Forests of southern Bahia, Brazil. Zootaxa 3702, 459–472. https://doi.org/10.11646/zootaxa.3702.5.5.
Thomé, M.T.C., Zamudio, K.R., Giovanelli, J.G.R., Haddad, C.F.B., Baldissera, F.A., Alexandrino, J., 2010. Phylogeography of endemic toads and post-Pliocene persistence of the Brazilian Atlantic Forest. Mol. Phylogenet. Evol. 55, 1018–1031. https://doi.org/10.1016/j.ympev.2010.02.003.
Thomé, M.T.C., Zamudio, K.R., Haddad, C.F.B., Alexandrino, J., 2014. Barriers, rather than refugia, underlie the origin of diversity in toads endemic to the Brazilian Atlantic Forest. Mol. Ecol. 23, 6152–6164. https://doi.org/10.1111/mec.12986.
Thomé, M.T.C., Sequeira, F., Brusquetti, F., Carstens, B., Haddad, C.F.B., Rodrigues, M.T., Alexandrino, J., 2016. Recurrent connections between Amazon and Atlantic forests shaped diversity in Caatinga four-eyed frogs. J. Biogeogr. 43, 1045–1056. https://doi.org/10.1111/jbi.12685.
Toews, D.P.L., Brelsford, A., 2012. The biogeography of mitochondrial and nuclear discordance in animals. Mol. Ecol. 21, 3907–3930. https://doi.org/10.1111/j.1365-294X.2012.05664.x.
Toledo, L.F., Becker, C.G., Haddad, C.F.B., Zamudio, K.R., 2014. Rarity as an indicator of endangerment in Neotropical frogs. Biol. Conserv. 179, 54–62. https://doi.org/10.1016/j.biocon.2014.08.012.
Trindade-Filho, J., de Carvalho, E.A., Brito, D., Loyola, R.D., 2012. How does the inclusion of Data Deficient species change conservation priorities for amphibians in the Atlantic Forest? Biodivers. Conserv. 21, 2709–2718. https://doi.org/10.1007/s10531-012-0326-y.
Villalobos, F., Dobrovolski, R., Provete, D.B., Gouveia, S.F., 2013. Is rich and rare the common share? Describing biodiversity patterns to inform conservation practices for South American anurans. PLoS ONE 8, e56073. https://doi.org/10.1371/journal.pone.0056073.
Vrcibradic, D., Ariani, C.V., Van Sluys, M., Rocha, C.F.D., 2010. Amphibia, Leptodactylidae, *Paratelmatobius mantiqueira*: distribution extension. Check List 6, 1–2. https://doi.org/10.15560/6.1.001.
Wiens, J.J., Kuczynski, C.A., Smith, S.A., Mulcahy, D.G., Sites Jr., J.W., Townsend, T.M., Reeder, T.W., 2008. Branch lengths, support, and congruence: testing the phylogenomic approach with 20 nuclear loci in snakes. Syst. Biol. 57, 420–431. https://doi.org/10.1080/10635150802166053.
Wollenberg, K.C., Vieites, D.R., Glaw, F., Vences, M., 2011. Speciation in little: the role of range and body size in the diversification of Malagasy mantellid frogs. BMC Evol. Biol. 11, 1–15. https://doi.org/10.1186/1471-2148-11-217.
Zachos, J., Pagani, M., Sloan, L., Thomas, E., Billups, K., 2001. Trends, rhythms, and aberrations in global climate 65 Ma to present. Science 292, 686–693. https://doi.org/10.1126/science.1059412.
Zaher, H., Aguiar, E., Pombal Jr., J.P., 2005. *Paratelmatobius gaigeae* (Cochran, 1938) rediscovered (Amphibia, Anura, Leptodactylidae). Arq. Mus. Nac. 63, 321–328.
Zalán, P.V., Oliveira, J.A.B., 2005. Origem e evolução estrutural do sistema de riftes cenozóicos do Sudeste do Brasil. Bol. Geocienc. Petrobras 13, 269–300.

# SUPPLEMENTARY FILES

Table S1. GenBank accession numbers for sequences of Paratelmatobiinae employed in this study. Sequences generated for this article are in **bold**.

| SPECIES | VOUCHER | FIELD NUMBER | LOCALITY | GMYC LINEAGE | SPECIES TREE LINEAGE | H1 | COI | CYT-B | POMC | RAG-1 | RHOD | TNS3 | TYR |
|---|---|---|---|---|---|---|---|---|---|---|---|---|---|
| *C. bokermanni* | CFBH 44748* | RBF 625 | Penha, Santa Teresa, ES | *C. bokermanni* - Lin A | *C. bokermanni* - Lin 1 | KF534637/KF534647 | KF534656 | KF534665 | – | – | KF534674 | – | – |
| *C. bokermanni* | CFBH 44749* | RBF 648 | Penha, Santa Teresa, ES | *C. bokermanni* - Lin A | *C. bokermanni* - Lin 1 | KF534638/KF534648 | KF534657 | KF534666 | – | – | KF534675 | – | KF534683 |
| *C. bokermanni* | CFBH 44750* | RBF 652 | Penha, Santa Teresa, ES | *C. bokermanni* - Lin A | *C. bokermanni* - Lin 1 | KF534639/KF534649 | KF534658 | KF534667 | – | – | KF534676 | – | KF534684 |
| *C. bokermanni* | CFBH 44751* | RBF 653 | Penha, Santa Teresa, ES | *C. bokermanni* - Lin A | *C. bokermanni* - Lin 1 | KF534640/KF534650 | KF534659 | KF534668 | – | – | KF534677 | – | KF534685 |
| *C. bokermanni* | UFMG 14188 | MTTS 216 | Penha, Santa Teresa, ES | *C. bokermanni* - Lin A | *C. bokermanni* - Lin 1 | MN610833 | MN610691 | MN610723 | MN610760 | MN609872 | **MN933063** | **MN933192** | MN610797 |
| *C. bokermanni* | *UFMG 14189 | MTTS 217 | Penha, Santa Teresa, ES | *C. bokermanni* - Lin A | *C. bokermanni* - Lin 1 | MN610834 | MN610692 | MN610724 | MN610761 | MN609873 | **MN933064** | **MN933193** | MN610798 |
| *C. bokermanni* | UFMG 14190 | MTTS 218 | Penha, Santa Teresa, ES | *C. bokermanni* - Lin A | *C. bokermanni* - Lin 1 | MN610835 | MN610693 | MN610725 | MN610762 | MN609874 | **MN933065** | – | MN610799 |
| *C. bokermanni* | *CFBH 30709 | CHCpo 206 | Reserva Biológica Augusto Ruschi, Santa Teresa, ES | *C. bokermanni* - Lin A | *C. bokermanni* - Lin 1 | **MN917465** | **MN932373** | **MN932544** | **MN932714** | **MN932884** | – | – | **MN933267** |
| *C. bokermanni* | MNRJ 34933* | – | Estação Biológica de Santa Lúcia, Santa Teresa, ES | *C. bokermanni* - Lin B | *C. bokermanni* - Lin 1 | KC593358 | – | – | – | – | – | – | – |
| *C. bokermanni* | *MNRJ 38412 | – | Estação Biológica de Santa Lúcia, Santa Teresa, ES | *C. bokermanni* - Lin B | *C. bokermanni* - Lin 1 | KC593359 | MN610690 | MN610722 | MN610759 | MN609871 | **MN933066** | **MN933194** | MN610796 |
| *C. bokermanni* | UFMG 13767 | MTTS 169 | Parque Estadual do Forno Grande, Castelo, ES | *C. bokermanni* - Lin C | *C. bokermanni* - Lin 2 | MN610836 | MN610694 | MN610726 | MN610763 | MN609875 | **MN933067** | **MN933195** | MN610800 |
| *C. bokermanni* | UFMG 13770 | MTTS 173 | Parque Estadual do Forno Grande, Castelo, ES | *C. bokermanni* - Lin C | *C. bokermanni* - Lin 2 | MN610837 | MN610695 | MN610727 | MN610764 | MN609876 | – | **MN933196** | MN610801 |
| *C. bokermanni* | UFMG 13774 | MTTS 177 | Parque Estadual do Forno Grande, Castelo, ES | *C. bokermanni* - Lin C | *C. bokermanni* - Lin 2 | MN610838 | MN610696 | MN610728 | MN610765 | MN609877 | – | – | MN610802 |
| *C. bokermanni* | UFMG 14198 | MTTS 226 | Parque Estadual do Forno Grande, Castelo, ES | *C. bokermanni* - Lin C | *C. bokermanni* - Lin 2 | MN610839 | MN610697 | MN610729 | MN610766 | - | **MN933068** | – | MN610803 |
| *C. bokermanni* | *UFMG 14199 | MTTS 227 | Parque Estadual do Forno Grande, Castelo, ES | *C. bokermanni* - Lin C | *C. bokermanni* - Lin 2 | MN610840 | MN610698 | MN610730 | MN610767 | MN609878 | **MN933069** | – | MN610804 |
| *C. bokermanni* | UFMG-G 1496-1 | MTTS-G 04 | Parque Estadual do Forno Grande, Castelo, ES | *C. bokermanni* - Lin C | *C. bokermanni* - Lin 2 | MN610841 | MN610699 | MN610731 | MN610768 | MN609879 | – | – | MN610805 |
| *C. bokermanni* | UFMG-G 1496-2 | MTTS-G 04 | Parque Estadual do Forno Grande, Castelo, ES | *C. bokermanni* - Lin C | *C. bokermanni* - Lin 2 | MN610842 | MN610700 | MN610732 | MN610769 | MN609880 | – | – | MN610806 |
| *C. itambe* | *UFMG 13377 | MTTS 131 | Parque Estadual do Pico do Itambé, Santo Antônio do Itambé, MG | *C. itambe* | *C. itambe* | MN610846 | KY362549 | MN610735 | MN610772 | MN609883 | – | – | MN610809 |
| *C. itambe* | UFMG 13376 | MTTS 130 | Parque Estadual do Pico do Itambé, Santo Antônio do Itambé, MG | *C. itambe* | *C. itambe* | MN610845 | KY362548 | MN610734 | MN610771 | MN609882 | **MN933070** | **MN933197** | MN610808 |
| *C. itambe* | UFMG 13379 | MTTS 133 | Parque Estadual do Pico do Itambé, Santo Antônio do Itambé, MG | *C. itambe* | *C. itambe* | MN610847 | KY362550 | MN610736 | MN610773 | MN609884 | **MN933071** | – | MN610810 |
| *C. itambe* | UFMG 13381 | MTTS 135 | Parque Estadual do Pico do Itambé, Santo Antônio do Itambé, MG | *C. itambe* | *C. itambe* | MN610848 | KY362551 | MN610737 | MN610774 | MN609885 | **MN933072** | **MN933198** | MN610811 |
| *C. itambe* | UFMG-G 1477 | – | Parque Estadual do Pico do Itambé, Santo Antônio do Itambé, MG | *C. itambe* | *C. itambe* | MN610844 | KY362547 | MN610733 | MN610770 | MN609881 | **MN933073** | – | MN610807 |
| *C. izecksohni* | CFBH 44755* | RBF 350 | Alto Santo Antônio, Santa Teresa, ES | *C. izecksohni* - Lin A | *C. izecksohni* | KF534632/KF534641 | KF534651 | KF534660 | – | – | KF534669* | – | KF534678 |

| | | | | | | | | | | | | | |
|---|---|---|---|---|---|---|---|---|---|---|---|---|---|
| *C. izecksohni* | CFBH 44756* | RBF 351 | Alto Santo Antônio, Santa Teresa, ES | *C. izecksohni* - Lin A | *C. izecksohni* | KF534633/KF534642 | KF534652 | KF534661 | – | – | KF534670 | – | KF534679 |
| *C. izecksohni* | RBF 517* | RBF 517 | Alto Santo Antônio, Santa Teresa, ES | *C. izecksohni* - Lin A | *C. izecksohni* | KF534634/KF534644 | KF534653 | KF534662 | – | – | KF534671* | – | KF534680 |
| *C. izecksohni* | UFMG 13747 | MTTS 124 | Alto Santo Antônio, Santa Teresa, ES | *C. izecksohni* - Lin A | *C. izecksohni* | MN610852 | MN610706 | MN610743 | MN610780 | MN609891 | **MN933074** | – | MN610817 |
| *C. izecksohni* | UFMG 14174 | MTTS 202 | Alto Santo Antônio, Santa Teresa, ES | *C. izecksohni* - Lin A | *C. izecksohni* | MN610854 | MN610708 | MN610745 | MN610782 | MN609893 | **MN933075** | – | MN610819 |
| *C. izecksohni* | UFMG 14175 | MTTS 203 | Alto Santo Antônio, Santa Teresa, ES | *C. izecksohni* - Lin A | *C. izecksohni* | MN610855 | MN610709 | MN610746 | MN610783 | MN609894 | – | – | MN610820 |
| *C. izecksohni* | *UFMG 14176 | MTTS 204 | Alto Santo Antônio, Santa Teresa, ES | *C. izecksohni* - Lin A | *C. izecksohni* | MN610856 | MN610710 | MN610747 | MN610784 | MN609895 | – | – | MN610821 |
| *C. izecksohni* | UFMG 14178 | MTTS 206 | Alto Santo Antônio, Santa Teresa, ES | *C. izecksohni* - Lin A | *C. izecksohni* | MN610857 | MN610711 | MN610748 | MN610785 | MN609896 | – | – | MN610822 |
| *C. izecksohni* | UFMG 14180 | MTTS 208 | Alto Santo Antônio, Santa Teresa, ES | *C. izecksohni* - Lin A | *C. izecksohni* | MN610858 | MN610712 | MN610749 | MN610786 | MN609897 | **MN933076** | – | MN610823 |
| *C. izecksohni* | UFMG-G 1495-1 | MTTS-G 01-1 | Alto Santo Antônio, Santa Teresa, ES | *C. izecksohni* - Lin A | *C. izecksohni* | MN610859 | MN610713 | MN610750 | MN610787 | MN609898 | **MN933077** | – | MN610824 |
| *C. izecksohni* | UFMG-G 1495-2 | MTTS-G 01-2 | Alto Santo Antônio, Santa Teresa, ES | *C. izecksohni* - Lin A | *C. izecksohni* | MN610860 | MN610714 | MN610751 | MN610788 | MN609899 | – | – | MN610825 |
| *C. izecksohni* | *UFMG 13748 | MTTS 125 | Hill in front of Escola Superior São Francisco de Assis, Santa Teresa, ES | *C. izecksohni* - Lin A | *C. izecksohni* | MN610853 | MN610707 | MN610744 | MN610781 | MN609892 | **MN933078** | – | MN610818 |
| *C. izecksohni* | *CFBH 44757* | RBF 592 | Penha, Santa Teresa, ES | *C. izecksohni* - Lin A | *C. izecksohni* | KF534635/KF534645 | KF534654 | KF534663 | – | – | KF534672 | – | KF534681 |
| *C. izecksohni* | CFBH 44758* | RBF 598 | Penha, Santa Teresa, ES | *C. izecksohni* - Lin A | *C. izecksohni* | KF534636/KF534646 | KF534655 | KF534664 | – | – | KF534673 | – | KF534682 |
| *C. izecksohni* | UFMG 13757 | MTTS 159 | Estação Biológica de Santa Lúcia, Santa Teresa, ES | *C. izecksohni* - Lin B | *C. izecksohni* | MN610849 | MN610701 | MN610738 | MN610775 | MN609886 | – | – | MN610812 |
| *C. izecksohni* | UFMG 13759 | MTTS 161 | Estação Biológica de Santa Lúcia, Santa Teresa, ES | *C. izecksohni* - Lin B | *C. izecksohni* | MN610850 | MN610702 | MN610739 | MN610776 | MN609887 | – | – | MN610813 |
| *C. izecksohni* | UFMG 13791 | MTTS 196 | Estação Biológica de Santa Lúcia, Santa Teresa, ES | *C. izecksohni* - Lin B | *C. izecksohni* | MN610851 | MN610703 | MN610740 | MN610777 | MN609888 | **MN933079** | – | MN610814 |
| *C. izecksohni* | UFMG 13792 | MTTS 197 | Estação Biológica de Santa Lúcia, Santa Teresa, ES | *C. izecksohni* - Lin B | *C. izecksohni* | **MN917466** | MN610704 | MN610741 | MN610778 | MN609889 | **MN933080** | **MN933199** | MN610815 |
| *C. izecksohni* | *UFMG 13793 | MTTS 198 | Estação Biológica de Santa Lúcia, Santa Teresa, ES | *C. izecksohni* - Lin B | *C. izecksohni* | **MN917467** | MN610705 | MN610742 | MN610779 | MN609890 | **MN933081** | **MN933200** | MN610816 |
| *C. septentrionalis* | MZUESC 14363 | ID 881 | Parque Nacional da Serra das Lontras, Arataca, BA | *C. septentrionalis* | *C. septentrionalis* | **MN917468** | MN610715 | MN610752 | MN610789 | MN609900 | **MN933082** | **MN933201** | MN610826 |
| *C. septentrionalis* | MZUESC 21668 | ID 885 | Parque Nacional da Serra das Lontras, Arataca, BA | *C. septentrionalis* | *C. septentrionalis* | **MN917469** | MN610716 | MN610753 | MN610790 | MN609901 | **MN933083** | – | MN610827 |
| *C. septentrionalis* | *MZUSP 150209 | MTR 16370 | Parque Nacional da Serra das Lontras, Arataca, BA | *C. septentrionalis* | *C. septentrionalis* | **MN917470** | KC603985 | **MN932545** | **MN932715** | **MN932885** | **MN933084** | **MN933202** | **MN933268** |
| *Crossodactylodes* sp. 1 | UFMG 13768 | MTTS 170 | Parque Estadual do Forno Grande, Castelo, ES | *Crossodactylodes* sp. 1 | *Crossodactylodes* sp. 1 | **MN917471** | **MN932374** | **MN932546** | **MN932716** | **MN932886** | – | – | **MN933269** |
| *Crossodactylodes* sp. 1 | UFMG 13771 | MTTS 174 | Parque Estadual do Forno Grande, Castelo, ES | *Crossodactylodes* sp. 1 | *Crossodactylodes* sp. 1 | **MN917472** | **MN932375** | **MN932547** | **MN932717** | **MN932887** | **MN933085** | – | **MN933270** |
| *Crossodactylodes* sp. 1 | UFMG 13772 | MTTS 175 | Parque Estadual do Forno Grande, Castelo, ES | *Crossodactylodes* sp. 1 | *Crossodactylodes* sp. 1 | **MN917473** | **MN932376** | **MN932548** | **MN932718** | **MN932888** | **MN933086** | **MN933203** | **MN933271** |
| *Crossodactylodes* sp. 1 | UFMG 13775 | MTTS 178 | Parque Estadual do Forno Grande, Castelo, ES | *Crossodactylodes* sp. 1 | *Crossodactylodes* sp. 1 | **MN917474** | **MN932377** | **MN932549** | **MN932719** | **MN932889** | – | **MN933204** | **MN933272** |
| *Crossodactylodes* sp. 1 | *UFMG 14201 | MTTS 229 | Parque Estadual do Forno Grande, Castelo, ES | *Crossodactylodes* sp. 1 | *Crossodactylodes* sp. 1 | **MN917475** | **MN932378** | **MN932550** | **MN932720** | **MN932890** | **MN933087** | – | **MN933273** |
| *Crossodactylodes* sp. 1 | UFMG 14202 | MTTS 230 | Parque Estadual do Forno Grande, Castelo, ES | *Crossodactylodes* sp. 1 | *Crossodactylodes* sp. 1 | **MN917476** | **MN932379** | **MN932551** | **MN932721** | **MN932891** | – | – | **MN933274** |
| *Crossodactylodes* sp. 1 | UFMG-G 1497 | MTTS-G 07 | Parque Estadual do Forno Grande, Castelo, ES | *Crossodactylodes* sp. 1 | *Crossodactylodes* sp. 1 | **MN917477** | **MN932380** | **MN932552** | **MN932722** | **MN932892** | **MN933088** | – | **MN933275** |
| *Crossodactylodes* sp. 2 | CFBH-T 22741 | RBF 1544 | Pedra do Garrafão, Santa Maria de Jetibá, ES | *Crossodactylodes* sp. 2 | *Crossodactylodes* sp. 2 | **MN917478** | **MN932381** | **MN932553** | **MN932723** | **MN932893** | **MN933089** | – | **MN933276** |

| | | | | | | | | | | | | | |
|---|---|---|---|---|---|---|---|---|---|---|---|---|---|
| *Crossodactylodes* sp. 2 | *CFBH-T 22742 | RBF 1545 | Pedra do Garrafão, Santa Maria de Jetibá, ES | *Crossodactylodes* sp. 2 | *Crossodactylodes* sp. 2 | **MN917479** | **MN932382** | **MN932554** | **MN932724** | **MN932894** | **MN933090** | – | **MN933277** |
| *Crossodactylodes* sp. 3 | CFBH 44887 | MTTS 480 | Parque Estadual da Serra Negra, Itamarandiba, MG | *Crossodactylodes* sp. 3 | *Crossodactylodes* sp. 3 | **MN917480** | **MN932383** | **MN932555** | **MN932725** | **MN932895** | **MN933091** | **MN933205** | **MN933278** |
| *Crossodactylodes* sp. 3 | CFBH 44888 | MTTS 485 | Parque Estadual da Serra Negra, Itamarandiba, MG | *Crossodactylodes* sp. 3 | *Crossodactylodes* sp. 3 | **MN917481** | **MN932384** | **MN932556** | **MN932726** | **MN932896** | **MN933092** | **MN933206** | **MN933279** |
| *Crossodactylodes* sp. 3 | CFBH 44889 | MTTS 501 | Parque Estadual da Serra Negra, Itamarandiba, MG | *Crossodactylodes* sp. 3 | *Crossodactylodes* sp. 3 | **MN917482** | **MN932385** | **MN932557** | **MN932727** | **MN932897** | – | **MN933207** | **MN933280** |
| *Crossodactylodes* sp. 3 | CFBH 44890 | MTTS 538 | Parque Estadual da Serra Negra, Itamarandiba, MG | *Crossodactylodes* sp. 3 | *Crossodactylodes* sp. 3 | **MN917483** | **MN932386** | **MN932558** | – | **MN932898** | **MN933093** | – | **MN933281** |
| *Crossodactylodes* sp. 3 | *CFBH-T 22743 | MTTS-G 88 | Parque Estadual da Serra Negra, Itamarandiba, MG | *Crossodactylodes* sp. 3 | *Crossodactylodes* sp. 3 | **MN917484** | **MN932387** | **MN932559** | **MN932728** | **MN932899** | – | – | **MN933282** |
| *Crossodactylodes* sp. 3 | UFMG 19824 | – | Parque Estadual da Serra Negra, Itamarandiba, MG | *Crossodactylodes* sp. 3 | *Crossodactylodes* sp. 3 | **MN917485** | **MN932388** | **MN932560** | **MN932729** | **MN932900** | – | **MN933208** | **MN933283** |
| *P. cardosoi* | CFBH 16774 | LRM 464 | Parque Estadual da Serra do Mar (Núcleo Curucutu), Itanhaém, SP | *P. cardosoi* - Lin A | *P. cardosoi* - Lin 1 | **MN917486** | **MN932389** | **MN932561** | **MN932730** | **MN932901** | **MN933094** | **MN933209** | – |
| *P. cardosoi* | CFBH 16775 | LRM 465 | Parque Estadual da Serra do Mar (Núcleo Curucutu), Itanhaém, SP | *P. cardosoi* - Lin A | *P. cardosoi* - Lin 1 | **MN917487** | **MN932390** | **MN932562** | **MN932731** | **MN932902** | – | **MN933210** | – |
| *P. cardosoi* | CFBH 16778 | LRM 468 | Parque Estadual da Serra do Mar (Núcleo Curucutu), São Paulo, SP | *P. cardosoi* - Lin A | *P. cardosoi* - Lin 1 | **MN917488** | **MN932391** | **MN932563** | **MN932732** | **MN932903** | – | **MN933211** | – |
| *P. cardosoi* | *CFBH 16779 | LRM 469 | Parque Estadual da Serra do Mar (Núcleo Curucutu), São Paulo, SP | *P. cardosoi* - Lin A | *P. cardosoi* - Lin 1 | **MN917489** | **MN932392** | **MN932564** | **MN932733** | **MN932904** | **MN933095** | **MN933212** | **MN933284** |
| *P. cardosoi* | CFBH 17679 | LRM 527 | Parque Estadual da Serra do Mar (Núcleo Curucutu), São Paulo, SP | *P. cardosoi* - Lin A | *P. cardosoi* - Lin 1 | **MN917490** | **MN932393** | **MN932565** | **MN932734** | **MN932905** | – | **MN933213** | – |
| *P. cardosoi* | CFBH 44648 | JPCM 420 | Parque Estadual da Serra do Mar (Núcleo Curucutu), São Paulo, SP | *P. cardosoi* - Lin A | *P. cardosoi* - Lin 1 | **MN917491** | **MN932394** | **MN932566** | **MN932735** | **MN932906** | **MN933096** | **MN933214** | **MN933285** |
| *P. cardosoi* | CFBH 28957* | – | Paranapiacaba, Santo André, SP | *P. cardosoi* - Lin B | *P. cardosoi* - Lin 1 | **MN917492** | **MN932395** | – | **MN932736** | **MN932907** | – | – | **MN933286** |
| *P. cardosoi* | CFBH 29004* | – | Paranapiacaba, Santo André, SP | *P. cardosoi* - Lin B | *P. cardosoi* - Lin 1 | **MN917493** | **MN932396** | – | **MN932737** | **MN932908** | – | – | – |
| *P. cardosoi* | CTMZ 7118 | VT 685 | Paranapiacaba, Santo André, SP | *P. cardosoi* - Lin B | *P. cardosoi* - Lin 1 | **MN917494** | **MN932397** | **MN932567** | **MN932738** | **MN932909** | – | **MN933215** | – |
| *P. cardosoi* | CTMZ 7163 | VT 735 | Paranapiacaba, Santo André, SP | *P. cardosoi* - Lin B | *P. cardosoi* - Lin 1 | **MN917495** | **MN932398** | **MN932568** | **MN932739** | **MN932910** | – | – | **MN933287** |
| *P. cardosoi* | CTMZ 7213* | VT 796 | Paranapiacaba, Santo André, SP | *P. cardosoi* - Lin B | *P. cardosoi* - Lin 1 | **MN917496** | – | – | **MN932740** | **MN932911** | – | – | – |
| *P. cardosoi* | CTMZ 7239* | VT 829 | Paranapiacaba, Santo André, SP | *P. cardosoi* - Lin B | *P. cardosoi* - Lin 1 | **MN917497** | **MN932399** | – | **MN932741** | **MN932912** | – | – | **MN933288** |
| *P. cardosoi* | MTR 9850 | MTR 9850 | Paranapiacaba, Santo André, SP | *P. cardosoi* - Lin B | *P. cardosoi* - Lin 1 | **MN917498** | **MN932400** | – | **MN932742** | **MN932913** | **MN933097** | – | **MN933289** |
| *P. cardosoi* | *MTR 10424* | MTR 10424 | Paranapiacaba, Santo André, SP | *P. cardosoi* - Lin B | *P. cardosoi* - Lin 1 | **MN917499** | **MN932401** | **MN932569** | **MN932743** | **MN932914** | – | – | – |
| *P. cardosoi* | MTR 10436 | MTR 10436 | Paranapiacaba, Santo André, SP | *P. cardosoi* - Lin B | *P. cardosoi* - Lin 1 | **MN917500** | **MN932402** | **MN932570** | **MN932744** | **MN932915** | – | – | **MN933290** |
| *P. cardosoi* | MZUSP 145372* | VT 1415 | Paranapiacaba, Santo André, SP | *P. cardosoi* - Lin B | *P. cardosoi* - Lin 1 | **MN917501** | **MN932403** | – | **MN932745** | **MN932916** | – | – | – |
| *P. cardosoi* | MZUSP 145373 | VT 1418 | Paranapiacaba, Santo André, SP | *P. cardosoi* - Lin B | *P. cardosoi* - Lin 1 | **MN917502** | **MN932404** | **MN932571** | **MN932746** | **MN932917** | – | **MN933216** | – |
| *P. cardosoi* | MZUSP 145374* | VT 1435 | Paranapiacaba, Santo André, SP | *P. cardosoi* - Lin B | *P. cardosoi* - Lin 1 | **MN917503** | – | – | **MN932747** | **MN932918** | **MN933098** | – | – |
| *P. cardosoi* | *MZUSP 145375 | VT 1439 | Paranapiacaba, Santo André, SP | *P. cardosoi* - Lin B | *P. cardosoi* - Lin 1 | **MN917504** | **MN932405** | **MN932572** | **MN932748** | **MN932919** | – | **MN933217** | **MN933291** |
| *P. cardosoi* | CFBH 38989 | JG 28 | Parque das Neblinas, Bertioga, SP | *P. cardosoi* - Lin B | *P. cardosoi* - Lin 1 | **MN917505** | **MN932406** | **MN932573** | **MN932749** | **MN932920** | **MN933099** | – | – |

| | | | | | | | | | | | | | | |
|---|---|---|---|---|---|---|---|---|---|---|---|---|---|---|
| *P. cardosoi* | CFBH 38990 | JG 29 | Parque das Neblinas, Bertioga, SP | *P. cardosoi* - Lin B | *P. cardosoi* - Lin 1 | **MN917506** | **MN932407** | **MN932574** | **MN932750** | **MN932921** | – | **MN933218** | – |
| *P. cardosoi* | CFBH 41879 | BB 550 | Parque das Neblinas, Mogi das Cruzes, SP | *P. cardosoi* - Lin B | *P. cardosoi* - Lin 1 | **MN917507** | **MN932408** | **MN932575** | **MN932751** | **MN932922** | **MN933100** | – | – |
| *P. cardosoi* | CFBH 41880 | BB 551 | Parque das Neblinas, Mogi das Cruzes, SP | *P. cardosoi* - Lin B | *P. cardosoi* - Lin 1 | **MN917508** | **MN932409** | **MN932576** | **MN932752** | **MN932923** | **MN933101** | – | **MN933292** |
| *P. cardosoi* | UFMG 3237 | – | Parque das Neblinas, Mogi das Cruzes, SP | *P. cardosoi* - Lin B | *P. cardosoi* - Lin 1 | **MN917509** | MN610717 | MN610754 | MN610791 | MN609902 | – | – | MN610828 |
| *P. cardosoi* | UFMG 20709 | MTTS 406 | Parque das Neblinas, Mogi das Cruzes, SP | *P. cardosoi* - Lin B | *P. cardosoi* - Lin 1 | **MN917510** | **MN932410** | **MN932577** | **MN932753** | **MN932924** | **MN933102** | – | – |
| *P. cardosoi* | *UFMG 21326* | MTTS 411 | Parque das Neblinas, Mogi das Cruzes, SP | *P. cardosoi* - Lin B | *P. cardosoi* - Lin 1 | **MN917511** | **MN932411** | **MN932578** | **MN932754** | **MN932925** | – | – | – |
| *P. cardosoi* | *CFBH 31094* | H 77 | Fazenda Capivari, São Paulo, SP | *P. cardosoi* - Lin C | *P. cardosoi* - Lin 1 | **MN917512** | **MN932412** | **MN932579** | **MN932755** | – | – | – | – |
| *P. cardosoi* | CFBH 40512 | PSS 34 | Parque Natural Municipal Fazenda do Carmo, São Paulo, SP | *P. cardosoi* - Lin C | *P. cardosoi* - Lin 1 | **MN917513** | **MN932413** | **MN932580** | **MN932756** | **MN932926** | – | **MN933219** | – |
| *P. cardosoi* | *CFBH 40513 | PSS 35 | Parque Natural Municipal Fazenda do Carmo, São Paulo, SP | *P. cardosoi* - Lin C | *P. cardosoi* - Lin 1 | **MN917514** | **MN932414** | **MN932581** | **MN932757** | **MN932927** | **MN933103** | – | **MN933293** |
| *P. cardosoi* | *CFBH 11622 | LRM 260 | Parque Natural Municipal Varginha, São Paulo, SP | *P. cardosoi* - Lin C | *P. cardosoi* - Lin 1 | **MN917515** | **MN932415** | **MN932582** | **MN932758** | **MN932928** | **MN933104** | **MN933220** | – |
| *P. cardosoi* | *CFBH 43043 | TC 471 | São Bernardo do Campo, SP | *P. cardosoi* - Lin C | *P. cardosoi* - Lin 1 | **MN917516** | **MN932416** | **MN932583** | **MN932759** | **MN932929** | – | – | **MN933294** |
| *P. cardosoi* | ITH 0938* | ITH 0938 | São Bernardo do Campo, SP | *P. cardosoi* - Lin C | *P. cardosoi* - Lin 1 | – | JX298372 | JX298413 | JX298143 | JX298195 | – | – | JX298242 |
| *P. cardosoi* | *MZUSP 125001 | ITH 32 | São Bernardo do Campo, SP | *P. cardosoi* - Lin C | *P. cardosoi* - Lin 1 | **MN917517** | **MN932417** | **MN932584** | **MN932760** | **MN932930** | **MN933105** | – | – |
| *P. cardosoi* | MZUSP 125002 | ITH 39 | São Bernardo do Campo, SP | *P. cardosoi* - Lin C | *P. cardosoi* - Lin 1 | **MN917518** | KU494619 | **MN932585** | **MN932761** | **MN932931** | – | **MN933221** | – |
| *P. cardosoi* | MZUSP 125003 | ITH 49 | São Bernardo do Campo, SP | *P. cardosoi* - Lin C | *P. cardosoi* - Lin 1 | **MN917519** | **MN932418** | **MN932586** | **MN932762** | **MN932932** | **MN933106** | – | – |
| *P. cardosoi* | MZUSP 125004* | ITH 50 | São Bernardo do Campo, SP | *P. cardosoi* - Lin C | *P. cardosoi* - Lin 1 | **MN917520** | **MN932419** | **MN932587** | **MN932763** | **MN932933** | – | – | – |
| *P. cardosoi* | MZUSP 125005 | ITH 51 | São Bernardo do Campo, SP | *P. cardosoi* - Lin C | *P. cardosoi* - Lin 1 | **MN917521** | **MN932420** | **MN932588** | **MN932764** | **MN932934** | – | – | **MN933295** |
| *P.* cf. *cardosoi* | *CFBH-T 5854 | CAB 1833 | Biritiba Mirim, SP | *P.* cf. *cardosoi* - Lin D | *P.* cf. *cardosoi* - Lin 2 | **MN917522** | **MN932421** | **MN932589** | **MN932765** | **MN932935** | **MN933107** | **MN933222** | **MN933296** |
| *P.* cf. *cardosoi* | *CFBH 6469 | – | Biritiba Ussu, Mogi das Cruzes, SP | *P.* cf. *cardosoi* - Lin D | *P.* cf. *cardosoi* - Lin 2 | **MN917523** | **MN932422** | **MN932590** | **MN932766** | **MN932936** | **MN933108** | – | – |
| *P.* cf. *cardosoi* | CFBH 6470* | – | Biritiba Ussu, Mogi das Cruzes, SP | *P.* cf. *cardosoi* - Lin D | *P.* cf. *cardosoi* - Lin 2 | **MN917524** | **MN932423** | **MN932591** | **MN932767** | **MN932937** | – | – | – |
| *P.* cf. *cardosoi* | CFBH-T 22744 | MCL 172 | Estação Biológica de Boracéia, Salesópolis, SP | *P.* cf. *cardosoi* - Lin D | *P.* cf. *cardosoi* - Lin 2 | **MN917525** | **MN932424** | **MN932592** | **MN932768** | **MN932938** | – | – | **MN933297** |
| *P.* cf. *cardosoi* | CFBH-T 22745 | MCL 173 | Estação Biológica de Boracéia, Salesópolis, SP | *P.* cf. *cardosoi* - Lin D | *P.* cf. *cardosoi* - Lin 2 | **MN917526** | **MN932425** | **MN932593** | **MN932769** | **MN932939** | **MN933109** | – | – |
| *P.* cf. *cardosoi* | CFBH-T 22746 | MCL 174 | Estação Biológica de Boracéia, Salesópolis, SP | *P.* cf. *cardosoi* - Lin D | *P.* cf. *cardosoi* - Lin 2 | **MN917527** | **MN932426** | **MN932594** | **MN932770** | **MN932940** | – | – | **MN933298** |
| *P.* cf. *cardosoi* | MTR 11712* | MTR 11712 | Estação Biológica de Boracéia, Salesópolis, SP | *P.* cf. *cardosoi* - Lin D | *P.* cf. *cardosoi* - Lin 2 | **MN917528** | – | – | **MN932771** | **MN932941** | – | – | – |
| *P.* cf. *cardosoi* | MTR 11713 | MTR 11713 | Estação Biológica de Boracéia, Salesópolis, SP | *P.* cf. *cardosoi* - Lin D | *P.* cf. *cardosoi* - Lin 2 | **MN917529** | **MN932427** | **MN932595** | **MN932772** | **MN932942** | **MN933110** | – | – |
| *P.* cf. *cardosoi* | MTR 16666* | MTR 16666 | Estação Biológica de Boracéia, Salesópolis, SP | *P.* cf. *cardosoi* - Lin D | *P.* cf. *cardosoi* - Lin 2 | **MN917530** | – | – | **MN932773** | **MN932943** | – | **MN933223** | – |
| *P.* cf. *cardosoi* | *MTR 16672* | MTR 16672 | Estação Biológica de Boracéia, Salesópolis, SP | *P.* cf. *cardosoi* - Lin D | *P.* cf. *cardosoi* - Lin 2 | **MN917531** | **MN932428** | **MN932596** | **MN932774** | **MN932944** | – | – | – |
| *P.* cf. *cardosoi* | MTR 21343 | MTR 21343 | Estação Biológica de Boracéia, Salesópolis, SP | *P.* cf. *cardosoi* - Lin D | *P.* cf. *cardosoi* - Lin 2 | **MN917532** | **MN932429** | **MN932597** | **MN932775** | **MN932945** | **MN933111** | – | **MN933299** |
| *P.* cf. *cardosoi* | MTR 26414* | MTR 26414 | Estação Biológica de Boracéia, Salesópolis, SP | *P.* cf. *cardosoi* - Lin D | *P.* cf. *cardosoi* - Lin 2 | **MN917533** | – | – | **MN932776** | **MN932946** | – | – | **MN933300** |

| | | | | | | | | | | | | | |
|---|---|---|---|---|---|---|---|---|---|---|---|---|---|
| *P. gaigeae* | *MZUSP 132604 | EEB 448 | Estação Ecológica do Bananal, Bananal, SP | *P. gaigeae* | *P. gaigeae* | **MN917534** | **MN932430** | **MN932598** | **MN932777** | **MN932947** | **MN933112** | – | **MN933301** |
| *P. gaigeae* | MZUSP 138657 | – | Estação Ecológica do Bananal, Bananal, SP | *P. gaigeae* | *P. gaigeae* | **MN917535** | **MN932431** | **MN932599** | **MN932778** | **MN932948** | **MN933113** | – | **MN933302** |
| *P. gaigeae* | MZUSP 138658 | – | Estação Ecológica do Bananal, Bananal, SP | *P. gaigeae* | *P. gaigeae* | **MN917536** | **MN932432** | **MN932600** | **MN932779** | **MN932949** | **MN933114** | – | **MN933303** |
| *P. gaigeae* | MZUSP 153317 | RS 1086 | Estação Ecológica do Bananal, Bananal, SP | *P. gaigeae* | *P. gaigeae* | **MN917537** | **MN932433** | **MN932601** | **MN932780** | **MN932950** | **MN933115** | **MN933224** | **MN933304** |
| *P. gaigeae* | MZUSP 153326 | EA 423 | Estação Ecológica do Bananal, Bananal, SP | *P. gaigeae* | *P. gaigeae* | **MN917538** | **MN932434** | **MN932602** | **MN932781** | **MN932951** | **MN933116** | **MN933225** | – |
| *P. gaigeae* | *CFBH 36079 | PCAG 1948 | Parque Nacional da Serra da Bocaina, São José do Barreiro, SP | *P. gaigeae* | *P. gaigeae* | **MN917539** | **MN932435** | **MN932603** | **MN932782** | **MN932952** | **MN933117** | **MN933226** | – |
| *P. gaigeae* | CFBH-T 20053 | – | Parque Nacional da Serra da Bocaina, São José do Barreiro, SP | *P. gaigeae* | *P. gaigeae* | **MN917540** | **MN932436** | **MN932604** | **MN932783** | **MN932953** | – | **MN933227** | **MN933305** |
| *P. gaigeae* | CFBH-T 20054 | – | Parque Nacional da Serra da Bocaina, São José do Barreiro, SP | *P. gaigeae* | *P. gaigeae* | **MN917541** | **MN932437** | **MN932605** | **MN932784** | **MN932954** | **MN933118** | – | **MN933306** |
| *P. gaigeae* | MNRJ 90730 | – | Parque Nacional da Serra da Bocaina, São José do Barreiro, SP | *P. gaigeae* | *P. gaigeae* | **MN917542** | **MN932438** | **MN932606** | **MN932785** | **MN932955** | **MN933119** | – | **MN933307** |
| *P. gaigeae* | UFMG 15006 | PCAG 1925 | Parque Nacional da Serra da Bocaina, São José do Barreiro, SP | *P. gaigeae* | *P. gaigeae* | **MN917543** | MN610718 | MN610755 | MN610792 | MN609903 | – | – | MN610829 |
| *P. poecilogaster* | CFBH 28959 | – | Paranapiacaba, Santo André, SP | *P. poecilogaster* - Lin A | *P. poecilogaster* - Lin 1 | **MN917544** | **MN932439** | **MN932607** | **MN932786** | **MN932956** | **MN933120** | – | **MN933308** |
| *P. poecilogaster* | CFBH 28960 | – | Paranapiacaba, Santo André, SP | *P. poecilogaster* - Lin A | *P. poecilogaster* - Lin 1 | **MN917545** | **MN932440** | **MN932608** | **MN932787** | **MN932957** | **MN933121** | **MN933228** | **MN933309** |
| *P. poecilogaster* | *CFBH-T 2434 | – | Paranapiacaba, Santo André, SP | *P. poecilogaster* - Lin A | *P. poecilogaster* - Lin 1 | **MN917547** | **MN932441** | **MN932610** | **MN932789** | **MN932959** | **MN933122** | **MN933229** | **MN933311** |
| *P. poecilogaster* | CFBH 28983* | – | Paranapiacaba, Santo André, SP | *P. poecilogaster* - Lin B | *P. poecilogaster* - Lin 1 | **MN917546** | – | **MN932609** | **MN932788** | **MN932958** | – | – | **MN933310** |
| *P. poecilogaster* | *MZUSP 145312 | VT 1319 | Paranapiacaba, Santo André, SP | *P. poecilogaster* - Lin B | *P. poecilogaster* - Lin 1 | **MN917548** | **MN932442** | **MN932611** | **MN932790** | **MN932960** | **MN933123** | **MN933230** | **MN933312** |
| *P. poecilogaster* | MZUSP 145315* | VT 1322 | Paranapiacaba, Santo André, SP | *P. poecilogaster* - Lin B | *P. poecilogaster* - Lin 1 | **MN917549** | – | – | – | **MN932961** | **MN933124** | – | – |
| *P. poecilogaster* | CFBH 41817 | BB 414 | Parque das Neblinas, Bertioga, SP | *P. poecilogaster* - Lin B | *P. poecilogaster* - Lin 1 | **MN917550** | **MN932443** | **MN932612** | **MN932791** | **MN932962** | – | – | **MN933313** |
| *P. poecilogaster* | CFBH 41818 | BB 416 | Parque das Neblinas, Bertioga, SP | *P. poecilogaster* - Lin B | *P. poecilogaster* - Lin 1 | **MN917551** | **MN932444** | **MN932613** | **MN932792** | **MN932963** | – | – | **MN933314** |
| *P. poecilogaster* | CFBH 41819 | BB 417 | Parque das Neblinas, Bertioga, SP | *P. poecilogaster* - Lin B | *P. poecilogaster* - Lin 1 | **MN917552** | **MN932445** | **MN932614** | **MN932793** | **MN932964** | – | – | **MN933315** |
| *P. poecilogaster* | *MZUSP 136756 | AUMC 376 | Parque das Neblinas, Bertioga, SP | *P. poecilogaster* - Lin B | *P. poecilogaster* - Lin 1 | **MN917553** | **MN932446** | **MN932615** | – | **MN932965** | **MN933125** | **MN933231** | **MN933316** |
| *P. poecilogaster* | UFMG 3240 | – | Parque das Neblinas, Bertioga, SP | *P. poecilogaster* - Lin B | *P. poecilogaster* - Lin 1 | **MN917554** | MN610719 | MN610756 | MN610793 | MN609904 | – | – | MN610830 |
| *P. poecilogaster* | UFMG 21317* | MTTS 403 | Parque das Neblinas, Bertioga, SP | *P. poecilogaster* - Lin B | *P. poecilogaster* - Lin 1 | **MN917555** | **MN932447** | **MN932616** | – | **MN932966** | – | – | **MN933317** |
| *P. poecilogaster* | UFMG 21320 | MTTS 405 | Parque das Neblinas, Bertioga, SP | *P. poecilogaster* - Lin B | *P. poecilogaster* - Lin 1 | **MN917556** | **MN932448** | **MN932617** | **MN932794** | **MN932967** | **MN933126** | – | **MN933318** |
| *P. poecilogaster* | *CFBH 35955 | – | Estrada Paraty-Cunha, Paraty, RJ | *P. poecilogaster* - Lin C | *P. poecilogaster* - Lin 2 | **MN917557** | **MN932449** | **MN932618** | **MN932795** | **MN932968** | **MN933127** | – | **MN933319** |
| *P. poecilogaster* | *MNRJ 65044 | – | Estrada Paraty-Cunha, Paraty, RJ | *P. poecilogaster* - Lin C | *P. poecilogaster* - Lin 2 | **MN917558** | **MN932450** | **MN932619** | **MN932796** | **MN932969** | **MN933128** | **MN933232** | **MN933320** |
| *P. poecilogaster* | *MNRJ 75864 | – | Estrada Paraty-Cunha, Paraty, RJ | *P. poecilogaster* - Lin C | *P. poecilogaster* - Lin 2 | **MN917559** | **MN932451** | **MN932620** | **MN932797** | **MN932970** | **MN933129** | – | **MN933321** |
| *P. poecilogaster* | CFBH 27851 | – | Parque Estadual da Serra do Mar (Núcleo Cunha), Cunha, SP | *P. poecilogaster* - Lin C | *P. poecilogaster* - Lin 2 | **MN917560** | **MN932452** | **MN932621** | **MN932798** | **MN932971** | **MN933130** | – | **MN933322** |

| | | | | | | | | | | | | | |
|---|---|---|---|---|---|---|---|---|---|---|---|---|---|
| *P. poecilogaster* | *CFBH 44688 | TC 291 | Parque Estadual da Serra do Mar (Núcleo Cunha), Cunha, SP | *P. poecilogaster* - Lin C | *P. poecilogaster* - Lin 2 | **MN917561** | **MN932453** | **MN932622** | **MN932799** | **MN932972** | **MN933131** | **MN933233** | **MN933323** |
| *P. poecilogaster* | CFBH 7730 | – | Parque Estadual da Serra do Mar (Núcleo Santa Virgínia), São Luiz do Paraitinga, SP | *P. poecilogaster* - Lin D | *P. poecilogaster* - Lin 2 | **MN917562** | **MN932454** | **MN932623** | **MN932800** | **MN932973** | **MN933132** | **MN933234** | **MN933324** |
| *P. poecilogaster* | *CFBH 7731 | – | Parque Estadual da Serra do Mar (Núcleo Santa Virgínia), São Luiz do Paraitinga, SP | *P. poecilogaster* - Lin D | *P. poecilogaster* - Lin 2 | **MN917563** | KU494620 | **MN932624** | **MN932801** | **MN932974** | – | **MN933235** | **MN933325** |
| *P. poecilogaster* | CFBH-T 1423 | – | Parque Estadual da Serra do Mar (Núcleo Santa Virgínia), São Luiz do Paraitinga, SP | *P. poecilogaster* - Lin D | *P. poecilogaster* - Lin 2 | **MN917564** | KU494621 | **MN932625** | **MN932802** | **MN932975** | **MN933133** | – | **MN933326** |
| *P. segallai* | *CFBH 35790 | – | Parque Estadual Pico do Marumbi, Piraquara, PR | *P. segallai* - Lin A | *P. segallai* - Lin 1 | DQ283098 | **MN932455** | **MN932626** | **MN932803** | **MN932976** | **MN933134** | – | **MN933327** |
| *P. segallai* | CFBH 43545 | MTTS 430 | Parque Estadual Pico do Marumbi, Piraquara, PR | *P. segallai* - Lin A | *P. segallai* - Lin 1 | MK791309 | **MN932456** | **MN932627** | **MN932804** | **MN932977** | – | – | **MN933328** |
| *P. segallai* | CFBH 43549 | MTTS 450 | Parque Estadual Pico do Marumbi, Piraquara, PR | *P. segallai* - Lin A | *P. segallai* - Lin 1 | MK791310 | **MN932457** | **MN932628** | **MN932805** | **MN932978** | – | – | **MN933329** |
| *P. segallai* | CFBH 43552 | MTTS 451 | Parque Estadual Pico do Marumbi, Piraquara, PR | *P. segallai* - Lin A | *P. segallai* - Lin 1 | MK791311 | **MN932458** | **MN932629** | **MN932806** | **MN932979** | **MN933135** | – | **MN933330** |
| *P. segallai* | CFBH 43554 | MTTS 453 | Parque Estadual Pico do Marumbi, Piraquara, PR | *P. segallai* - Lin A | *P. segallai* - Lin 1 | MK791312 | **MN932459** | **MN932630** | **MN932807** | **MN932980** | **MN933136** | **MN933236** | – |
| *P. segallai* | CFBH 43555* | MTTS 426 | Parque Estadual Pico do Marumbi, Piraquara, PR | *P. segallai* - Lin A | *P. segallai* - Lin 1 | MK791313 | **MN932460** | **MN932631** | – | **MN932981** | **MN933137** | – | – |
| *P.* cf. *segallai* | CFBH-T 22747 | H 0247 | Juquitiba, SP | *P.* cf. *segallai* - Lin B | *P.* cf. *segallai* - Lin 2 | **MN917565** | **MN932461** | **MN932632** | **MN932808** | **MN932982** | **MN933138** | **MN933237** | **MN933331** |
| *P.* cf. *segallai* | CFBH-T 22748 | H 0248 | Juquitiba, SP | *P.* cf. *segallai* - Lin B | *P.* cf. *segallai* - Lin 2 | **MN917566** | **MN932462** | **MN932633** | **MN932809** | **MN932983** | – | – | **MN933332** |
| *P.* cf. *segallai* | *MTR 10363 | MTR 10363 | Reserva Florestal do Morro Grande, Cotia, SP | *P.* cf. *segallai* - Lin B | *P.* cf. *segallai* - Lin 2 | **MN917567** | **MN932463** | **MN932634** | **MN932810** | **MN932984** | **MN933139** | – | **MN933333** |
| *P.* cf. *segallai* | *CFBH 43420 | MN 07 | Bairro Araçaeiro, Guapiara, SP | *P.* cf. *segallai* - Lin C | *P.* cf. *segallai* - Lin 2 | MK791306 | **MN932464** | **MN932635** | **MN932811** | **MN932985** | **MN933140** | **MN933238** | **MN933334** |
| *P.* cf. *segallai* | *CFBH 8365* | – | Fazenda João XXIII, Pilar do Sul, SP | *P.* cf. *segallai* - Lin C | *P.* cf. *segallai* - Lin 2 | MK791307 | **MN932465** | **MN932636** | **MN932812** | **MN932986** | – | – | – |
| *P.* cf. *segallai* | CFBH-T 397 | – | Fazenda João XXIII, Pilar do Sul, SP | *P.* cf. *segallai* - Lin C | *P.* cf. *segallai* - Lin 2 | MK791308 | **MN932466** | **MN932637** | **MN932813** | **MN932987** | **MN933141** | **MN933239** | **MN933335** |
| *P.* cf. *segallai* | CFBH 40789** | JWRJ 112 | Parque Estadual Carlos Botelho, Capão Bonito, SP | *P.* cf. *segallai* - Lin C | *P.* cf. *segallai* - Lin 2 | **MN917568** | **MN932467** | **MN932638** | **MN932814** | **MN932988** | – | – | – |
| *P.* cf. *segallai* | *CFBH-T 22749 | AF 1626 | Parque Estadual Carlos Botelho, Capão Bonito, SP | *P.* cf. *segallai* - Lin C | *P.* cf. *segallai* - Lin 2 | **MN917569** | **MN932468** | **MN932639** | **MN932815** | **MN932989** | **MN933142** | – | **MN933336** |
| *P.* cf. *segallai* | CFBH 38426** | FRS 660 | Parque Estadual Carlos Botelho, São Miguel Arcanjo, SP | *P.* cf. *segallai* - Lin C | *P.* cf. *segallai* - Lin 2 | **MN917570** | **MN932469** | **MN932640** | **MN932816** | **MN932990** | – | – | – |
| *P.* cf. *segallai* | CFBH 38427 | FRS 661 | Parque Estadual Carlos Botelho, São Miguel Arcanjo, SP | *P.* cf. *segallai* - Lin C | *P.* cf. *segallai* - Lin 2 | **MN917571** | **MN932470** | **MN932641** | **MN932817** | **MN932991** | **MN933143** | – | – |
| *P.* cf. *segallai* | *CFBH 40684* | JWRJ 07 | Parque Estadual Carlos Botelho, São Miguel Arcanjo, SP | *P.* cf. *segallai* - Lin C | *P.* cf. *segallai* - Lin 2 | **MN917572** | **MN932471** | **MN932642** | **MN932818** | **MN932992** | – | – | – |
| *P.* cf. *segallai* | CFBH 40686 | JWRJ 09 | Parque Estadual Carlos Botelho, São Miguel Arcanjo, SP | *P.* cf. *segallai* - Lin C | *P.* cf. *segallai* - Lin 2 | **MN917573** | **MN932472** | **MN932643** | **MN932819** | **MN932993** | **MN933144** | – | **MN933337** |
| *P.* cf. *segallai* | *MZUSP 135989* | HZB 192 | Parque Estadual Carlos Botelho, São Miguel Arcanjo, SP | *P.* cf. *segallai* - Lin C | *P.* cf. *segallai* - Lin 2 | **MN917574** | **MN932473** | **MN932644** | **MN932820** | **MN932994** | – | – | – |
| *P.* cf. *segallai* | MZUSP 135992 | HZB 335 | Parque Estadual Carlos Botelho, São Miguel Arcanjo, SP | *P.* cf. *segallai* - Lin C | *P.* cf. *segallai* - Lin 2 | **MN917575** | **MN932474** | **MN932645** | **MN932821** | **MN932995** | – | **MN933240** | – |

| | | | | | | | | | | | | | |
|---|---|---|---|---|---|---|---|---|---|---|---|---|---|
| *P.* cf. *segallai* | MZUSP 135993 | HZB 558 | Parque Estadual Carlos Botelho, São Miguel Arcanjo, SP | *P.* cf. *segallai* - Lin C | *P.* cf. *segallai* - Lin 2 | **MN917576** | **MN932475** | **MN932646** | **MN932822** | **MN932996** | **MN933145** | – | **MN933338** |
| *P.* cf. *segallai* | *MZUSP 141657 | JU 21 | Parque Estadual Jurupará, Ibiúna, SP | *P.* cf. *segallai* - Lin C | *P.* cf. *segallai* - Lin 2 | **MN917577** | **MN932476** | **MN932647** | **MN932823** | **MN932997** | **MN933146** | **MN933241** | – |
| *P.* cf. *segallai* | MZUSP 141658* | JU 22 | Parque Estadual Jurupará, Ibiúna, SP | *P.* cf. *segallai* - Lin C | *P.* cf. *segallai* - Lin 2 | **MN917578** | **MN932477** | **MN932648** | – | **MN932998** | – | – | – |
| *P.* cf. *segallai* | *MZUSP 141659 | JU 46 | Parque Estadual Jurupará, Ibiúna, SP | *P.* cf. *segallai* - Lin C | *P.* cf. *segallai* - Lin 2 | **MN917579** | **MN932478** | **MN932649** | **MN932824** | **MN932999** | **MN933147** | – | – |
| *P.* cf. *segallai* | *CFBH 23302 | TP 44 | Piedade, SP | *P.* cf. *segallai* - Lin C | *P.* cf. *segallai* - Lin 2 | **MN917580** | **MN932479** | **MN932650** | **MN932825** | **MN933000** | **MN933148** | – | – |
| *P.* cf. *segallai* | MZUSP 124959 | ITH 388 | Piedade, SP | *P.* cf. *segallai* - Lin C | *P.* cf. *segallai* - Lin 2 | **MN917581** | **MN932480** | **MN932651** | **MN932826** | **MN933001** | **MN933149** | – | – |
| *P.* cf. *segallai* | MZUSP 136422* | H 61 | Piedade, SP | *P.* cf. *segallai* - Lin C | *P.* cf. *segallai* - Lin 2 | **MN917582** | **MN932481** | **MN932652** | **MN932827** | **MN933002** | – | – | – |
| *P.* cf. *segallai* | MZUSP 136425 | H 78 | Piedade, SP | *P.* cf. *segallai* - Lin C | *P.* cf. *segallai* - Lin 2 | **MN917583** | **MN932482** | **MN932653** | **MN932828** | **MN933003** | **MN933150** | **MN933242** | **MN933339** |
| *P.* cf. *segallai* | *MZUSP 136431 | H 118 | Piedade, SP | *P.* cf. *segallai* - Lin C | *P.* cf. *segallai* - Lin 2 | **MN917584** | **MN932483** | **MN932654** | **MN932829** | **MN933004** | – | – | **MN933340** |
| *P.* cf. *segallai* | *CFBH 16536 | – | Tapiraí, SP | *P.* cf. *segallai* - Lin C | *P.* cf. *segallai* - Lin 2 | MK791305 | **MN932484** | **MN932655** | **MN932830** | **MN933005** | **MN933151** | – | – |
| *P.* cf. *segallai* | CFBH 44857* | RJS 744 | Estação Ecológica de Juréia-Itatins, Iguape, SP | *P.* cf. *segallai* - Lin D | *P.* cf. *segallai* - Lin 3 | **MN917585** | **MN932485** | – | – | – | – | – | – |
| *P.* cf. *segallai* | CFBH 44863* | RJS 750 | Estação Ecológica de Juréia-Itatins, Iguape, SP | *P.* cf. *segallai* - Lin D | *P.* cf. *segallai* - Lin 3 | **MN917586** | – | – | – | – | – | – | – |
| *P.* cf. *segallai* | CFBH 44865* | RJS 752 | Estação Ecológica de Juréia-Itatins, Iguape, SP | *P.* cf. *segallai* - Lin D | *P.* cf. *segallai* - Lin 3 | **MN917587** | – | – | – | – | – | – | – |
| *P.* cf. *segallai* | CFBH 44866* | RJS 753 | Estação Ecológica de Juréia-Itatins, Iguape, SP | *P.* cf. *segallai* - Lin D | *P.* cf. *segallai* - Lin 3 | **MN917588** | – | – | – | – | – | – | – |
| *P.* cf. *segallai* | *CFBH 44886 | MTTS 400 | Estação Ecológica de Juréia-Itatins, Iguape, SP | *P.* cf. *segallai* - Lin D | *P.* cf. *segallai* - Lin 3 | **MN917589** | **MN932486** | **MN932656** | **MN932831** | **MN933006** | **MN933152** | **MN933243** | **MN933341** |
| *P. yepiranga* | *MZUSP 136697 | AUMC 280 | Parque das Neblinas, Bertioga, SP | *P. yepiranga* | *P. yepiranga* | **MN917590** | **MN932487** | **MN932657** | **MN932832** | **MN933007** | **MN933153** | **MN933244** | **MN933342** |
| *P. yepiranga* | MZUSP 136698 | AUMC 281 | Parque das Neblinas, Bertioga, SP | *P. yepiranga* | *P. yepiranga* | **MN917591** | **MN932488** | **MN932658** | **MN932833** | **MN933008** | **MN933154** | **MN933245** | **MN933343** |
| *Paratelmatobius* sp. | MTR 11682 | MTR 11682 | Estação Biológica de Boracéia, Salesópolis, SP | *Paratelmatobius* sp. | *Paratelmatobius* sp. | **MN917592** | **MN932489** | **MN932659** | **MN932834** | **MN933009** | **MN933155** | **MN933246** | **MN933344** |
| *Paratelmatobius* sp. | MTR 23373 | MTR 23373 | Estação Biológica de Boracéia, Salesópolis, SP | *Paratelmatobius* sp. | *Paratelmatobius* sp. | **MN917593** | **MN932490** | **MN932660** | **MN932835** | **MN933010** | **MN933156** | **MN933247** | **MN933345** |
| *Paratelmatobius* sp. | *MTR 23374 | MTR 23374 | Estação Biológica de Boracéia, Salesópolis, SP | *Paratelmatobius* sp. | *Paratelmatobius* sp. | **MN917594** | **MN932491** | **MN932661** | **MN932836** | **MN933011** | **MN933157** | – | **MN933346** |
| *R. cardosoi* | *JC 1112 | JC 1112 | Mucugê, BA | *R. cardosoi* - Lin A | *R. cardosoi* - Lin 1 | **MN917595** | **MN932492** | **MN932662** | **MN932837** | **MN933012** | KC604106 | **MN933248** | **MN933347** |
| *R. cardosoi* | MTR 19805 | MTR 19805 | Mucugê, BA | *R. cardosoi* - Lin A | *R. cardosoi* - Lin 1 | **MN917596** | **MN932493** | **MN932663** | – | **MN933013** | **MN933158** | **MN933249** | **MN933348** |
| *R. cardosoi* | MTR 19924 | MTR 19924 | Mucugê, BA | *R. cardosoi* - Lin A | *R. cardosoi* - Lin 1 | **MN917597** | **MN932494** | **MN932664** | **MN932838** | **MN933014** | – | – | **MN933349** |
| *R. cardosoi* | MZFS 2415* | FJ 117 | Parque Municipal de Mucugê, Mucugê, BA | *R. cardosoi* - Lin A | *R. cardosoi* - Lin 1 | KC593361 | – | KC593351 | – | – | – | – | KC593368 |
| *R. cardosoi* | UFMG 4274 | FSFL 4287 | Parque Nacional da Chapada Diamantina, Mucugê, BA | *R. cardosoi* - Lin A | *R. cardosoi* - Lin 1 | **MN917598** | **MN932495** | **MN932665** | **MN932839** | **MN933015** | **MN933159** | – | **MN933350** |
| *R. cardosoi* | UFMG 4349 | FSFL 4211 | Parque Nacional da Chapada Diamantina, Mucugê, BA | *R. cardosoi* - Lin A | *R. cardosoi* - Lin 1 | **MN917599** | **MN932496** | **MN932666** | **MN932840** | **MN933016** | – | – | **MN933351** |
| *R. cardosoi* | UFMG 4606 | FSFL 4093 | Toca do Vaqueiro, Mucugê, BA | *R. cardosoi* - Lin A | *R. cardosoi* - Lin 1 | **MN917600** | MN610720 | MN610757 | MN610794 | MN609905 | **MN933160** | – | MN610831 |
| *R. cardosoi* | *MTR 22434 | MTR 22434 | Morro do Chapéu, BA | *R. cardosoi* - Lin B | *R. cardosoi* - Lin 2 | **MN917601** | **MN932497** | **MN932667** | **MN932841** | **MN933017** | **MN933161** | **MN933250** | **MN933352** |

| | | | | | | | | | | | | | |
|---|---|---|---|---|---|---|---|---|---|---|---|---|---|
| *R. cardosoi* | MTR 22497 | MTR 22497 | Morro do Chapéu, BA | *R. cardosoi* - Lin B | *R. cardosoi* - Lin 2 | **MN917602** | **MN932498** | **MN932668** | **MN932842** | **MN933018** | **MN933162** | **MN933251** | **MN933353** |
| *S. sawayae* | *CFBH 6072 | – | Parque Estadual Pico do Marumbi, Piraquara, PR | *S. sawayae* - Lin A | *S. sawayae* - Lin 1 | DQ283099 | **MN932499** | **MN932669** | **MN932843** | **MN933019** | DQ283815 | – | **MN933354** |
| *S. sawayae* | CFBH 43229 | MTTS 391 | Parque Estadual Pico do Marumbi, Piraquara, PR | *S. sawayae* - Lin A | *S. sawayae* - Lin 1 | **MN917603** | **MN932500** | **MN932670** | **MN932844** | **MN933020** | **MN933163** | – | **MN933355** |
| *S. sawayae* | CFBH 44871 | MTTS 463 | Parque Estadual Pico do Marumbi, Piraquara, PR | *S. sawayae* - Lin A | *S. sawayae* - Lin 1 | **MN917604** | **MN932501** | **MN932671** | **MN932845** | **MN933021** | – | – | **MN933356** |
| *S. sawayae* | CFBH 44872 | MTTS 464 | Parque Estadual Pico do Marumbi, Piraquara, PR | *S. sawayae* - Lin A | *S. sawayae* - Lin 1 | **MN917605** | **MN932502** | **MN932672** | – | **MN933022** | **MN933164** | – | **MN933357** |
| *S. sawayae* | CFBH 44876 | MTTS 469 | Parque Estadual Pico do Marumbi, Piraquara, PR | *S. sawayae* - Lin A | *S. sawayae* - Lin 1 | **MN917606** | **MN932503** | **MN932673** | **MN932846** | **MN933023** | **MN933165** | **MN933252** | **MN933358** |
| *S. sawayae* | CFBH 44877 | MTTS 470 | Parque Estadual Pico do Marumbi, Piraquara, PR | *S. sawayae* - Lin A | *S. sawayae* - Lin 1 | **MN917607** | **MN932504** | **MN932674** | **MN932847** | **MN933024** | – | – | **MN933359** |
| *S. sawayae* | *CFBH-T 11239 | CEC 973 | Serro e Gemido, São José dos Pinhais, PR | *S. sawayae* - Lin A | *S. sawayae* - Lin 1 | **MN917608** | **MN932505** | **MN932675** | **MN932848** | **MN933025** | **MN933166** | **MN933253** | **MN933360** |
| *S. sawayae* | CFBH-T 11243 | CEC 974 | Serro e Gemido, São José dos Pinhais, PR | *S. sawayae* - Lin A | *S. sawayae* - Lin 1 | **MN917609** | **MN932506** | **MN932676** | **MN932849** | **MN933026** | – | – | **MN933361** |
| *S. sawayae* | *CFBH-T 18300 | CEC 1278 | Serro e Gemido, São José dos Pinhais, PR | *S. sawayae* - Lin A | *S. sawayae* - Lin 1 | **MN917610** | **MN932507** | **MN932677** | **MN932850** | **MN933027** | **MN933167** | – | **MN933362** |
| *S. sawayae* | *FURB 22434 | JPCM 138 | Tijucas do Sul, PR | *S. sawayae* - Lin A | *S. sawayae* - Lin 1 | **MN917611** | **MN932508** | **MN932678** | **MN932851** | **MN933028** | **MN933168** | – | **MN933363** |
| *S. sawayae* | *FURB 19456 | – | Reserva Biológica do Sassafrás, Doutor Pedrinho, SC | *S. sawayae* - Lin B | *S. sawayae* - Lin 2 | **MN917612** | **MN932509** | **MN932679** | **MN932852** | **MN933029** | **MN933169** | **MN933254** | **MN933364** |
| *S. sawayae* | FURB 19598 | – | Reserva Biológica do Sassafrás, Doutor Pedrinho, SC | *S. sawayae* - Lin B | *S. sawayae* - Lin 2 | **MN917613** | **MN932510** | **MN932680** | **MN932853** | **MN933030** | **MN933170** | – | **MN933365** |
| *S. sawayae* | FURB 19599 | – | Reserva Biológica do Sassafrás, Doutor Pedrinho, SC | *S. sawayae* - Lin B | *S. sawayae* - Lin 2 | **MN917614** | **MN932511** | **MN932681** | **MN932854** | **MN933031** | – | – | **MN933366** |
| *S. sawayae* | FURB 19600 | – | Reserva Biológica do Sassafrás, Doutor Pedrinho, SC | *S. sawayae* - Lin B | *S. sawayae* - Lin 2 | **MN917615** | **MN932512** | **MN932682** | **MN932855** | **MN933032** | – | – | **MN933367** |
| *S. sawayae* | *CHUFSC 2893 | – | Área de Relevante Interesse Ecológico Costeira de Zimbros, Bombinhas, SC | *S. sawayae* - Lin C | *S. sawayae* - Lin 2 | **MN917616** | **MN932513** | **MN932683** | **MN932856** | **MN933033** | **MN933171** | **MN933255** | **MN933368** |
| *S. sawayae* | CFBH 43197 | MTTS 359 | Braço Paula Ramos, Massaranduba, SC | *S. sawayae* - Lin C | *S. sawayae* - Lin 2 | **MN917617** | **MN932514** | **MN932684** | **MN932857** | **MN933034** | – | **MN933256** | **MN933369** |
| *S. sawayae* | *CFBH 43198 | MTTS 360 | Braço Paula Ramos, Massaranduba, SC | *S. sawayae* - Lin C | *S. sawayae* - Lin 2 | **MN917618** | **MN932515** | **MN932685** | **MN932858** | **MN933035** | **MN933172** | **MN933257** | **MN933370** |
| *S. sawayae* | *CFBH 43199 | MTTS 361 | Braço Paula Ramos, Massaranduba, SC | *S. sawayae* - Lin C | *S. sawayae* - Lin 2 | **MN917619** | **MN932516** | **MN932686** | **MN932859** | **MN933036** | **MN933173** | – | **MN933371** |
| *S. sawayae* | UFMG 15676* | BFZ 275 | Castelo dos Bugres, Joinville, SC | *S. sawayae* - Lin C | *S. sawayae* - Lin 2 | **MN917620** | **MN932517** | **MN932687** | **MN932860** | **MN933037** | – | – | – |
| *S. sawayae* | UFMG 15677 | BFZ 276 | Castelo dos Bugres, Joinville, SC | *S. sawayae* - Lin C | *S. sawayae* - Lin 2 | **MN917621** | **MN932518** | **MN932688** | **MN932861** | **MN933038** | – | – | **MN933372** |
| *S. sawayae* | *UFMG 15678 | BFZ 277 | Castelo dos Bugres, Joinville, SC | *S. sawayae* - Lin C | *S. sawayae* - Lin 2 | **MN917622** | MN610721 | MN610758 | MN610795 | MN609906 | – | – | MN610832 |
| *S. sawayae* | *UFMG 17192 | – | Castelo dos Bugres, Joinville, SC | *S. sawayae* - Lin C | *S. sawayae* - Lin 2 | **MN917623** | **MN932519** | **MN932689** | **MN932862** | **MN933039** | **MN933174** | – | **MN933373** |
| *S. sawayae* | UFMG 17193 | – | Castelo dos Bugres, Joinville, SC | *S. sawayae* - Lin C | *S. sawayae* - Lin 2 | **MN917624** | **MN932520** | **MN932690** | **MN932863** | **MN933040** | **MN933175** | **MN933258** | **MN933374** |
| *S. sawayae* | UFMG 17194 | – | Castelo dos Bugres, Joinville, SC | *S. sawayae* - Lin C | *S. sawayae* - Lin 2 | **MN917625** | **MN932521** | **MN932691** | **MN932864** | **MN933041** | – | – | **MN933375** |
| *S. sawayae* | CFBH 44869 | LFU 26 | Estrada Geral de Ourinhos, Botuverá, SC | *S. sawayae* - Lin C | *S. sawayae* - Lin 2 | **MN917626** | **MN932522** | **MN932692** | **MN932865** | **MN933042** | **MN933176** | **MN933259** | **MN933376** |
| *S. sawayae* | *CFBH 44870 | LFU 103 | Estrada Geral de Ourinhos, Botuverá, SC | *S. sawayae* - Lin C | *S. sawayae* - Lin 2 | **MN917627** | **MN932523** | **MN932693** | **MN932866** | **MN933043** | **MN933177** | – | **MN933377** |

| | | | | | | | | | | | | | |
|---|---|---|---|---|---|---|---|---|---|---|---|---|---|
| *S. sawayae* | CFBH 44892 | JPCM 625 | Morro do Baú, Ilhota, SC | *S. sawayae* - Lin C | *S. sawayae* - Lin 2 | **MN917628** | **MN932524** | **MN932694** | **MN932867** | **MN933044** | **MN933178** | – | **MN933378** |
| *S. sawayae* | CFBH 44893 | JPCM 626 | Morro do Baú, Ilhota, SC | *S. sawayae* - Lin C | *S. sawayae* - Lin 2 | **MN917629** | **MN932525** | **MN932695** | **MN932868** | **MN933045** | **MN933179** | – | **MN933379** |
| *S. sawayae* | *CFBH 44894 | JPCM 627 | Morro do Baú, Ilhota, SC | *S. sawayae* - Lin C | *S. sawayae* - Lin 2 | **MN917630** | **MN932526** | **MN932696** | **MN932869** | **MN933046** | – | **MN933260** | **MN933380** |
| *S. sawayae* | *CFBH 29996 | LFU 156 | Pedreira Vale do Selke, Blumenau, SC | *S. sawayae* - Lin C | *S. sawayae* - Lin 2 | **MN917631** | **MN932527** | **MN932697** | **MN932870** | **MN933047** | **MN933180** | – | **MN933381** |
| *S. sawayae* | *FURB 22451 | – | Reserva Particular do Patrimônio Natural Emílio Fiorentino Battistella, Corupá, SC | *S. sawayae* - Lin C | *S. sawayae* - Lin 2 | **MN917632** | **MN932528** | **MN932698** | **MN932871** | **MN933048** | **MN933181** | **MN933261** | **MN933382** |
| *S. sawayae* | *CFBH 3185 | – | São Bento do Sul, SC | *S. sawayae* - Lin C | *S. sawayae* - Lin 2 | **MN917633** | **MN932529** | **MN932699** | **MN932872** | **MN933049** | **MN933182** | **MN933262** | **MN933383** |
| *Scythrophrys* sp. | *CFBH 9369 | – | Industria dos Fosfatados Catarinenses, Anitápolis, SC | *Scythrophrys* sp. | *Scythrophrys* sp. | **MN917634** | **MN932530** | **MN932700** | **MN932873** | **MN933050** | **MN933183** | **MN933263** | **MN933384** |
| *Scythrophrys* sp. | CFBH 9371 | – | Industria dos Fosfatados Catarinenses, Anitápolis, SC | *Scythrophrys* sp. | *Scythrophrys* sp. | **MN917635** | **MN932531** | **MN932701** | **MN932874** | **MN933051** | **MN933184** | – | – |
| *Scythrophrys* sp. | *CFBH-T 22738 | – | Parque Estadual da Serra do Tabuleiro, São Bonifácio, SC | *Scythrophrys* sp. | *Scythrophrys* sp. | **MN917636** | **MN932532** | **MN932702** | – | **MN933052** | **MN933185** | – | **MN933385** |
| *Scythrophrys* sp. | CFBH-T 22739* | TAB 147 | Parque Estadual da Serra do Tabuleiro, São Bonifácio, SC | *Scythrophrys* sp. | *Scythrophrys* sp. | **MN917637** | **MN932533** | **MN932703** | – | **MN933053** | – | – | **MN933386** |
| *Scythrophrys* sp. | CFBH-T 22740 | TAB 152 | Parque Estadual da Serra do Tabuleiro, São Bonifácio, SC | *Scythrophrys* sp. | *Scythrophrys* sp. | **MN917638** | **MN932534** | **MN932704** | **MN932875** | **MN933054** | – | – | **MN933387** |
| *Scythrophrys* sp. | *MNRJ 91707* | – | Parque Estadual da Serra do Tabuleiro, São Bonifácio, SC | *Scythrophrys* sp. | *Scythrophrys* sp. | **MN917639** | **MN932535** | **MN932705** | **MN932876** | **MN933055** | – | – | – |
| *Scythrophrys* sp. | MNRJ 91708 | – | Parque Estadual da Serra do Tabuleiro, São Bonifácio, SC | *Scythrophrys* sp. | *Scythrophrys* sp. | **MN917640** | **MN932536** | **MN932706** | **MN932877** | **MN933056** | **MN933186** | – | **MN933388** |
| *Scythrophrys* sp. | UFMG 18509 | PCAG 2099 | Parque Estadual da Serra do Tabuleiro, São Bonifácio, SC | *Scythrophrys* sp. | *Scythrophrys* sp. | **MN917641** | **MN932537** | **MN932707** | **MN932878** | **MN933057** | **MN933187** | **MN933264** | **MN933389** |
| *Scythrophrys* sp. | UFMG 20656 | MTTS 422 | Sítio Soapé, Rancho Queimado, SC | *Scythrophrys* sp. | *Scythrophrys* sp. | **MN917642** | **MN932538** | **MN932708** | **MN932879** | **MN933058** | **MN933188** | – | **MN933390** |
| *Scythrophrys* sp. | *UFMG 20657 | MTTS 424 | Sítio Soapé, Rancho Queimado, SC | *Scythrophrys* sp. | *Scythrophrys* sp. | **MN917643** | **MN932539** | **MN932709** | **MN932880** | **MN933059** | **MN933189** | – | **MN933391** |
| *Scythrophrys* sp. | UFMG 21349 | MTTS 420 | Sítio Soapé, Rancho Queimado, SC | *Scythrophrys* sp. | *Scythrophrys* sp. | **MN917644** | **MN932540** | **MN932710** | – | **MN933060** | **MN933190** | **MN933265** | **MN933392** |
| *Scythrophrys* sp. | UFMG 21350 | MTTS 421 | Sítio Soapé, Rancho Queimado, SC | *Scythrophrys* sp. | *Scythrophrys* sp. | **MN917645** | **MN932541** | **MN932711** | **MN932881** | **MN933061** | **MN933191** | – | **MN933393** |
| *Scythrophrys* sp. | UFMG 21351 | MTTS 423 | Sítio Soapé, Rancho Queimado, SC | *Scythrophrys* sp. | *Scythrophrys* sp. | **MN917646** | **MN932542** | **MN932712** | **MN932882** | **MN933062** | – | – | **MN933394** |

before voucher number
*included in the GMYC analysis

after voucher number
*excluded for the species tree analysis

after accession number (RHOD)
*excluded from matrix (contamination detected)

Table S2. GenBank accession numbers for outgroup sequences employed in this study. Sequences generated for this article are in **bold**.

| SPECIES | FAMILY | H1 | COI | CYT-B | POMC | RAG-1 | RHOD | TYR |
|---|---|---|---|---|---|---|---|---|
| *Acris gryllus* | Hylidae | AY843560 | KT388396 | EF988136 | EF988249 | AY844359 | AY844534 | AY844020 |
| *Adenomera andreae* | Leptodactylidae | KC520683 | KC520689 | JQ321766 | KC604061 | KC604037 / KF674220 | KC604094 | KC520698 |
| *Agalychnis callidryas / A. moreletii* | Phyllomedusidae | DQ283423 | FJ766570 | GQ365916 | EF158395 | KX208666 | AY844537 | DQ283018 |
| *Allobates femoralis* | Aromobatidae | AY364543 | DQ502811 | HQ290531 | HQ290831 | DQ503327 | DQ503215 | DQ503156 |
| *Allophryne ruthveni* | Allophrynidae | AY843564 | KU494331 | AY843786 | AY819077 | AY844361 | AY844538 | KC604076 |
| *Alsodes gargola / A. neuquensis* | Alsodidae | AY843565 | JX203891 | JX564852 | KP295561 | AY844362 | AY844539 | – |
| *Amazophrynella minuta* | Bufonidae | AY843582 | DQ502828 | AY843804 | AY819081 | DQ503337 | AY844555 | EF364362 |
| *Anaxyrus boreas / A. canorus* | Bufonidae | AY680239 | MG421083 | HM563929 | KJ532285 | KJ609661 | KJ532270 | – |
| *Aplastodiscus perviridis* | Hylidae | AY843569 | KU184041 | AY843791 | – | AY844366 | AY844543 | AY844025 |
| *Atelognathus patagonicus* | Batrachylidae | AY843571 | JX203909 | MH974605 | KP295562 | AY844368 | AY844545 | AY844027 |
| *Barycholos pulcher / B. ternetzi* | Craugastoridae | EU186727 / EU186709 | KU494358 | JX298401 | JX298136 | KX208662 | DQ283810 | DQ282921 |
| *Batrachyla leptopus* | Batrachylidae | AY843572 | JX203910 | MH301156 | KP295563 | AY844369 | AY844546 | AY844028 |
| *Boana multifasciata* | Hylidae | AY843648 | JN970762 | AY843887 | GQ366036 | AY844436 | AY844633 | AY844093 |
| *Brachycephalus ephippium* | Brachycephalidae | DQ283091 | KU494370 | HQ435706 | GQ345256 | GQ345290 | DQ283806 | DQ282917 |
| *Bufo gargarizans / B. japonicus* | Bufonidae | AB303363 | AB303363 | AB303363 | JN653306 | AB612057 | DQ283905 | AB612059 |
| *Callimedusa tomopterna* | Phyllomedusidae | JX564887 | JX564887 | JX564887 | GQ366068 | AY844497 | GQ366157 | GQ366219 |
| *Calyptocephalella gayi* | Calyptocephalellidae | JX298374 | JX298374 | JX298374 | AY819090 | KX208684 | DQ284036 | JX298244 |
| *Ceratophrys aurita* | Ceratophryidae | KP295604 | KP295685 | KP295727 | KP295564 | KP295585 | KP295704 | KP295665 |
| *Craugastor brasfordii / C. podiciferus / C. rhodopis* | Craugastoridae | EF493360 | KR862892 | GQ345197 | GQ345258 | GQ345292 | DQ283960 | DQ282968 |
| *Crossodactylus schmidti* | Hylodidae | AY843579 | DQ502738 | AY843801 / HQ290528 | HQ290828 | DQ503298 | AY844552 | AY844031 |
| *Cryptobatrachus fuhrmanni / C. remotus* | Hemiphractidae | JX564861 | JX564861 | JX564861 | KR270358 | – | - | KR270387 |

| | | | | | | | | |
|---|---|---|---|---|---|---|---|---|
| *Cycloramphus boraceiensis* | Cycloramphidae | DQ283097 | DQ502856 | DQ502588 | – | DQ503357 | DQ283813 | DQ282924 |
| *Dendropsophus triangulum* | Hylidae | AY843680 | KY406664 | AY843926 | KY406706 | AY844464 | AY844673 | AY844122 |
| *Duttaphrynus melanostictus* | Bufonidae | AY458592 | AY458592 | AY458592 | KU183100 | KX208729 | DQ283967 | – |
| *Edalorhina perezi* | Leptodactylidae | AY843585 | – | AY843807 | – | KP145992 | AY844558 | – |
| *Eleutherodactylus planirostris* | Eleutherodactylidae | DQ283107 | JF769002 | HQ831615 | HQ831974 | – | DQ283821 | DQ282929 |
| *Engystomops petersi/ E. pustulosus* | Leptodactylidae | FJ668193 | KR862978 | GU086762 | KC604054 | GQ375544 | FJ668241 | – |
| *Espadarana prosoblepon* | Centrolenidae | JX564857 | JX564857 | JX564857 | AY819085 | EU663453 | AY364404 | – |
| *Eupsophus roseus / E. nahuelbutensis* | Alsodidae | AY843587 | DQ502852 | MK180910 | KC604074 | JX204087 | AY844560 | AY844036 |
| *Gastrotheca pseustes / Gastrotheca sp.* | Hemiphractidae | JX564866 | JX564866 | JX564866 | KC844986 | KX208740 | AY844563 | AY844039 |
| *Hyalinobatrachium fleischmanni* | Centrolenidae | JX564869 | JX564869 | JX564869 | EU663224 | EU663503 | DQ284043 | – |
| *Hydrolaetare* cf. *caparu* | Leptodactylidae | KC603953 / KC603954 | KC603988 | KC603975 | KC604050 | KC604035 | KC604107 | KC604081 |
| *Hyla annectans* | Hylidae | KM271781 | KM271781 | KM271781 | KP742500 | AY844388 | AY844574 | AY844045 |
| *Hylodes phyllodes / H. nasus* | Hylodidae | DQ283096 | DQ502873 | DQ502606 | GQ345272 | DQ503367 | DQ503253 | DQ282923 |
| *Hyloscirtus palmeri* | Hylidae | AY843650 | FJ766738 | AY843890 | AY819158 | AY844439 | AY844636 | AY844095 |
| *Hyloxalus yasuni* | Dendrobatidae | KT221612 | KT221612 | KT221612 | HQ290850 | MF614367 | MF614419 | MF624164 |
| *Incilius nebulifer* | Bufonidae | AY680252 | JN867983 | HQ290525 | KJ532288 | KJ609666 | EF372225 | HQ290885 |
| *Insuetophrynus acarpicus* | Rhinodermatidae | JX204223 | JX203938 | JX204005 | – | JX204088 | JX204152 | – |
| *Ischnocnema guentheri / I. juipoca / I. parva* | Brachycephalidae | JX267303 | KU494498 | HQ435717 | GQ345257 | GQ345291 | DQ283809 | JX267734 |
| *Lepidobatrachus asper* | Ceratophryidae | KP295626 | KP295696 | KP295739 | KP295574 | KP295598 | KP295718 | KP295679 |
| *Leptodactylus latrans* | Leptodactylidae | AY843688 | KC603989 | KC603976 | KC604055 | AY844470 | AY844681 | KC604082 |
| *Leptodactylus mystaceus* | Leptodactylidae | **MN958079** | KC603992 | KC603979 | KC604058 | KC604036 | KC604108 | JN691817 |
| *Lithodytes lineatus* | Leptodactylidae | AY843690 | KC604003 | JQ321833 | KC604060 | AY844472 | AY844683 | AY844129 |
| *Melanophryniscus klappenbachi* | Bufonidae | AY843699 | DQ502739 | AY843944 | KP295580 | DQ503299 | DQ283765 | – |
| *Niceforonia brunnea / N. dolops* | Craugastoridae | EF493357 | – | GQ345203 | GQ345264 | GQ345298 | GQ345304 | EF493484 |

| | | | | | | | | |
|---|---|---|---|---|---|---|---|---|
| *Nymphargus bejaranoi* | Centrolenidae | AY843576 | – | AY843798 | EU663239 | EU663522 | KP295725 | AY844029 |
| *Odontophrynus americanus* | Odontophrynidae | AY843704 | JX203939 | AY843949 | JX298141 | FJ685706 | AY844695 | JX298239 |
| *Osteocephalus taurinus* | Hylidae | JX564881 | JX564881 | JX564881 | JX875747 | AY844485 | AY844700 | AY844140 |
| *Peltophryne lemur / P. peltocephalus* | Bufonidae | DQ158465 | JF434558 | KX788998 | DQ158306 | KX208706 | – | – |
| *Physalaemus cuvieri* | Leptodactylidae | AY843729 | JQ627310 | AY843975 | AY819096 | AY844499 | AY844717 | – |
| *Physalaemus nattereri* | Leptodactylidae | DQ337208 | KC603984 | KC603965 | KC604053 | – | – | KC604079 |
| *Pleurodema brachyops* | Leptodactylidae | AY843733 | KP295702 | AY843979 | KP295582 | AY844503 | AY844721 | – |
| *Pristimantis curtipes / P. thymelensis* | Craugastoridae | EF493513 | EF493513 | EF493513 | AY819092 | KX208737 | – | EF493503 |
| *Proceratophrys avelinoi* | Odontophrynidae | KP295643 | **MN932371** | FJ685671 | KP295583 | FJ685711 | KF214204 | DQ282903 |
| *Pseudis paradoxa* | Hylidae | AY843740 | KP149190 | AY843986 | AY819102 | AY844506 | AY844727 | AY844167 |
| *Pseudopaludicola falcipes* | Leptodactylidae | AY843741 | KP295703 | KC593350 | KC604051 | AY844507 | AY844728 | AY844168 |
| *Ranitomeya ventrimaculata* | Dendrobatidae | HQ290979 | DQ502928 | HQ290556 | HQ290856 | DQ503399 | DQ503272 | HQ290916 |
| *Ranoidea caerulea* | Pelodryadidae | AY843692 | AY883980 | AY843938 | AY819149 | AY323767 | AY844685 | AY844131 |
| *Rhinella marina* | Bufonidae | DQ283062 | KR012546 | DQ415597 | DQ158316 | KX208677 | DQ283789 | KR012509 |
| *Rhinoderma darwinii* | Rhinodermatidae | DQ283324 | DQ502858 | JX564891 | KP295584 | KX208660 | AY364403 | – |
| *Schismaderma carens* | Bufonidae | DQ283425 | – | – | DQ158266 | KX208663 | DQ284027 | – |
| *Scinax staufferi / S. madeirae* | Hylidae | AY843761 | KJ004277 | AY844006 | GQ366071 | AY844523 | AY844748 | AY844183 |
| *Strabomantis biporcatus / S. bufoniformis / S. sulcatus* | Craugastoridae | DQ283165 | FJ766635 | GQ345204 | GQ345265 | KX208649 | – | DQ282942 |
| *Telmatobius bolivianus / T. truebae / Telmatobius sp.* | Telmatobiidae | JF703234 | JF703234 | JF703234 | AY819097 | AY583344 | AY844757 | DQ347182 |
| *Thoropa taophora* | Cycloramphidae | DQ283331 | DQ502874 | JX298411 | GQ345271 | FJ685702 | GQ345307 | JX298241 |
| *Vitreorana eurygnatha* | Centrolenidae | AY843595 | **MN932372** | **MN932543** | **MN932713** | **MN932883** | AY844567 | **MN933266** |

Table S3: Primers and PCR conditions used to amplify mitochondrial and nuclear loci. Each PCR reaction was carried out in a final volume of 25ul and contained 1 uL of genomic DNA, 2X PCR Master Mix Amplicon II, 0.5 uL (10 pmol) of each primer. PCR conditions were as follows: an initial hold for 1 min at 95 ºC; 40 to 45 cycles of 95 ºC for 30 s, [primer pair annealing temperature] for 30 s and 68 ºC for 1 min, followed by a final hold of 68 ºC for 3 min, and terminating the reaction at 12 ºC. F: forward primers; R: Reverse primers.

| Gene | Primer name | Sequence (5'→3') | Direction | Reference | Annealing temperature |
|---|---|---|---|---|---|
| H1 (12S-tRNA$^{valine}$-16S) | MVZ59 | ATAGCACGTAAAAYGCTDAGATG | F | Graybeal (1997) | |
| | 12S L48 | ATGCAAGYMTCMGCRYCCCNGTGA | F | Walker et al. (2018) | |
| | 12S H978 | CTTACCRTGTTACGACTTRCCT | R | Walker et al. (2018) | |
| | 12S F-H | CTTGGCTCGTAGTTCCCTGGCG | R | Goebel et al. (1999) | |
| | 12S A-L | AAACTGGGATTAGATACCCCACTAT | F | Goebel et al. (1999) | 50 ºC |
| | tRNAval-H | GGTGTAAGCGARAGGCTTTKGTTAAG | R | Goebel et al. (1999) | |
| | 12sL13 | TTAGAAGAGGCAAGTCGTAACATGGTA | F | Feller and Hedges (1998) | |
| | H10 | TGCTTACGCTACCTTTGCACGGT | F | Hedges (1994) | |
| | 16Sar-L | CGCCTGTTTATCAAAAACAT | F | Palumbi et al. (1991) | |
| | 16Sbr-H | CCGGTCTGAACTCAGATCACGT | R | Palumbi et al. (1991) | |
| COI | AnF1 | ACHAAYCAYAAAGAYATYGG | F | Lyra et al. (2017) | UP reaction (45 ºC/50 ºC) |
| | AnR1 | CCRAARAATCARAADARRTGTTG | R | Lyra et al. (2017) | Lyra et al. (2017) |
| cyt-*b* | MVZ15 | GAACTAATGGCCCACACWWTACGNAA | F | Goebel et al. (1999) | |
| | CytbAR-H | TAWAAGGGTCTTCTACTGGTTG | R | Goebel et al. (1999) | 50 ºC |
| | CytbF | TTTCTAGCAATACAYTACACAGCYGAT | F | **This study** | |
| | CytbC-R | CTACTGGTTGTCCTCCGATTCATGT | R | **This study** | |
| POMC | POMC-1 | AATGTATYAAAGMMTGCAAGATGGWCCT | F | Wiens et al. (2005) | 52 ºC |
| | POMC-2 | TAYTGRCCCTTYTTGTGGGCRTT | R | Wiens et al. (2005) | |
| RAG-1 | RAG-1 TG1F | CCAGCTGGAAATAGGAGAAGTCTA | F | Grant et al. (2006) | |
| | RAG-1 TG1R | CTGAACAGTTTATTACCGGACTCG | R | Grant et al. (2006) | |
| Rhod | RHOD 1A | ACCATGAACGGAACAGAAGGYCC | F | Bossuyt and Milinkovitch (2000) | 58 ºC |
| | RHOD 1C | CCAAGGGTAGCGAAGAARCCTTC | R | Bossuyt and Milinkovitch (2000) | |

| | | | | | |
|---|---|---|---|---|---|
| TNS3 | WL421 | CAGTGTTGGAGAAGATGGTATGTC | R | Smith et al. (2007) | 50 ºC |
| | WL423 | CAGCATAGGTACTTTATCATCATCAG | F | Smith et al. (2007) | |
| Tyr | Tyr1C | GGCAGAGGAWCRTGCCAAGATGT | F | Bossuyt and Milinkovitch (2000) | |
| | Tyr1G | TGCTGGGCRTCTCTCCARTCCCA | R | Bossuyt and Milinkovitch (2000) | 57 ºC |
| | Tyr 1HAdeno | ACATTGTTG GGCATCTCTCC | F | Fouquet et al. (2012) | |
| | Tyr 1I-Adeno6 | CAACTCTCC TTTGGGTCCTC | R | Fouquet et al. (2012) | |

**References**

Bossuyt, F., Milinkovitch, M.C., 2000. Convergent adaptive radiations in Madagascan and Asian ranid frogs reveal covariation between larval and adult traits. Proc. Natl. Acad. Sci. USA 97, 6585–6590. https://doi.org/10.1073/pnas.97.12.6585.

Feller, A.E., Hedges, S.B., 1998. Molecular evidence for the early history of living amphibians. Mol. Phylogenet. Evol. 9, 509–516. http://dx.doi.org/10.1006/mpev.1998.0500.

Fouquet, A., Noonan, B.P., Rodrigues, M.T., Pech, N., Gilles, A., Gemmell, N.J., 2012. Multiple quaternary refugia in the eastern Guiana Shield revealed by comparative phylogeography of 12 frog species. Syst. Biol. 61, 461–489. http://dx.doi.org/10.1093/sysbio/syr130.

Grant, T., Frost, D.R., Caldwell, J.P., Gagliardo, R., Haddad, C.F.B., Kok, P.J.R., Means, D.B., Noonan, B.P., Schargel, W.E., Wheeler, W.C., 2006. Phylogenetic systematics of dart-poison frogs and their relatives (Amphibia: Athesphatanura: Dendrobatidae). Bull. Am. Mus. Natl. Hist. 299, 6–262. http://dx.doi.org/10.5531/sd.sp.14.

Graybeal, A., 1997. Phylogenetic relationships of bufonid frogs and tests of alternate macroevolutionary hypotheses characterizing their radiation. Zool. J. Linn. Soc. 119, 297–338. http://dx.doi.org/10.1111/j.1096-3642.1997.tb00139.x.

Goebel, A.M., Donnelly, J.M., Atz, M.E., 1999. PCR primers and amplification methods for 12S ribosomal DNA, the control region, cytochrome oxidase I, and cytochrome b in bufonids and other frogs, and an overview of PCR primers which have amplified DNA in amphibians successfully. Mol. Phylogenet. Evol. 11, 163–199. http://dx.doi.org/ 10.1006/mpev.1998.0538.

Hedges, S.B., 1994. Molecular evidence for the origin of birds. Proc. Natl. Acad. Sci. USA 91, 2621–2624. https://doi.org/10.1073/pnas.91.7.2621.

Lyra, M.L., Haddad, C.F.B., de Azeredo-Espin, A.M.L., 2017. Meeting the challenge of DNA barcoding Neotropical amphibians: polymerase chain reaction optimization and new COI primers. Mol. Ecol. Resour. 17, 966–980. https://doi.org/10.1111/1755- 0998.12648.

Palumbi, S.R., Martin, A.P., Kessing, B.D., McMillan, W.O., 1991. Detecting population structure using mitochondrial DNA, in: Hoelzel, A.R. (Ed.), Genetic Ecology of Whales and Dolphins. International Whaling Commission, Cambridge, pp. 203–215.

Smith, S.A., Arif, S., de Oca, A.N.M., Wiens, J.J., 2007. A phylogenetic hotspot for 1045 evolutionary novelty in Middle American treefrogs. Evolution 61, 2075–2085. https://doi.org/10.1111/j.1558-5646.2007.00173.x.

Walker, M., Lyra, M.L., Haddad, C.F.B., 2018. Phylogenetic relationships and cryptic species diversity in the Brazilian egg-brooding tree frog, genus *Fritziana* Mello-Leitão 1937 (Anura: Hemiphractidae) Mol. Phylogenet. Evol. 123, 59–72. https://doi.org/10.1016/j.ympev.2018.02.012.

Wiens, J.J., Fetzner, J.W., Parkinson, C.L., Reeder, T.W., 2005. Hylid frog phylogeny and sampling strategies for speciose clades. Syst. Biol. 54, 778–807. http://dx.doi.org/10. 1080/10635150500234625.

Table S4: Best-fitting models and data partitions for each analysis.

**multigene matrix (AICc = 325378.15)**

| Partition | Model (Bayesian Inference) | Model (Maximum Likelihood) |
|---|---|---|
| COI 1st position | GTR + I + G | GTR + G |
| COI 2nd position | GTR + I | GTR + G |
| COI 3rd position | GTR + G | GTR + G |
| cyt-*b* 1st position | SYM + I + G | GTR + G |
| cyt-*b* 2nd position | GTR + I + G | GTR + G |
| cyt-*b* 3rd position | GTR + G | GTR + G |
| H1 | GTR + I + G | GTR + G |
| POMC 1st position | GTR + I + G | GTR + G |
| POMC 2nd position, RAG-1 1st position, TNS3 (1st and 2nd positions), Tyr 2nd position | GTR + I + G | GTR + G |
| POMC and RAG-1 3rd positions | GTR + I + G | GTR + G |
| RAG-1 2nd position | GTR + I + G | GTR + G |
| Rhod 1st position | GTR + I + G | GTR + G |
| Rhod 2nd position | GTR + I + G | GTR + G |
| Rhod 3rd position | GTR + G | GTR + G |
| TNS3 3rd position | K80 + I | GTR + G |
| Tyr 3rd position | GTR + G | GTR + G |
| Tyr1st position | SYM + I + G | GTR + G |

**mtDNA matrix - Bayesian Inference MrBayes (AICc = 74189.10)**

| Partition | Model |
|---|---|
| COI 1st position | GTR + G |
| COI 2nd position | GTR + I |
| COI 3rd position | GTR + I + G |
| cyt-*b* 1st position | SYM + I + G |
| cyt-*b* 2nd position | HKY + I + G |
| cyt-*b* 3rd position | GTR + G |
| H1 | GTR + I + G |

**nDNA matrix - Bayesian Inference MrBayes (AICc = 17194.10)**

| Partition | Model |
|---|---|
| POMC, RAG-1, and Rhod (1st positions), TNS3 (1st and 2nd positions), Tyr (1st and 2nd positions) | GTR + I + G |
| POMC, and RAG-1 (2nd positions) | GTR + I |
| POMC, Rhod, and Tyr (3rd positions) | HKY + G |
| RAG-1 and TNS3 (3rd positions) | SYM + G |
| Rhod 2nd position | F81 + I |

**mtDNA matrix - Beast2**

| Partition | Model |
|---|---|
| COI | TRN + I + G |
| cyt-*b* | GTR + I + G |
| H1 | GTR + I + G |

**multigene matrix - StarBeast2**

| Partition | Model |
|---|---|
| mtDNA | GTR + I + G |
| POMC | GTR + I + G |
| RAG-1 | TRN + I + G |
| Rhod | HKY + I + G |
| TNS3 | HKY + G |
| Tyr | SYM + I + G |

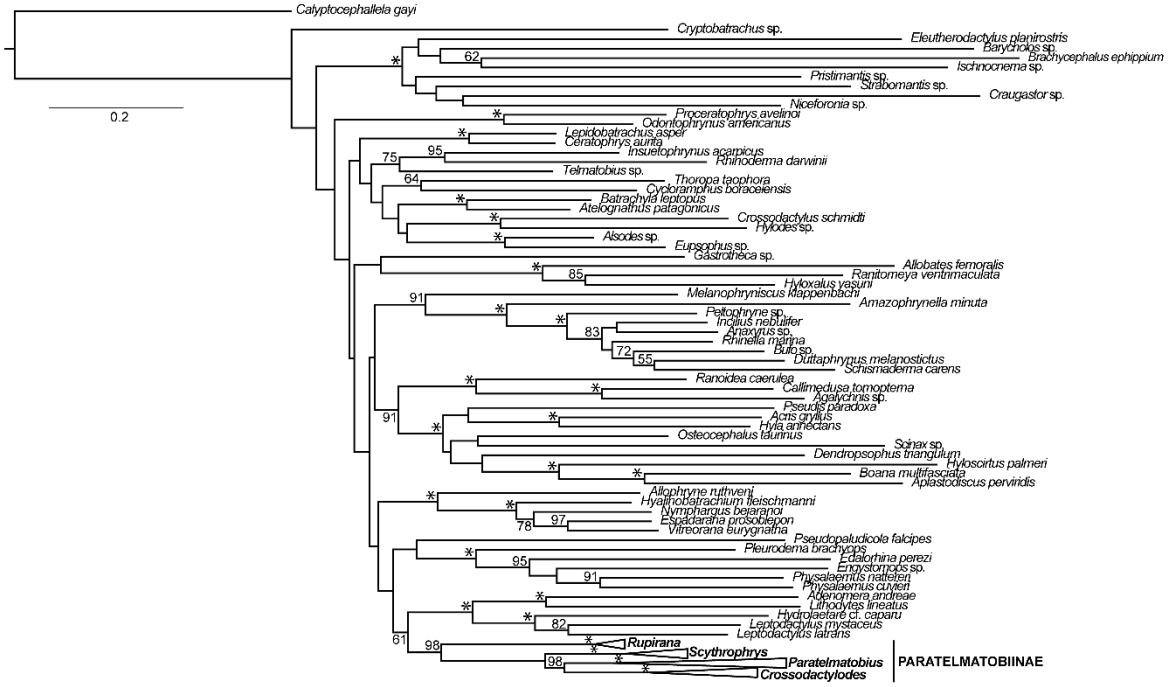


**Figure S1.** The tree from maximum likelihood inference of concatenenated mtDNA (H1, COI, cyt-b) and nDNA (POMC, RAG-1, Rhod, TNS3, Tyr) genes showing the relationships of the four genera of Paratelmatobiinae with the outgroups. Maximum likelihood bootstraps are shown next to the nodes. Asterisks (*) indicate fully supported nodes.

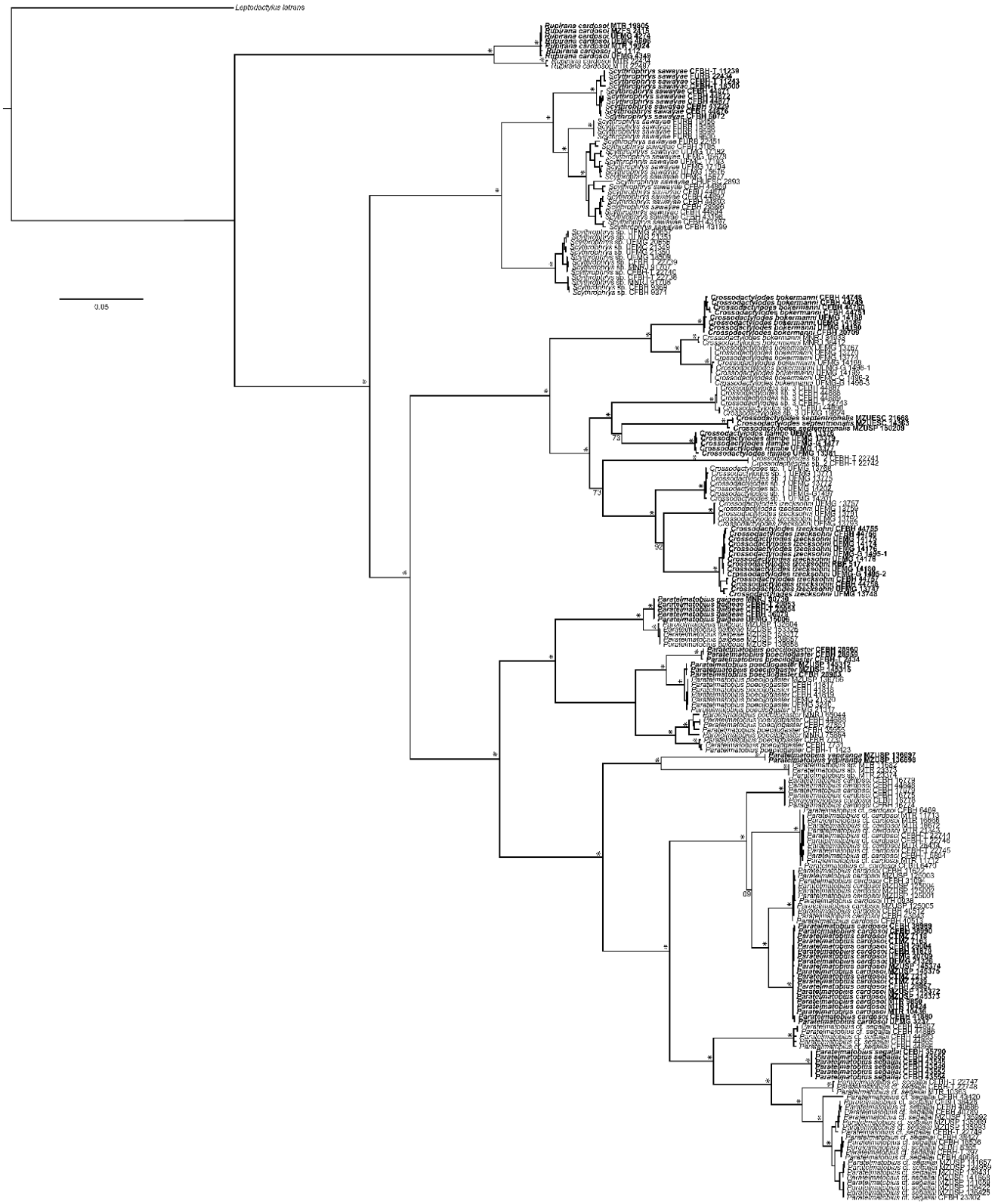


**Figure S2.** The 50% majority rule consensus tree from Bayesian phylogenetic inference of concatenenated mtDNA (H1, COI, cyt-b) genes showing the relationships within Paratelmatobiinae. Posterior probabilities and next to the nodes. Asterisks (*) indicate fully supported nodes.

**Figure S3.** The 50% majority rule consensus tree from Bayesian phylogenetic inference of concatenenated nDNA (POMC, RAG-1, Rhod, TNS3, Tyr) genes showing the relationships within Paratelmatobiinae. Posterior probabilities are shown next to the nodes. Asterisks (*) indicate fully supported nodes.

# CAPÍTULO III

## A new species of *Paratelmatobius* (Anura: Leptodactylidae: Paratelmatobiinae) from the Atlantic Forest of southern Brazil

*Zootaxa* 4648 (3): 473–493
https://www.mapress.com/j/zt/
Copyright © 2019 Magnolia Press

**Article**

ISSN 1175-5326 (print edition)
**ZOOTAXA**
ISSN 1175-5334 (online edition)

https://doi.org/10.11646/zootaxa.4648.3.4
http://zoobank.org/urn:lsid:zoobank.org:pub:6EFC650A-E3DF-4DC0-932F-3226C476CB57

# A new species of *Paratelmatobius* (Anura: Leptodactylidae: Paratelmatobiinae) from the Atlantic Forest of southern Brazil

MARCUS THADEU TEIXEIRA SANTOS[1,2,7], SÍLVIA HELENA DE OLIVEIRA[1], THIAGO RIBEIRO DE CARVALHO[1], BÁRBARA FERNANDES ZAIDAN[3,4], NELSON RODRIGUES DA SILVA[5,6], BIANCA VON MÜLLER BERNECK[1] & PAULO CHRISTIANO ANCHIETTA GARCIA[3,4,7]

*[1]Laboratório de Herpetologia, Departamento de Zoologia e Centro de Aquicultura (CAUNESP), Instituto de Biociências, Universidade Estadual Paulista (UNESP), 13506-900, Rio Claro, São Paulo, Brazil.*
*[2]Programa de Pós-graduação em Zoologia, Instituto de Biociências, Universidade Estadual Paulista (UNESP), 13506-900, Rio Claro, São Paulo, Brazil.*
*[3]Laboratório de Herpetologia, Departamento de Zoologia, Instituto de Ciências Biológicas, Universidade Federal de Minas Gerais (UFMG), 31270-901, Belo Horizonte, Minas Gerais, Brazil.*
*[4]Programa de Pós-graduação em Zoologia, Instituto de Ciências Biológicas, Universidade Federal de Minas Gerais (UFMG), 31270-901, Belo Horizonte, Minas Gerais, Brazil.*
*[5]Instituto de Ciências Biológicas e da Saúde, Universidade Federal de Alagoas, 57072-900 Maceió, Alagoas, Brazil.*
*[6]Setor de Zoologia, Museu de História Natural, Universidade Federal de Alagoas, 57010-020 Maceió, Alagoas, Brazil.*
*[7]Corresponding authors. E-mails: mthadeusantos@gmail.com, pcagarcia@gmail.com*

## Abstract

A new species of *Paratelmatobius* is described from the Brazilian Atlantic Forest in the state of Paraná in southern Brazil. Adults, tadpoles, and vocalizations are described. Morphological traits and phylogenetic analysis place the new species within the *P. cardosoi* group. The new species can be readily distinguished from its congeners by its advertisement call being composed of two note types and comprised of a series of 2–4 notes. The new species is classified as an explosive breeder, having reproductive activity strongly associated with heavy rainfall. This discovery highlights the importance of intensifying survey efforts in the Atlantic Forest, a domain with high levels of species richness and endemism.

**Key words:** Advertisement call, External morphology, Serra do Mar, State of Paraná, Tadpoles, Taxonomy

## Introduction

The leptodactylid frog genus *Paratelmatobius* Lutz & Carvalho, 1958, is part of the subfamily Paratelmatobiinae Ohler & Dubois, 2012, along with the genera *Crossodactylodes* Cochran, 1938, *Rupirana* Heyer, 1999, and *Scythrophrys* Lynch, 1971 (Fouquet *et al*. 2013a). The genus is endemic to the Brazilian Atlantic Forest, occurring only in the Serra do Mar and Serra da Mantiqueira mountain ranges (Pombal & Haddad 1999; Garcia *et al*. 2009), and currently comprises six species characterized by bright and contrasting colors on the venter (Pombal & Haddad 1999). Members of this genus are arranged in two morphological groups (Pombal & Haddad 1999). The *P. cardosoi* group includes *P. cardosoi* Pombal & Haddad, 1999; *P. mantiqueira* Pombal & Haddad, 1999; and *P. yepiranga* Garcia, Berneck & Costa, 2009, and is diagnosed by possessing head not flattened, vocal slits in males, first finger longer than second, medial margin of the first toe not fringed or webbed, and nuptial pad (in males) not divided (Pombal & Haddad 1999; Garcia *et al*. 2009). The *P. lutzii* group comprises *P. gaigeae* (Cochran, 1938); *P. lutzii* Lutz & Carvalho, 1958; and *P. poecilogaster* Giaretta & Castanho, 1990, and is diagnosed by possessing head flattened, males lacking vocal slits, first finger as long as or shorter than second, medial margin of the first toe fringed or webbed, and nuptial pad (in males) divided in two portions (Pombal & Haddad 1999; Garcia *et al*. 2009). DNA sequences of mitochondrial ribosomal genes support this arrangement (Lourenço *et al*. 2008), although sequences from *P. lutzii*, *P. mantiqueira*, and *P. yepiranga* are not available to date. Additionally, species of the *P. cardosoi*

*Accepted by D. Baldo: 10 Jun. 2019; published: 31 Jul. 2019*

group are characterized by remarkable gains in heterochromatin adjacent to the nucleolus organizer region (NOR) when compared to species of the *P. lutzii* group (Lourenço *et al*. 2008).

In general, species of *Paratelmatobius* are considered relatively rare due to their restricted geographical distributions (Garcia *et al*. 2009), their use of specific microhabitats, and their limited breeding season (Pombal & Haddad 1999). This is evidenced by the long periods by which some species of *Paratelmatobius* go unrecorded. For example, it took 73 years to find *Paratelmatobius gaigeae* again since its original discovery (Zaher *et al*. 2005); *P. mantiqueira* was known only from its type series until a single female was found 52 years later (Vrcibradic *et al*. 2010); and *P. lutzii* remains unrecorded since 1978, even after many field surveys at the type locality (Pombal & Haddad 1999).

Field surveys conducted in the Serra do Mar mountain range in the state of Paraná in southern Brazil, and the examination of specimens from different herpetological collections, have allowed us to identify a new species of *Paratelmatobius* belonging to the *P. cardosoi* group. Herein we describe this new species based on the external morphology of adults and tadpoles, and its vocalization. We also provide its phylogenetic placement and comment on its geographical distribution, natural history, and conservation. The new species was already mentioned in the literature and it was identified as: *Paratelmatobius* sp. (aff. *cardosoi*) in Lourenço *et al*. (2003); *Paratelmatobius* sp. in Frost *et al*. (2006) and Grant *et al*. (2006); and *Paratelmatobius* sp. 1 (aff. *cardosoi*) in Lourenço *et al*. (2008).

## Material and methods

**Adult Morphology and Species Description.** Specimens were euthanized in 5% lidocaine solution, fixed in 10% commercial grade formalin, and preserved in 70% ethanol. Voucher specimens are housed in the Célio F. B. Haddad Amphibian Collection, Rio Claro, São Paulo, Brazil (CFBH); Amphibian Collection of Centro de Coleções Taxonômicas da Universidade Federal de Minas Gerais, Belo Horizonte, Minas Gerais, Brazil (UFMG); Amphibian Collection of Museu Nacional, Rio de Janeiro, Rio de Janeiro, Brazil (MNRJ); Herpetological Collection of the Museu de Zoologia da Universidade de São Paulo, São Paulo, São Paulo, Brazil (MZUSP); and Herpetological Collection of Museu de História Natural Capão da Imbuia, Curitiba, Paraná, Brazil (MHNCI). For comparisons with other species, we used information from original descriptions or redescriptions (i.e., Giaretta & Castanho 1990; Pombal & Haddad 1999; Zaher *et al*. 2005; Garcia *et al*. 2009) and specimens examined from herpetological collections (Appendix I). Terminology for morphological characters follows Duellman (1970), Heyer *et al*. (1990), and Duellman & Lehr (2009). Morphometric characters follow Duellman (1970) for snout-vent length (SVL), head length (HL), head width (HW), tympanum diameter (TD), eye diameter (ED), eye to nostril distance (END), nostril to tip of snout distance (NSD), internarial distance (IND), tibia length (TBL) and foot length (FL); Heyer *et al*. (1990) for hand length (HAL), thigh length (THL) and tarsal length (TAL); Garcia *et al*. (2003) for distance between the anterior margins of eyes (AMD); Duellman *et al*. (1997) for forearm length (FAL); and Greene & Funk (2009) for arm length (AL), arm width (AW) and forearm width (FAW). The measurements SVL, HL, HW, AL, FAL, HAL, THL, TBL, TAL, and FL were taken to the nearest 0.1 mm using a digital caliper under a Zeiss Stemi SV 11 stereomicroscope, whereas the measurements ED, END, NSD, IND, AMD, TD, AW, and FAW were taken using an ocular micrometer coupled to the stereomicroscope. We only measured SVL from specimens in poor preservation condition. Sex was determined by the presence of vocal slits and nuptial pads in males, and the presence of mature oocytes in females. All geographic coordinates are in the system datum WGS84.

**Tadpoles.** We collected an amplectant pair at the type locality on 9 September 2005 and kept them in a plastic bag until spawning. We placed the clutch in an aquarium filled with water collected from the same pond in which the amplectant pair was found, and followed the development of eggs and tadpoles until they reached a desirable stage. Tadpoles were euthanized in 5% lidocaine solution and fixed in 10% commercial grade formalin on 26 October 2005. Vouchers are housed in the Tadpole Collection of Centro de Coleções Taxonômicas da Universidade Federal de Minas Gerais, Belo Horizonte, Minas Gerais, Brazil (UFMG). Descriptions and measurements of external morphology were based on nine tadpoles in stages 29–34 (Gosner 1960; lot UFMG 1830).

Tadpole measurements and terminology follow Altig & McDiarmid (1999) for total length (TL), body length (BL), tail length (TAL), maximum tail height (MTH), internarial distance (IND), interorbital distance (IOD), tail muscle height (TMH), tail muscle width (TMW); Lavilla & Scrocchi (1986) for body height (BH), body width (BW), body width at eye level (BWE), body width at narial level (BWN), eye-snout distance (ESD), eye-nostril distance (END), nostril-snout distance (NSD), eye diameter (ED), narial diameter (ND), snout-spiracle distance

(SSD), and oral disc width (ODW); Grosjean (2005) for dorsal fin height (DFH) and ventral fin height (VFH); and Pinheiro *et al*. (2012) for spiracle length (SL) and spiracle distal edge height (SDEH). All measurements were taken to the nearest 0.01 mm with ImageJ version 1.52a (Schneider *et al*. 2012). We used an adjustable platform to support tadpoles immersed in water to obtain high quality photos (Schacht & McBrayer 2009).

**Recording and Acoustic Analysis.** We recorded two males at the type locality on 18 January 2018 using a Marantz PMD 661 digital recorder and a Sennheiser ME66/K6 unidirectional microphone. Sound recordings are housed in the acoustic repository of CFBH collection. The first male was recorded at 22:30 h at an air temperature of 20.5ºC (recording MTTS 002, unvouchered); the second male was recorded at 23:50 h at an air temperature of 19.0ºC (recording MTTS 001, voucher CFBH 43545). Recordings (stored as mono wave files) were made at a sampling rate of 44.1 kHz and a sample size of 16 bits. A 500-Hz high-pass filter (48 dB) was applied to sound files in Audacity version 2.1.1 (Audacity Team 2017) to reduce background noise caused by rain. Acoustic analysis was conducted in Raven Pro version 1.5 (Bioacoustics Research Program 2014). Spectrogram parameters were set as follows: Window Size = 256 samples, Window Type = Hann, 3 dB Filter Bandwidth = 248 Hz, Overlap = 90% (locked), Hop Size = 0.59 ms, DFT Size = 1024 samples (locked), Grid Spacing = 43.1 Hz, and Spectrogram Color Map = "cool". Sound figures were produced using Seewave version 1.7.3 (Sueur *et al*. 2008) in R version 3.2.2 (R Core Team 2015). Seewave settings were as follows: window = Hann, FFT overlap = 90%, FFT size = 256 samples, and color scale = 30 relative dB. Acoustic definitions and terminology follow those of Cocroft & Ryan (1995). Temporal call traits were measured manually from oscillograms, except for call rise time, which was obtained through the Peak Time measurement function; spectral call traits were obtained through the following measurement functions: Peak Frequency (dominant frequency), and Frequency 5% and 95% (minimum and maximum frequencies, respectively). The only exception from the definitions proposed by Cocroft & Ryan (1995) was for the acoustic trait "pulse rate", which was obtained by dividing pulse number by note duration, given that pulses are juxtaposed throughout the duration of notes or simply did not have accurate between-pulse silent gaps. In addition to the two recordings analyzed, a third recording from the type locality (PCAG 12) was available at CFBH, but it was not included in the quantitative analysis because of low sound input and the overlap of call emissions of neighboring males.

**Molecular phylogenetics and genetic distances**. The phylogenetic placement of the new species was provided by Lourenço *et al*. (2008), who referred to it as *Paratelmatobius* sp. 1. However, that analysis did not include the genera *Crossodactylodes* and *Rupirana*, which were subsequently included in Paratelmatobiinae (Fouquet *et al*. 2013a). For this reason, we assembled a matrix with sequences of rRNA gene fragments of the heavy strand transcription unit 1 (H1—12S and 16S, plus the intervening $tRNA^{valine}$ segment) of *Paratelmatobius* available from GenBank and complemented it with sequences obtained in the present study (Table 1). For the ingroup we included sequences of the new species and three of the six nominal species of *Paratelmatobius*, since sequences were not available for *P. lutzii*, *P. mantiqueira*, and *P. yepiranga*. In addition, we included sequences of specimens with uncertain taxonomic status: (1) specimens morphologically similar to *P. segallai* (see Remarks), but with some differences in the karyotype (see Lourenço *et al*. 2008), here identified as *Paratelmatobius* cf. *segallai* (*Paratelmatobius* sp. 3 in Lourenço *et al*. 2008); and (2) specimens morphologically similar to *P. cardosoi* but with some differences in the karyotype (see Lourenço *et al*. 2008), here identified as *Paratelmatobius* cf. *cardosoi* (*Paratelmatobius* sp. 2 in Lourenço *et al*. 2008). We selected outgroup taxa based on the results of Pyron & Wiens (2011), Fouquet *et al*. (2013a), and Pyron (2014), and included GenBank sequences of the other three genera of Paratelmatobiinae (*Crossodactylodes*, *Rupirana*, and *Scythrophrys*). We also included GenBank sequences of *Leptodactylus*, *Adenomera* (Leptodactylinae), *Physalaemus*, and *Pleurodema* (Leiuperinae), for sampling the other two subfamilies of Leptodactylidae. We used a sequence of *Allophryne ruthveni* (Allophrynidae) to root the trees based on its close relationship with Leptodactylidae (Pyron & Wiens 2011; Pyron 2014).

We extracted genomic DNA from ethanol-preserved tissues using a standard ammonium acetate extraction protocol adapted from Maniatis *et al*. (1982). Primers employed for amplification and sequencing of H1 are MVZ59 (Graybeal 1997); 12S F-H, 12S A-L and tRNAval-H (Goebel *et al*. 1999); 12S L48 and 12S-H978 (Walker *et al*. 2018); 12SL13 (Feller & Hedges 1998); 16S H10 (Hedges 1994); and 16SAR and 16SBR (Palumbi *et al*. 1991). Reaction conditions follow Walker *et al*. (2018). We purified PCR products with a mix of thermosensitive alkaline phosphatase (FastAP) and Exonuclease I using the manufacturer's protocol (Thermo Fisher Scientific Inc.), with minor modifications presented by Lyra et al. (2017). We used a mix of 0.5 unit of FastAP and 1 unit of Exonuclease I diluted in 2.45 µL of ultrapure water per 20 µL PCR reaction, incubated for 30 min at 37°C followed by 5 min at 95°C. The resulting amplified fragments were sequenced by Macrogen Inc. of Seoul, South Korea. Chromatograms were checked manually, assembled, and edited using Geneious v.7 (Biomatters Ltd.).

**TABLE 1**. Sample information for DNA sequences of heavy strand transcription unit 1 (12S and 16S, plus the intervening tRNAvaline segment) generated for this article **(in bold)** and obtained from GenBank used in the molecular phylogenetic analysis: species; museum voucher; field/tissue collection number; locality; GenBank accession number; and the original publication of sequences. For some sequences, vouchers are indicated with field or tissue numbers in GenBank; when possible we also provided the museum number. Museum acronyms (only those not provided in "Materials and Methods"): AMNH-A: Amphibians Collection of American Museum of Natural History, New York, United States; BC: Tissue Collection of Laboratory of "Biologia Celular", Instituto de Biologia, Universidade Estadual de Campinas, Campinas, São Paulo, Brazil. CFBH-T: Célio F. B. Haddad Amphibian Tissue Collection, Rio Claro, São Paulo, Brazil; MZFS: Museu de Zoologia de Feira de Santana, Universidade Estadual de Feira de Santana, Feira de Santana, Bahia, Brazil. Abbreviations for Brazilian states: BA: Bahia; ES: Espírito Santo; MG: Minas Gerais; PR: Paraná; SC: Santa Catarina; and SP: São Paulo. Other abbreviations: AF: field number of Antoine Fouquet; and MAD: field number of Maureen A. Donnelly.

| Species | Voucher number | Field/tissue number | Locality | Accession number | Reference |
|---|---|---|---|---|---|
| *Adenomera andreae* | – | 317 AF | Parare, French Guyana | KC520683 | Fouquet *et al*. (2013b) |
| *Allophryne ruthveni* | – | MAD 1512 | Kabocali camp, Guyana | AY843564 | Faivovich *et al.* (2005) |
| *Crossodactylodes bokermanni* | MNRJ 38412 | – | Santa Teresa, ES, Brazil | KC593359 | Fouquet *et al*. (2013a) |
| *Crossodactylodes izecksohni* | UFMG 13747 | – | Santa Teresa, ES, Brazil | KP146086 | Lourenço *et al*. (2015) |
| *Leptodactylus fuscus* | AMNH-A 139088 | – | Southern Rupununi Savanna, Guyana | DQ283404 | Frost *et al.* (2006) |
| *Paratelmatobius cardosoi* | CFBH 3264 | – | Santo André, SP, Brazil | EU224402 | Lourenço *et al*. (2008) |
| *Paratelmatobius cardosoi* | CFBH 3265 | – | Santo André, SP, Brazil | EU224403 | Lourenço *et al*. (2008) |
| *Paratelmatobius cardosoi* | CFBH 3267 | – | Santo André, SP, Brazil | EU224404 | Lourenço *et al*. (2008) |
| *Paratelmatobius* cf. *cardosoi* | CFBH 6469 | – | Mogi das Cruzes, SP, Brazil | EU224412 | Lourenço *et al*. (2008) |
| *Paratelmatobius* cf. *cardosoi* | CFBH 6470 | – | Mogi das Cruzes, SP, Brazil | EU224413 | Lourenço *et al*. (2008) |
| *Paratelmatobius* cf. *cardosoi* | CFBH 13307 | BC 61.24 | Mogi das Cruzes, SP, Brazil | EU224414 | Lourenço *et al*. (2008) |
| *Paratelmatobius* cf. *segallai* | CFBH 5448 | – | São Miguel Arcanjo, SP, Brazil | EU224409 | Lourenço *et al*. (2008) |
| *Paratelmatobius* cf. *segallai* | – | BC 61.29 | São Miguel Arcanjo, SP, Brazil | EU224410 | Lourenço *et al*. (2008) |
| *Paratelmatobius* cf. *segallai* | – | BC 61.30 | São Miguel Arcanjo, SP, Brazil | EU224411 | Lourenço *et al*. (2008) |
| ***Paratelmatobius* cf. *segallai*** | **CFBH 43420** | **MN 07** | **Guapiara, SP, Brazil** | **MK791306** | **This study** |
| ***Paratelmatobius* cf. *segallai*** | **CFBH 8365** | **CFBH-T 1613** | **Pilar do Sul, SP, Brazil** | **MK791307** | **This study** |
| ***Paratelmatobius* cf. *segallai*** | – | **CFBH-T 397** | **Pilar do Sul, SP, Brazil** | **MK791308** | **This study** |
| ***Paratelmatobius* cf. *segallai*** | **CFBH 16536** | **CFBH-T 5485** | **Tapiraí, SP, Brazil** | **MK791305** | **This study** |
| *Paratelmatobius gaigeae* | CFBH 7156 | – | Bananal, SP, Brazil | EU224397 | Lourenço *et al*. (2008) |
| *Paratelmatobius poecilogaster* | CFBH 7731 | – | São Luís do Paraitinga, SP, Brazil | EU224398 | Lourenço *et al*. (2008) |

*.....continued on the next page*

**TABLE 1. (Continued)**

| Species | Voucher number | Field/tissue number | Locality | Accession number | Reference |
|---|---|---|---|---|---|
| *Paratelmatobius poecilogaster* | CFBH 3251 | – | Santo André, SP, Brazil | EU224399 | Lourenço *et al*. (2008) |
| *Paratelmatobius poecilogaster* | CFBH 3253 | – | Santo André, SP, Brazil | EU224400 | Lourenço *et al*. (2008) |
| *Paratelmatobius poecilogaster* | – | BC 33.17 | Santo André, SP, Brazil | EU224401 | Lourenço *et al*. (2008) |
| *Paratelmatobius segallai* | CFBH 35790 | CFBH-T 240 | Piraquara, PR, Brazil | EU224408 | Lourenço *et al*. (2008) |
| *Paratelmatobius segallai* | MZUSP 137905 | BC 61.17 | Piraquara, PR, Brazil | EU224405 | Lourenço *et al*. (2008) |
| *Paratelmatobius segallai* | MZUSP 137908 | BC 61.20 | Piraquara, PR, Brazil | EU224406 | Lourenço *et al*. (2008) |
| *Paratelmatobius segallai* | MZUSP 137910 | BC 61.22 | Piraquara, PR, Brazil | EU224407 | Lourenço *et al*. (2008) |
| ***Paratelmatobius segallai*** | **CFBH 43545** | – | **Piraquara, PR, Brazil** | **MK791309** | **This study** |
| ***Paratelmatobius segallai*** | **CFBH 43549** | – | **Piraquara, PR, Brazil** | **MK791310** | **This study** |
| ***Paratelmatobius segallai*** | **CFBH 43552** | – | **Piraquara, PR, Brazil** | **MK791311** | **This study** |
| ***Paratelmatobius segallai*** | **CFBH 43554** | – | **Piraquara, PR, Brazil** | **MK791312** | **This study** |
| ***Paratelmatobius segallai*** | **CFBH 43555** | – | **Piraquara, PR, Brazil** | **MK791313** | **This study** |
| *Pleurodema brachyops* | AMNH-A 139118 | – | Southern Rupununi Savanna, Guyana | AY843733 | Faivovich *et al*. (2005) |
| *Physalaemus signifer* | – | CFBH-T 7508 | Congonhas do Campo, MG, Brazil | KP146090 | Lourenço *et al*. (2015) |
| *Scythrophrys sawayae* | CFBH 6072 | CFBH-T 241 | Piraquara, PR, Brazil | EU224415 | Lourenço *et al*. (2008) |
| *Scythrophrys sawayae* | CFBH 3185 | – | São Bento do Sul, SC, Brazil | EU224417 | Lourenço *et al*. (2008) |
| *Rupirana cardosoi* | MZFS 2415 | – | Mucugê, BA, Brazil | KC593361 | Fouquet *et al*. (2013a) |

We performed a multiple sequence alignment in MAFFT v.7 online version, using the G-INS-i strategy, and default transition/transversion cost ratio and gap opening penalty (Katoh & Standley 2013). We used PartitionFinder v.2.1.1 (Lanfear *et al*. 2017) to select the optimal partition scheme and nucleotide substitution models for each data block using linked model of branch lengths with greedy search algorithm. For this analysis, we defined three *a priori* partitions, including 12S, tRNAvaline, and 16S, separately. The best model was selected through Bayesian Information Criterion (BIC). We performed a Bayesian phylogenetic inference analysis using MrBayes v. 3.2.6. (Ronquist *et al*. 2012), implemented in the online CIPRES Science gateway portal (Miller *et al*. 2010), with two parallel runs, using four chains (one cold) with 2 x $10^7$ generations each. The first 25% of the total trees were discarded as burn-in and the remaining trees were summarized in a majority-rule consensus tree and used to calculate Bayesian posterior probabilities (BPP). We verified the convergence and minimal effective sample sizes (ESS > 200) of the parameters in Tracer v. 1.6 (Rambaut *et al*. 2014).

We computed uncorrected p-distances for all samples of *Paratelmatobius* using Mega 7 (Kumar *et al*. 2016). For this, we used the entire fragment of H1 and considered substitutions to include transitions + transversions, uniform rates among sites, and gaps/missing data as pairwise deletion.

## Results

***Paratelmatobius segallai* sp. nov.**
http://zoobank.org/urn:lsid:zoobank.org:act:3E3050DE-37E1-463C-B961-1A3293007FBA
(Figs. 1–2; Table 2)

**Holotype.** CFBH 43545, adult male from Brazil: state of Paraná: municipality of Piraquara: Parque Estadual Pico do Marumbi: Mananciais da Serra: "Salto" trail (25°29′53.18″S, 48°58′53.45″W, 1040 m above sea level), collected on 18 January 2018 by M.T.T. Santos, and J.P.C. Monteiro.

**Paratypes.** All adults (40 males, and 10 females), collected at the type locality, or in its surroundings. CFBH 43546–43549 (females), CFBH 43550–43554 (males), UFMG 20769–20776 (males), MNRJ 92342–92345 (males), MHNCI 10879–10882 (males), collected on 17–19 January 2018 by M.T.T. Santos, and J.P.C. Monteiro; same locality as the holotype. CFBH 43555–43557 (males), collected on 17 January 2018 by M.T.T. Santos, and J.P.C. Monteiro, in the surroundings of the type locality (trail to the water tank "Carambola", 25°29′20.09″S, 48°58′34.71″W, 1036 m above sea level). MZUSP 137887, 137889, 137894, 137898 (females), MZUSP 136882, 137888, 137890–93, 137895–97 (males), UFMG 7335 (male), UFMG 7336 (female), MHNCI 2970–72 (males), collected on 31 October to 2 November 1999 by P.C.A. Garcia, M.V. Segalla, and R. Lingnau; same locality as the holotype. CFBH 35790 (male), CFBH 35791 (female), UFMG 20586 (male), collected on 11–13 October 2002 by P.C.A. Garcia, and M.V. Segalla; same locality as the holotype. MZUSP 137560 (male), collected on 8 October 2005 by M.V. Segalla; same locality as the holotype.

**Generic allocation.** We assign this new species to the genus *Paratelmatobius* based on its morphological similarity to congeners (presence of well-developed fringes on toes, and belly with blotches of vivid coloration in life) and corroborate this inference with a phylogenetic hypothesis based on a mtDNA dataset (detailed below in the section "Molecular phylogenetics and genetic distances").

**Diagnosis.** This new species of *Paratelmatobius* is diagnosable from all congeners by the following combination of characters: (1) advertisement call composed of two note types (A and B); (2) calls emitted in series of 2–4 notes; (3) call duration varying 26–64 ms; (4) note A with 4–10 pulses; (5) absence of an isolated pulse on the onset of notes; (6) dominant frequency (both note types) ranging 2455–3230 Hz; (7) snout not flattened; (8) tympanic annulus visible through the skin; (9) males with vocal slits; (10) presence of a well-developed mandibular tubercle; (11) finger I longer than II; (12) tip of finger III pointed; (13) medial margin of the first toe not fringed or webbed; (14) foot fringed, not webbed (15) presence of tubercles on upper eyelid; (16) nuptial pads with pigmented keratinized spicules; (17) nuptial pads continuous, not divided; (18) toe tips not expanded; (19) dorsolateral fold well-developed; (20) in life, belly and ventral surfaces of arms and forearms blotched with orange; (21) in life, external margins of throat lacking orange blotches; (22) adult male SVL 17.2–23.1.

**Comparisons with congeners (characters of the comparative species in parentheses).** *Paratelmatobius segallai* **sp. nov.** is distinguished from all congeners by its advertisement call being composed of two note types that are always emitted in a series of 2–4 notes; Fig. 4A–C (calls composed of a single note type emitted isolated or

in intermittent series; Cardoso & Haddad 1990; Giaretta & Castanho 1990; Garcia *et al*. 2009; Giaretta & Magrini 2013). In addition, the advertisement call of *Paratelmatobius* **sp. nov.** distinguishes it from *P. cardosoi* and *P. yepiranga* by being shorter: both notes combined range of 26–64 ms (70–130 ms in *P. cardosoi*, Pombal & Haddad 1999; 490–660 ms in *P. yepiranga*, Garcia *et al*. 2009). The new species further differs from *P. yepiranga* by having note A composed of 4–10 pulses—note B is not clearly pulsed; Fig. 4B–C (16–22 pulses; Garcia *et al*. 2009). It differs from *P. gaigeae* by the absence of an isolated pulse on the onset of either note A or B (presence; Giaretta & Magrini 2013). It differs from *P. poecilogaster* by having a higher dominant frequency in both note types: combined range of 2455–3230 Hz (1800–2500 Hz; Giaretta & Castanho 1990). To date, the vocalizations of *P. lutzii* and *P. mantiqueira* are unknown.

*Paratelmatobius segallai* **sp. nov.** is distinguished from species of the *P. lutzii* group (*P. lutzii*, *P. gaigeae*, and *P. poecilogaster*) by having: snout not flattened (flattened); tympanic annulus present and visible through the skin (tympanic annulus absent in *P. lutzii*, and concealed by the skin in *P. gaigeae* and *P. poecilogaster*); presence of vocal slits in males (absence); presence of mandibular tubercle (absence); finger I longer than II (finger I shorter than II in *P. lutzii* and *P. poecilogaster*, and finger I as long as finger II in *P. gaigeae*); tip of finger III pointed (rounded); medial margin of the first toe not fringed or webbed (webbed in *P. lutzii*, and fringed in *P. gaigeae* and *P. poecilogaster*); nuptial pads in males not divided (divided in two portions); ventral coloration in life with a gray background blotched with orange (black background with white and red stains in *P. lutzii*; dark brown background with pinkish red blotches and white dots in *P. gaigeae*; and orange background with black, red, and white blotches in *P. poecilogaster*). The new species further differs from *P. lutzii* by the presence of tubercles on the upper eyelid (absence); presence of pigmented keratinized spicules on nuptial pads of males (absence); and foot fringed (foot webbed). The new species is also distinguished from *P. poecilogaster* by the tips of toes not expanded (expanded). *Paratelmatobius segallai* is distinguished from *P. cardosoi* by the presence of tubercles on the upper eyelid (absence); a well-developed mandibular tubercle (poorly developed); and a well-developed dorsolateral fold (poorly developed). It differs from *P. mantiqueira* by having larger males, SVL 17.2–23.1 mm (SVL 14.4–16.7 mm); well-developed dorsolateral fold (moderately developed); and the tip of finger III pointed (rounded). The new species differs from *P. yepiranga* by the absence of orange blotches on external margins of throat in life (presence).

**Description of holotype.** Adult male, SVL 18.4 mm; body robust; head wider than long (HW/HL 1.15); head width 0.36 SVL; head length 0.31 SVL; snout not flattened, rounded in dorsal and lateral views; END shorter than ED (END/ED 0.82); canthus rostralis slightly curved in dorsal view and rounded in cross-section; loreal region slightly concave; nostrils slightly protuberant, oval, dorsolaterally directed; interorbital area more than twice as long as ED (AMD/ED 2.41). Eyes large and protuberant (ED/HL 0.31; ED/HW 0.27), laterally oriented; upper eyelid margin with small scattered tubercles and a prominent tubercle in its medial region. Tympanic membrane undifferentiated; tympanic annulus medium-sized (TD/ED 0.55), visible through the skin; supratympanic fold poorly developed, covering the upper portion of tympanic annulus. Well-developed ventrolaterally-oriented mandibular tubercle present on the posterior third of lower jaw. Dorsolateral fold well-developed but fragmented, extending from the posterior corner of the eye to the inguinal region.

Choanae small, nearly rounded, spaced 1.8 mm from each other. Dentigerous processes of vomers poorly distinguishable, oblique, positioned posterior to the level of the choanae, broadly separated from each other. Tongue ovoid, with lateral constriction on its anterior third, free behind for about one third of its length. Vocal slits short, located at the level of the posterior third of tongue; vocal sac externally indistinct. Single, small tooth-like process present on front of lower jaw with a socket between premaxillae.

Forelimb robust, hypertrophied, lacking fold or fringe, well-developed tubercle present on the anterior surface of arm; fingers short, robust; tips of fingers I, II and IV rounded, tip of finger III slightly pointed; relative length of fingers II < I < IV < III; finger I broadly widened, with nuptial pad formed by numerous keratinized spicules covering most of its lateral margin and dorsal surface; subarticular tubercles large, flat, oval in ventral view on finger I, and round in ventral view on fingers II–IV; supernumerary tubercles absent; inner metacarpal tubercle flat, elliptical; outer metacarpal tubercle large, flat, and nearly round in ventral view.

Hindlimb medium-sized and moderately robust (THL/SVL 0.47; TBL/SVL 0.45), bearing two transverse irregular dermal crests on dorsal surfaces of thigh and tibia; tarsal fold absent; toes medium-sized, robust, with narrow and rounded tips, similar in size to those on fingers; relative length of toes I < II < V < III < IV; toes not webbed, bearing developed and flexible lateral fringes, except in medial margin of toe I; fringes joined between toes II and III, III and IV, and IV and V; subarticular tubercles small, flat, oval in ventral view on toe I, and rounded in ventral

view on toes II–V; supernumerary tubercles absent; inner metatarsal tubercle large, flat, and elliptical in ventral view; outer metatarsal tubercle small, nearly rounded in ventral view, conical in profile.

Skin shagreen except on belly (smooth) and on posterior surface of thigh around the cloaca (coarsely granular). Cloacal opening directed posteriorly, at upper level of thighs, covered above by a poorly developed cloacal flap.

**Measurements (mm).** SVL 18.4, HL 5.8, HW 6.6, ED 1.8, END 1.5, NSD 1.5, IND 2.1, AMD 4.4, TD 1.2, AL 4.6, AW 2.3, FAL 4.5, FAW 2.7, HAL 4.3, THL 8.6, TBL 8.2, TAL 4.3, FL 8.4.

**Coloration (Figs. 1–2).** In life, dorsum brown with scattered whitish flecks. Dorsal surface between the orbits dark brown. A light brown V-shaped blotch present on posterior third of head delimited anteriorly by whitish flecks, and posteriorly by a thin whitish line. A grayish brown, somewhat quadrangular blotch is present in the scapular region; an oblique band of the same color, connected to this blotch, extends into the inguinal region from each of the posterior corners. A pale yellow middorsal stripe extends from the medial third of the body to cloacal region, which is fragmented anteriorly and continuous posteriorly. Loreal region light brown. A whitish dorsolateral fold extends from behind the eye to inguinal region. Flank with a dark-brown band dorsally delimited by the whitish dorsolateral fold. This band possesses two expansions anteriorly: one triangle-shaped, between eye and arm insertion; the other a vertical bar just posterior to the arm insertion. Ventral to the dark-brown band the flank is brown with several dark brown and blueish flecks and blotches. Tubercles on eyelids, posterior third of mandible, and proximal third of arm whitish. Limbs brown dorsally with scattered whitish flecks and tubercles. Spicules on nuptial pad black. Toes, and dermal crests on thighs and tibia pale yellow. Anterior surface of thigh dark brown. Anterior and posterior surfaces of arm, and inner and outer surfaces of tibia with dark brown transverse bars. An inverted V-shaped thin dark-brown mark extends from the cloacal region to the posterior surfaces of thighs. Ventral surfaces of hand and toes light brown. Ventral surfaces of throat, chest, hindlimbs, and distal third of forearms grayish brown with scattered whitish and blueish blotches and spots. Ventral surfaces of arms and proximal half of forearms orange. Belly with large orange blotches covering almost its entire surface, over a grayish brown background. Ventral surface of inguinal region with small orange blotches. Iris copper-colored with dark brown reticulations.

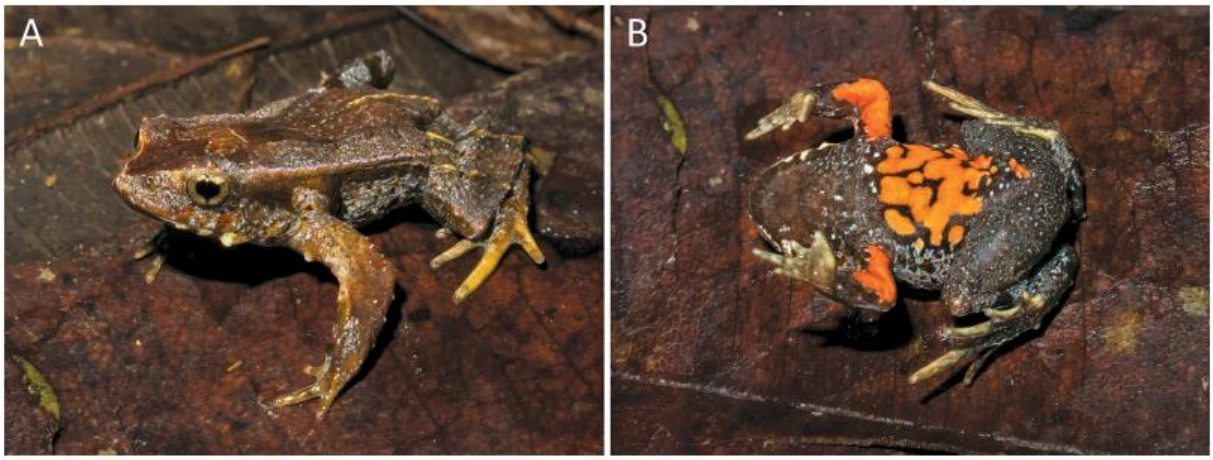


**FIGURE 1.** *Paratelmatobius segallai*, holotype in life (CFBH 43545, male, SVL 18.4 mm). (A) dorsal view; (B) ventral view.

In preservative, the colors fade, turning into pale tones with scattered melanophores. Dorsal blotches become less distinct. The pale-yellow colors of the middorsal stripe, toes, and dermal crests of the thighs and tibia become whitish. The blueish blotches on flanks and venter become whitish. The orange colors of the ventral surfaces of the forelimbs, belly, and inguinal region become paler (Fig. 2).

**Variation.** Males are distinguished from females by the presence of nuptial pads, and hypertrophy of arms and forearms (males AW/AL 0.44–0.59, mean 0.52; females AW/AL 0.31–0.39, mean 0.36; and males FAW/FAL 0.50–0.66, mean 0.58; females FAW/FAL 0.35–0.42, mean 0.39; Table 2). In addition, males possess wider thumbs than females. In general females are larger than males (females SVL mean = 20.6 mm, n = 9; males SVL mean = 18.5 mm, n = 37), but a male specimen (CFBH 43552) is the largest individual of the type series (maximum values of all measurements taken correspond to this individual; Table 2). The tubercles on posterior third of the mandible and on proximal third of arm vary in degree of development. The middorsal stripe varies in size, width, and degree of fragmentation. In some specimens the stripe is large and reaches the quadrangular blotch in the scapular region (MHNCI 10881, MNRJ 92343, 92345, UFMG 20770, 20775), while in others it is very small and covers just the

posterior third of the body, reaching the cloacal region (CFBH 43551, 43554, MHNCI 10880, 10882, UFMG 20769, 20774). Some specimens possess an orange blotch on the posterior third of the tarsus (CFBH 43555, 43549, MHNCI 10880, 10882). Some specimens possess few (CFBH 43549, MHNCI 10880, MNRJ 92343) or several (UFMG 20773) white spots in the pectoral region. One specimen (CFBH 43552) possesses a lighter coloration of the dorsum and the blotches of the belly, which are more yellowish. The mandibular tubercle of one specimen (MHNCI 10881) is orange. One specimen (MNRJ 92342) has dark brown labial bars and possesses a greater number of dark brown bars and blotches on the limbs, and a darker band on the flanks. The coloration of the specimens that were collected between 1999 and 2005 are more faded (dorsum light brown, blotches of belly cream and less visible markings).

**Tadpole.** Maximum total length 19.95 mm (at stage 34; Table 3). Body 0.37–0.40 times TL, depressed (BH/BW = 0.70–0.83), elliptical in dorsal view, rounded depressed in lateral view, with peribranchial region slightly convex, and abdominal region convex (Fig. 3A, B). Snout rounded in dorsal (BWN/BWE = 0.66–0.73) and lateral views. Eyes 0.15–0.19 times BW, dorsally located (IOD/BWE = 0.49–0.57), dorsolaterally directed. Nostrils elliptical, dorsal, located halfway between eyes and tip of snout (NSD/ESD = 0.43–0.53), anterolaterally directed and with a continuous and elevated rim, without fleshy projection. Spiracle sinistral, lateral (SDEH/BH = 0.38–0.43), posterodorsally directed, 0.10–0.13 times BL, opening between the middle and posterior thirds of body (SSD/BL = 0.65–0.72); inner wall fused to body with a small free edge. Lateral line system indistinct. Intestinal switchback point located at the center of abdominal region or dislocated to the left (Fig. 3C). Vent tube dextral, posteriorly directed, small, fused to ventral fin and positioned at its ventral margin (Fig. 3A, C). Tail with medium height (TH/TAL = 0.29–0.33), moderately slender musculature (TMH/BH = 0.40–0.46), not reaching the rounded tail tip; dorsal fin height approximately the same as that of ventral fin (AND/ANV = 1.02–1.10). Dorsal fin height 0.09–0.13 times TAL, with slightly convex external margin; emerging on the posterior third of body; maximum height at the posterior third of tail. Ventral fin height 0.08–0.12 times TAL, with slightly convex external margin; originates at base of tail, concealed by vent tube (Fig. 3A). Oral disc 0.38–0.45 times BW, ventral, laterally emarginated; a single row of marginal papillae aligned on the anterior labium and alternated on the posterior labium, with a wide dorsal gap; papillae reduced or absent on lateral emarginations; one submarginal papilla anteriorly on each side; labial tooth row formula (LTRF) 2(2)/3(1), A1=A2; P1=P2=P3; jaw sheaths narrow, finely serrated; upper jaw sheath arc-shaped and lower sheath "V"-shaped (Fig. 3D).

**TABLE 2**. Measurements and proportions for the type series of *Paratelmatobius segallai*. Values (mm) are reported as ranges (mean ± SD). See text for explanation of measurement abbreviations.

| | Measurement | | | Body ratios | |
|---|---|---|---|---|---|
| | Males ($n$ = 37, except for SVL, $n$ = 41) | Females ($n$ = 9, except for SVL, $n$ = 10) | | Males ($n$ = 37) | Females ($n$ = 9) |
| SVL | 17.2–23.1 (18.6 ± 1.0) | 19.5–22.0 (20.6 ± 0.8) | HW / HL | 1.13–1.18 | 1.12–1.18 |
| HL | 5.5–7.1 (5.9 ± 0.2) | 6.3–6.8 (6.6 ± 0.2) | HL / SVL | 0.30–0.33 | 0.31–0.34 |
| HW | 6.4–8.3 (6.8 ± 0.3) | 7.4–8.0 (7.6 ± 0.2) | HW / SVL | 0.38–0.37 | 0.36–0.38 |
| ED | 1.8–2.2 (1.9 ± 0.1) | 1.9–2.1 (1.9 ± 0.1) | END / ED | 0.74–0.85 | 0.77–0.86 |
| END | 1.4–1.8 (1.5 ± 0.1) | 1.5–1.7 (1.6 ± 0.1) | AMD / ED | 2.24–2.52 | 2.35–2.65 |
| NSD | 1.4–2.0 (1.6 ± 0.1) | 1.5–1.8 (1.7 ± 0.1) | AMD /HL | 0.72–0.80 | 0.69–0.77 |
| IND | 2.0–2.7 (2.1 ± 0.1) | 2.3–2.5 (2.4 ± 0.1) | AMD / HW | 0.62–0.70 | 0.61–0.67 |
| AMD | 4.2–5.4 (4.5 ± 0.2) | 4.7–5.0 (4.8 ± 0.1) | ED / HL | 0.29–0.35 | 0.28–0.30 |
| TD | 1.1–1.5 (1.1 ± 0.1) | 1.2–1.5 (1.4 ± 0.1) | ED / HW | 0.25–0.31 | 0.24–0.27 |
| AL | 4.3–6.1 (4.7 ± 0.3) | 4.3–4.9 (4.6 ± 0.2) | TD / ED | 0.56–0.66 | 0.62–0.74 |
| AW | 2.0–3.4 (2.4 ± 0.2) | 1.5–1.9 (1.7 ± 0.1) | TD / HL | 0.18–0.21 | 0.18–0.22 |
| FAL | 4.1–5.9 (4.5 ± 0.3) | 4.7–5.6 (5.0 ± 0.2) | AW / AL | 0.44–0.59 | 0.31–0.39 |
| FAW | 2.1–3.8 (2.6 ± 0.3) | 1.7–2.3 (2.0 ± 0.2) | FAW / FAL | 0.50–0.66 | 0.35–0.42 |
| HAL | 4.0–5.6 (4.4 ± 0.3) | 4.2–4.9 (4.6 ± 0.2) | FAL / SVL | 0.22–0.27 | 0.22–0.27 |
| THL | 8.1–10.8 (8.6 ± 0.5) | 8.7–9.5 (9.1 ± 0.3) | HAL / SVL | 0.22–0.25 | 0.21–0.25 |
| TBL | 7.7–10.5 (8.4 ± 0.4) | 8.3–9.1 (8.7 ± 0.2) | THL / SVL | 0.44–0.48 | 0.43–0.46 |
| TAL | 4.3–5.6 (4.6 ± 0.3) | 4.7–5.3 (4.9 ± 0.2) | TBL / SVL | 0.42–0.48 | 0.41–0.44 |
| FL | 7.5–10.2 (8.5 ± 0.4) | 8.3–9.6 (8.9 ± 0.4) | FL / SVL | 0.43–0.49 | 0.39–0.46 |

**Coloration of tadpole in preservative.** Body brown with scattered dark brown dots; caudal musculature beige with scattered dark brown dots, mainly on its anterior third; dorsal and ventral fins, spiracle and myomeres on medial and posterior thirds of tail musculature translucent; few to numerous small white dots scattered along the body, dorsal and ventral fins and caudal musculature. The intestinal mass is visible both ventrally and laterally.

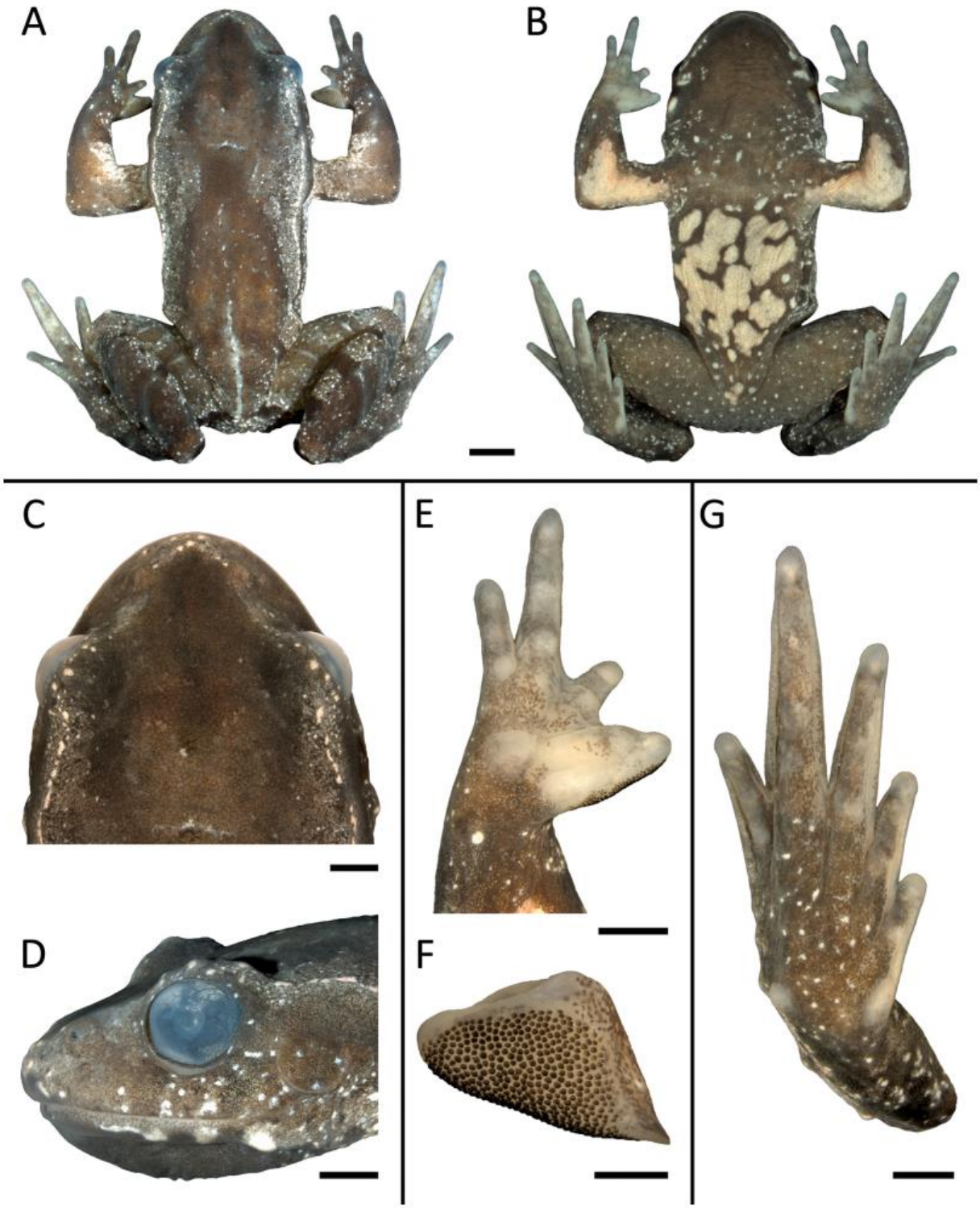


**FIGURE 2.** *Paratelmatobius segallai*, holotype (CFBH 43545). (A) Dorsal view, (B) ventral view; scale bar = 2 mm. (C) Head in dorsal view, (D) head in lateral view, (E) right hand in ventral view; scale bars = 1 mm. (F) Finger I in dorsal view showing nuptial pad in detail; scale bar = 0.5 mm. (G) Right foot in ventral view, scale bar = 1 mm.

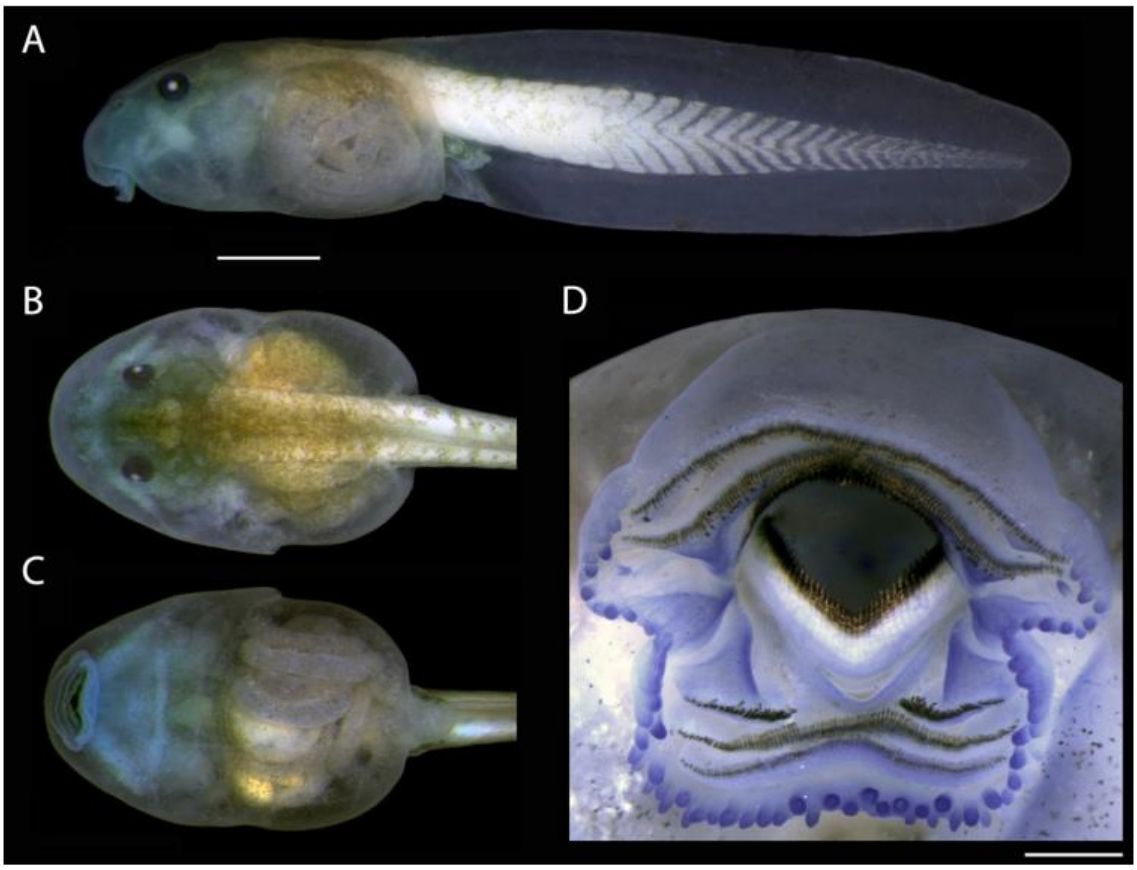


**FIGURE 3.** Tadpole of *Paratelmatobius segallai* (lot UFMG 1830) at stage 34. Body and tail shown in (A) lateral, (B) dorsal, and (C) ventral views (scale = 2.0 mm). (D) Oral disc (scale = 0.5 mm). Tadpole was stained with methylene blue for a better contrast of oral structures.

**TABLE 3**. Measurements (in mm) of tadpoles of *Paratelmatobius segallai* from the type locality (UFMG 1830, stages 29–34). Data presented as mean ± standard deviation (range). For abbreviations, see text.

| Measurements | | | |
|---|---|---|---|
| TL | 19.35 ± 1.25 (16.74–19.95) | ESD | 1.87 ± 0.06 (1.81–2.03) |
| BL | 7.10 ± 0.32 (6.52–7.40) | END | 1.07 ± 0.06 (0.98–1.14) |
| TAL | 12.13 ± 0.96 (10.22–12.74) | NSD | 0.91 ± 0.09 (0.81–1.07) |
| MTH | 3.75 ± 0.32 (3.21–4.11) | ED | 0.59 ± 0.06 (0.56–0.73) |
| IND | 1.36 ± 0.11 (1.13–1.44) | ND | 0.15 ± 0.02 (0.14–0.19) |
| IOD | 2.02 ± 0.14 (1.75–2.16) | SSD | 4.68 ± 0.24 (4.39–5.06) |
| TMH | 1.52 ± 0.14 (1.36–1.69) | ODW | 1.84 ± 0.09 (1.64–1.92) |
| TMW | 1.27 ± 0.11 (1.07–1.37) | DFH | 1.19 ± 0.19 (0.94–1.51) |
| BH | 3.56 ± 0.28 (2.95–3.80) | VFH | 1.14 ± 0.21 (0.86–1.47) |
| BW | 4.48 ± 0.19 (4.23–4.76) | SL | 0.81 ± 0.08 (0.74–0.96) |
| BWE | 3.68 ± 0.08 (3.60–3.80) | SDEH | 1.34 ± 0.16 (1.13–1.63) |
| BWN | 2.53 ± 0.09 (2.38–2.67) | | |

**Comparison with congeners' tadpoles.** Tadpole morphology is known for five species of *Paratelmatobius*: *P. cardosoi* (Cardoso & Haddad 1990; Pombal & Haddad 1999), *P. poecilogaster* (Giaretta & Castanho 1990; Pombal & Haddad 1999), *P. yepiranga* (Garcia *et al*. 2009), *P. gaigeae* (Domenico *et al*. 2014), and *P. segallai* (present study). Tadpoles of *P. lutzii* and *P. mantiqueira* remain undescribed. The tadpole of *P. segallai* is distinguished from *P. poecilogaster* by possessing a single row of alternated marginal papillae on the posterior labium (three rows;

Pombal & Haddad 1999), and shorter total length—19.9 mm at Stage 34 (25.8 mm at Stage 37; Pombal & Haddad 1999). It differs from *P. gaigeae* by possessing an elliptical body in dorsal view (ovoid), a single row of marginal papillae aligned on the anterior labium and alternated on the posterior labium (single row, alternated on anterior and posterior labia), a wider dorsal gap of marginal papillae (less wide), and narrow jaw sheaths (wide). It differs from *P. yepiranga* by the absence of submarginal papillae on the posterior labium (presence) and by possessing narrow jaw sheaths (wide). It differs from *P. cardosoi* by possessing a single row of marginal papillae aligned on the anterior labium and alternated on the posterior labium (single row, alternated on anterior and posterior labia).

**Advertisement call.** The vocalization of *P. segallai* (Fig. 4) consists of a series of 2–4 notes (n = 30; calls of two males). Notes comprising the advertisement call (= note series) are classified into two distinct types: notes A and B. Note A is defined by having well-marked pulses throughout the note and a higher amplitude in comparison with note B. On the other hand, note B possesses varying degrees of amplitude modulations (AMs), from a pattern of no modulation throughout the note, to an intermediate pattern of AMs, but irregularly distributed and/or weakly modulated in these notes, to a pattern of several AMs throughout the note, with variable modulation rates and depths between peaks and valleys (Fig. 4). Because of this variation we chose not to apply the term "pulse" to the highly variable AM patterns present in notes B.

The two note types are arranged in different combinations, with two-note calls "B + A" and three-note calls "B + A + B" being the most frequent emission patterns of one of the recorded males (57% and 36% of calls, respectively; recording MTTS 001, voucher CFBH 43545, holotype), whereas two-note calls "B + A" and three-note calls "B + A + A" were equally frequent in the other recorded male (50% of calls each; recording MTTS 002, unvouchered). The emission of isolated notes (either A or B) was rarely observed in call recordings and only on occasions when two males were calling in antiphony, which we assume to be a variant of the most frequent calling emission patterns described earlier related to male-male acoustic interactions. Calling rate ranged 33–69 calls per minute (50.9 ± 25.3; n = 2 males), and the interval between notes (in a note series) lasted 74–177 (111.7 ± 26.8; n = 44) ms.

Note A lasted 27–61 (44.9 ± 5.7; n = 40) ms, with rise time ranging 2–65 (32.3 ± 5.9; n = 40) %. Pulse number ranged 4–10 (6.6 ± 0.6, n = 41), and was emitted at a rate of 125–222 (147.1 ± 4.7; n = 41) pulses per second. The linear frequency modulation throughout the note was very subtle. The dominant frequency ranged 2756–3230 (2966 ± 140; n = 40) Hz, the minimum frequency 2412–2885 (2657 ± 96; n = 40) Hz and the maximum frequency 3058–4091 (3365 ± 223; n = 40) Hz. Note B lasted 26–64 (45.0 ± 9.0; n = 33) ms, with rise time ranging 4–83 (43.6 ± 10.8; n = 33) %. The linear frequency modulation throughout the notes was very subtle. The dominant frequency ranged 2455–3187 (2764 ± 86; n = 33) Hz, the minimum frequency 1852–2541 (2210 ± 96; n = 33) Hz, and the maximum frequency 2842–4433 (3400 ± 588; n = 33) Hz.

**Geographic distribution.** *Paratelmatobius segallai* is known to occur only at its type locality (municipality of Piraquara, state of Paraná, in the Serra do Mar mountain range, southern Brazil), which represents the southernmost record of the genus (Fig. 5). For geographic coordinates, see the sections "Holotype" and "Paratypes".

**Natural history.** The new species occurs in remnants of high montane dense ombrophilous Atlantic Forest, in well-preserved fragments. We visited the type locality (Piraquara, state of Paraná) in October-November 1999, October 2002, October 2005, January 2006, November 2017, and January 2018. Despite drizzly weather in November 2017, we did not observe any vocalizing males of *Paratelmatobius segallai* nor did we find any individuals. On all other occasions we visited the area during and after long periods of heavy rains (at least a week) and found many individuals near temporary pools, some of which were calling. In January 2018, we observed many individuals of *P. segallai* (males, females and amplectant pairs) exposed and/or walking on the leaf litter shortly after a heavy rain ceased. According to our observations, *P. segallai* can be classified as an explosive breeder (Wells 1977), with its reproductive activity being strongly associated with heavy rainfall.

Adult males of *Paratelmatobius segallai* call at night and occasionally during the day from within or on the edge of small, shallow muddy-bottom pools, usually positioned with their body partially submerged. When disturbed, individuals dive quickly to the bottom of the pools. These pools were usually next to rivulets. Amplexus is axillary. Eggs are submerged and attached to leaves or to the margin of pools. Clutches are composed of few eggs (less than 30) that are relatively large and uniformly dark-pigmented. Larvae of *P. segallai* are exotrophic, lentic and benthic (guild IIA1; McDiarmid & Altig 1999), completing their development in temporary pools inside the forest.

Another species of Paratelmatobiinae, *Scythrophrys sawayae*, was syntopic with *Paratelmatobius segallai* at the type locality. Despite males of both species calling simultaneously, their advertisement calls were easily distinguishable by temporal (e.g., pulse number and rate) and spectral (dominant frequency) traits. Individuals of *S. sawayae* were more abundant and shared the calling and breeding microhabitat with *P. segallai*.

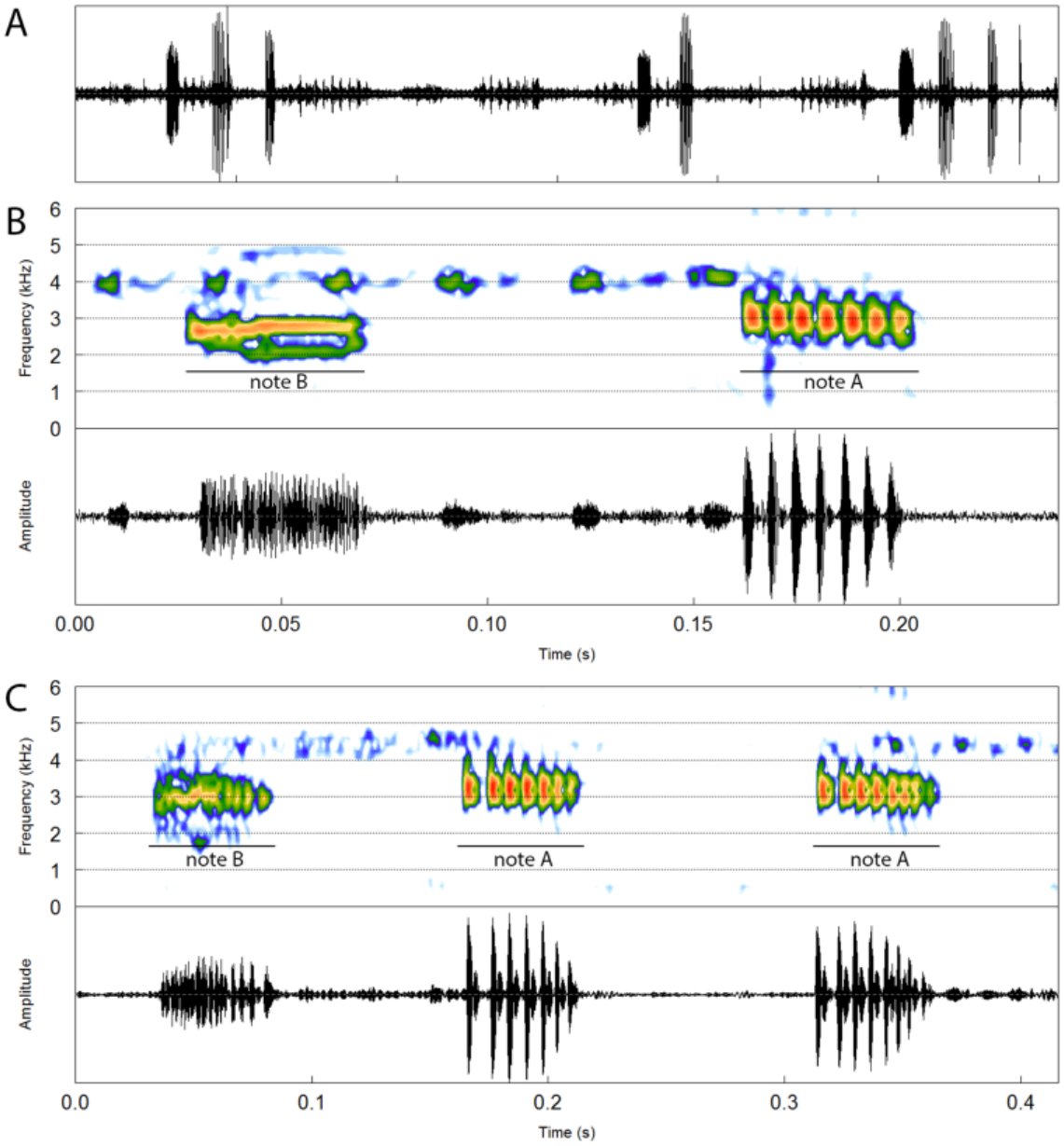


**FIGURE 4.** Advertisement call of *Paratelmatobius segallai*. (A) Oscillogram section from recording MTTS 001 (voucher CFBH 43545, holotype) containing three calls (ticks on the time axis correspond to 0.5 s). The multi-pulsed call in the background at ca. 4 kHz is the call of syntopic *Scythrophrys sawayae*. (B) Spectrogram and oscillogram of the two-note call in A: note B followed by note A. (C) Spectrogram and oscillogram of a three-note call from recording MTTS 002 (unvouchered): note B followed by two notes A.

**Molecular phylogenetics and genetic distances.** The optimal MAFFT similarity-alignment comprised 2440 characters. The BIC in Partition Finder identified one subset, GTR + I + G, for 12S, tRNA$^{valine}$, and 16S, BIC: 29876.8386125. The Bayesian phylogenetic inference analysis recovered a monophyletic and well-supported *Paratelmatobius* (BPP = 100), and placed *P. segallai* in the *P. cardosoi* group (Fig. 6). Within this group, *P. segallai* was recovered as the sister taxon of *Paratelmatobius* cf. *segallai*, a morphologically related lineage for which more data are still needed for a specific assignment (see the section Remarks below). The clade comprising these taxa

formed the sister group of *P. cardosoi* + *Paratelmatobius* cf. *cardosoi*. These four taxa formed the sister group of the sampled species of the *P. lutzii* group (*P. gaigeae* and *P. poecilogaster*). All relationships among recognized species and lineages with uncertain taxonomic status of *Paratelmatobius* were well-supported (BPP = 100). The uncorrected p-distances of H1 fragment between recognized species of *Paratelmatobius* varied from 6.4% to 11.9% (Table 4).

**Etymology.** The specific epithet honors the Brazilian herpetologist Magno V. Segalla for having collected the first specimens of the new species, and for his substantial contributions to the study and conservation of amphibians in southern Brazil.

**Remarks.** We carefully examined the external morphology of specimens from the municipalities of Capão Bonito, Guapiara, Iporanga, Piedade, Pilar do Sul, São Miguel Arcanjo, and Tapiraí, in the state of São Paulo (Appendix I), including the vouchers CFBH 8365, 16536, and 43420, which were included in our phylogenetic analysis (*Paratelmatobius* cf. *segallai*; Fig. 6). The morphology of these specimens is largely congruent with that described for the type series of *P. segallai*, considering all the morphological diagnostic characters that were possible to evaluate (characters # 7–19 and 22). We only found some variation in the arrangement of blotches on belly. In some specimens the blotches are similar to those of the type series of *P. segallai* (e.g., CFBH 8365, 8370, 16535–16536, 40684, 40686), whereas in other specimens the blotches may be small and sparse (e.g., CFBH 3724–3726, 8366, 43420–43421, 40681, 40789, 40794), or medium-sized and slightly merged (e.g., CFBH 3722–3723, 8367–8368, 16537, 23302, 36008–36011, 38426–38427). A few specimens possess a midventral line crossing the throat and the pectoral region (CFBH 16536, 38427) or only the pectoral region (CFBH 8366).

In addition, we accessed the only available call recording for the populations of São Paulo State (APA 001, housed at CFBH from the municipality of Pilar do Sul). Because of the low sound input of calls recorded, we were able to analyze only some qualitative features. These features are in accordance with the diagnosis of *P. segallai* (characters # 1–2, 5; note A is pulsed).

However, karyotypic differences between specimens from the type locality of *Paratelmatobius segallai* (Piraquara) and specimens of *Paratelmatobius* cf. *segallai* from São Miguel Arcanjo were reported by Lourenço *et al*. (2008): e.g., the nucleolar organizer region (NOR) site is adjacent to a large heterochromatic block of the short arm of the chromosome 9 in specimens from Piraquara, whereas it is in the long arm of chromosome 8 in specimens from São Miguel Arcanjo.

The uncorrected p-distance between *Paratelmatobius segallai* and *Paratelmatobius* cf. *segallai* (2.9–3.1%) is similar to the distances between *P. cardosoi* and *Paratelmatobius* cf. *cardosoi* (2.5%) and between the two lineages of *P. poecilogaster* (4.0%); Table 4. These distances might indicate that there are structured intraspecific lineages within these taxa; alternatively, this might indicate the presence of cryptic distinct evolving lineages corresponding to undescribed species. In the case of *P. segallai* and *Paratelmatobius* cf. *segallai*, the genetic distances can also be attributed to the sampling gap (i.e., 135 km) between the single occurrence locality for *P. segallai* and the southernmost sampled locality for *Paratelmatobius* cf. *segallai* (see distribution point 6 in Fig. 5). Therefore, a more comprehensive study, including specimens from other localities and with the addition of nuclear DNA fragments and other mitochondrial fragments, is required for a better understanding of the diversification processes that occurred in *Paratelmatobius*.

We used an integrative approach to describe the new species, with evidence from adult and tadpole morphology, advertisement call, and DNA sequences. For this reason and considering the karyotypic differences reported by Lourenço *et al*. (2008), we believe that additional data are necessary to an accurate assignment of the populations in São Paulo State.

## Discussion

Pombal & Haddad (1999) proposed two species groups for *Paratelmatobius* based on morphological characters. Garcia *et al*. (2009) redefined the diagnostic characteristics for each of the species groups, and the present study found the external morphology of *P. segallai* to be congruent with the characteristics defined for the *P. cardosoi* species group. DNA-based phylogenetic analyses corroborate the definition of these species groups (Lourenço *et al.* 2008; present study), with the genetic distances between recognized species from different groups varying 10.7–11.9%, whereas the distances between species within groups varying 6.4–7.5% (Table 4). Sequences from *P. lutzii*, *P. mantiqueira*, and *P. yepiranga* remain unavailable and their addition may contribute to a better understanding of the evolutionary relationships within the genus.

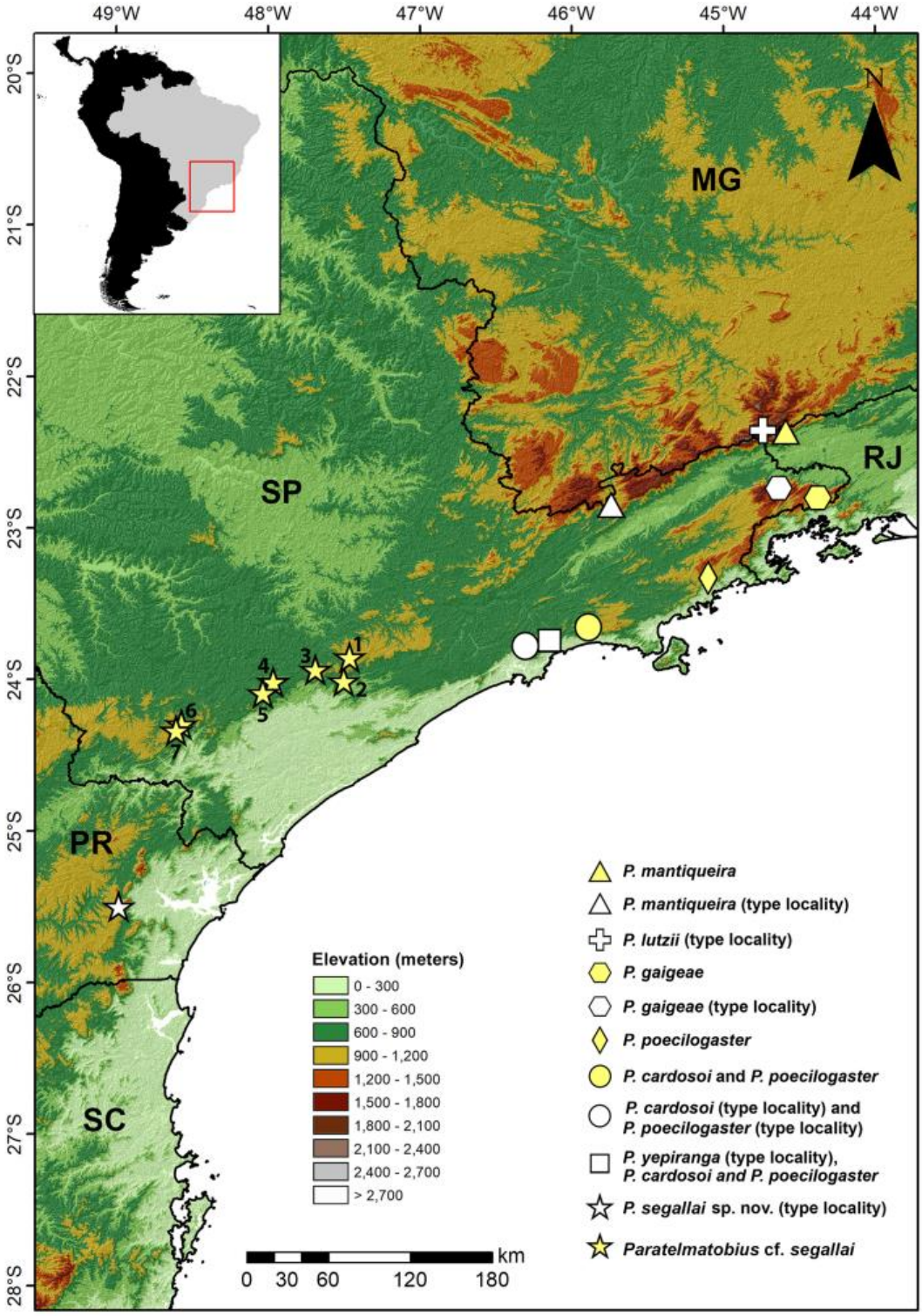


**FIGURE 5.** Geographic distribution of *Paratelmatobius segallai* and congeners from the Atlantic Forest of southeastern and southern Brazil. White solid symbols represent the type locality of each species. Numbered yellow stars represent the known records for *Paratelmatobius* cf. *segallai* in the municipalities of (1) Piedade; (2) Tapiraí; (3) Pilar do Sul; (4) São Miguel Arcanjo; (5) Capão Bonito; (6) Guapiara, and (7) Iporanga (records obtained from Célio F. B. Haddad Amphibian Collection, Rio Claro, São Paulo, Brazil). Occurrence records for the other species were obtained from: Garcia *et al*. (2009); Giaretta & Magrini (2013); Giasson (2008); Pombal & Haddad (1999); Vrcibradic *et al*. (2010); Zaher *et al*. (2005).

**TABLE 4.** Uncorrected p-distances (percentage) of mitochondrial H1 fragment (ca. 2400 bp) among species and lineages of *Paratelmatobius*. Intraspecific or intra-lineage distances are highlighted in gray (in diagonal). Interspecific or inter-lineage distances are shown under the diagonal. Data are shown as range (mean) where appropriate. N/C = not calculated, because there was only one individual. Lin = Lineage.

| Uncorrected p-distances | *P. cardosoi* | *P.* cf. *cardosoi* | *P. gaigeae* | *P. poecilogaster* Lin A | *P. poecilogaster* Lin B | *P.* cf. *segallai* | *P. segallai* |
|---|---|---|---|---|---|---|---|
| *P. cardosoi* | 0.0 (n = 3) | | | | | | |
| *P.* cf. *cardosoi* | 2.5 | 0.0 (n = 3) | | | | | |
| *P. gaigeae* | 10.7 | 11.1 | N/C | | | | |
| *P. poecilogaster* Lin A | 11.2–11.3 (11.3) | 11.5–11.7 (11.6) | 6.4 | 0.0–0.1 (0.1, n = 3) | | | |
| *P. poecilogaster* Lin B | 11.0 | 11.3 | 6.7 | 4.0 | N/C | | |
| *P.* cf. *segallai* | 7.8–8.0 (7.9) | 7.7–7.9 (7.8) | 11.5–11.8 (11.6) | 12.0–12.4 (12.2) | 11.5–11.9 (11.6) | 0.0–1.3 (0.6, n = 7) | |
| *P. segallai* | 7.5 | 7.5–7.6 (7.6) | 11.2 | 11.7–11.9 (11.8) | 11.7–11.8 (11.8) | 2.9–3.1 (3.0) | 0.0 (n = 9) |

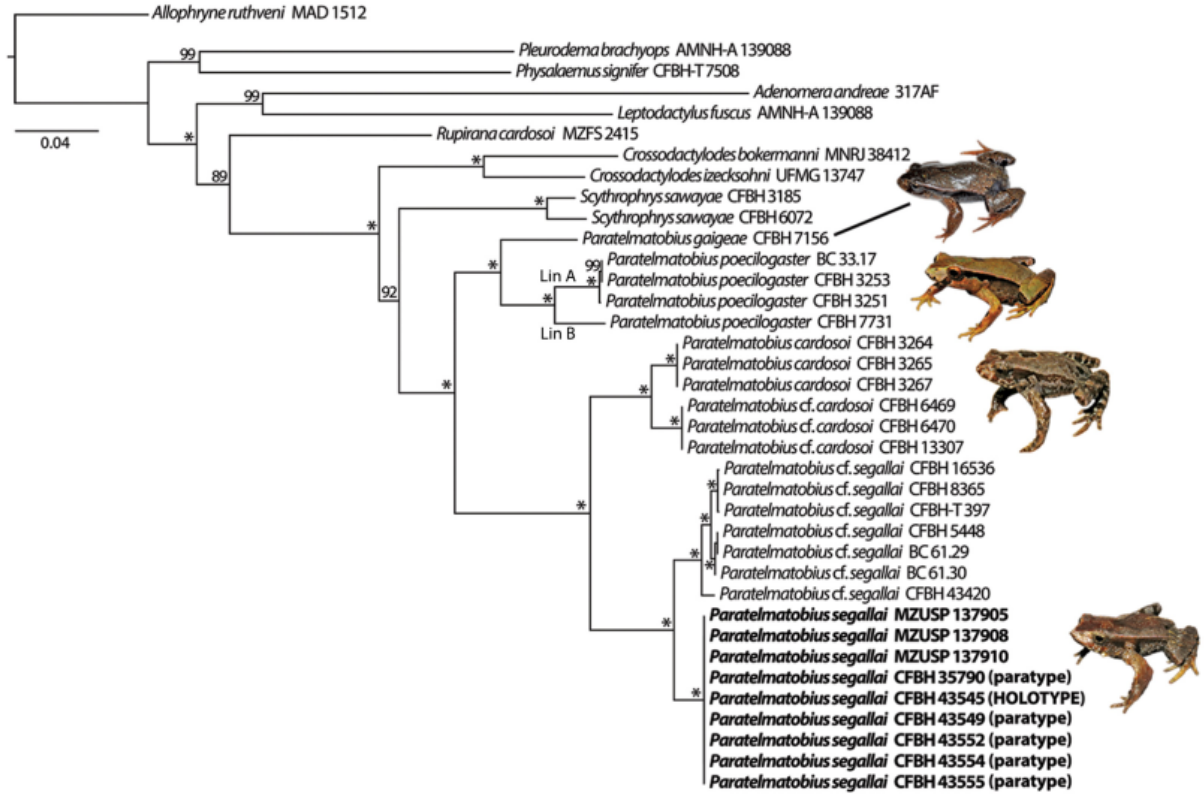


**FIGURE 6.** The 50% majority rule consensus tree resulting from Bayesian phylogenetic inference based on 2440 aligned base pairs of the heavy strand transcription unit 1 (H1—12S and 16S, plus the intervening $tRNA^{valine}$ segment). Values to the left of clades are node Bayesian posterior probabilities (BPP). Asterisks (*) indicate 100% values. Terminals in bold represent the new species. Lin = Lineage.

*Paratelmatobius segallai* occurs in the Parque Estadual Pico do Marumbi, a full protection conservation unit in the state of Paraná. Although this might mitigate negative impacts to this population, the resources available for the management and supervision of conservation units are scarce, leading to difficulty in avoiding impacts related to human activities, such as illegal hunting, logging, and fire which represent current threats to the species' habitat. The description of *P. segallai*, along with other recent anuran species discoveries in mountain ranges of the Brazilian Atlantic Forest (e.g., Bornschein *et al*. 2015; Malagoli *et al*. 2017), emphasizes the incompleteness of current knowledge regarding the true species richness of this domain. Biodiversity loss, driven by the destruction and fragmentation of natural habitats (Ribeiro *et al*. 2009) within a biodiversity hotspot for conservation priorities (Myers *et al*. 2000), highlights the urgency for the Brazilian government to take a more committed stance towards conservation policies and actions in the Atlantic Forest. Investments in comprehensive faunal inventories are crucial for new taxonomic discoveries and to help attenuate a massive loss of species, especially before their scientific discovery, and thus safeguard Brazilian biodiversity heritage.

## Acknowledgments

We are indebted to J.P.C. Monteiro for her invaluable assistance with fieldwork and for her help with an earlier version of the manuscript. We thank C.F.B. Haddad for logistical support. We are grateful to J.P. Pombal, Jr. (MNRJ), H. Zaher (MZUSP), C.F.B. Haddad (CFBH), A.A. Giaretta (AAG-UFU), and J.C. Moura-Leite (MHNCI) for loaning specimens under their care. We thank the staff of IAP-PR and SANEPAR, especially A.C.R. Barros, for logistical support and allowing access to Parque Estadual Pico do Marumbi, Mananciais da Serra, Piraquara, PR. We are grateful to the Centro de Estudos de Insetos Sociais (CEIS), UNESP, Rio Claro, Brazil, for allowing the utilization

of the facilities for molecular analyses. We thank M.L. Lyra, S.S.C. Lamerato-Costa and L.R. Malagoli for laboratory assistance; F. Leal for help with image editing; J.G.R. Giovanelli for help with map; and A.A. Giaretta for the photograph of *P. gaigeae*. We are grateful to P.D.P. Pinheiro, T.L. Pezzuti, A. Valencia-Aguilar, D. Baldo and two anonymous reviewers for comments and suggestions that improved the manuscript. P. Shea and K. Mercier helped with English, and E.R. Wild made an English review. Specimens were collected under collection permits ICMBio-IBAMA 094/99, 197/05, 59179-1, and 59366-2, IAP/PR 38.17, and CEUA-IB, Unesp, Rio Claro-SP 24/2017. This work was financially supported by the Brazilian agency FAPESP (#2013/50741-7 and #2014/50342-8) and by Fundação Grupo Boticário de Proteção à Natureza. MTTS is supported by a CAPES scholarship. BVMB thanks FAPESP (#2013/18807-8); TRC is supported by a FAPESP postdoctoral fellowship (#2017/08489-0). PCAG thanks CNPq for a research productivity fellowship, and FAPESP (05/56228-3 and 06/57853-1).

## References

Altig, R. & McDiarmid, R.W. (1999) Body plan: development and morphology. *In*: McDiarmid, R.W. & Altig, R. (Eds.), *Tadpoles: The Biology of Anuran Larvae*. The University of Chicago Press, Chicago, pp. 24–51.

Audacity Team (2017) *Audacity (R): Free Audio Editor and Recorder. Version 2.2.1*. Boston, Massachusetts. [program]

Bioacoustics Research Program (2014) *Raven Pro: Interactive Sound Analysis Software. Version 1.5*. The Cornell Lab of Ornithology, Ithaca, New York. [program]

Bornschein, M.R., Firkowski, C.R., Baldo, D., Ribeiro, L.F., Belmonte-Lopes, R., Corrêa, L., Morato, S.A.A. & Pie, M.R. (2015) Three new species of phytotelm-breeding *Melanophryniscus* from the Atlantic Rainforest of southern Brazil (Anura: Bufonidae). *PLOS ONE*, 10, e0142791. https://doi.org/10.1371/journal.pone.0142791

Cardoso, A.J. & Haddad, C.F.B. (1990) Redescrição e biologia de *Paratelmatobius gaigeae* (Anura, Leptodactylidae). *Papéis Avulsos de Zoologia*, 37, 125–132.

Cochran, D.M. (1938) Diagnoses of new frogs from Brazil. *Proceedings of the Biological Society of Washington*, 51, 41–42.

Cocroft, R.B. & Rian, M.J. (1995) Patterns of advertisement call evolution in toads and chorus frogs. *Animal Behaviour*, 49, 283–303. https://doi.org/10.1006/anbe.1995.0043

Domenico, E.A., Haddad, C.F.B. & Zaher, H. (2014) Natural history of *Paratelmatobius gaigeae* (Amphibia, Anura, Leptodactylidae): description of the tadpole and advertisement call. *Journal of Herpetology*, 48, 430–433. https://doi.org/10.1670/12-275

Duellman, W.E. (1970) *Hylid frogs of Middle America*. *Monographs of the Museum of Natural History*. University of Kansas, Lawrence, Kansas, xi + 753 pp., 72 pls.

Duellman, W.E., De La Riva, I. & Wild, E.R. (1997) Frogs of the *Hyla armata* and *Hyla pulchella* groups in the Andes of South America, with definitions and analyses of phylogenetic relationships of Andean groups of *Hyla*. *Scientific Papers, Natural History Museum, The University of Kansas*, 3, 1–41. https://doi.org/10.5962/bhl.title.48689

Duellman, W.E. & Lehr, E. (2009) *Terrestrial Breeding Frogs (Strabomantidae) in Peru*. Natur und Tier-Verlag, Münster, 382 pp.

Faivovich, J., Haddad, C.F.B., Garcia, P.C.A., Frost, D.R., Campbell, J.A. & Wheeler, W.C. (2005) Systematic review of the frog family Hylidae, with special reference to Hylinae: phylogenetic analysis and taxonomic revision. *Bulletin of the American Museum of Natural History*, 294, 1–240. https://doi.org/10.1206/0003-0090(2005)294[0001:SROTFF]2.0.CO;2

Feller, A.E. & Hedges, S.B. (1998) Molecular evidence for the early history of living amphibians. *Molecular Phylogenetics and Evolution*, 9, 509–516. https://doi.org/10.1006/mpev.1998.0500

Fouquet, A., Blotto, B.L., Maronna, M.M., Verdade, V.K., Junc, F.A., De S, R. & Rodrigues, M.T. (2013a) Unexpected phylogenetic positions of the genera *Rupirana* and *Crossodactylodes* reveal insights into the biogeography and reproductive evolution of leptodactylid frogs. *Molecular Phylogenetics and Evolution*, 67, 445–457. https://doi.org/10.1016/j.ympev.2013.02.009

Fouquet, A., Pineau, K., Rodrigues, M.T., Mailles, J., Schneider, J.B., Ernst, R. & Dewynter, M. (2013b) Endemic or exotic: the phylogenetic position of the Martinique volcano frog *Allobates chalcopis* (Anura: Dendrobatidae) sheds light on its origin and challenges current conservation strategies. *Systematics and Biodiversity*, 11, 87–101. https://doi.org/10.1080/14772000.2013.764944

Frost, D.R., Grant, T., Faivovich, J., Bain, R., Haas, A., Haddad, C.F.B, de Sá, R.O., Donnellan, S.C., Raxworthy, C.J., Wilkinson, M., Channing, A., Campbell, J.A., Blotto, B.L., Moler, P., Drewes, R.C., Nussbaum, R.A., Lynch, J.D., Green, D. & Wheeler, W.C. (2006) The amphibian tree of life. *Bulletin of the American Museum of Natural History*, 297, 1–370. https://doi.org/10.1206/0003-0090(2006)297[0001:TATOL]2.0.CO;2

Garcia, P.C.A., Berneck, B.V.M. & Costa, C.O.R. (2009) A new species of *Paratelmatobius* (Amphibia, Anura, Leptodactylidae) from Atlantic Rain Forest of Southeastern Brazil. *South American Journal of Herpetology*, 4, 217–224. https://doi.org/10.2994/057.004.0303

Garcia, P.C.A., Vinciprova, G. & Haddad, C.F.B. (2003) The taxonomic status of *Hyla pulchella joaquini* (Anura: Hylidae) with description of its tadpole and vocalization. *Herpetologica*, 59, 350–363. https://doi.org/10.1655/01-54

Giaretta, A.A. & Castanho, L.M. (1990) Nova espécie de *Paratelmatobius* (Amphibia, Anura, Leptodactylidae) da Serra do Mar, Brasil. *Papéis Avulsos de Zoologia, São Paulo*, 37, 133–139.

Giaretta, A.A. & Magrini, L. (2013) Calls of *Paratelmatobius gaigeae* (Cochran 1938) (Anura, Leptodactylidae). *Herpetology Notes*, 6, 171–176.

Giasson, L.O.M. (2008) *Atividade sazonal e uso do ambiente por anfíbios da Mata Atlântica no alto da Serra do Mar*. Ph.D. thesis, Universidade Estadual Paulista, São Paulo, 132 pp.

Goebel, A.M., Donnelly, J.M. & Atz, M.E. (1999) PCR primers and amplification methods for 12S ribosomal DNA, the control region, cytochrome oxidase I, and cytochrome b in bufonids and other frogs, and an overview of PCR primers which have amplified DNA in amphibians successfully. *Molecular Phylogenetics and Evolution*, 11, 163–199. https://doi.org/10.1006/mpev.1998.0538

Gosner, K.L. (1960) A simplified table for staging anuran embryos and larvae with notes on identification. *Herpetologica*, 16, 183–190.

Grosjean, S. (2005) The choice of external morphological characters and developmental stages for tadpole-based anuran taxonomy: a case study in *Rana* (*Sylvirana*) *nigrovittata* (Blyth, 1855) (Amphibia, Anura, Ranidae). *Contributions to Zoology*, 74, 61–76. https://doi.org/10.1163/18759866-0740102005

Grant, T., Frost, D.R., Caldwell, J.P., Gagliardo, R., Haddad, C.F.B. & Kok, P.J.R. (2006) Phylogenetic systematics of dart-poison frogs and their relatives (Amphibia: Athesphatanura: Dendrobatidae). *Bulletin of the American Museum of Natural History*, 299, 1–262. https://doi.org/10.1206/0003-0090(2006)299[1:PSODFA]2.0.CO;2

Graybeal, A. (1997) Phylogenetic relationships of bufonid frogs and tests of alternate macroevolutionary hypotheses characterizing their radiation. *Zoological Journal of the Linnean Society*, 119, 297–338. https://doi.org/10.1111/j.1096-3642.1997.tb00139.x

Greene, A.E. & Funk, W.C. (2009) Sexual selection on morphology in an explosive breeding amphibian, the columbia spotted frog (*Rana luteiventris*). *Journal of Herpetology*, 43, 244–251. https://doi.org/10.1670/08-112R.1

Hedges, S.B. (1994) Molecular evidence for the origin of birds. *Proceedings of the National Academy of Sciences of the United States of America*, 91, 2621–2624. https://doi.org/10.1073/pnas.91.7.2621

Heyer, W.R., Rand, A.S., Cruz, C.A.G., Peixoto, O.L. & Nelson, C. (1990) Frogs of Boracéia. *Arquivos de Zoologia do Estado de São Paulo*, 31, 271–272.

Heyer, W.R. (1999) A new genus and species of frog from Bahia, Brazil (Amphibia: Anura: Leptodactylidae) with comments on the zoogeography of the Brazilian campos rupestres. *Proceedings of the Biological Society of Washington*, 112, 19–30.

Katoh, K. & Standley, D.M. (2013) MAFFT multiple sequence alignment software Version 7: Improvements in performance and usability. *Molecular Biology and Evolution*, 30, 772–780. https://doi.org/10.1093/molbev/mst010

Kumar, S., Stecher, G. & Tamura, K. (2016) MEGA7: Molecular Evolotionary Genetics Analysis version 7.0 for bigger datasets. *Molecular Biology and Evolution*, 33, 1870–1874. https://doi.org/10.1093/molbev/msw054

Lanfear, R., Frandsen, P.B., Wright, A.M., Senfeld, T. & Calcott, B. (2017) PartitionFinder 2: New Methods for Selecting Partitioned Models of Evolution for Molecular and Morphological Phylogenetic Analyses. *Molecular Biology and Evolution*, 34, 772–773. https://doi.org/10.1093/molbev/msw260

Lavilla, E.O. & Scrocchi, G.J. (1986) Morfometría larval de los géneros de Telmatobiinae (Anura: Leptodactylidae) de Argentina y Chile. *Physis*, 44, 39–43.

Lourenço, L.B., Garcia, P.C.A. & Recco-Pimentel, S.M. (2003) Cytogenetics of a new species of *Paratelmatobius cardosoi* group (Anura: Leptodactylidae), with the description of an apparent case of pericentric inversion. *Amphibia-Reptilia*, 24, 47–55. https://doi.org/10.1163/156853803763806939

Lourenço, L.B., Bacci-Júnior, M., Martins, V.G., Recco-Pimentel, S.M. & Haddad, C.F.B. (2008) Molecular phylogeny and karyotype differentiation in *Paratelmatobius* and *Scythrophrys* (Anura, Leptodactylidae). *Genetica*, 132, 255–266. https://doi.org/10.1007/s10709-007-9169-y

Lourenço, L.B., Targueta, C.P., Baldo, D., Nascimento, J., Garcia, P.C.A., Andrade, G.V., Haddad, C.F.B. & Recco-Pimentel, S.M. (2015) Phylogeny of frogs from the genus *Physalaemus* (Anura, Leptodactylidae) inferred from mitochondrial and nuclear gene sequences. *Molecular Phylogenetics and Evolution*, 92, 204–216.

https://doi.org/10.1016/j.ympev.2015.06.011
Lutz, B. & Carvalho, A.L. (1958) Novos anfíbios anuros das Serras Costeiras do Brasil. *Memórias do Instituto Oswaldo Cruz, Rio de Janeiro*, 56, 239–249.
https://doi.org/10.1590/S0074-02761958000100012
Lyra, M.L., Haddad, C.F.B. & Azeredo-Espin, A.M.L. (2017) Meeting the challenge of DNA barcoding Neotropical amphibians: polymerase chain reaction optimization and new COI primers. *Molecular Ecology Resources*, 17, 966–980.
https://doi.org/10.1111/1755-0998.12648
Lynch, J.D. (1971) Evolutionary relationships, osteology, and zoogeography of leptodactyloid frogs. *Miscellaneous Publication. Museum of Natural History, University of Kansas*, 53, 1–238.
Malagoli, L.R., De Sá, F.P., Canedo, C. & Haddad, C.F.B. (2017) A New Species of *Hylodes* (Anura, Hylodidae) from Serra do Mar, Southeastern Brazil: The Fourth with Nuptial Thumb Tubercles. *Herpetologica*, 73, 136–147.
https://doi.org/10.1655/HERPETOLOGICA-D-16-00069
Maniatis, T., Fritsch, E.F. & Sambrook, J. (1982) *Molecular Cloning: A Laboratory Manual*. Cold Spring Harbor Laboratory Press, Cold Spring Harbor, New York, X + 545S.
McDiarmid, R.W. & Altig, R. (1999) Research: materials and techniques. *In*: McDiarmid, R.W. & Altig, R. (Eds.), *Tadpoles: The Biology of Anuran Larvae*. The University of Chicago Press, Chicago, pp. 7–23.
Miller, M.A., Pfeiffer, W. & Schwartz, T. (2010) Creating the CIPRES Science Gateway for inference of large phylogenetic trees. *Proceedings of the Gateway Computing Environments Workshop*, 2010, 1–8.
https://doi.org/10.1109/GCE.2010.5676129
Myers, N., Mittermeier, R.A., Mittermeier, C.G., da Fonseca, G.A.B. & Kent, J. (2000) Biodiversity hotspots for conservation priorities. *Nature*, 403, 853–858.
https://doi.org/10.1038/35002501
Ohler, A. & Dubois, A. (2012) Validation of two familial nomina nuda of Amphibia Anura. *Alytes*, 28, 162–167.
Palumbi, S.R., Martin, A.P., Kessing, B.D. & McMillan, W.O. (1991) Detecting population structure using mitochondrial DNA. *In*: Hoelzel, A.R. (Ed.), *Genetic Ecology of Whales and Dolphins*. International Whaling Comission, Cambridge, pp. 271–278.
Pinheiro, P.D.P., Pezzuti, T.L. & Garcia, P.C.A. (2012) The tadpole and vocalizations of *Hypsiboas polytaenius* (Cope, 1870) (Anura, Hylidae, Hylinae). *South American Journal of Herpetology*, **7**, 123–133.
https://doi.org/10.2994/057.007.0202
Pombal, Jr.J.P. & Haddad, C.F.B. (1999) Frogs of the genus *Paratelmatobius* (Anura: Leptodactylidae) with descriptions of two new species. *Copeia*, 1999, 1014–1026.
https://doi.org/10.2307/1447976
Pyron, R.A. & Wiens, J.J. (2011) A large-scale phylogeny of Amphibia with over 2800 species, and a revised classification of extant frogs, salamanders, and caecilians. *Molecular Phylogenetics and Evolution*, 61, 543–583.
https://doi.org/10.1016/j.ympev.2011.06.012
Pyron, R.A. (2014) Biogeographic analysis reveals ancient continental vicariance and recent oceanic dispersal in amphibians. *Systematic Biology*, 63, 779–797.
https://doi.org/10.1093/sysbio/syu042
R Core Team (2015) *R: a language and environment for statistical computing. Version 3.2.2*. R foundation for statistical computing, Vienna. [program]
Rambaut, A., Suchard, M.A., Xie, D. & Drummond, A.J. (2014) *Tracer. Version 1.6*. Available from: http://tree.bio.ed.ac.uk/software/tracer (accessed 16 June 2019)
Ribeiro, M.C., Metzger, J.P., Martensen, A.C., Ponzoni, F.J. & Hirota, M.M. (2009) The Brazilian Atlantic forest: how much is left, and how is the remaining forest distributed? Implications for conservation. *Biological Conservation*, 142, 1141–1153.
https://doi.org/10.1016/j.biocon.2009.02.021
Ronquist, F., Teslenko, M., van der Mark, P., Ayres, D.L., Darling, A., Höhna, S., Larget, B., Liu, L., Suchard, M.A. & Huelsenbeck, J.P. (2012) MrBayes 3.2: efficient Bayesian phylogenetic inference and model choice across a large model space. *Systematic Biology*, 61, 539–542.
https://doi.org/10.1093/sysbio/sys029
Schacht, M.C. & McBrayer, L.D. (2009) A Method for Constructing an Adjustable Plataform to Obtain Lateral Photographs of Larval Anurans. *Herpetological review*, 40, 303–304.
Schneider, C.A., Rasband, W.S. & Eliceiri, K.W. (2012) NIH Image to ImageJ: 25 years of image analysis. *Nature methods*, 9, 671–675.
https://doi.org/10.1038/nmeth.2089
Sueur, J., Aubin, T. & Simonis, C. (2008) Seewave, a new modular tool for sound analysis and synthesis. *Bioacoustics*, 18, 213–226.
https://doi.org/10.1080/09524622.2008.9753600
Vrcibradic, D., Ariani, C.V., Van Sluys, M. & Rocha, C.F.D. (2010) Amphibia, Leptodactylidae, *Paratelmatobius mantiqueira*: Distribution extension. *Check List*, 6, 1–2.
https://doi.org/10.15560/6.1.001

Walker, M., Lyra, M.L. & Haddad, C.F.B. (2018) Phylogenetic relationships and cryptic species diversity in the Brazilian egg-brooding tree frog, genus *Fritziana* Mello-Leitão 1937 (Anura: Hemiphractidae). *Molecular Phylogenetics and Evolution*, 123, 59–72.
https://doi.org/10.1016/j.ympev.2018.02.012

Wells, K.D. (1977) The social behaviour of anuran amphibians. *Animal Behaviour*, 25, 666–693.
https://doi.org/10.1016/0003-3472(77)90118-X

Zaher, H., Aguiar, E. & Pombal Jr., J.P. (2005) *Paratelmatobius gaigeae* (Cochran, 1938) re-discovered (Amphibia, Anura, Leptodactylidae). *Arquivos do Museu Nacional*, 63, 321–328.

**APPENDIX I. Specimens examined**

*Paratelmatobius cardosoi*: BRAZIL: SÃO PAULO: Bertioga, Parque das Neblinas (CFBH 38980, 38982, 38989–38990, UFMG 3237); Itanhaém, Parque Estadual da Serra do Mar, Núcleo Curucutu (CFBH 16770, 16780, 22130, 27718); Santo André, Paranapiacaba (CFBH 862–865 [paratypes], 37757 [topotype]).

*Paratelmatobius* cf. *segallai*: BRAZIL: SÃO PAULO: Capão Bonito, Parque Estadual Carlos Botelho (CFBH 40789, MZUSP 135993); Guapiara, Bairro Araçaeiro (CFBH 43420–43421); Iporanga, Parque Estadual Turístico do Alto Ribeira (CFBH 25616); Piedade (CFBH 23302); Pilar do Sul, Fazenda João XXIII (CFBH 3722–3726, 8365–8370); São Miguel Arcanjo, Parque Estadual Carlos Botelho (CFBH 36008–36011, 38426–38427, 40681, 40684, 40686, 40794, MZUSP 135979, 135981–135983, 135985–135992); Tapiraí (CFBH 16535–16537).

*Paratelmatobius gaigeae*: BRAZIL: SÃO PAULO: Bananal, Estação Ecológica do Bananal (CFBH 7156, MZUSP 138657, 138659, 138661); São José do Barreiro, Parque Nacional da Serra da Bocaina (AAG-UFU 810–816, CFBH 36069–36070, 36079, UFMG 15004–15008 [topotypes]).

*Paratelmatobius lutzii*: BRAZIL: MINAS GERAIS: Itamonte, Parque Nacional de Itatiaia, Brejo da Lapa (CFBH 295, MZUSP 94622–94654 [topotypes]).

*Paratelmatobius mantiqueira*: BRAZIL: SÃO PAULO: Campos do Jordão, Cidade Azul (MZUSP 15133 [holotype], 15128–15132, 15134–15142 [paratypes]); RIO DE JANEIRO: Resende, Fazenda Marimbondo (MNRJ 51501).

*Paratelmatobius poecilogaster*: BRAZIL: SÃO PAULO: Bertioga, Parque das Neblinas (UFMG 3238–3240); Santo André, Paranapiacaba (CFBH 6266 [paratype], 866, 3253, 3254, 12004, 12005, 28959, 28960, 29983 [topotypes]); São Luís do Paraitinga, Parque Estadual da Serra do Mar, Núcleo Santa Virgínia (CFBH 7730–7734, 7935–7939, 9880–9883).

*Paratelmatobius yepiranga*: BRAZIL: SÃO PAULO: Bertioga, Parque das Neblinas (MZUSP 137563 [holotype], 136696–136698 [paratypes]).

## CONCLUSÕES GERAIS

A partir de expedições de campo e dados obtidos em coleções herpetológicas, obtivemos uma matriz com ampla amostragem de linhagens da subfamília Paratelmatobiinae, que nos permitiu melhorar o entendimento da taxonomia e da história evolutiva do grupo. As principais conclusões são comentadas abaixo:

- O gênero *Crossodactylodes*, até então pouco estudado, foi recuperado como monofilético e bem suportado. A taxonomia de *Crossodactylodes* foi aprimorada a partir de novas diagnoses para o gênero e cada uma de suas espécies. O gênero pode ser diagnosticado por sete sinapomorfias putativas em caracteres morfológicos e de história natural, sendo que alguns desses caracteres parecem ter relação com o hábito bromelígena. Além disso, dados sobre distribuição geográfica, história natural e conservação foram atualizados. Dessa forma, nosso estudo contribuiu para o aumento do conhecimento sobre o gênero e poderá beneficiar futuras descrições de espécies.
- A subfamília Paratelmatobiinae e os gêneros nela contidos foram recuperados como monofiléticos, com altos valores de suporte em análise filogenética multigênica que incluiu 11 das 14 espécies conhecidas. Além disso, outras linhagens evolutivamente independentes, incluindo cinco espécies potencialmente novas, foram delimitadas. Os tempos de divergência estimados sugerem um cenário complexo para a diversificação de Paratelmatobiinae, que se iniciou no Eoceno e Oligoceno com as divergências intergenéricas e continuou principalmente no Mioceno, com as divergências intragenéricas. Mudanças climáticas passadas, eventos neotectônicos e características associadas à história natural das espécies de Paratelmatobiinae possivelmente influenciaram a diversificação.
- A nova espécie de *Paratelmatobius* descrita (*P. segallai*) pertence ao grupo de espécies de *P. cardosoi*. A espécie é diagnosticável de seus táxons congenéricos por apresentar canto de anúncio composto por dois tipos de notas, emitidos em séries de duas a quatro notas, além de outras diferenças acústicas e morfológicas. *Paratelmatobius segallai* apresenta reprodução explosiva, associada a períodos de fortes chuvas. A descrição de *P. segallai* sugere que o conhecimento sobre a diversidade da Mata Atlântica ainda se encontra subestimado, enfatizando a importância de novos inventários faunísticos e estudos taxonômicos.

## PERSPECTIVAS

Diante dos resultados obtidos, podem-se traçar algumas perspectivas:

- Investigar os posicionamentos filogenéticos de *Crossodactylodes pintoi*, *Paratelmatobius lutzii* e *P. mantiqueira* por meio de sequências de DNA obtidas a partir de espécimes históricos depositados em coleções herpetológicas.

- Realizar estudos taxonômicos focados nas linhagens não descritas que foram recuperadas em nossas análises, quando possível integrando outros sistemas de caracteres, como bioacústicos e larvais, aos dados genéticos e morfológicos.

- Investigar os processos evolutivos relacionados à diversificação de diferentes linhagens proximamente relacionadas a partir do uso de modelos demográficos alternativos.

- Investigar a biogeografia histórica das linhagens de Paratelmatobiinae por meio de modelos de reconstrução de distribuição ancestral.